A Resorbable Polymeric Microreservoir Device for Controlled Release Drug Delivery

by

Amy Catherine Richards Grayson

B.S., Materials Science and Engineering
Massachusetts Institute of Technology, 1997

Submitted to the Department of Materials Science and Engineering
and the
Program in Polymer Science and Technology
in Partial Fulfillment of the Requirements for the Degree of
Doctor of Philosophy in Polymer Science

at the

Massachusetts Institute of Technology
June 2003

Signature of Author…….
Amy C. R. Grayson
Department of Materials Science and Engineering
April 23, 2003

Certified by…….
Robert S. Langer
Kenneth J. Germeshausen Professor of Chemical and Biomedical Engineering
Thesis Supervisor

Certified by…….
Michael J. Cima
Sumitomo Electric Industries Professor of Engineering
Thesis Supervisor

Accepted by…….....
Harry L. Tuller
Professor of Ceramics and Electronic Materials
Chair, Departmental Committee on Graduate Students

A Resorbable Polymeric Microreservoir Device for Controlled Release Drug Delivery

by
Amy Catherine Richards Grayson

Submitted to the Department of Materials Science and Engineering
and the
Program in Polymer Science and Technology
April 23, 2003
in partial fulfillment of the requirements for the degree of
Doctor of Philosophy in Polymer Science

ABSTRACT

The method by which a drug is delivered can have a significant effect on the drug's therapeutic efficacy. Pulsatile delivery of certain drugs and molecules (such as hormones) has been shown to more efficacious than continuous delivery, as the fluctuation in concentration levels *in vivo* more closely mimics the natural physiological processes of the human body. However, there is a shortage of systems that are capable of delivering drugs in this manner, particularly if it is desired to have a self-contained system that does not require external stimulation to trigger device function.

The objectives of this thesis were to design, fabricate, test, and characterize a biodegradable polymeric microreservoir device that is capable of delivering multiple pulses of drugs in a reproducible manner. This polymeric microreservoir device contains an array of reservoirs that are each covered by a thin membrane of a degradable polymer. Control over the release of drugs from the device was achieved by changing the molecular weight of the reservoir membranes. The current prototypes have 36 reservoirs, but the size and geometry of the polymeric chip could be designed to optimize device performance depending on the application for which it will be used. Changing the membrane materials or thicknesses could change the time at which the chemicals are released from the reservoirs. Each reservoir on the device could potentially have a different set of membrane characteristics, enabling release of the contents of each reservoir at a different time.

A fabrication process for these devices was developed, that consists of two compression-molding steps, followed by microinjection of the reservoir membranes from solution and subsequent drying of the membranes under vacuum and elevated temperature. The devices are then loaded with the drugs to be released and sealed at room temperature. This fabrication process avoids exposure of the drugs to solvents and high temperatures that may adversely affect their stability. Further, the compression-molding process used to fabricate the main body of the device, as well as minimal solvent used in the fabrication of the reservoir membranes, were designed to minimize adverse effects upon *in vivo* implantation due to residual solvent.

Poly(L-lactic acid) was selected as the component material for the device substrate, while the reservoir membranes were made from copolymers of poly(lactic-co-glycolic acid) having varying molecular weights. The degradation behaviors of these materials have been extensively studied both *in vitro* and *in vivo*, and they have been shown to be quite biocompatible. Studies showed that the degradation of the reservoir membranes *in vitro* and subsequent release times of chemicals from the reservoirs is a function of both the membrane thicknesses and environmental temperature.

Proof-of-principle release studies showed up to four pulses of radiolabeled molecules (^{14}C-dextran, ^{3}H-heparin, and ^{125}I-HGH) from single devices, both with one chemical per device (four pulses per chemical) as well as two chemicals per device (two pulses per chemical). Bioactivity measurements showed that heparin released from the devices *in vitro* retains activity up to at least 143 days. *In vitro* release studies and characterization of partition coefficients showed that the pulsatile delivery of smaller, more lipophilic molecules is more challenging, and may require further device modification.

Proof-of-principle *in vivo* release studies demonstrated delivery of two pulses of ^{14}C-mannitol in rats from prototype devices having reservoir membranes made from two different polymers. More pulses could be achieved *in vivo* by increasing the number of different reservoir membrane materials used. The more rapid release kinetics observed *in vivo* compared to the *in vitro* results suggests more rapid degradation of the reservoir membranes. This hypothesis was supported by results obtained from *in vivo* biodegradation studies.

A greater understanding of the mechanisms by which the reservoir membranes open will aid in attaining greater reproducibility of device performance. Additionally, more thorough study of the interactions between the drug and the membrane materials may help to develop a framework for understanding how device performance and release time can be predicted based on the chemistry of the drugs of interest. Finally, optimization of the membrane materials for *in vivo* device usage is paramount for progress towards achieving a clinically useful drug delivery system.

Thesis Supervisor: Robert Langer
Title: Kenneth J. Germeshausen Professor of Chemical and Biomedical Engineering

Thesis Supervisor: Michael J. Cima
Title: Sumitomo Electric Industries Professor of Engineering

Thesis Errata Sheet

Author Amy C. R. Grayson

Primary Dept. Materials Science and Engineering

Degree(s) Ph.D. **Graduation date** Jun 2003

Thesis title

A Resorbable Polymeric Microreservoir Device for Controlled Release Drug Delivery

Brief description of errata sheet

Figures 5.25, 9.1, and 9.2 of the thesis and the accompanying text in the captions and body incorrectly state the reservoir membrane thicknesses of the devices as 150 microns. The actual membrane thicknesses are 318-330 microns. This errata sheet provides corrected text for these errors.

Number of pages 5 (11 maximum, including this page)

▶ **Author**: I request that the attached errata sheet be added to my thesis. I have attached two copies prepared as prescribed by the current *Specifications for Thesis Preparation*.

Signature of author _____ Date _____

▶ **Thesis Supervisor** or **Dept. Chair**: I approve the attached errata sheet and recommend its addition to the student's thesis.

Signature _____ Date _____

Name _____ ☐ Thesis supervisor ☐ Dept. Chair

▶ **Dean for Graduate Education**: I approve the attached errata sheet and direct the Institute Archives to insert it into all copies of the student's thesis held by the MIT Libraries, both print and electronic.

Signature _____ Date _____

Name _____

page 15, Figure 5.25 caption, line 2

Original text: "WITH ^{14}C-MANNITOL AND HAVING 150 μM THICK PLGA11 AND PLGA64 RESERVOIR MEMBRANES WITH"

Corrected text: "WITH ^{14}C-MANNITOL AND HAVING 318–327 μM THICK PLGA11 AND PLGA64 RESERVOIR MEMBRANES WITH"

page 17, Figure 9.1 caption, line 2

Original text: "DEVICES HAVING PLGA11 AND PLGA64 RESERVOIR MEMBRANES, EACH LOADED WITH …"

Corrected text: "DEVICES HAVING 318–327 μM THICK PLGA11 AND PLGA64 RESERVOIR MEMBRANES, EACH LOADED WITH …"

page 17, Figure 9.2 caption, line 2

Original text: "DEVICES (□△◇○) HAVING PLGA11 AND PLGA64 RESERVOIR MEMBRANES, EACH LOADED WITH…"

Corrected text: "DEVICES (□△◇○) HAVING 321–330 μM THICK PLGA11 AND PLGA64 RESERVOIR MEMBRANES, EACH LOADED WITH…"

page 42, paragraph 2, line 2

Original text: "experiments reported in this thesis. The volume of membrane solution…"

Corrected text: "experiments reported in this thesis, although occasionally devices with membranes of 175–330 μm thickness were used. The volume of membrane solution…"

page 44, paragraph 1, last line

Original text: "volumes ranged from 100 to 200 nL, for predicted final membrane thicknesses of 150 μm."

Corrected text: "volumes ranged from approximately 110 to 265 nL for predicted final membrane thicknesses of 150 μm, and up to 500 nL were injected for thicker membranes."

page 149, paragraph 2, line 3

Original text: "**Error! Reference source not found.** also shows longer $t_{1/2}$ values for 150 μm thick films that"

Corrected text: "**Table 5-3** also shows longer $t_{1/2}$ values for 150 μm thick films that"

page 152, paragraph 2, lines 1–3

Original text: "Similarly, comparison of release results at 37°C *in vitro* from devices having 150 μm thick **PLGA11** and **PLGA64** membranes and loaded with ^{14}C-mannitol (experimental methods are presented in Chapter 9) show excellent agreement with results obtained…"

Corrected text: "Similarly, release results at 37°C *in vitro* from devices having 318–327 μm thick **PLGA11** and **PLGA64** membranes and loaded with ^{14}C-mannitol (experimental methods are presented in Chapter 9) can be compared with results obtained…"

page 153, Figure 5.25 caption, line 2

Original text: "mannitol and having 150 μm thick **PLGA11** and **PLGA64** reservoir membranes…"

Corrected text: "mannitol and having 318–327 μm thick **PLGA11** and **PLGA64** reservoir membranes…"

page 153, paragraph 1 below Figure 5.25

Original text: "These results suggest that perhaps once the molecular weight of the membrane material drops below a critical value, in the range of 4,000 to 7,000 daltons, the membrane becomes so mechanically weak that it ruptures and releases the contents of the reservoir. It seems unlikely that the membrane opens due to simple dissolution of the low molecular weight chains, as others have reported a critical weight average molecular weight of 1,050 to 1,150 for water solubility of poly(D,L-lactic acid) oligomers[15], which is much lower than the 4,000–7,000 molecular weight that seems to be significant for membrane opening in the studies reported here."

Corrected text: "A prediction of the molecular weight range for **PLGA11** and **PLGA64** membrane failure at 37°C must take into account the possibility of size-dependent degradation related to the differences in thicknesses of the device membranes in **Figure 5.25** and the films used in the degradation study. For the **PLGA11** material, **Table 5-3** shows that 150 μm films degraded slightly slower, as indicated by a longer half-life, than 50 μm films at 25°C with no media change. The release times at 25°C summarized in **Table 5-2** show that **PLGA11** membranes of thicknesses ranging from 150 to 275 μm do not consistently show a size-dependence of degradation rate. Therefore it is unclear whether 150 μm membranes would

release earlier or later than the 318–327 μm membranes shown in **Figure 5.25**. In the most extreme case, assuming faster degradation of thinner membranes, immediate release of 150 μm **PLGA11** membranes would correlate to a molecular weight of 12,700 daltons, the highest measured molecular weight for this polymer at the start of the degradation study. If **PLGA11** does exhibit size-dependent degradation and a consequent faster degradation of thicker objects, however, the expected release time of 150 μm membranes would occur after that observed for the 318–327 μm membranes at days four to six. The molecular weight for failure of 150 μm thick **PLGA11** membranes would therefore be equal to or less than the measured molecular weight range of 4,400–6,500 daltons measured between days four and seven for the 150 μm films at 37°C with media change.

PLGA64 clearly appears to undergo size-dependent degradation at 25°C and at the length scale of interest (150–330 μm) for **Figure 5.25**, in contrast to **PLGA11**. The release times summarized in **Table 5-2** for the **PLGA64** membranes at 25°C show faster degradation of 250 and 275 μm membranes than for 175 and 150 μm membranes, respectively. If this size dependent degradation were extrapolated to 37°C and thicker membranes we would expect that 150 μm membranes would show release later than that observed for the 318–327 μm membranes between days 12 to 15 in **Figure 5.25**. The molecular weight for failure of 150 μm thick **PLGA64** membranes would therefore be similar to or less than the measured molecular weight of 5,300 daltons at 14 days for 150 μm thick **PLGA64** films at 37°C with media change.

The comparison of release and degradation results at 25 and 37°C suggests that perhaps once the molecular weight of the membrane material drops below a critical value, in the range of 5,000 to 13,000 daltons, the membrane becomes so mechanically weak that it ruptures and releases the contents of the reservoir. The upper limit of molecular weight for membrane rupture may in fact be lower than estimated here, however molecular weight data for degradation of 150 μm thick **PLGA28** and **PLGA64** films beyond 49 days at 25°C, and 150 μm membrane release data at 37°C would be required to determine the upper limit more precisely. It seems unlikely that the membrane opens due to simple dissolution of the low molecular weight chains, as others have reported a critical weight average molecular weight of 1,050 to 1,150 for water solubility of poly(D,L-lactic acid) oligomers[15], which is much lower than the 5,000–13,000 molecular weight that seems to be significant for membrane opening in the studies reported here.

page 230, paragraph 1, lines 6–7

Original text: "…Predicted membrane thicknesses were 150 μm for all devices. On each device…"

Corrected text: "…Predicted membrane thicknesses were 318–327 μm for devices tested *in vitro*, and 321–330 μm for devices tested *in vivo*. On each device…"

page 232, Figure 9.1 caption, line 2

Original text: "**PLGA11** and **PLGA64** reservoir membranes, each loaded with…"

Corrected text: "318–327 μm thick **PLGA11** and **PLGA64** reservoir membranes, each loaded with…"

page 233, Figure 9.2 caption, line 2

Original text: "having **PLGA11** and **PLGA64** reservoir membranes, each loaded with…"

Corrected text: "having 321–330 μm thick **PLGA11** and **PLGA64** reservoir membranes, each loaded with…"

page 267, paragraph 4, lines 2–3

Original text: "…the polymer molecular weight dropping below 5,000–7,000 daltons, the results reported in Chapter 7…"

Corrected text: "…the polymer molecular weight dropping below 5,000–13,000 daltons, the results reported in Chapter 7…"

TABLE OF CONTENTS

LIST OF FIGURES

LIST OF TABLES

ACKNOWLEDGEMENTS

After so many years at MIT, it is difficult to believe that I am finally leaving. The line that runs through my mind these days is "Boston, you're my home," from the song "Dirty Water" by the Standells. After four years as an undergraduate at MIT and another six (!) as a graduate student, I really do feel like Boston is my home, and my family can vouch for my acquired Boston accent. I've lived here for ten out of my 27 years, which is longer than I have lived anywhere else! But now it is time to move on to other things, and to do that I must thank all those without whom I could not have made it this far.

Bob Langer and Michael Cima, for your guidance and patience and helping me to grow as a scientist, researcher, engineer, and person. Thank you for taking a chance on me, when I really had no idea what I was getting into and just wanted to work on this project because I thought it was really cool. I have learned so many valuable things, not just about research, from both of you.

My thesis committee members (past and present), Chris Scott, Paul Laibinis, Michael Rubner, and Darrell Irvine. Thank you for your insights and suggestions and making sure that I knew my stuff. And thank you for your willingness to serve in the departmental rotation know as "Amy's thesis committee."

My collaborators, Betty Tyler and Dr. Henry Brem at Johns Hopkins University, and Gabriela Voskerician and Dr. James Anderson at Case Western Reserve University. Our work together on the *in vivo* studies has been invaluable in giving me a broader perspective of biomaterials and drug-delivery systems.

Lenny Rigione and John Centorino, for always being willing to help me learn how to use equipment, and seeming genuinely interested in my answers to your questions about how my experiments were going.

Barbara Layne, Connie Beal, and Ilda Moura Thompson, for your invaluable work to make sure that all rules and budgets were followed, equipment was purchased when I needed it, and for your help with scheduling appointments and meetings.

Those who have gone before me in Langer Lab, for showing me that it really is possible to graduate: Karen, Sachiko, Amir, and Jennifer.

Those who will come after me in the Langer and Cima labs, for sharing your enthusiasm with an old and bitter n^{th} year student: Grace and Yawen.

My compatriots and fellow students in both the Langer and Cima labs, for commiseration, mutual support, and laughter: Joe, Tommy, Eric, Audrey, Rebecca, Mindy, and Ryan.

My UROPS, Rebecca, Joyce, and Casey, for all of the hard work, weekend pipetting, and radiation safety training that you endured. The data you collected were an important part of this thesis, and I truly would have gone crazy without your help to take off a few weekends from the lab.

My course 3 buddies, Ben, Neil, and Vicky, we have finally all made it!

Insung, your discussions and insights truly helped me to refocus when I desperately needed it.

John Santini, first my tutor, then my friend, mentor, and microchip predecessor, thank you for your scientific insights, as well as for always taking a moment out of your day to talk to me when I needed it.

The students of 2nd East at East Campus where I was a graduate resident tutor, for letting me get to know you and watch you grow. I appreciate the friendships we formed and I thank you for keeping me young at heart for a little while longer.

My friends from Ashdown, swim team, and water polo, thank you for reminding me that there is life and fun outside of lab.

Diana and Deb, for lending an ear to listen whenever I needed it.

My family: Mom, Dad, Jess, and Chuck, for being there no matter what, and having faith that I would get through this.

And to my husband,
Jay,
What would I do without you?
I'm finally done!

1 Background and Introduction

1.1 Overview of Controlled Release

The method by which a drug is delivered can have a significant effect on the drug's therapeutic efficacy[1,2]. Conventional drug delivery systems such as tablets[3–5], pumps[6–8], implants (Gliadel, for example[9,10]), injectable microspheres (such as Lupron Depot[11]), and patches[12] often produce a sharp initial increase in concentration to a peak above the therapeutic range, followed by a fast decrease in concentration to a level below the therapeutic range. Many polymeric implants achieve pulsatile release of a chemical via triggering by specific stimuli (changes in pH[13–15] or temperature[16–18], exposure to ultrasound[19,20], enzymes[21], or light[22], or changes in electric[23–27] or magnetic[19,28] fields or molecules present in the human body, such as antigens[29] or water). Externally-worn pumps are also used for pulsatile delivery. A newer approach uses microfabricated silicon devices for controlled release of drugs[30,31]. These devices potentially allow the release of hundreds of individual doses of drugs or chemicals (including both liquids and solids) with no moving parts from a single device on demand. However, these devices are not self-contained or biodegradable, and require components such as a power supply and clock or timer.

In certain applications it may be desirable for a drug delivery system to release pulses of drug without the application of an external stimulus or a change in the local environment surrounding the device. For example, many hormones such as insulin[32], gonadotropin releasing hormone and growth hormone releasing hormone are more effective when delivered in pulses over the course of a day[33,34], but this is cumbersome and inconvenient to achieve by using an externally-triggered device. Therefore, there is a therapeutic need that could potentially be met by polymeric drug delivery systems that are capable of releasing pulses of drugs without the device performance being tied to an environmental change (such as local pH or application of a current).

Thus far, the only reports in the literature of a polymeric system that can achieve pulsatile release without the application of an external stimulus or change in the local environment of the device, are of PLGA devices that have concentrically compression-molded alternating layers of polymer loaded with drug, or having no drug[35,36]. Two pulses of model drugs have been

demonstrated from these devices *in vitro*, as well as one pulse *in vivo*. However, this system may be limited in the number of dosages that it could deliver, due to the fabrication process by which it is made.

1.2 A Resorbable Polymeric Microreservoir Device for Drug Delivery

We propose here a resorbable polymeric microreservoir device, shown schematically in **Figure 1.1** below, that could be used to deliver multiple pulses of drug.

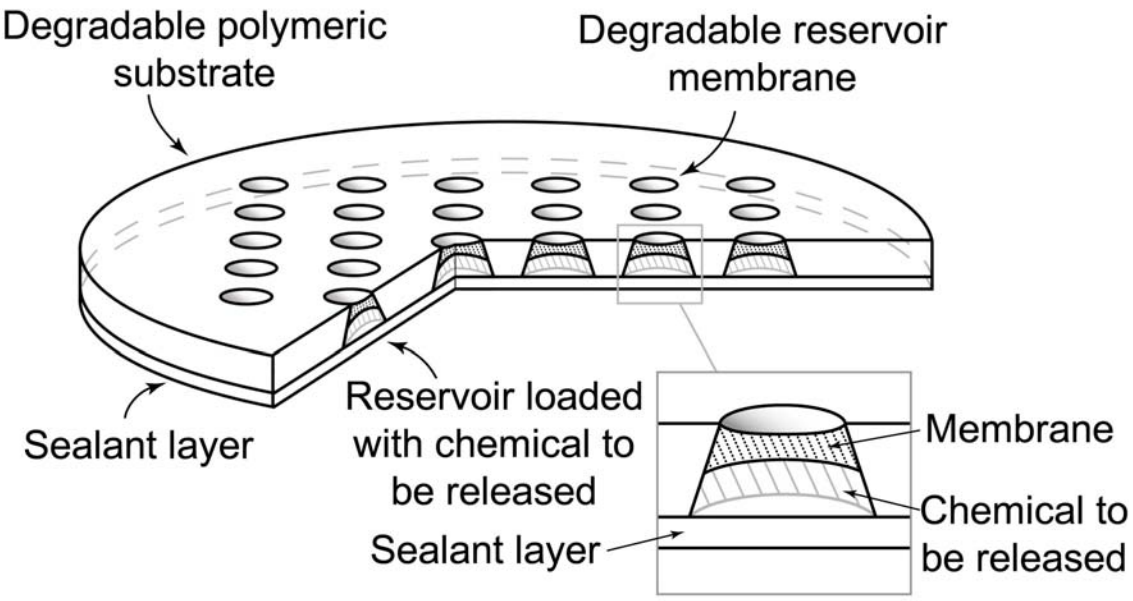

Figure 1.1 Schematic of polymeric microreservoir device. Figure by Erica Beade.

The goal of our polymeric microreservoir device is to reproducibly achieve multiple pulses of drugs from a single device, with no initial burst effect. This device concept is based on previous work that has been done to develop an active, silicon-based microchip for controlled release[30]. The polymeric microreservoir device presented in this thesis contains an array of reservoirs that are each covered by a thin membrane of a degradable polymer. Control over the release of drugs from the device is achieved by changing the characteristics of the reservoir membranes. Increasing the thickness or the molecular weight of the membrane material, or using a more slowly degraded polymer, for example, could change the time at which the chemicals are released from the reservoirs. Each reservoir on the device could potentially have a different set of membrane characteristics, enabling release of the contents of each reservoir at a different time.

While the current prototypes shown in **Figure 1.1** have 36 reservoirs, the size and geometry of the polymeric chip could be tailored depending on the application for which it will be used. For example, an 18 mm x 18 mm square device having 289 conical reservoirs (each with a large opening 500 μm in diameter and a small opening 45 μm in diameter) could hold enough ethinyl estradiol for one year of estrogen replacement therapy. Similar applications involving potent hormones (contraception, for example) or other chemicals could be envisioned.

One of the unique advantages of this drug delivery system is that it allows separation of the components that control device performance from those that affect drug stability. The formulation that controls the drug release (the reservoir membranes) is to a first approximation independent of any formulation that may be included in the reservoir to control the drug stability. This is vastly different from other drug delivery systems that have been developed. Lupron Depot, for example, is a commercially available injectable microsphere formulation that releases leuprorelin acetate, a superagonist of luteinizing hormone releasing hormone (LH-RH), for treatment of hormone-dependent cancers and endocrine diseases[11,37]. Sustained blood levels of leuprorelin acetate have been found to be more effective for treating the disorders of interest, and therefore a constant release rate of drug from the microspheres is ideal. However, the release characteristics of the drug (amount of initial burst and sustained release rate) from the microspheres are affected by the drug loading, oligomer content, and particle size of the microspheres. In one study of numerous formulations made from varying molecular weights of PLA and PLGA, for example, optimal results were obtained for leuprorelin acetate delivered from PLA microspheres having an average molecular weight of 15,000, < 0.1% of water-soluble oligomer content, and with a drug loading of 12%. But even this "optimized" formulation showed a burst of leuprorelin acetate (<10% of the initial drug loading) on the first day *in vivo*[37]. The limitations of formulation specificity are not unique to Lupron Depot. Although PLA, PGA, and PLGA copolymers are widely studied and used for drug delivery systems, the flexibility that can be achieved through variation of molecular weight, oligomer content, copolymer ratio, particle size, and drug loading, is often underutilized when a formulation must be optimized for a specific drug release profile. In contrast, the flexibility offered by PLA, PGA, and PLGA copolymers can be fully exploited by the polymeric microreservoir device by simply changing the reservoir membrane characteristics independently of the drug formulation that is to be released from the device, and vice versa. Increasing the drug loading of the microreservoir

device, for example, can be achieved simply by loading more of the drug into each reservoir, or loading more reservoirs with the drug. This would not affect the drug release rate and would require no redesign of the membrane formulation. In contrast, changing the drug loading of Lupron Depot microspheres would require changing the polymer molecular weight or any number of other variables in order to maintain the drug release rate. This flexibility of the polymeric microreservoir device may offer an additional degree of freedom when considering the design of a drug delivery system for a given application, as the drug formulation will not be intimately tied to the release formulation. This may potentially allow greater utility of the microreservoir device as a platform for a broad range of drug-delivery applications, rather than being limited to treatment of only one or a few specific conditions.

The microreservoir device has a number of other advantages. It has no moving parts and thus is not susceptible to mechanical failure, unlike external pumps and internal micropumps. Additionally, it could potentially deliver a wide variety of chemicals in solid, liquid, or gel form (this is not the case with pumps or patches), and could also achieve release of a desired substance or substances over a prolonged period of time, from days to weeks to even months or years, depending on the number of reservoirs that are filled with the substance and the characteristics of the reservoir membranes. This offers a distinct advantage over tablets used for oral delivery of drugs, which typically can achieve only one to three pulses of drug over the course of a day as the tablet passes through the gastrointestinal tract. The microchip is also an improvement over existing implantable, polymeric, controlled release systems due to the fact that it is not limited to the release of only one or a few chemical substances. In theory, every reservoir on the chip could be filled with a different substance or drug. Additionally, the fabrication and filling processes for the microchip are such that the drugs put into the chip are not exposed to any high temperatures or harsh chemicals. Thus the stability of the drugs is not compromised, in contrast to solvent-intensive fabrication procedures for microspheres and some other types of polymeric implants.

1.3 Thesis Objectives

The specific goals of this Ph.D. thesis are as follows:

1) To develop a fabrication process and select appropriate component materials for the microreservoir device substrate and reservoir membranes, as well as to develop a method for filling the devices with the drug to be released (Chapters 2 and 3).

2) To demonstrate chemical release from the microreservoir devices *in vitro* (Chapter 4).
3) To characterize the degradation of the membrane materials *in vitro* and to determine the effect of membrane thickness and environmental temperature on their degradation rates (Chapter 5).
4) To characterize the factors affecting the kinetics of drug release, specifically the partition coefficients, molecular weights, and reservoir loadings (osmotic P effects) of the drugs of interest (Chapters 6 and 7).
5) To demonstrate biological activity of molecules released from the microreservoir device *in vitro* (Chapter 8).
6) To demonstrate chemical release from the devices *in vivo* (Chapter 9).
7) To characterize the biodegradation and biocompatibility of reservoir membrane materials *in vivo* in order to better understand their *in vivo* performance (Chapter 10).

1.4 References

1. E. E. Bakken and K. Heruth, "Temporal control of drugs, an engineering perspective," *Ann. New York Acad. Sci.* 618 (1991) 422–427.

2. A. J. Kost and R. Langer, "Responsive polymeric delivery systems," *Adv. Drug Delivery Rev.* 6 (1991) 19–50.

3. B. M. Wu, S. W. Borland, R. A. Giordano, L. G. Cima, E. M. Sachs, and M. J. Cima, "Solid free-from fabrication of drug delivery devices," *J. Control Release* 40 (1996) 77–87.

4. W. E. Katstra, R. D. Palazzolo, C. W. Rowe, B. Giritlioglu, P. Teung, and M. J. Cima, "Oral dosage forms fabricated by Three Dimensional Printing," *J. Control Release* 66 (2000) 1–9.

5. C. W. Rowe, W. E. Katstra, R. D. Palazzolo, B. Giritlioglu, P. Teung, and M. J. Cima, "Multimechanism oral dosage forms fabricated by three dimensional printing," *J. Control Release* 66 (2000) 11–17.

6. N. Santoro, "Efficacy and safety of intravenous pulsatile gonadotropin-releasing hormone: Lutrepulse for injection," *Am. J. Obstet. Gynecol*. 163 (1990) 1759–1764.

7. G. W. Creasy and M. E. Jaffe, "Pulsatile delivery systems," *Ann. NY Acad. Sci*. 618 (1991) 548–557.

8. G. W. Creasy and M. E. Jaffe, "Endocrine/reproductive pulsatile delivery systems," *Adv. Drug Delivery Rev*. 6 (1991) 51–56.

9. P. Sampath and H. Brem, "Implantable slow-release chemotherapeutic polymers for the treatment of malignant brain tumors," *Journal of the Moffitt Cancer Center* 5 (1998) 130–137.

10. *Physician's Desk Reference* (Ed.: R. Arky), Medical Economics Company, Montvale, NJ, USA, 1998, pp. 2587–2589.

11. *Physician's Desk Reference* (Ed.: R. Arky), Medical Economics Company, Montvale, NJ, USA, 1998, pp. 3139–3150.

12. L. Brown and R. Langer, "Transdermal delivery of drugs," *Ann. Rev. Med.* 39 (1988) 221–229.

13. R. A. Siegel, M. Falamarzian, B. A. Firestone, and B. C. Moxley, "pH-controlled release from hydrophobic/polyelectrolyte copolymer hydrogels," *J. Controlled Release* 8 (1988) 179-182.

14. J. H. Kim, J. Y. Kim, Y. M. Lee, and K. Y. J. Kim, "Controlled release of riboflavin and insulin through crosslinked poly (vinyl alcohol)/chitosan blend membrane," *Appl. Polym. Sci*. 44 (1992) 1923–1828.

15. A. Gutowska, J. S. Bark, I. C. Kwon, Y. H. Bae, Y. Cha, and S. W. Kim, "Squeezing hydrogels for controlled oral drug delivery," *J. Controlled Release* 48 (1997) 141–148.

16. Y. H. Bae, T. Okano, R. Hsu, and S. W. Kim, "Thermo-sensitive polymers as on-off switches for drug release," *Makromol. Chem. Rapid Commun*. 8 (1987) 481–485.

17. A. S. Hoffman, A. Afrassiabi, and L. C. Dong, "Thermally reversible hydrogels: II. delivery and selective removal of substances from aqueous solutions," *J. Controlled Release* 4 (1986) 213–222.

18. T. Okano, Y. H. Bae, and S. W. Kim, in Pulsed and Self-Regulated Drug Delivery, Ed.: J. Kost, CRC Press, Boca Raton, FL, USA, 17–45 (1990).

19. J. Kost and R. Langer, in Pulsed and Self-Regulated Drug Delivery, Ed.: J. Kost, CRC Press, Boca Raton, FL, USA, 3–16 (1990).

20. J. Kost, K. Leong, and R. Langer, "Ultrasound-enhanced polymer degradation and release of incorporated substances," *Proc. Natl. Acad. Sci. USA* 86 (1989) 7663–7666.

21. F. Fischel-Ghodsian, L. Brown, E. Mathiowitz, D. Brandenburg, and R. Langer, "Enzymatically controlled drug delivery," *Proc. Natl. Acad. Sci. USA* 85 (1988) 2403–2406.

22. E. Mathiowitz and M. D. Cohen, "Polyamide microcapsules for controlled release. V. photochemical release," *J. Membr. Sci*. 40 (1989) 67–86.

23. I. C. Kwon, Y. H. Bae, and S. W. Kim, "Electrically erodible polymer gel for controlled release of drugs," *Nature* 354 (1991) 291–293.

24. Y. H. Bae, I. C. Kwon, and S. W. Kim, in Polymeric Drugs and Drug Administration, Ed.: R. M. Ottenbrite, American Chemical Society, Washington, DC, USA, 98–110 (1994).

25. L. L. Miller, "Electrochemically controlled release of drug ions from conducting polymers," *Mol. Cryst. Liq. Cryst.* 160 (1998) 297–301.

26. M. Hepel and Z. Fijalek, in Polymeric Drugs and Drug Administration, Ed.: R. M. Ottenbrite, American Chemical Society, Washington, DC, USA, 79–97 (1994).

27. S. F. Schwendeman, G. L. Amidon, and R. J. Levy, "Determinants of the modulated release of antiarrhythmic drugs by iontophoresis through polymer membranes," *Macromolecules* 26 (1993) 2264–2272.

28. E. R. Edelman, J. Kost, H. Bobeck, and R. Langer, "Regulation of drug release from polymer matrices by oscillating magnetic fields," *J. Biomed. Mater. Res*. 19 (1985) 67–83.

29. Y. Suzuki, M. Tanihara, Y. Nishimura, K. Suzuki, Y. Kakimaru, and Y. Shimizu, "A new drug delivery system with controlled release of antibiotic only in the presence of infection," *J. Appl. Biomat*. 42 (1998) 112–116.

30. J. T. Santini Jr., M. J. Cima, and R. Langer, "A controlled-release microchip," *Nature* 397 (1999) 335–338.

31. J. T. Santini Jr., A. C. Richards, R. Scheidt, M. J. Cima, and R. Langer, "Microchips as controlled drug-delivery devices," *Angew. Chem. Int. Ed.* 39 (2000) 2396–2407.

32. D. R. Matthews, D. A. Lang, M. A. Burnett, and R. C. Turner, "Control of pulsatile insulin secretion in man," *Diabetologia* 24 (1983) 231–237.

33. M. C. Gelato and G. R. Merriam, "Growth hormone releasing hormone," *Ann. Rev. Physiol.* 48 (1986) 569–591.

34. R. L. Reid, R. Fretts, and D. A. V. Vugt, "The theory and practice of ovulation induction with gonadotropin-releasing hormone," *American Journal of Obstetrics and Gynecology* 158 (1988) 176–185.

35. A. Göpferich, "Bioerodible implants with programmable drug release," *J. Controlled Release* 44 (1997) 271–281.

36. W. Vogelhuber, P. Rotunno, E. Magni, A. Gazzaniga, T. Spruß, G. Bernhardt, A. Buschauer, and A. Göpferich, "Programmable biodegradable implants," *J. Controlled Release* 73 (2001) 75–88.

37. H. Okada, "One- and three-month release injectable microspheres of the LH-RH superagonist leuprorelin acetate," *Adv. Drug Delivery Rev.* 28 (1997) 43–70.

2 Device Fabrication

2.1 Introduction and Motivation

2.1.1 Introduction

The polymeric microreservoir device currently consists of a reservoir-containing substrate made out of poly(lactic acid) (**PLA)**, and reservoir membranes made from copolymers of **PLA** and poly(glycolic acid) (**PGA**). These materials were selected as components of the device due to their biocompatibility and biodegradation characteristics, but other materials could also be used to fabricate devices similar in concept and operation to the device discussed here. This chapter describes the fabrication methods that were used to manufacture the devices, specifically substrate fabrication by compression molding and the formation of reservoir membranes by microinjection.

2.1.2 Motivation

A variety of biodegradable polymers have been used in drug delivery applications, most commonly poly(ε-caprolactone), polyanhydrides, poly(lactic acid) (PLA), poly(glycolic acid) (PGA), and copolymers of PLA and PGA (PLGA). The fabrication methods that are used often depend on the desired final geometry of the drug delivery device, as well as the thermal (T_g and T_m), physical (density and modulus), and chemical (solubility) properties of the polymer. Solvent film casting, melt spinning of fibers, and extrusion of rods[1] have been reported for objects made from PLGA. However, with the exception of compression- and other molding techniques, most fabrication methods are capable of producing only very simple shapes (films and cylinders, for example). Solvent evaporation, spray drying, and emulsion techniques are common for microsphere systems[2–4] (Lupron Depot®, for example[5]). Larger depot systems are often fabricated by compression molding[6], melt casting[7], or solvent casting[8] of a mixture of the polymer and drug of interest, or by encapsulating a drug within a semipermeable membrane (such as the Norplant system[9]). Significant burst release upon implantation (or commencement of an *in vitro* release study)[6,10], is typically followed by sustained release (constant release rate) of the drug from many of these systems. This may be undesirable for certain therapeutic

applications in which pulsatile release of the active agent, or the absence of an initial burst release, are desired for maximum therapeutic efficacy.

Several considerations are of importance in the development of a fabrication method for our polymeric microreservoir device. First, the goal of delivering multiple pulses of active substances from a number of small reservoirs necessitates a more complex geometry than can be formed by spray drying, extrusion, or film casting. Second, it is desired for the microreservoir device to be completely dense (nonporous), as well as have good mechanical strength and a degradation time of at least one month in the body. Low or no porosity, as well as a long degradation time, are desired in order to prevent drug leakage or dose dumping from the device. Good mechanical strength is desired in order to prevent fracture or fragility of the device for commercial production and loading, shelf stability, and ease of implantation by the surgeon in a patient. Third, it is highly desirable to minimize the amount of residual solvent in our device, given the long-term goal of implantation in a human patient. The U.S. Food and Drug Administration (FDA) has very strict requirements on residual solvent concentrations, typically requiring less than a few hundred parts per million (ppm) of the types of solvents (chloroform and dichloromethane, for example) in which the component materials of our microreservoir device are soluble[11]. Injection and compression molding provide solventless fabrication methods that allow the production of a device that satisfies all of the above requirements. Lab-scale injection molding equipment was not available through MIT's facilities at the time the polymer microreservoir prototypes were developed. Therefore, compression-molding was selected as the optimal fabrication method for the substrate.

The two most important considerations for the fabrication of the reservoir membranes are reproducibility of the fabrication method, and the ability to fabricate the membranes (the formulation that controls drug release) separately from loading the device with the drug formulation (which controls the drug stability). Maximal control over device performance can be attained by limiting the number of factors that affect drug release. In the case of our device, the reservoir membranes are the feature by which the drug release is controlled. Therefore, the fabrication process for the reservoir membranes must be applicable to a variety of different materials, yet allow precise control over the characteristics of the membranes (thickness, porosity, and geometry) while providing some degree of physical separation of the membrane from the drug formulation. While other methods such as ultrasonic bonding or solvent welding could be

used to fabricate the membranes that seal the reservoirs, microinjection is a relatively straightforward and simple one-step process.

Based on these considerations, a fabrication procedure was developed that consisted of solventless two-step compression molding of the substrate, followed by microinjection of the membrane polymers in solution and subsequent drying under vacuum to form the reservoir membranes. Details of these procedures are discussed in the following sections.

2.2 Materials and Methods

2.2.1 Materials

Poly(L-lactic acid) (**PLA**, M_w 194 Kilodaltons (Kd), Medisorb® 100 L), poly(glycolic acid) (**PGA**, Medisorb® 100 PGA) and poly(D,L-lactic-*co*-glycolic acid) polymer powders of molecular weights (M_w) 4.4 Kd (**PLGA4.4**, Medisorb® 5050 DL 1A), 11 Kd (**PLGA11**, Medisorb® 5050 DL 2A), 28 Kd (**PLGA28**, Medisorb® 5050 DL 3A), and 64 Kd (**PLGA64**, Medisorb® 5050 DL 4A) were obtained from Alkermes (Cincinnati, Ohio). The properties of the polymers that were used to make the membranes on the microreservoir devices are summarized in **Table 2-1** below. Reagent grade dichloromethane (methylene chloride), 1,1,1,3,3,3-hexafluoro-2-propanol (HFIP), and HPLC grade methyl alcohol were purchased from Sigma-Aldrich (St. Louis, MO). Ethyl alcohol, 190 proof, was obtained from Pharmco (Brookfield, CT). Ideal 9144 Masking Tape was obtained from American Biltrite, Inc. (Lowell, MA).

Table 2-1 Molecular weights, copolymer mole ratios, and approximate degradation times reported by the manufacturer for the **PLGA4.4**, **PLGA11**, **PLGA28**, and **PLGA64** poly(lactic-co-glycolic acid) copolymers used to make the reservoir membranes on the microreservoir devices.

Polymer designation	**M_w**	**L:G mole ratio**	**Chain End Group**	**Degradation time *in vitro* at 37°C**
PLGA4.4	4,400	51:49	-COOH	1-2 weeks
PLGA11	11,000	53:47	-COOH	2-3 weeks
PLGA28	28,000	54:46	-COOH	3-4 weeks
PLGA64	64,000	54:46	-COOH	3-4 weeks

2.2.2 Methods

2.2.2.1 Substrate Fabrication

2.2.2.1.1 Poly(L-lactic acid) Purification

Poly(L-lactic acid) (**PLA**) as received from the manufacturer was purified and processed into a powder form. This was done for two reasons. First, it was desired to remove any residual lactide monomer (between 0.4 and 4.1% as reported by the manufacturer) in the polymer. The presence of residual lactide in the final device could affect the degradation rate of the polymer, as well as contribute to the formation of porosity. Diffusion of residual lactide from the substrate of the final device into the environment surrounding the device (saline solution *in vitro*, for example) might leave behind pores, through which the drug loaded into the device could diffuse. Second, the purification step provides a powder form of the polymer, which is more easily molded than the granules that were received from the manufacturer.

The PLA was purified by first placing approximately ten grams of the polymer in a 250 mL glass beaker, along with a magnetic stir bar and approximately 200 to 250 mL of dichloromethane. The solution was gently mixed on a magnetic stir plate until complete dissolution of the polymer was achieved. The solution was then slowly poured into approximately 1.5 L of methanol (a nonsolvent for **PLA**, but a solvent for lactide monomer) that was magnetically stirred in a 2 L beaker. The **PLA** solution was poured into this larger beaker in a slow steady stream, causing the formation of a continuous thin fiber as the **PLA** precipitated out of solution, similar to a wet fiber spinning process[12]. The fibrous mats were periodically removed from the solution using a pair of tweezers. When the methanol solution became cloudy, due to the increasing amounts of dichloromethane and lactide monomer in solution, the solution was poured out of the beaker and replaced with fresh methanol before the precipitation process was continued.

After precipitation of the **PLA** was complete, the fibers were dried under approximately 93.5% vacuum (~6.7 kPa) for at least five days in order to allow complete evaporation of the methanol. The fibers were then chilled either on dry ice, or immersed in liquid nitrogen. Fibers were placed in a Tekmar A-10 Analytical Mill attached to a Cole-Parmer Polystat refrigerated recirculator with the temperature set to 0°C, and chopped into powder.

2.2.2.1.2 Substrate Molding

Schematics showing the device fabrication procedure are shown in **Figure 2.1** and **Figure 2.2**. Device substrates were fabricated from approximately 0.38–0.4 g of purified **PLA** (T_g = 53°C, T_m = 176°C). The powder was loaded into a 15/32" (11.9 mm) inner diameter die, as shown in **Figure 2.1**, and molded in a Carver Lab Press, Type C, for one minute and 30 seconds at approximately 2,000 load pounds and 25°C. This load (pounds-force) is applied to the area of the die plunger having a diameter of 15/32" and an area of 0.1726 in^2, and therefore is commensurate with an applied pressure to the powder within the die of 11,500 psi or 80 MPa. This step produces a round white disk, or preform, similar to a tablet.

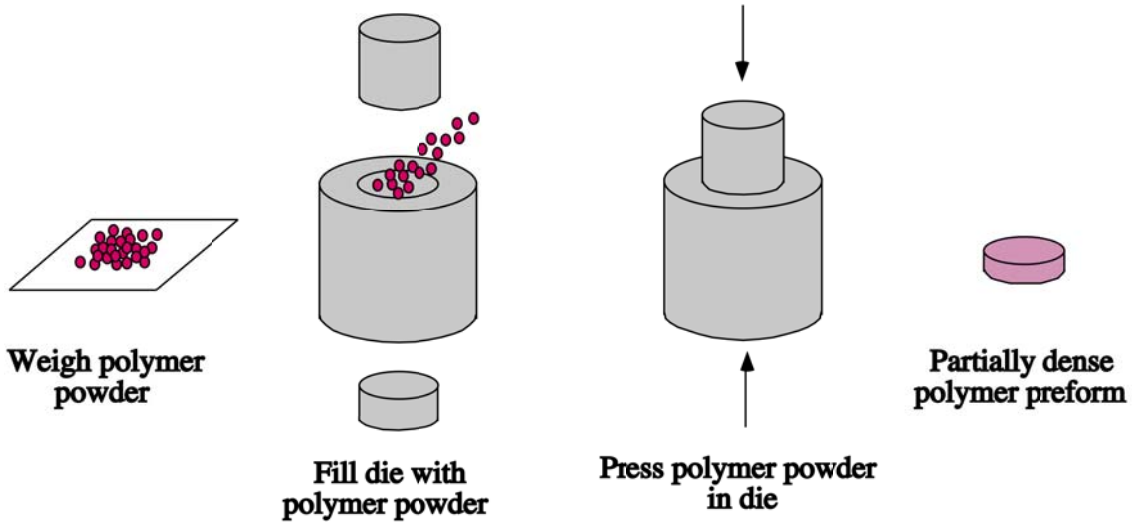

Figure 2.1 Schematic of first compression molding step at room temperature, in which the **PLA** polymer preform that will become the device substrate is formed.

Early efforts to fabricate devices included an intermediate compression step, in which the preform was molded above the T_g of the polymer between two Teflon sheets, either with or without the presence of aluminum shims. The preform is next molded at 182°C on an aluminum die plate for ten minutes to form a completely dense substrate. A pressure of approximately 2,500 pounds-force was applied to the die once the polymer preform had completely melted, after five or six minutes. The aluminum die plate was treated with (tridecafluoro-1,1,2,2-tetrahydrooctyl) trichlorosilane for eight hours at room temperature to functionalize the surface with a fluorocarbon, as shown schematically in **Figure 2.3**. This functionalization aided in release of the devices from the die plate. Surface functionalization was used instead of

application of a mold release agent (such as myristic or stearic acid) to avoid the introduction of a molecule that might adhere to or leave a residue on the surface of the device.

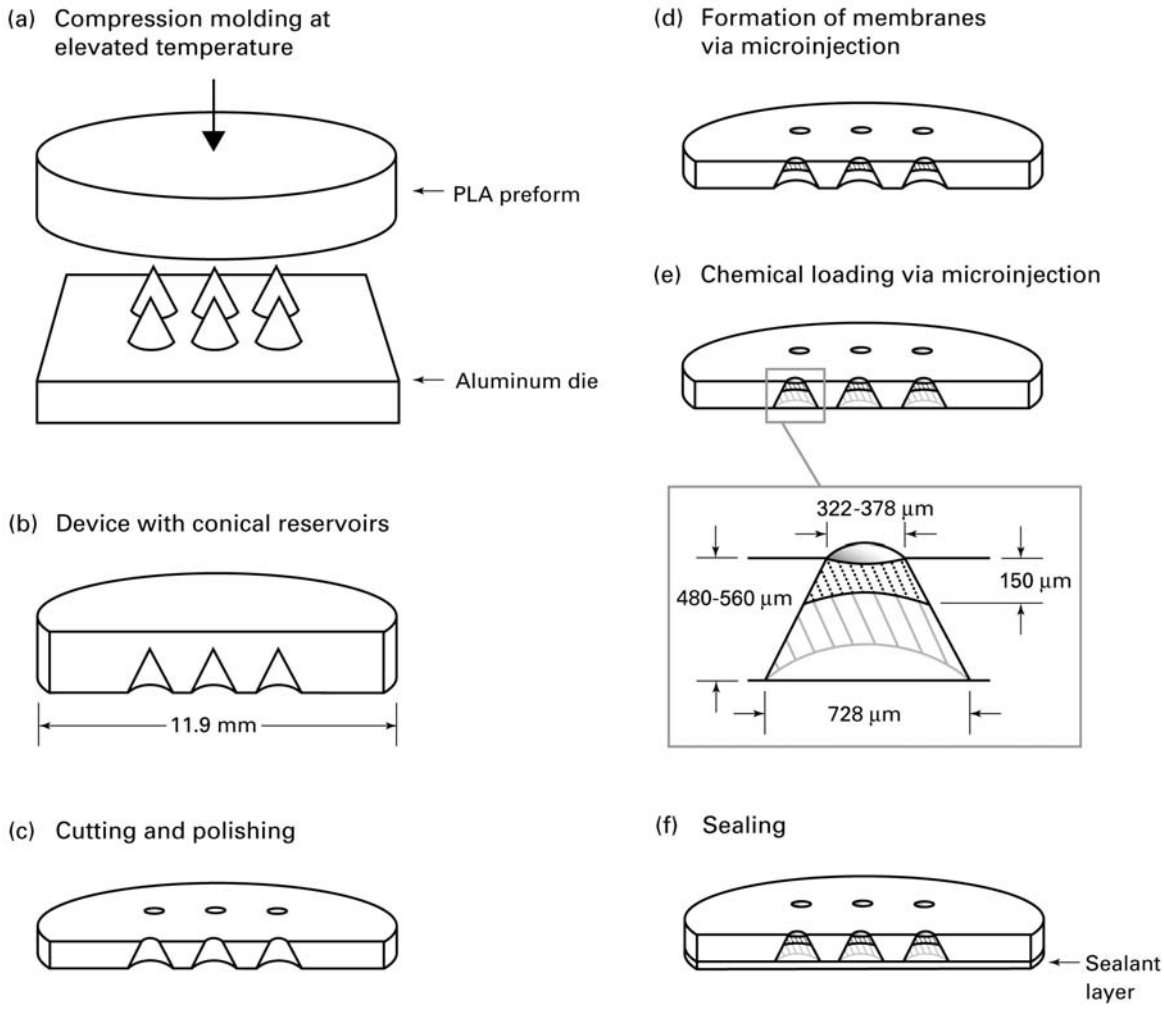

Figure 2.2 Schematic showing fabrication process for polymeric microreservoir device: (a) Second compression molding step at $T>T_g$ of the polymer, in which the conical reservoirs are formed in the polymer preform that was compression molded at 25°C by compression molding with an aluminum die having conical protrusions on it, (b) Cut-away schematic of device substrate showing partial penetration of conical reservoirs into substrate, (c) Device substrate after being polished with silicon carbide paper, showing truncation of conical reservoirs (complete penetration of reservoirs through device substrate), (d) Cut-away schematic showing reservoirs with microinjected membranes, (e) Cut-away schematic showing device after microinjection of chemical to be released. Enlargement of reservoir shows meniscus shape of reservoir membrane and typical dimensions of device features, (f) Cut-away schematic showing device after sealing with a layer of electroplating mask tape. Figure by Erica Beade.

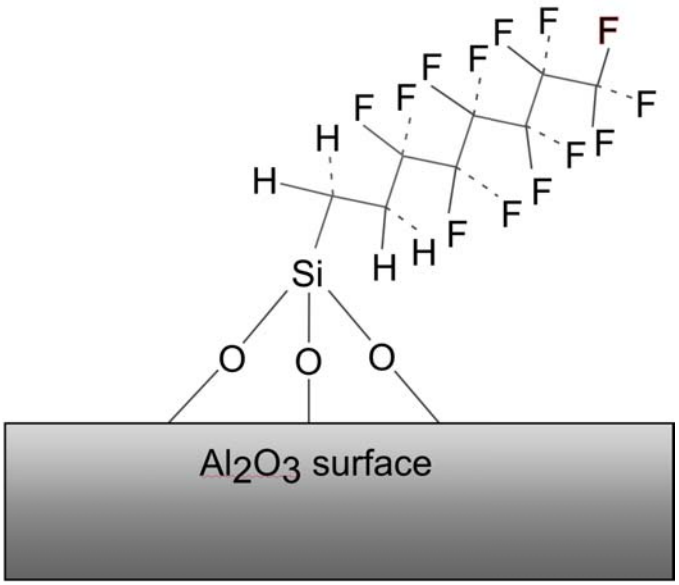

Figure 2.3 Schematic of aluminum surface treated with (tridecafluoro-1,1,2,2-tetrahydrooctyl) trichlorosilane.

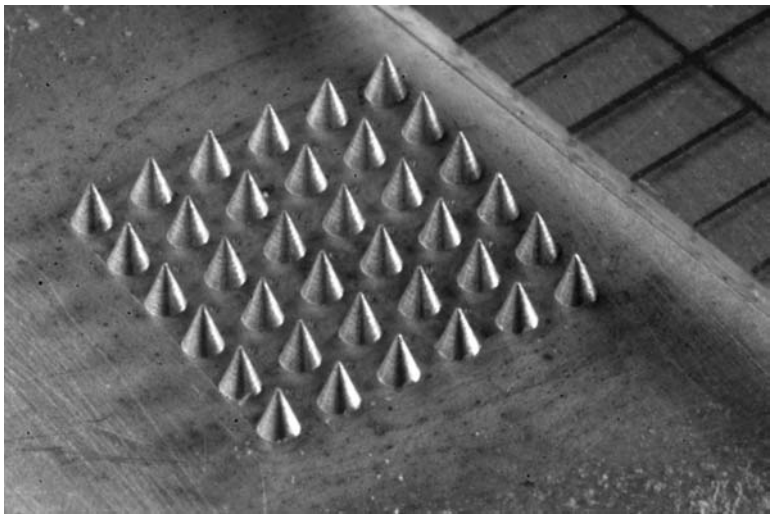

Figure 2.4 Photograph of 6 × 6 array of conical protrusions (1000 μm tall, base angle of cones = 70°) on aluminum die plate. Tick marks on ruler indicate 1/16" (~1600 μm). Photo by Richard Holman.

Conical protrusions on the aluminum die plate, shown in **Figure 2.4** above, formed reservoirs in the **PLA** substrate. The reservoirs had a diameter at the large end of the cone of 728 μm, an angle of 70°, and an approximate depth of 1000 μm. The molding setup consists of three aluminum plates. The first (base) plate has four sets of these conical protrusions. A second plate sits on top of the base plate. This second plate is 2 mm thick and has four ½" diameter holes in which the preforms are placed, and which are located directly over the arrays of conical indenters on the base plate. Finally, a third flat plate that does not have any holes or protrusions is placed on top of the whole assembly. This entire assembly, with four preforms loaded in it, is placed in

the lab press that has both platens heated to a specified temperature. A thermocouple (Omega HH21 microprocessor thermometer, J-K-T thermocouple) is placed in a small hole machined through the base plate, lying directly under the center of the plate, in order to monitor the temperature close to the performs. The conical reservoirs initially penetrated partially through the substrate.

Substrate material was removed from one side of the device, truncating the conical reservoirs and providing two openings for reservoirs, one on each side of the device. The material was removed by polishing the devices on an Ecomet IV polisher/grinder with an attached Euromet I Power Head, 50-6150 Controlled Material Removal Accessory, 60-5455 Specimen Loading Plate, and 60-5450 Maxi-Lok Chuck Assembly (Beuhler Ltd., Lake Bluff, IL). Diamond stops on the 50-6150 were set so that the thickness of the devices was reduced by approximately 1.2 mm. Samples were polished with 240 grit Carbimet paper until the diamond stops contacted the surface of the polishing wheel, typically between one minute and one minute and forty-five seconds. The diamond stops were then removed from the 50-6150, and the devices were polished for thirty seconds using 600 grit Carbimet paper, and thirty seconds using 1200 grit MicroCut paper. All polishing media were silicon carbide paper obtained from Buehler Ltd. The thickness of the devices after polishing typically ranged from 400 to 825 μm, but variation within a given batch of devices was normally less than this.

2.2.2.1.3 Visual Inspection

Devices were inspected using an Olympus BH2 optical microscope with Olympus TH3 light source (Olympus, Melville, NY). Photos were taken either with Polaroid film using an Olympus PM-10AK camera, or with a Pixera digital camera using Pixera Viewfinder software on a Dell Dimension L566cx computer. Microscopy was performed in order to check for porosity, as well as to measure the size of the reservoir openings. The reservoir opening size was then used to calculate the volume of polymer solution needed for a membrane of a specified thickness, as discussed in section 2.2.2.2.1 below.

2.2.2.1.4 Density Measurements

The densities of the devices were determined from several measurements of their weights, performed using a Mettler model AE 160 balance with Mettler 33360 Density Determination Kit.

Typically a device was dried in a desiccator attached to a Precision Vacuum Pump Model DD50 for approximately 13 minutes (experimentally determined as sufficient time for drying via periodic measurements of the change in weight), and then weighed to determine the dry weight (W_{dry}). The device was then immersed in a beaker of 90 or 100% (190 or 200 proof) ethanol and left under vacuum for another 20 minutes or until no out gassing of air from the device was observed, in order to completely saturate the device with ethanol. The device was then suspended in a beaker of ethanol (same % as was used for initial saturation) and weighed (W_{susp}). The device was blotted dry to remove any excess liquid from the surface, and finally weighed a third time to determine the saturated weight (W_{sat}). The ambient temperature was recorded in order to determine the density of the ethanol. The apparent, bulk, and relative densities, as well as the percentages of open and closed porosity, can be determined from application of the Archimedean Principle, which states that the buoyant force (F_b) on a submerged object is equal to the weight of the fluid that is displaced by the object. This can be expressed mathematically as follows:

$$F_b = \frac{W_{dry} \times \rho_{EtOH}}{\rho_{apparent}}$$

Equation 2-a

where W_{dry} = dry weight of the microreservoir device, ρ_{EtOH} is the density of ethanol at the ambient temperature, and $\rho_{apparent}$ is the apparent density of the microreservoir device. The buoyant force is related to the dry and suspended weights of the device according to the following relation:

$$F_b = W_{dry} - W_{susp}$$

Equation 2-b

Combining Equation 2-a and Equation 2-b, the apparent density can be calculated from the experimentally determined values as follows:

$$\rho_{apparent} = \frac{W_{dry} \times \rho_{EtOH}}{W_{dry} - W_{susp}}$$

Equation 2-c

Similarly, the bulk density, which is the weight per unit volume of a sample including any pore space, can be calculated as follows:

$$\rho_{bulk} = \frac{W_{dry} \times \rho_{EtOH}}{W_{sat} - W_{susp}}$$

Equation 2-d

The percentage of open porosity (P_o) is then found from the equation:

$$P_o = \left(\frac{W_{sat} - W_{dry}}{W_{sat} - W_{susp}} \right) \times 100$$

Equation 2-e

The density ($\rho_{relative}$) of the microreservoir device relative to the theoretical density ($\rho_{theoretical}$) of the polymer from which it is fabricated is found according to the relation:

$$\rho_{relative} = \left(\frac{\rho_{bulk}}{\rho_{theoretical}} \right) \times 100$$

Equation 2-f

Finally, the percentage of closed porosity (P_c) can be found via subtraction as follows:

$$P_c = 100 - \rho_{relative} - P_o$$

Equation 2-g

2.2.2.2 Reservoir Membrane Fabrication

It was desired to use a membrane fabrication process that would allow precise control over the thickness of the membranes, as well as allowing flexibility to change the membrane material if desired. Further, it was desirable for the membranes to be nonporous, as well as have a small residual solvent volume, as discussed in section 2.1.2. Microinjection meets both of these requirements.

2.2.2.2.1 Reservoir Membrane Microinjection

The accuracy of the microinjector is a function of several variables. The first is the mechanical step size that is programmed into the micro pump controller. An internal seated screw having a set number of turns (steps) rotates and thus moves the plunger of the syringe. Because the number of steps is fixed, the volume per step varies depending on the size of the syringe used. For example, a volume per step of 0.529 nL/step is used for a ten μL syringe, while 5.29 nL/step is used for a 100 μL syringe. The second factor is the solvent used. Due to the small volumes that are injected (typically from 20–150 nL), evaporation of the solvent due to the vapor pressure may cause a significant decrease in the droplet volume, and corresponding increase in the concentration of the droplet. Additionally, variation in the amount of elapsed time between injections may cause evaporation of different volumes and thus change the local concentration of the solute or chemical in the needle tip.

Membranes were prepared in the reservoirs by injection of PLGA in 1,1,1,3,3,3-hexafluoro-2-propanol solutions (12%v/v). Solutions of **PLGA4.4**, **PLGA11**, **PLGA28**, and **PLGA64** were used to make four different types of membranes in each device. Injection was performed using a system purchased from World Precision Instruments (Sarasota, FL), consisting of a UMP-1 Ultra Micro Pump with a Micro-4 controller, Kite-R micromanipulator with a TB-1 tilting base and 5464 five pound weight for the tilting base, and a PZMT Trinocular stereo microscope with 13338 Adapter Ring Light, R-8-8-WPI01 fiber optic ring light, and NOVA Novaflex fiber optic light source. Solutions were injected from a 1710RN 100 μL gas tight glass syringe with a 0160831 1" 31 gauge removable needle, blunt tip (both items from Hamilton Co., Reno, NV).

A conical shape was chosen for the reservoirs in order to aid in membrane formation. The membrane solution was injected into the side of the device having the larger diameter reservoir openings. The Young-Laplace equation offers a physical explanation for what will happen to the membrane solution once it is injected into a reservoir. For a truncated conical reservoir containing a volume of liquid that has radii of curvature R_1 and R_2, where $R_1 > R_2$ (shown schematically in **Figure 2.5** below), the Young-Laplace equation is[13]:

$$\Delta P = \gamma\left(\frac{2}{R_2} - \frac{2}{R_1}\right)$$

Equation 2-h

where ΔP = the pressure difference (proportional to the stress) between the two sides of the interface and γ = surface tension of the liquid.

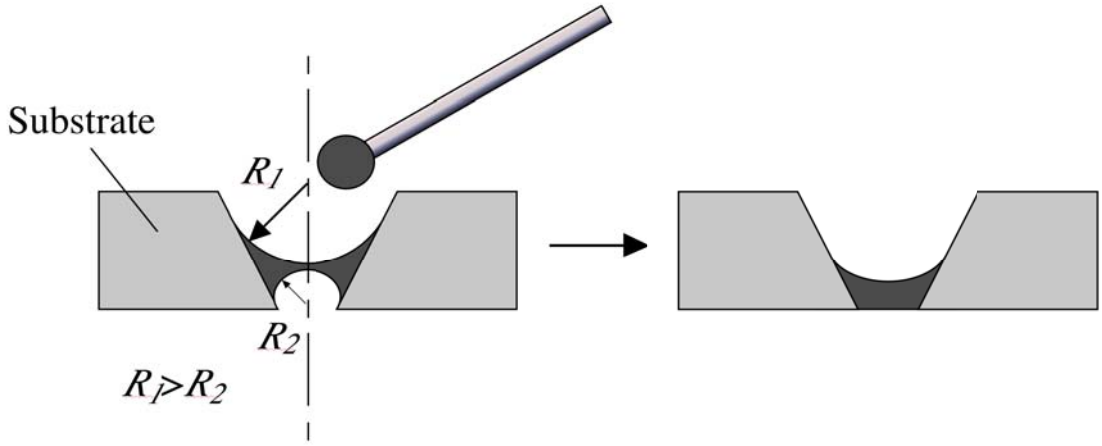

Figure 2.5 Schematic of reservoir geometry showing microinjection of membrane solution into reservoir and formation of a fluid volume having radii of curvature R_1 and R_2, and subsequent drying of the solution as capillary pressure drags the fluid volume to the small end of the reservoir.

There will be a corresponding pressure or stress that pulls the droplet in the direction of the narrow end of the reservoir, since the radius of curvature (R_2) of the liquid is smaller on that side of the droplet. Thus, capillary action will drag the membrane solution to the narrow end of the conical reservoirs, forming the membrane close to the opposite surface of the device upon drying. Wetting of the membrane solution on the reservoir walls was observed experimentally. The conical shape of the reservoirs also minimizes the area of the membrane that is exposed to the release environment. This geometry may be beneficial in helping to control the degradation of the membrane and release of the chemical, as it minimizes effects from the pressure of the fluid or mechanical disturbances to the membrane from the surrounding environment.

Reservoir membranes were typically designed to be approximately 150 μm thick in the experiments reported in this thesis. The volume of membrane solution injected into each device varied due to the slight variations in device thickness and the corresponding size of the reservoir openings. The volume of solution injected into each reservoir was calculated from the volume fraction of polymer in the solution, the specific geometry of each device, and the desired final membrane thickness. We assumed that (1) upon drying, the surface of the membrane at the small end of the cone frustum is coplanar with the surface of the device, i.e. that there is no meniscus,

(2) that the two surfaces of the membrane are parallel and flat, and (3) that the membrane is completely dense after drying. The frustum of a cone having a height (membrane thickness) h has bases with radii R_1 for the larger radius and R_2 for the smaller radius. The value of h is calculated as:

$$h = (R_1 - R_2) \times \tan A$$

Equation 2-i

where A = angle of the base of the cone = 70° for our geometry. A conical frustum with the relevant dimensions indicated is shown in **Figure 2.6** below.

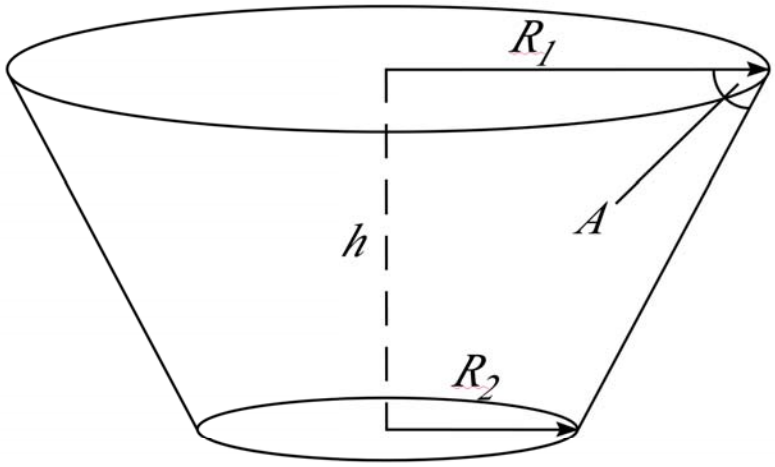

Figure 2.6 Conical frustum, taken as model geometry for reservoir membranes, having height (membrane thickness) h, base angle A, and radii R_1 and R_2.

The total volume (V) of the frustum of the cone, which is the volume of the reservoir membrane, is calculated as:

$$V = \frac{1}{3}\pi h \times \left(R_1^2 + R_2^2 + R_1 \times R_2\right)$$

Equation 2-j

The volume of membrane solution that must be injected (V_{inj}) to achieve this membrane volume and thus the desired membrane thickness is:

$$V_{inj} = \frac{V}{f_{poly}}$$

Equation 2-k

where f_{poly} is the volume fraction of polymer in the solution to be injected. Typical injected volumes ranged from 100 to 200 nL, for predicted final membrane thicknesses of 150 μm.

The devices were dried in a vacuum oven at 74–81°C and 93.5% (6.7 kPa) vacuum for approximately 48 hours after microinjection of the membrane solutions. Devices were suspended on glass slides so that the truncated ends of the reservoirs in which the membranes were located faced the bottom of the vacuum oven, but were not touching the surface of the oven. Typically no sagging of the membrane (membrane bulging out from the surface of the device) was observed after the membranes were dried. The membranes were inspected for defects after drying (such as air bubbles and pinholes) at 80X magnification using a PZMT Trinocular stereo microscope with 13338 Adapter Ring Light, R-8-8-WPI01 fiber optic ring light, and NOVA Novaflex fiber optic light source. Reservoirs having defect-free membranes were considered viable for use in release experiments, and selected reservoirs were loaded with the chemical(s) to be released.

2.2.2.2.2 Near-Infrared Characterization of Membranes

It is desirable to ensure that significant mixing between the reservoir membrane polymer and the substrate polymer does not occur during the microinjection process. In the case of the materials used in our prototype devices, poly(lactic acid) (**PLA**) and poly(lactic-co-glycolic acid) (**PLGA**), the degradation rates of these polymers are a function of both copolymer ratio (polymers having a higher ratio of **PLA** have slower degradation rates), as well as molecular weight (higher molecular weight polymers have longer degradation times, see Chapter 5 for a more thorough discussion). The substrate polymer not only is pure **PLA**, but also has a higher molecular weight than the membrane polymers. Both of these factors could lead to a decrease in the degradation rates of the reservoir membranes. Further, the solvent that is used to make the membrane polymer solutions (1,1,1,3,3,3-hexafluoro-2-propanol) is also a solvent for the

substrate polymer (**PLA**). While use of a co-solvent will allow a small amount of beneficial mixing between the membrane and substrate polymers and therefore ensure that the reservoir is completely sealed, significant mixing would be highly undesirable.

Near-infrared (NIR) spectroscopy was used to characterize a representative microreservoir device in order to determine if significant mixing of the membrane and substrate polymers occurred during membrane microinjection. Near-infrared chemical imaging data was obtained with MatrixNIR (Spectral Dimensions, Inc., Olney, MD). The imaging system used in this study consists of a reflectance illumination source, a Liquid Crystal Tunable Filter (LCTF) for wavelength selection, collection and focusing optics, and an NIR sensitive Focal Plane Array (FPA). The focal plane array is a 320 × 240 pixel Indium Gallium Arsenide (InGaAs) array. Each pixel on the array corresponds to ~ 2.5 × 2.5 μm on the sample, providing a field of view (FOV) of approximately 0.8 × 0.6 mm.

The sample was illuminated in reflectance mode with four quartz tungsten halogen (QTH) sources. The diffuse reflected NIR energy was collected by a 15X Cassegrain objective, passed through the LCTF, and focused onto the FPA. The LCTF was tuned across the spectral range of interest, and images were recorded from the FPA at each selected wavelength. The LCTF had a 6 nm bandpass over the spectral range of interest.

The MatrixNIR instrument was controlled with data acquisition software, MatrixAcquire V 0.5.10 (Spectral Dimensions, Inc., Olney, MD). Data was collected over the spectral range 1100 ~ 1700 nm, at 10 nm increments. Sixteen frames were co-added at each wavelength step, and for each data set, two complete scans were co-added. Complete background data sets were also recorded on a Spectralon (SRS-99-010, Labsphere Inc., North Sutton, NH), an NIR reflectance standard. The data was analyzed with Isys V 2.0.0 (Spectral Dimensions, Inc., Olney, MD).

The raw sample data cubes were divided by spectralon data sets to eliminate the instrument response function, and then converted to standard reflectance units, log (1/R), by taking the inverse logarithm. The data was then analyzed using a multivariate method, Partial Least Squares (PLS) type II analysis[14], which is commonly used in chemometric analyses. Pure component spectra were taken from samples of pure poly(lactic acid) (**PLA**) powder molded at room temperature, and at room temperature and subsequently at 182°C, and poly (glycolic acid) (**PGA**) microinjected onto Mylar film, and **PGA** cast on and then removed from Mylar film

(freestanding film). These reference samples were selected because they mimic the processing conditions that the **PLA** and **PGA** components of the microreservoir device are exposed to during fabrication. Spectra from both of the **PLA** reference samples were similar, as were spectra from both of the **PGA** reference samples. Reference spectra from the **PLA** sample molded at room temperature and 182°C, and from the **PGA** freestanding film, were used to build a library, which was then used to analyze the sample data sets. The resulting PLS scores are correlated with the amounts of each component (**PLA** or **PGA**) that are present at a given location in the sample[15]. The PLS score images showed the relative concentrations of the library components. These scores were plotted as a function of the location on the sample.

2.2.2.2.3 Residual Solvent Determination

Membrane polymer samples were analyzed on a PerkinElmer Thermogravimetric Analyzer (model TGA7) to determine the residual solvent after experiencing similar processing conditions as those that reservoir membranes on a device are exposed to. Empty platinum TGA pans were filled with one of four solutions, having between 11.7 and 12.1% by volume of **PLGA4.4**, **PLGA11**, **PLGA28**, or **PLGA64** in 1,1,1,3,3,3-hexafluoro-2-propanol. The pans were dried under approximately 90% house vacuum for 48 hours at 77°C, and then sequentially run on a PerkinElmer TGA7 using nitrogen purge gas. The heating program is summarized in **Table 2-2** below. The residual solvent was determined as the percentage of weight lost over a temperature range (30–100°C) that encompasses the boiling temperature of 1,1,1,3,3,3-hexafluoro-2-propanol (58°C).

Table 2-2 Experimental parameters for TGA analysis of membrane polymers.

Condition	Starting Temperature (°C)	Ending Temperature (°C)	Rate (°C/min)	Time (min:sec)
Isothermal	30	30		3:00
Ramp	30	900	15	60:00
End		30		

2.3 Results and Discussion

2.3.1 Substrate Fabrication

2.3.1.1 Visual Inspection

Devices formed cohesive tablets after the initial compression-molding step at room temperature. The mechanical strength of the devices was such that no breakage or crumbling of the devices occurred during normal manipulation with tweezers or by hand. A photograph of a representative device (preform) at this point of the fabrication process is shown in **Figure 2.7** below.

Figure 2.7 Photograph of **PLA** preform after compression molding of polymer powder in 15/32" cylindrical die at 11,500 psi for one minute and thirty seconds at room temperature. Photo by Richard Holman.

A variety of molding temperatures, pressures, and times were tried in an attempt to optimize the experimental parameters for the second compression-molding step. Representative samples from some batches are discussed here. Early prototypes were fabricated with P-L-LGA (M_w 36,000, T_g 38°C) and had an intermediate hot compression molding step on Teflon sheets. These devices had insignificant pressure applied during the hot compression molding step on the aluminum die plate, and they showed porosity no matter what the temperature at which they were molded.

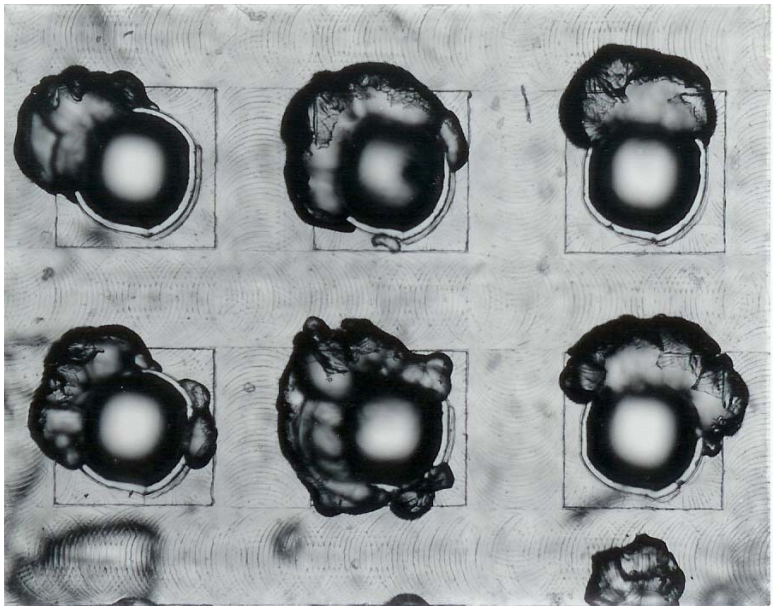

Figure 2.8 Optical microscopy photograph at 37.5X of device 070799-03 (hot compression molded at 66°C), showing six conical reservoirs with entrapped air bubbles (pores) localized around the reservoirs.

Figure 2.8, for example, shows a device that was compression molded on the aluminum plate at approximately 66°C, while **Figure 2.9** shows a device molded at 82°C, and **Figure 2.10** shows a device molded at 99°C.

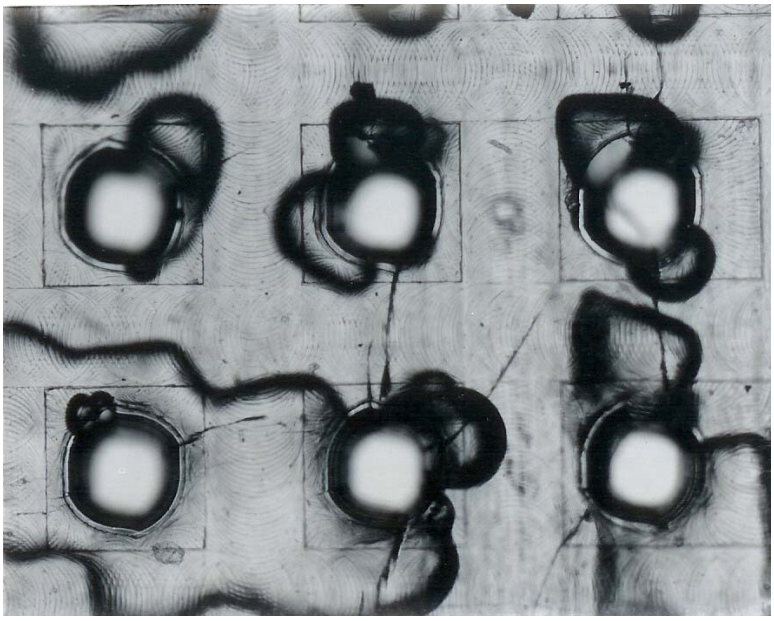

Figure 2.9 Optical microscopy photograph at 37.5X of device 070799-06 (hot compression-molded at 82°C), showing six conical reservoirs and air bubbles localized near reservoirs and spreading between reservoirs.

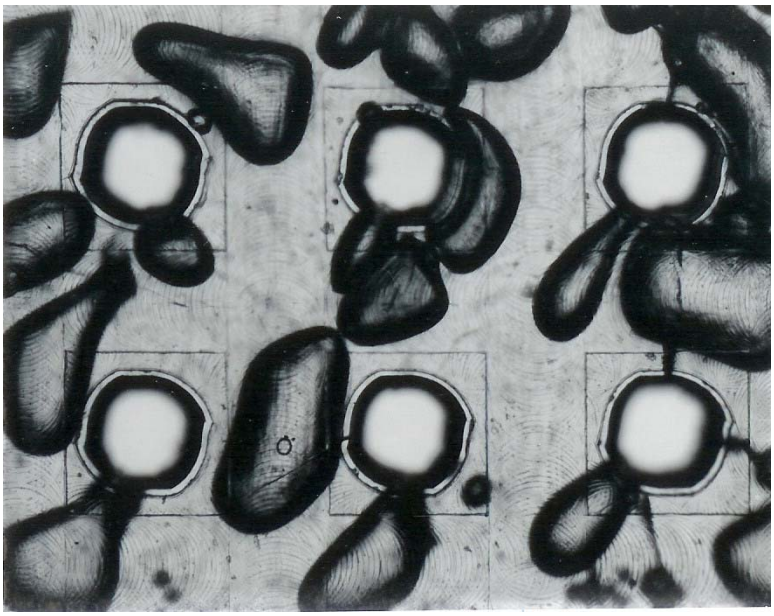

Figure 2.10 Optical microscopy photograph at 37.5X of device 070799-09 (hot compression-molded at 99°C) showing six reservoirs with distributed porosity throughout the device substrate.

It is clear from the photographs above that significant porosity was evident at all of the molding temperatures investigated in this particular batch of devices. The application of pressure during the molding process was found to drastically reduce the amount of porosity in the devices. Further, better results were obtained when the polymer was allowed to nearly completely melt before the load pressure was applied. One explanation for this might be that application of pressure to the die while the polymer was still solid actually nucleated air bubbles at the sites of the conical protrusions on the aluminum die as the preform was pressed onto the surface. When the polymer later melted, these air bubbles could have become entrapped in the polymer matrix. If no additional load pressure were applied, there would be no driving force, other than surface tension, to eliminate the air bubbles. However, if the order of processes were reversed (heating followed by the application of pressure), application of load pressure after the polymer had already melted would force the air bubbles through the liquid matrix and out to the surface of the device.

It was also observed that at short times, the visible porosity decreased as the length of time under load increased. However, after a certain point it was found that additional time under load did not appear to have any effect on eliminating the few remaining air bubbles. Devices were typically completely transparent and showed only a few air bubbles after being

compression molded at 182°C for 10 minutes and 2,500 load pounds. Sample devices having no visible porosity near the reservoirs are shown in **Figure 2.11** to **Figure 2.13**.

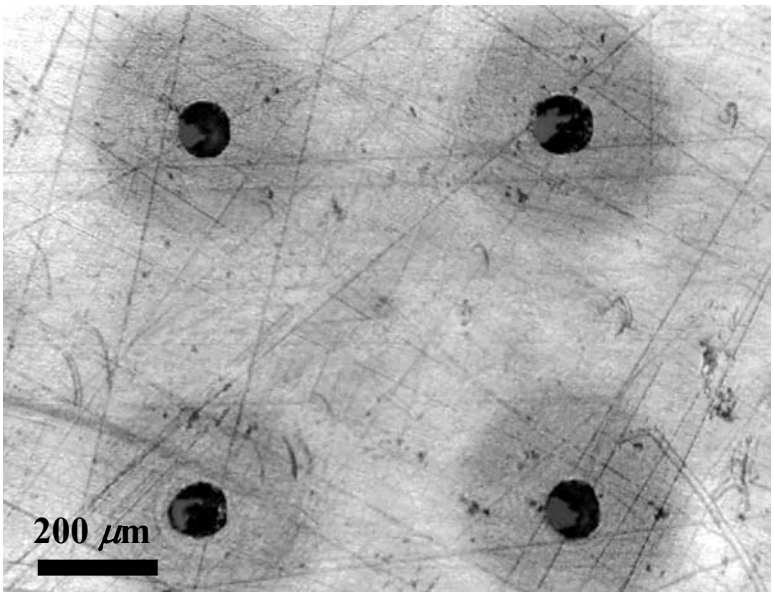

Figure 2.11 Optical microscopy photograph of device 123102-01 showing four reservoirs after polishing step. Dark regions in reservoir openings are polymer debris from polishing (removed before membrane microinjection). Lines on device surface are polishing artifacts.

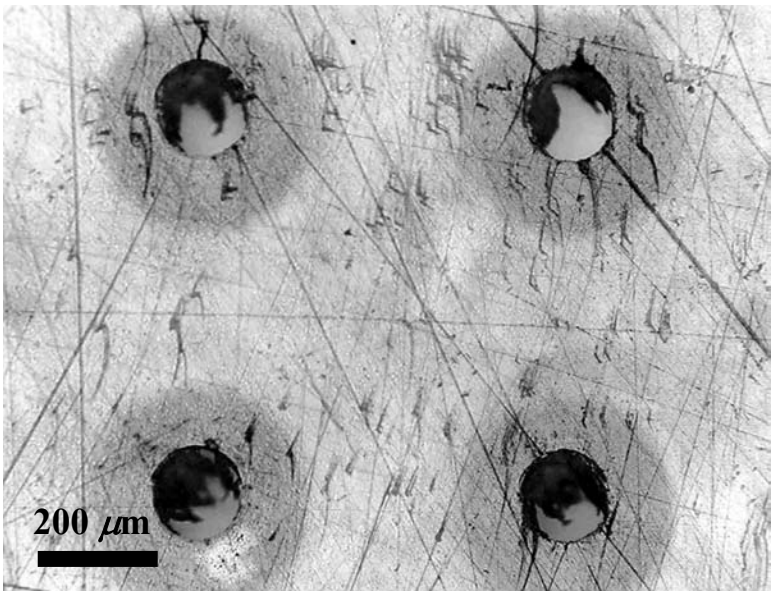

Figure 2.12 Optical microscopy photograph of device 123102-02 showing four reservoirs after polishing step. Dark regions in reservoir openings are polymer debris from polishing (removed before membrane microinjection). Lines on device surface are polishing artifacts.

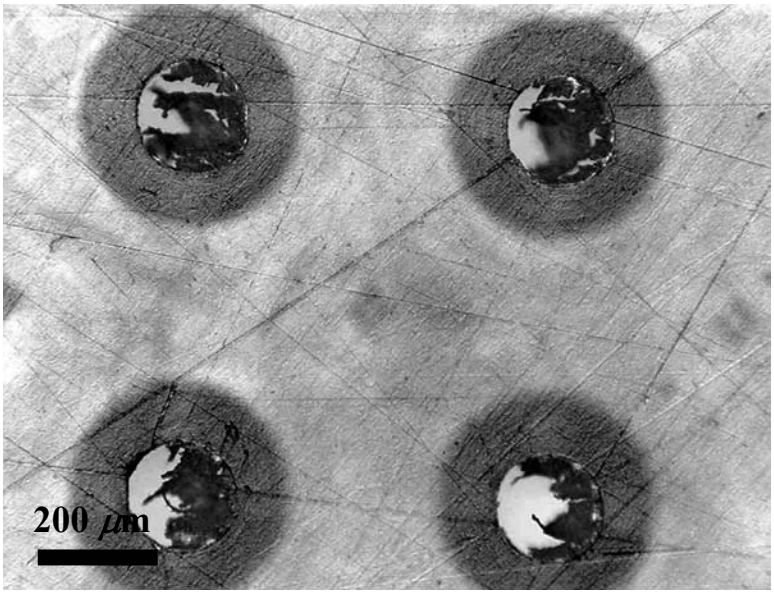

Figure 2.13 Optical microscopy photograph of device 123102-03 showing four reservoirs after polishing step. Dark regions in reservoir openings are polymer debris from polishing (removed before membrane microinjection). Lines on device surface are polishing artifacts.

Some variation in final device thickness was typical due to the variability in the polishing process. Diamond stops are used during the first polishing step, in which the coarsest polishing paper (240 grit) is used, but the stops are removed prior to polishing with the finer grits of paper (600 and 1200 grit) in subsequent steps. Load pressure was typically maintained at 14 pounds-force, but slight variations in device placement or pressure can affect how much material is removed from the surface of the devices. This, in turn, can affect the final thickness of a device and the size of the reservoir openings, as can be seen in a comparison of **Figure 2.11**, **Figure 2.12**, and **Figure 2.13**. One batch of devices, for example, had reservoir openings (small end of truncated conical reservoirs) that ranged from 170 to 385 μm in diameter, as measured by optical microscopy. The variation in reservoir diameters was minimized as much as possible when selecting devices from a given device batch for release studies. One representative batch of devices used for a release study had a ±40 μm variation in reservoir diameters, for example. As discussed in section 2.2.2.2.1, however (see Equations i-k), the volume of membrane solution that was injected into each reservoir was calculated based on the reservoir opening size and volume fraction of polymer in solution in order to give approximately the same desired membrane thickness for all devices, regardless of the size of the reservoir openings. No significant variation in release time due to variation in reservoir opening size was seen in the *in*

vitro release studies presented in Chapter 4. A photograph of a sample device after polishing is shown in **Figure 2.14**.

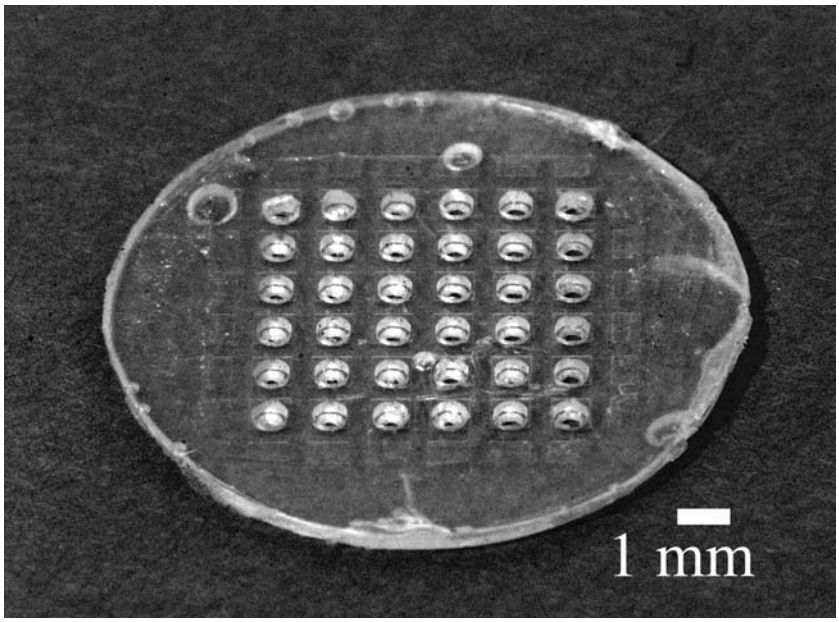

Figure 2.14 Photograph of prototype device after polishing, showing 6 × 6 array of truncated conical reservoirs. Photo by Richard Holman.

Optical microscopy of devices was used to determine which reservoirs were suitable for microinjection of membranes. Reservoirs that had air bubbles near or connected to them were deemed unsuitable for microinjection due to the possibility of nonuniform dissolution of the substrate material and consequent deformities in the reservoir membranes. Typical yield of usable reservoirs on a given device ranged from 70 to 100%, with 80–90% being more common.

2.3.1.2 Density Measurements

Density measurements were performed on early prototype devices fabricated from **PLGA** 65:35. Devices that had visible porosity (such as those in **Figure 2.8**, **Figure 2.9**, and **Figure 2.10**) typically had calculated relative densities of 94–99%. Open porosities ranged from 0.4–3.9%, and closed porosities from 0.02–1.7%. Density measurements were also performed on the **PLA** devices shown in **Figure 2.11** to **Figure 2.13**. These devices had a few air bubbles at their edges, as well as localized near a few reservoirs. The calculated relative densities, however, were much higher than for the PLGA devices that had visible porosity. Typical relative densities of 99–100% were measured, with open porosity values of 0–0.50%, and closed porosity of 0–0.92%. These devices were similar in appearance to many others that were fabricated and thus

these results can be considered representative. While the devices were not completely dense, the most important consideration is that typically very little porosity was seen in the regions surrounding the reservoirs, yielding a high percentage of usable reservoirs as discussed in 2.3.1.1.

2.3.2 Reservoir Membrane Fabrication

2.3.2.1 Reservoir Membrane Microinjection

Reservoir membranes were inspected using optical microscopy after they had been completely dried. Both sides of the membranes were inspected for defects such as air bubbles, pinholes, or surface irregularities such as wrinkles or dimples. Membranes that exhibited any of these features were considered unusable, as the degradation behavior and membrane opening times might be affected. SEM analysis of some device membranes was performed. An example membrane is shown in **Figure 2.15** below.

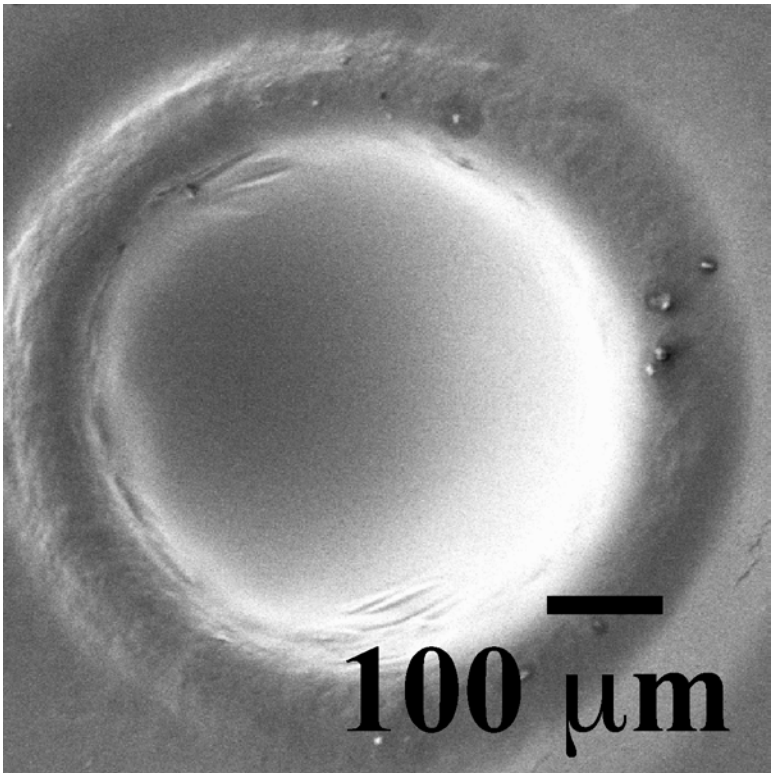

Figure 2.15 SEM of **PLGA64** reservoir membrane on **PLA** device. Photograph taken of front side of membrane that is exposed to release environment, opposite the side of the reservoir into which the membrane solution was microinjected.

As can be seen in **Figure 2.15**, the surface of the membrane on the side of the device that is exposed to the release environment (opposite to the side of the device that was microinjected)

is concave rather than planar, as was assumed in our calculations of the volume of membrane solution required to form a membrane of a desired thickness (see section 2.2.2.2.1 above). This was observed for most of the devices that were used for release studies, but attempts to cryomicrotome the devices in order to gain a better understanding of the membrane geometry were unsuccessful. The simplifying assumptions used in the calculations of membrane solution volume (see 2.2.2.2.1) were therefore left unchanged.

Membrane yield varied widely, depending on the size of the reservoir openings and the polymers from which the membranes were fabricated. The membrane solutions often did not form a cohesive structure in reservoirs that had very large openings (greater than ~375 μm at the small end of the reservoir), possibly due to rapid wetting of the large surface area. Additionally, although the membrane solutions typically had similar volume fractions of polymer regardless of the polymer that was used, it was found that the higher molecular weight polymers (**PLGA64** and **PLGA28**) produced more viscous solutions. These solutions sometimes did not completely wet the reservoir, as the high viscosity prevented the solution from coating the reservoir before the solvent evaporated. Additionally, the high viscosity at times prevented entrapped air bubbles from coalescing and bursting at the membrane surface, resulting in entrapped air bubbles within the reservoir membranes. On the other hand, the low viscosity (low molecular weight) solutions sometimes wetted the surface of the reservoir rapidly and broke in the center, and did not form a cohesive structure. Entrapped air bubbles, however, were not often seen in membranes made from the lower molecular weight polymers (specifically the **PLGA4.4**).

2.3.2.2 Near-Infrared Characterization of Membranes

A device was analyzed using near-IR spectroscopy to determine whether the membrane material (**PLGA**) blended with the substrate material (**PLA**) during membrane fabrication. It was desired to determine whether microinjection of the membrane polymer in a co-solvent for the membrane and substrate polymers caused mixing of the two polymers in the central region of the membrane during fabrication of the membranes. This mixing might affect the degradation time of the membrane and thus perhaps the release time of the chemicals from the reservoir. The substrate was fabricated from **PLA** and the membranes from **PGA,** instead of the **PLGA** copolymers used in the devices for the release studies, for maximum contrast in the spectra of the membrane and the substrate of the device. Pure component spectra were taken from a **PLA**

substrate that was fabricated in the same fashion as the sample device, and a pure **PGA** film. Spectra taken from the surface of the **PLA** sample device and the center of the **PGA** membrane on the sample device were identical to the **PLA** and **PGA** reference spectra.

The partial least squares (PLS) scores measure the correlation of the sample spectra with the reference spectra and indicate the relative contribution of each material (PLA and PGA) to the overall composition of the sample at a given location. The PLS scores obtained during the IR membrane characterization are shown in **Figure 2.16** and **Figure 2.17**. As is expected, the spectra obtained from the membrane region show a high correlation with the **PGA** reference spectra (**Figure 2.16**), while the spectra obtained from the substrate of the device show a high correlation with the **PLA** reference spectra (**Figure 2.17**), as indicated by the high PLS scaled score values.

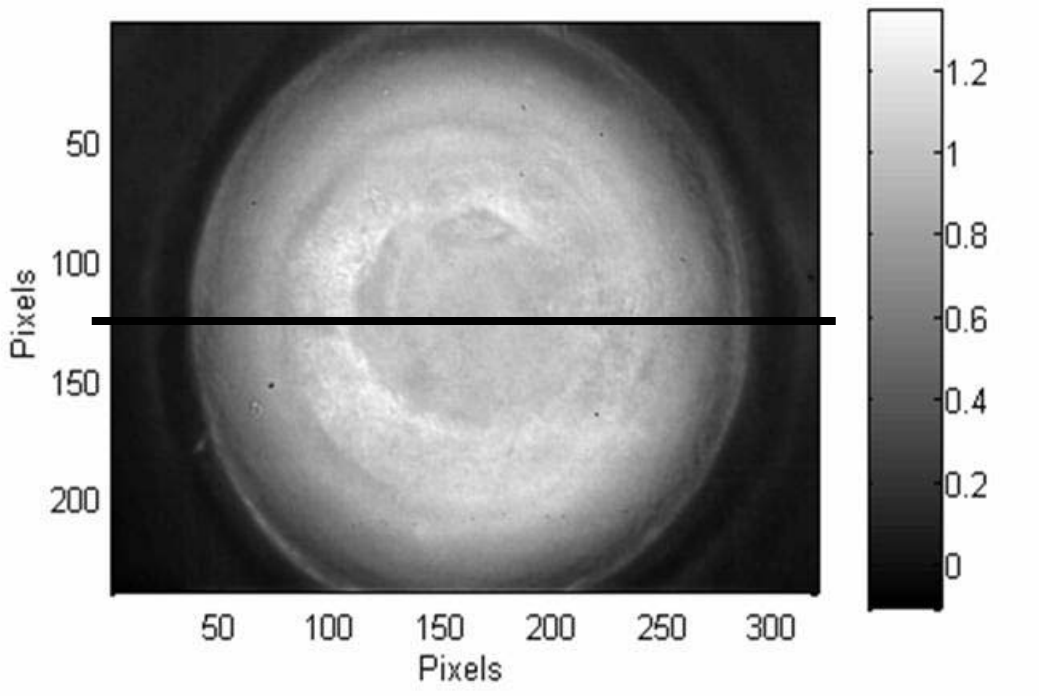

Figure 2.16 Near-infrared characterization of **PGA** membrane on **PLA** device. Image of reservoir with **PGA** membrane, showing PLS Score of **PGA** ranging from zero on the substrate of the device to one in the membrane region. Horizontal line indicates row 120, from which the PLS Scores are plotted in **Figure 2.18** along with PLS Score from **PLA** characterization shown in **Figure 2.17**.

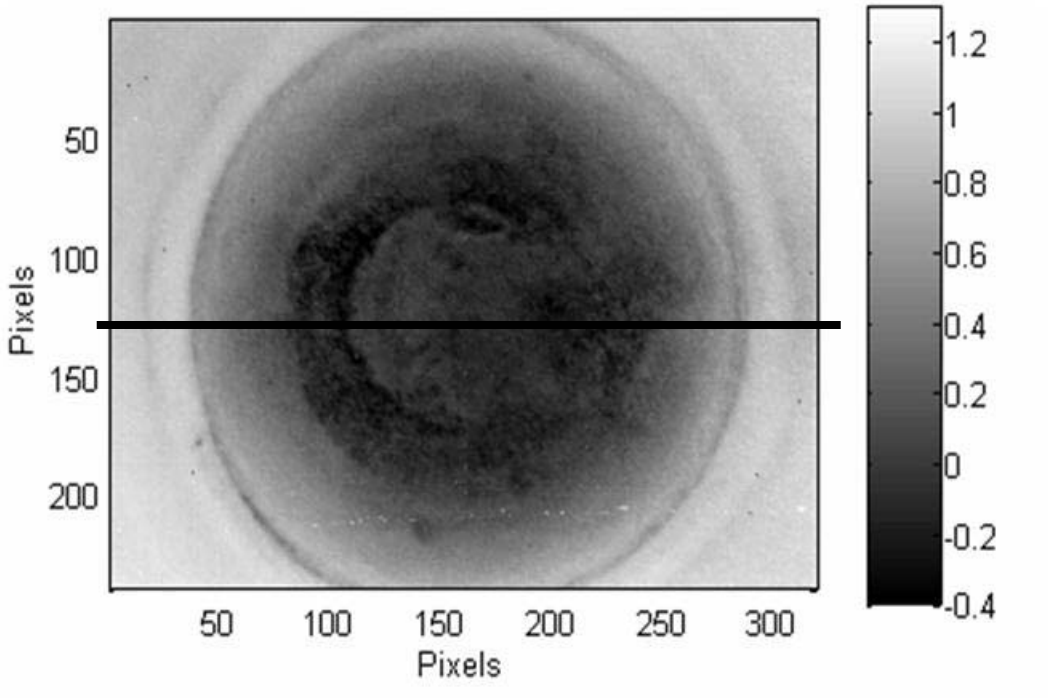

.

Figure 2.17 Near-infrared characterization of **PGA** membrane on **PLA** device. Image of reservoir with **PGA** membrane, showing PLS Score of **PLA** ranging from close to one on the substrate of the device to zero in the membrane region. Horizontal line indicates row 120, from which the PLS Scores are plotted in **Figure 2.18** along with PLS Score from **PGA** characterization shown in **Figure 2.16**.

Figure 2.18 shows a one-dimensional projection of the PLS scores along the horizontal centerlines (row 120) indicated in **Figure 2.16** and **Figure 2.17**. The **PLA** and **PGA** signals appear quite different in both the membrane region and the device substrate region, at the extreme edges of graph. The **PLA** and **PGA** signals also vary linearly in the taper region, which is the region in which the sidewall of the reservoir is at a 70° angle to the device surface. This result is expected, as the spectra that are collected in this region are due to the infrared radiation as is passes through both the substrate and the underlying reservoir region with **PGA**, as shown schematically in **Figure 2.19** below.

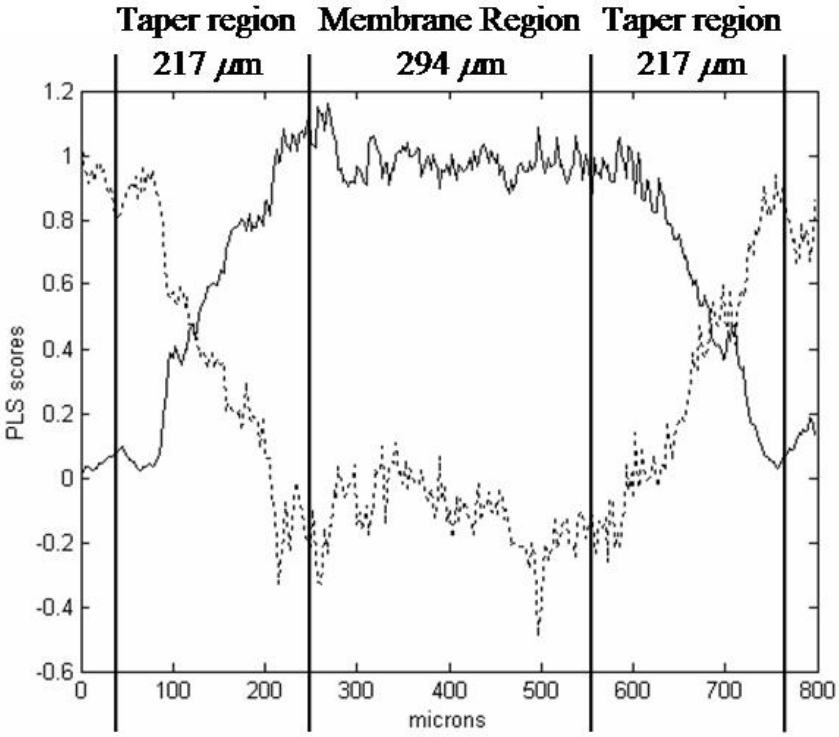

Figure 2.18 1-D projection of PLS Image Scores along horizontal axis at vertical center, row 120. Solid line indicates **PGA** score and dotted line indicates **PLA** score.

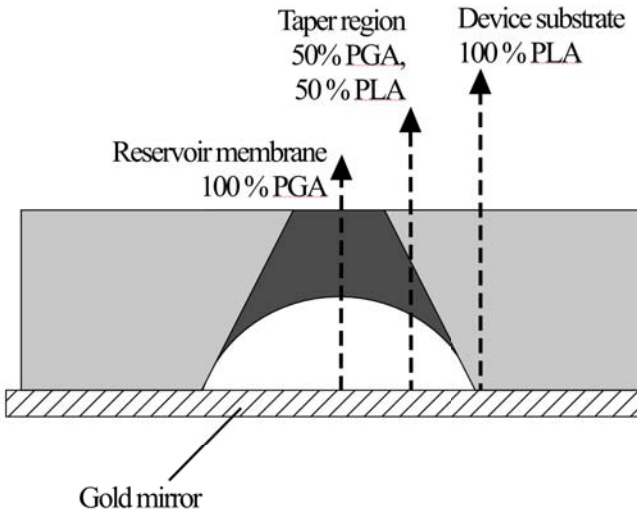

Figure 2.19 Schematic of experimental geometry used for collection of near-infrared spectra, showing device resting on gold mirror, and diffuse reflectance of quartz tungsten halogen illumination through the device thickness. In the substrate region of the device, the infrared signal that is collected is due solely to the substrate (**PLA**), while in the center of the reservoir membrane the signal will be due solely to the membrane (**PGA**). In the taper region of the reservoir, however, the detected signal is due to both the membrane and the substrate regions through which the illumination passes. In the idealized schematic, for example, the signal will be 50% **PGA** and 50% **PLA** spectra, as the linear thicknesses of the **PGA** and **PLA** regions through which the illumination passes are equal.

These results suggest that no significant mixing of the membrane polymer with **PLA** from the substrate occurred in the central region of the reservoir membrane during the fabrication of the membranes. This supports the hypothesis that the degradation time or opening of the membrane and the subsequent release of the chemicals from the reservoirs are not a function of mixing of the substrate and membrane materials.

2.3.2.3 Residual Solvent Determination

Microinjected reservoir membranes on polymeric devices were not used for this experiment, as the amount of polymer that is typically injected into a reservoir is too small to show a significant change in mass due to residual solvent evaporation. Typically 100–150 nL of a membrane polymer solution is injected into a reservoir on a device. For conditions of 12% volume fraction of polymer in the solution, and an approximate polymer density of 1.3 g/mL, this corresponds to a mass of 23.4 μg of polymer in a reservoir. If the residual solvent were 1% by weight (10,000 ppm), this would correspond to a mass change of 0.234 μg when the solvent was vaporized, which is not considerably larger than the microbalance sensitivity of 0.1 μg for the TGA that was used. Additionally, the TGA manufacturer recommends using samples 40–50 mg in size for residual solvent measurements. Therefore, larger membrane polymer masses than would be present in a microinjected device were used for these studies.

Sample sizes (polymer + solvent) ranged from approximately 14 to 30 mg, and the polymer samples were approximately 1–2 mm thick. The decomposition curves from 30 to 850°C for each material are shown in **Figure 2.20**. Although the decomposition of the polymers is clearly evident as a large decrease in the sample weight, there is no noticeable change in sample weight at 58°C, the boiling temperature of the HFIP. These preliminary results suggest that the amount of residual HFIP in the polymer samples is quite small.

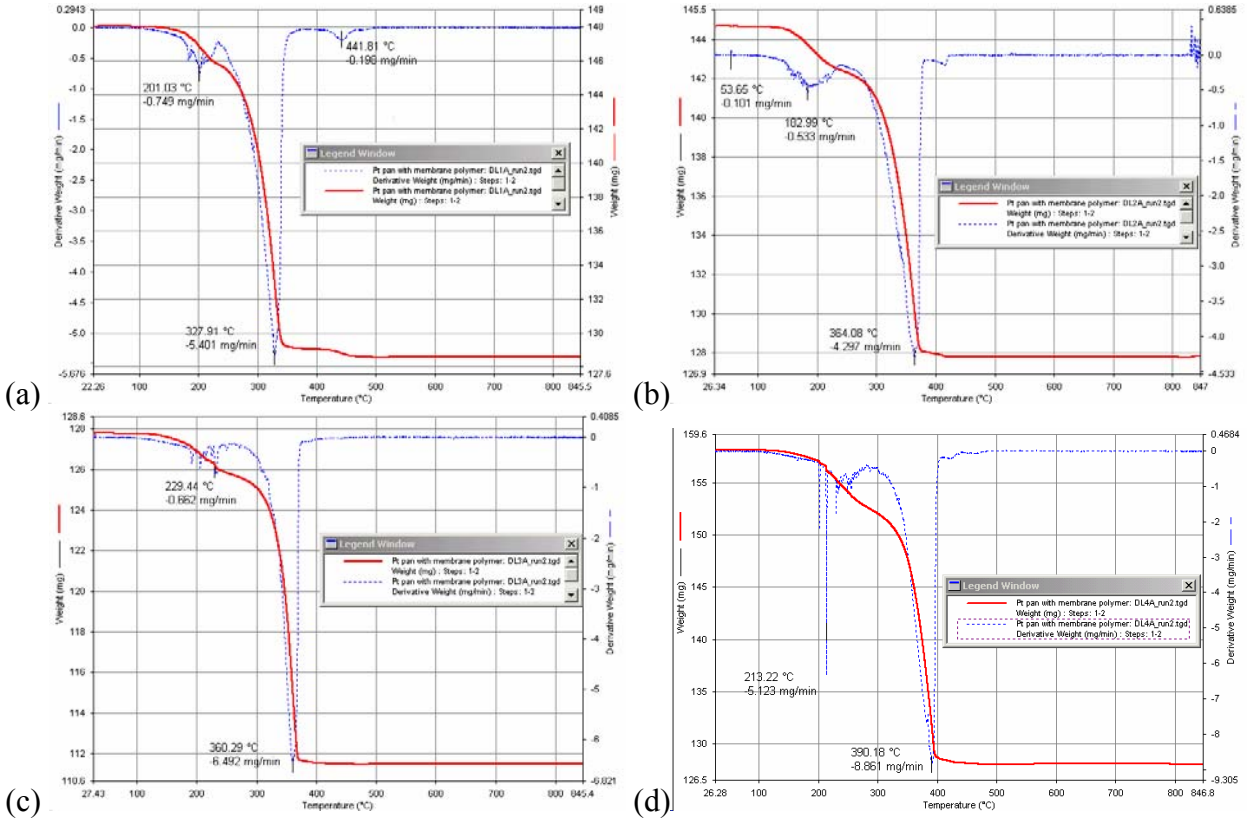

Figure 2.20 TGA decomposition curves from 30–850°C for (a) 19.463 mg of **PLGA4.4**, (b) 16.902 mg of **PLGA11**, (c) 16.301 mg of **PLGA28**, (d) 30.086 mg of **PLGA64** in platinum pans. Solid lines indicate the weights of the samples, dotted lines indicate the derivative weights (mg/min) of the samples.

More quantitative results were obtained upon closer inspection of the curves. Enlarged views of the decomposition curves from 30 to 260°C are shown in **Figure 2.21**. The mass of solvent lost was calculated as the change in weight as the temperature was increased from 30 to 100°C. The results are summarized in **Table 2-3** below.

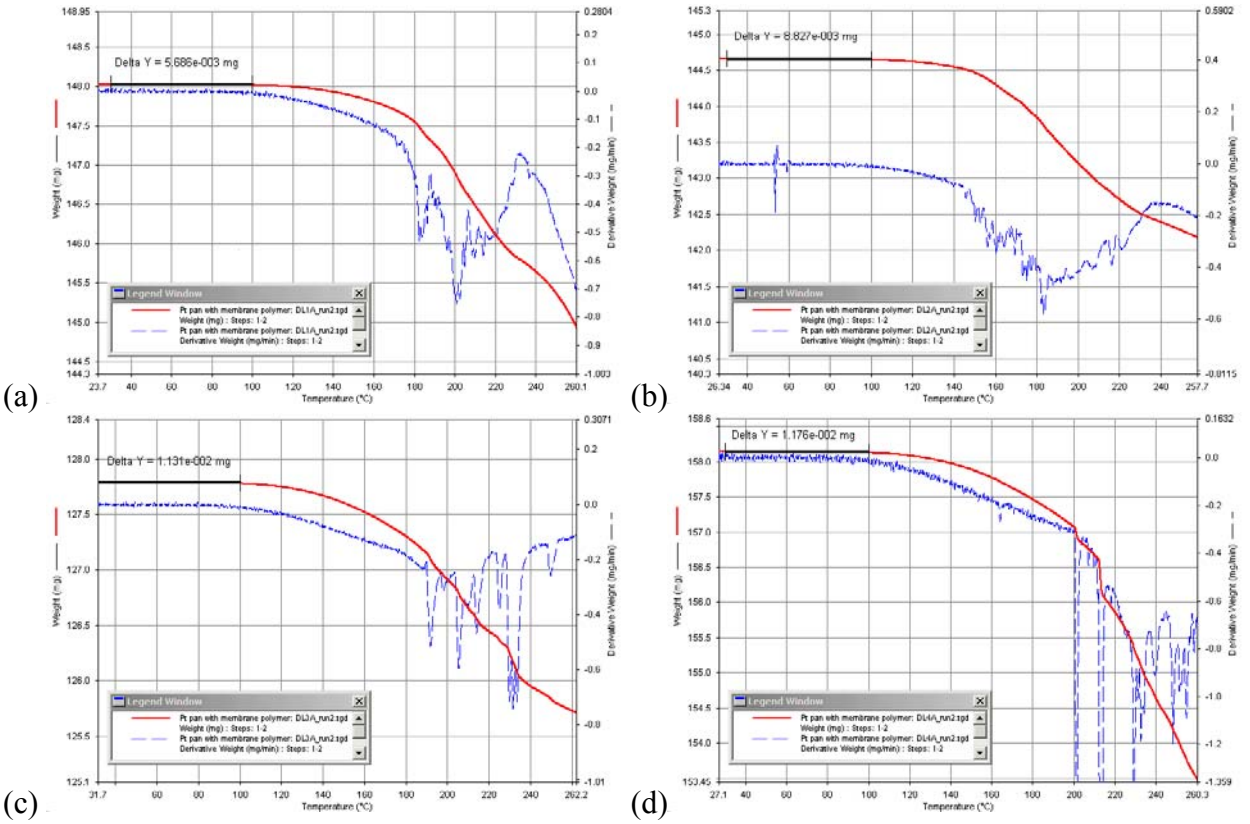

Figure 2.21 TGA decomposition curves from 30–260°C and weight losses from 30 to 100°C for (a) **PLGA4.4**, (b) **PLGA11**, (c) **PLGA28**, and (d) **PLGA64**. Solid lines indicate weights of samples, dashed lines indicate derivative weights (mg/min) of samples.

Table 2-3 Residual solvent in **PLGA4.4**, **PLGA11**, **PLGA28**, and **PLGA64** polymers after drying for 48 hours at 77°C. Solvent determined as weight change from 30 to 100°C.

Polymer	Initial Weight (mg)	Δ weight from 30–100°C (mg)	Solvent weight (%)	Solvent weight (ppm)
PLGA4.4	19.463	5.686×10^{-3}	2.92×10^{-2}	292
PLGA11	16.902	8.827×10^{-3}	5.22×10^{-2}	522
PLGA28	16.301	1.131×10^{-2}	6.94×10^{-2}	694
PLGA64	30.086	1.176×10^{-2}	3.91×10^{-2}	391

Overall, the measured quantities of residual solvent over the specified time period and temperature range are quite low. However, it is well known that some polymers will retain solvent for long periods of time. A more extended TGA study was therefore performed on one of the membrane polymer materials (**PLGA11**) to more accurately determine the residual solvent content. This sample had a mass of 14.08 mg and was held at 80°C for 22 hours. The TGA results are shown in **Figure 2.22** below.

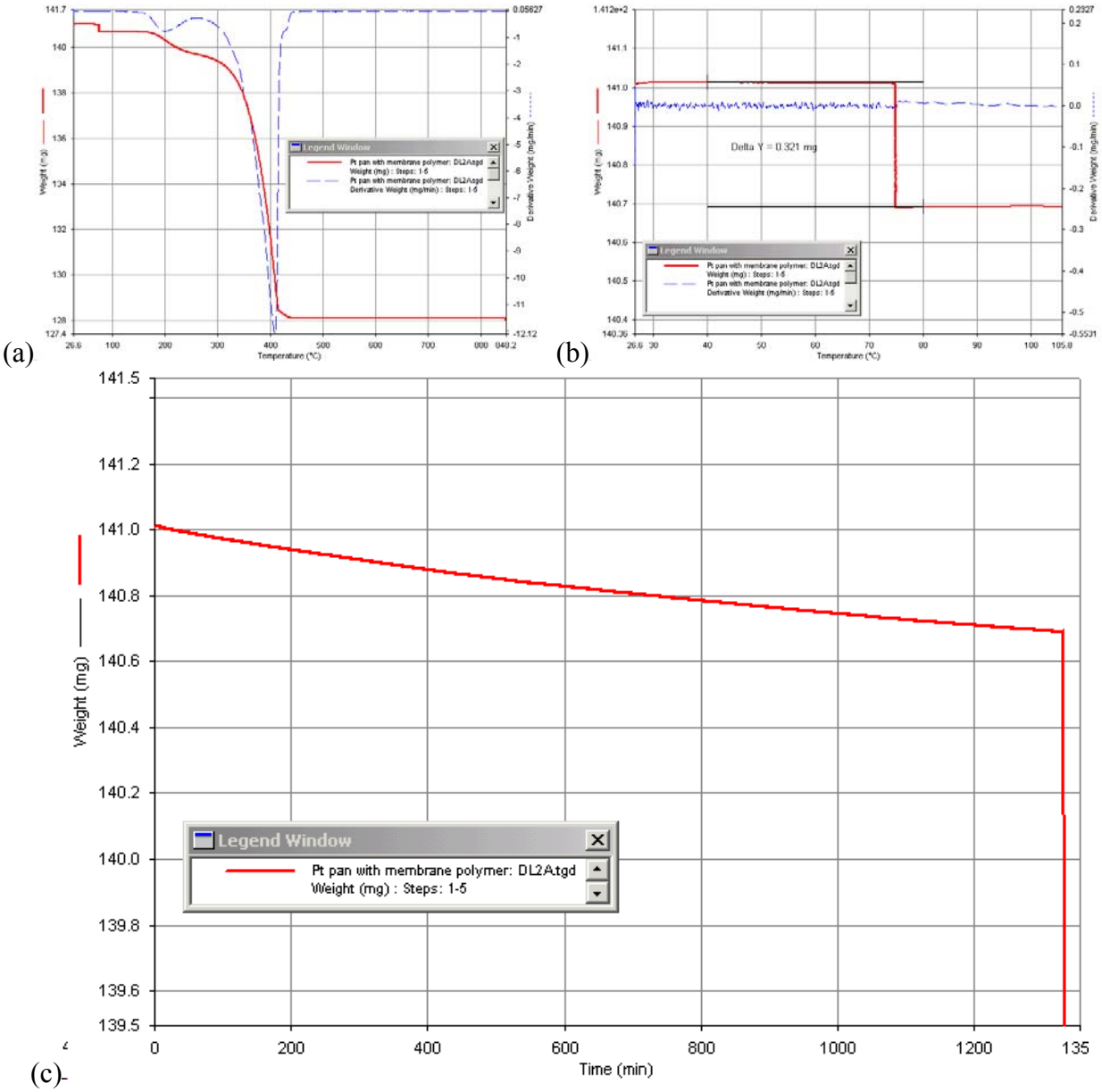

Figure 2.22 TGA decomposition curves for **PLGA11** sample held at 80°C for 22 hours: (a) TGA curve (weight loss versus temperature) from approximately 30 to 850°C, (b) close-up of TGA curve from approximately 30 to 105°C showing calculated weight loss of 0.321 mg from 40 to 80°C, (c) TGA curve of weight loss over time for the entire course of the experiment. Solid lines indicate weights of samples, dashed lines indicate derivative weights (mg/min) of samples.

The weight loss of 0.321 mg over the temperature range of 40–80°C shown in **Figure 2.22**(b) is much larger for this sample than was seen for the other samples which were not held at 80°C, and in fact corresponds to a residual solvent amount of 2.28%, or approximately 22800 ppm. Additionally, as can be seen from **Figure 2.22**(c), even after 22 hours at 80°C the sample weight was still decreasing, although the rate of mass loss appears to be diminishing as evidenced by the curvature of the line. These results suggest that complete evaporation of

residual solvent from the membrane polymers takes place over an extended period of time, and that for commercial applications a prolonged out gassing time is desirable.

Although HFIP is not classified by the FDA as a Class 1, 2, or 3 type solvent (solvent to be avoided, solvent to be limited, or solvent with low toxic potential), chloroform and dichloromethane are designated as Class 2 solvents and could be used instead of HFIP to fabricate the reservoir membranes and to ensure that the membrane fabrication process will be compatible with FDA guidelines. The higher vapor pressures of these two solvents, however, might make reproducible microinjection of the polymer solutions more difficult. The ppm values specified by the FDA for these two solvents range from 60 ppm for chloroform to 600 ppm for dichloromethane.

The FDA also specifies permissible daily exposure (PDE) limits for Class 2 solvents[16]. The PDE, in mg/day, can be found as follows:

$$\left(\frac{ppm_{\max}}{1000}\right) \times dose = PDE$$

Equation 2-l

where ppm_{max} = the maximum allowable ppm concentration according to the FDA and $dose$ = 10 g. For the microreservoir devices, the daily exposure can be found from the total mass of membrane polymer in the device and the ppm values obtained through our TGA analyses. A device having 36 reservoirs that each have 23.4 μg of membrane polymer would have a total membrane polymer mass of 842.4 μg, or 8.424×10^{-4} g. If we assume a maximum concentration of 22800 ppm of solvent within each of those membranes (according to the **PLGA11** sample that was held at 80°C for an extended period of time), then the total dosage of solvent can be calculated from Equation 2-l as:

$$\left(\frac{22800\,ppm}{1000}\right) \times \left(8.424 \times 10^{-4}\,g\right) = 0.019 mg/day = 19 \mu g/day$$

This is well below the range of PDE values (0.5 to 48.4 mg/day) specified for Class 2 solvents by the FDA[11]. Additionally, for a patient weighing approximately 150 lbs (68 kg), the 19.21 μg of

residual 1,1,1,3,3,3-hexafluoro-2-propanol calculated above for a prototype device would correspond to a dosage of:

$$\frac{19.21\mu g}{68.18kg} = 0.28\mu g / kg$$

which is much lower than the intraperitoneal LD50 (lethal dose at which 50% of test subjects are killed) reported for mice of 300 mg/kg. Additionally, the PDE specified by the FDA is the maximum allowable amount of solvent per day that can be released from a pharmaceutical body, for example a tablet that is administered daily. The microreservoir device, however, is designed for implantation and use over a much longer time period than one day, with possible device lifetimes up to a few years. It is highly unlikely that all of the residual solvent would be released in one day, given the extended period of time required for out gassing in the TGA studies reported here, and moreover the device would not be repeatedly administered to a patient.

Finally, it is likely that the residual solvent in the reservoir membranes is actually lower than the concentrations found during this study, as the membranes have a much smaller volume and thickness than the polymer samples in our TGA pans, and would therefore allow more rapid out gassing of the solvent. The samples analyzed in this study had masses of membrane polymers that were larger by a factor of nearly 10^3 and thicknesses that were approximately six times larger than those typically present in a microreservoir device.

2.4 Summary and Conclusions

We have developed a fabrication process for polymeric microreservoir devices that consists of two compression-molding steps, a polishing step, and microinjection of polymer solutions into the reservoirs to form the reservoir membranes. This process yields a device that fulfills our criteria of being able to deliver multiple pulses, as well as having low porosity (typical relative densities of 99–100% were obtained). The amount of residual solvent in membrane polymer samples appears to decrease quite slowly even at 80°C. Using a more volatile solvent or extending the curing time of the membranes prior to device loading may help to further minimize the amount of residual solvent. Additionally, near-infrared characterization of microinjected membranes on a device showed no significant mixing between membrane and

substrate materials, indicating that the release time of the reservoirs will be controlled by the characteristics of the membrane polymer and not by mixing phenomena. Although some variation in device thickness and corresponding reservoir opening diameter occurs as a consequence of the fabrication procedure, devices selected for a release experiment typically showed on average ±40 μm variation in reservoir diameter. The yield of usable reservoirs on a given device is generally between 80–90%, but the yield of microinjected membranes was found to vary widely, depending on the size of the reservoir and the polymer from which the membrane was made. Overall, the fabrication processes that were developed are applicable for a variety of materials, and do not appear to adversely affect the performance of the devices.

2.5 Acknowledgements

The near-infrared characterization of devices reported here was performed by Dr. Insung Choi, now at the Department of Chemistry, School of Molecular Science - BK21 and Center for Molecular Design and Synthesis, Korea Advanced Institute of Science and Technology, Daejeon 305-701, Korea.

2.6 References

1. R. K. Kulkarni, E. G. Moore, A. F. Hegyeli, and F. Leonard, "Biodegradable poly(lactic acid) polymers," *J. Biomed. Mater. Res.* 5 (1971) 169–181.

2. K. Fu, D. W. Pack, A. M. Klibanov, and R. Langer, "Visual evidence of acidic environment within degrading poly(lactic-co-glycolic acid) (PLGA) microspheres," *Pharm. Res.* 17 (2000) 100–106.

3. M. J. Blanco-Príeto, K. Besseghir, O. Zerbe, D. Andris, P. Orsolini, F. Heimgartner, H. P. Merkle, and B. Gander, "In vitro and in vivo evaluation of a somatostatin analogue released from PLGA microspheres," 67 (2000) 19–28.

4. L. M. Sanders, J. S. Kent, G. I. McRae, B.H. Vickery, T. R. Tice, and D. H. Lewis, "Controlled release of a luteinizing hormone-releasing hormone analogue from poly(*d*,*l*-lactide-co-glycolide) microspheres," *J. Pharm. Sci.* 73 (1984) 1294–1297.

5. H. Okada, "One- and three-month release injectable microspheres of the LH-RH superagonist leuprorelin acetate," *Adv. Drug Deliv. Rev.* 28 (1997) 43–70.

6. K. J. Brodbeck, S. Pushpala, and A. J. McHugh, "Sustained release of human growth hormone from PLGA solution depots," *Pharm. Res.* 16 (1999) 1825–1829.

7. J. F. Strasser, L. K. Fung, S. Eller, S. A. Grossman, and W. M. Saltzman, "Distribution of 1,3-bis(2-Chloroethyl)-1-Nitrosourea and tracers in the rabbit brain after interstitial delivery by biodegradable polymer implants," *J. Pharmacol. Exp. Ther.* 275 (1995) 1647–1655.

8. R. J. Tamargo, J. S. Myseros, J. I. Epstein, M. B. Yang, M. Chasin, and H. Brem, "Interstitial chemotherapy of the 9L gliosarcoma: controlled release polymers for drug delivery in the brain," *Cancer Res.* 53 (1993) 329–333.

9. I. Sivin, D. N. Robertson, J. Stern, H. B. Crozatto, S. Diaz, E. Coutinho, A. R. da Silva, F. A. Sanchez, A. Faundes, O. McDonald, P. Holma, N. C. Nielson, M. Osler, H. A. Nash, "Norplant: reversible implant contraception," *Studies in Family Planning* 11 (1980) 227–235.

10. X. Huang and C. S. Brazel, "On the importance and mechanisms of burst release in matrix-controlled drug delivery systems," *J. Controlled Release* 73 (2001) 121–136.

11. "Guidance for Industry, Q3C — Tables and List," U.S. Department of Health and Human Services, Food and Drug Administration, Center for Drug Evaluation and Research (CDER), and Center for Biologics Evaluation and Research (CBER), December 1997, ICH, Available: http://www.fda.gov/cder/guidance/Q3Ct&l.pdf

12. Z. Tadmor, C. G. and Gogos, *Principles of Polymer Processing*, John Wiley and Sons, New York, NY, USA, 1979, pp. 542–545.

13. A. W. Adamson and A. P. Gast, Physical Chemistry of Surfaces, 6th edition, John Wiley & Sons, Inc., New York, 1997.

14. P. Geladi and B. R. Kowalski, "Partial least-squares regression: a tutorial," *Anal. Chim. Acta*, 185 (1986) 1–17.

15. R. D. Tobias, "An introduction to partial least squares regression," URL: ftp://ftp.sas.com/techsup/download/technote/ts509.pdf

16. "Guidance for Industry, Q3C Impurities: Residual Solvents," U.S. Department of Health and Human Services, Food and Drug Administration, Center for Drug Evaluation and Research (CDER), and Center for Biologics Evaluation and Research (CBER), December 1997, ICH, Available: http://www.fda.gov/cder/guidance/Q3Cfnl.pdf

3 Chemical Loading and Device Sealing

3.1 Introduction and Motivation

3.1.1 Introduction

The method of microinjection is used to load devices with the chemicals to be released. This method is used to load proteins into cells, and can reliably deliver volumes down to 52 pL according to the manufacturer of the microinjector. Microinjection has also been used to load silicon microreservoir devices similar to these polymeric microreservoir devices[1]. Microinjection allows loading of different chemicals into different reservoirs on an individual basis, unlike other filling methods such as discontinuous dewetting[2]. Inkjet printing may also be used to load individual reservoirs with different chemicals, but the solution viscosity and composition strongly affect the volume of solution that is delivered from the inkjet printhead[1]. The accuracy of the microinjector, however, is also dependent on several factors that may vary according to the chemical that is loaded into the reservoirs.

A variety of methods are available for sealing the polymeric microreservoir devices. While microinjection of a sealant layer on the backside of the devices is most likely not feasible due to the complication of depositing the polymer solution on top of the drug within the reservoir, other methods may be considered. Solvent or ultrasonic bonding of thin polymer films to the backside of the device is the most obvious method. Ultrasonic bonding has been widely used in wire bonding, but has also been studied for application to plastic parts[3], as has solvent bonding[4]. Ultrasonic welding, however, may generate heat within the polymer[5–7] which could be detrimental to the drugs loaded in the microreservoir device, while solvent welding raises the issue of residual solvent, as discussed in section 2.1.2.

3.1.2 Motivation

A number of factors may affect the performance of the microinjector and therefore the amount of drug that is loaded into the reservoirs. Both the solvent in which the drug is dissolved and the geometry of the surface onto which the solution is microinjected may affect the volume of solution that is delivered from the microinjector. Therefore, the goal of the microinjector

studies reported here was to quantify the effect of these variables on the microinjector performance in order to determine whether or not their effect on the amount of drug loaded into the device was significant. This will enable accurate quantitation of the device performance later on, as typically it is desired to achieve mass balance (ideally 100% of the initial loading should be detected as released from the device) over the course of a release experiment.

Similarly, it is vitally important for the sealing method to produce a hermetic seal on the devices. Should this seal fail or leak, device performance cannot be confidently assessed. Leakage or breakage of the seal would make it impossible to determine if a detected release from a device was due to opening of the reservoir membranes or simply failure of the seal. The goal of the sealing experiments discussed below was therefore to ascertain whether the sealing method used was robust (no diffusion, leakage, or breakage) over the course of a typical release experiment.

3.2 Materials and Methods

3.2.1 Materials

Poly(L-lactic acid) (**PLA**, M_w 194 Kilodaltons (Kd), Medisorb® 100 L) was obtained from Alkermes (Cincinnati, Ohio). Fluorescein-dextran, M_w~70,000 daltons, was obtained from Molecular Probes (Eugene, OR). Fluorescein sodium salt and ^{14}C-dextran were obtained from Sigma-Aldrich (St. Louis, MO). ^{14}C-iodoantipyrine was obtained from Perkin Elmer Life Sciences (Boston, MA). Ideal 9144 Masking Tape was obtained from American Biltrite, Inc. (Lowell, MA).

3.2.2 Methods

3.2.2.1 Reservoir Filling

Reservoirs on devices were loaded with a solution of the chemical to be released via microinjection. Microinjection was performed using a system purchased from World Precision Instruments (Sarasota, FL), consisting of a UMP-1 Ultra Micro Pump with a Micro-4 controller, Kite-R micromanipulator with a TB-1 tilting base and 5464 five pound weight for the tilting base, and a PZMT Trinocular stereo microscope with 13338 Adapter Ring Light, R-8-8-WPI01 fiber

optic ring light, and NOVA Novaflex fiber optic light source. The experimental setup is shown in **Figure 3.1**.

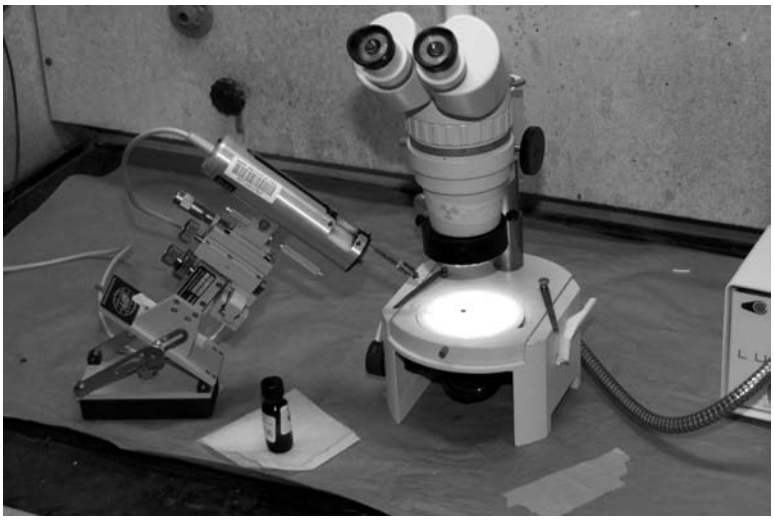

Figure 3.1 Experimental setup used for microinjection. The device to be loaded is placed on the stage of the stereomicroscope, and the chemical is loaded into the reservoirs from a syringe that is seated in a micromanipulator that can be tilted to allow optimal positioning of the needle tip. Photo by Rebecca Shawgo.

Solutions were injected from a variety of gastight syringes and needles. Typically ten, 50, or 100 μL syringes were used with gastight needles (all items from Hamilton Company, Reno, NV).

3.2.2.1.1 Effect of Solvent

One factor that may affect the microinjected volume is the solvent in which the drug solution is prepared. Evaporation of the solvent due to its vapor pressure may cause a decrease in the volume of the droplet at the end of the needle, and a corresponding increase in the concentration of the droplet. Additionally, the concentration of the drug in the solution that resides locally at the needle tip may also increase. Microinjection of radiolabeled solutions having different solvents was performed in order to determine the effect of vapor pressure on the measured microinjected amounts of radiolabeled chemicals.

Solutions of ^{14}C-iodoantipyrine (in ethanol) and ^{14}C-dextran, M_w~70,000 (in water) were injected into 7-mL glass scintillation vials. Five mL of ScintiSafe Plus, 50% (Fisher Scientific, Atlanta, GA) were added to each vial. The amount of radiolabel in each vial was quantified using a ^{14}C counting protocol on a Packard Tri-Carb liquid scintillation counter, Model U2200. Raw data (disintegrations per minute, *DPM*) were converted to microcuries (μCi) by using the

conversion factor 2.2 × 10^6 dpm = 1 μCi. The measured μCi value was then divided by the concentration, in μCi/mL, of the injected stock solution (C_{init}) to give the measured microinjected volume (V_{meas}) as follows:

$$V_{meas} = \frac{DPM}{\left[\left(2.2\times10^{6}\,\frac{dpm}{\mu Ci}\right)\times C_{init}\right]}$$

Equation 3-a

The small size of the solution droplets (typically 20 to 150 nL) may cause the vapor pressure to be changed by the droplet curvature. The vapor pressure of a solvent over a curved surface can be calculated from the Kelvin Equation[8]:

$$RT\ln\left(\frac{P}{P_0}\right) = \gamma\frac{V_m}{R_m}$$

Equation 3-b

where R = ideal gas constant, T = temperature, P = vapor pressure observed over curved surface, P_0 = normal vapor pressure of liquid, γ = surface tension, V_m = molar volume of liquid, and R_m = mean radius of curvature of the surface. The evaporation rate, Z (in moles/(m^2*sec)), due to the vapor pressure can then be found using the equation[8]:

$$Z = P\left(\frac{1}{2\pi MRT}\right)^{\frac{1}{2}}$$

Equation 3-c

where P = vapor pressure of the liquid, M = molar mass of the liquid, R = ideal gas constant and T = temperature. The number of molecules that evaporate in a given time interval from a droplet can be calculated using the results of Equation 3-c as follows:

$$N_L = Z\times S_A\times t$$

Equation 3-d

where N_L = number of molecules evaporated in time t (the time between consecutive microinjections), S_A = surface area of droplet, and Z = evaporation rate as calculated from Equation 3-c. These equations were used to determine whether or not the evaporation of the different solvents and subsequent increase in solution concentration were predicted to be significant under the experimental conditions that were used.

3.2.2.1.2 Effect of Surface Geometry

The geometry of the surface onto which the solution is microinjected may also affect the accuracy of the microinjector. The interfaces between the liquid solution, solid surface, and surrounding air are constrained by Young's equation[8]:

$$\cos\theta = \frac{\left(\gamma_{SV} - \gamma_{SL}\right)}{\gamma_{LV}}$$

Equation 3-e

where θ = contact angle between liquid and solid surfaces, γ_{SV} = surface tension between solid and gas (vapor) phases, γ_{SL} = surface tension between solid and liquid phases, and γ_{LV} = surface tension between liquid and gas (vapor) phases. The contact angle of the solution on curved and flat surfaces remains the same, but the solution droplet may break off from the needle differently for different surface geometries. Put another way, the droplet will break off from the needle tip such that the most energetically favorable state (minimized surface free energy) is achieved both for the liquid that remains on the needle tip and the liquid that is deposited on the surface of the device. This state will be different for liquid deposited in a reservoir compared to liquid deposited on a flat surface of the device.

In order to determine whether this effect is significant for the microreservoir devices, four different chemicals (fluorescein, fluorescein dextran, ^{14}C-dextran, and ^{14}C-iodoantipyrine) were injected onto the planar surfaces of poly(lactic acid) device substrates, as well as into the reservoirs of the devices. The devices were cut into pieces a few millimeters on a side prior to microinjection so that one device could be used for several measurements. A ten μL syringe was used to inject the solutions. Injection volumes were 24.87 nL and 99.48 nL (with the exception of fluorescein dextran). After microinjection, samples with fluorescent chemicals were placed in 4.5 mL polystyrene cuvettes along with 3 mL of 1X PBS. Cuvettes were covered with Parafilm

M® and gently shaken to allow the fluorescent molecules to dissolve in the saline solution. The fluorescence was measured on a PTI spectrofluorometer and the amount of fluorescent molecule in each cuvette was calculated using a standard curve. The microinjected volumes were then calculated based on the known molarities of the fluorescent stock solutions that were microinjected. Device pieces that were microinjected with radiolabeled solutions were placed in 7-mL scintillation vials. Five mL of ScintiSafe Plus 50% were added to each vial, and the amount of radiolabel present in each vial was measured using a ^{14}C counting protocol on a Packard Tri-Carb liquid scintillation counter, Model U2200. The microinjected volumes were then calculated using the known concentrations of the radiolabel stock solutions.

3.2.2.2 Device Sealing

The devices that were used in release studies were sealed using Ideal 9144 Masking Tape after microinjection and drying of the chemical solutions within the reservoirs. This procedure was performed using the PZMT stereo microscope. Tweezers and scissors were used to cut the tape to the appropriate size and affix the tape to the backsides (side opposite the membranes) of the devices. A hard object, such as the handle of the scissors or a metal spatula, was used to firmly press the tape to the surface of the device and to eliminate any air bubbles that were trapped between the tape and the device. The tape was inspected under the microscope to ensure that no air bubbles remained. This tape is designed for use in the production of printed circuit boards and provides protection from chemicals used in tin/lead stripping and gold finger plating operations.

An experiment was performed to test the stability of the tape used to seal the devices. Three unpolished devices (the conical reservoirs penetrated only partially through the substrate, as shown schematically in **Figure 2.2**(b)) with no reservoir membranes were each loaded with approximately 0.073 μCi of ^{14}C-dextran (M_w = 70,000). The backsides of the devices were then sealed with the 9144 masking tape and the devices were affixed to glass slides for stability. Devices were placed in jars containing 20 mL of 1X PBS and magnetically stirred at approximately 28–33°C. Samples of 1 mL of the release media were taken once daily, five days per week, from each of the jars. Fresh PBS was added back to the jars to replace the media that was removed. The media aliquots were assayed on the scintillation counter using a ^{14}C protocol to monitor the amount of ^{14}C-dextran that was released from the devices.

3.3 Results and Discussion

3.3.1 Reservoir Filling

3.3.1.1 Effect of Solvent

Two different radiolabeled solutions were microinjected in order to determine the effect of solvent vapor pressure on the accuracy of microinjection. A 100 μCi/mL solution of ^{14}C-iodoantipyrine (M_w = 314, model molecule for carmustine, a chemotherapy drug) in ethanol was microinjected into glass scintillation vials. A solution of 50 μCi/mL of ^{14}C-dextran (M_w ~ 70,000) in water was also microinjected into glass scintillation vials. Prior to injection into a vial, at least one injection was performed onto the surface of a glass slide in order to eliminate effects from any evaporation that may have occurred in the time that elapsed while switching vials. The MICRO4 controller was programmed to deliver 20, 40, 60, 80, 100, or 120 nL of solution. This corresponded to 19.57, 39.68, 59.79, 79.98, 99.48, and 119.5 nL injected based on the syringe volume of ten μL.

The measured microinjected volume for each set of injections was calculated according to Equation 3-a. The results are shown by the data points and dashed line (least squares fit) in **Figure 3.2** (^{14}C-iodoantipyrine) and **Figure 3.3** (^{14}C-dextran). The solid lines in **Figure 3.2** and **Figure 3.3** indicate the predicted theoretical microinjected volumes that were listed above and are based on the microinjector settings, step size, and syringe volume.

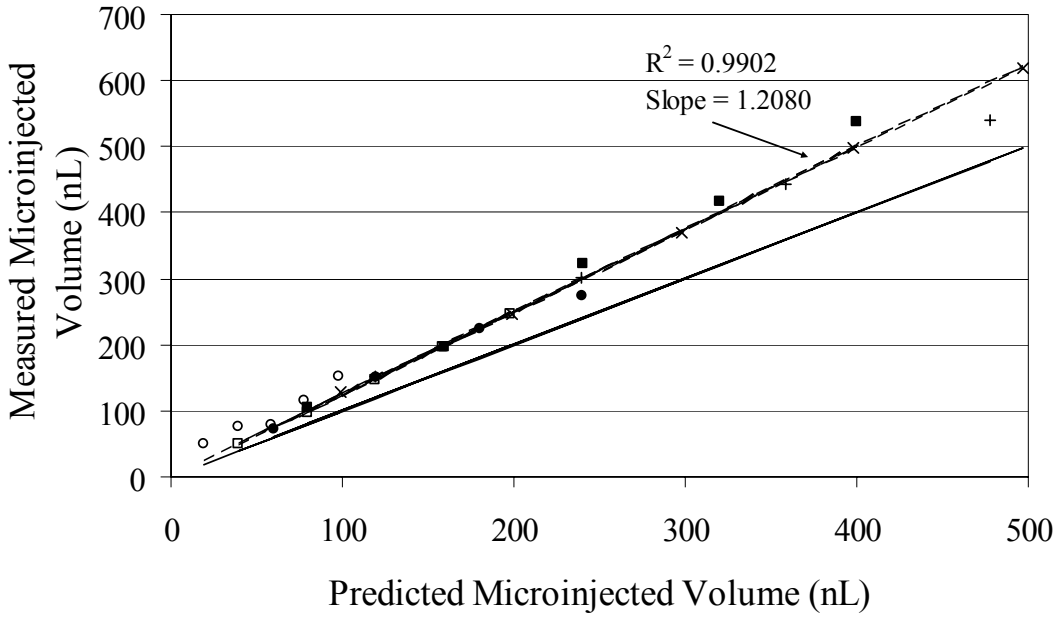

Figure 3.2 Measured vs. predicted microinjected volume for ^{14}C-iodoantipyrine in ethanol, injected from a ten μL syringe: ○ 20 nL injections, □ 40 nL injections, ● 60 nL injections, ■ 80 nL injections, × 100 nL injections, + 120 nL injections, solid line indicates theoretical predicted microinjected volume, dashed line indicates least-squares best fit line to data points.

The measured microinjected volume for iodoantipyrine samples was typically 20% greater than the predicted value (slope of trendline = 1.2080), as can be seen from **Figure 3.2**. In contrast, the measured microinjected volume for the dextran samples was only about 80% of the predicted value (slope of trendline = 0.8476), as can be seen in **Figure 3.3**. At smaller injection volumes (20 and 40 nL injections), the measured volume was typically closer to 60% of the predicted value.

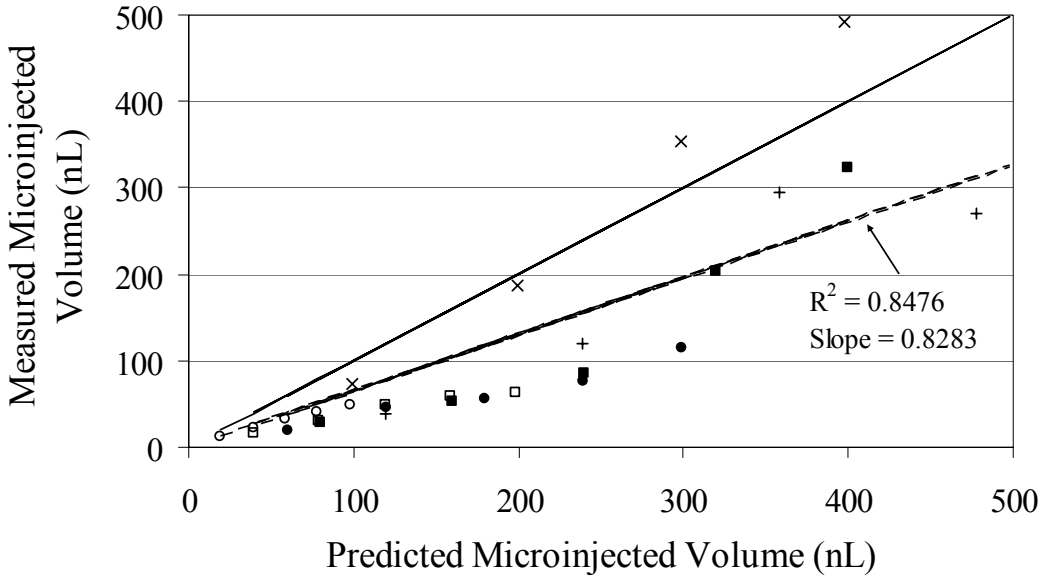

Figure 3.3 Measured vs. predicted microinjected volume for ^{14}C-dextran in water, injected from a ten μL syringe: ○ 20 nL injections, □ 40 nL injections, ● 60 nL injections, ■ 80 nL injections, × 100 nL injections, + 120 nL injections, solid line indicates theoretical predicted microinjected volume, dashed line indicates least-squares best fit line to data points.

The larger measured volume seen for the ^{14}C-iodoantipyrine samples may be due to solvent evaporation and consequent concentration of the solution in the local area of the needle tip. The vapor pressures for ethanol and water droplets of various volumes at 20°C (270°K) were calculated according to Equation 3-b, neglecting solute effects. The results are shown below in **Table 3-1**. The curvature due to the small droplet sizes does not appear to cause a large change in the vapor pressure of the two solvents at the temperature and volumes of interest.

Table 3-1 Vapor pressures at 270°K of ethanol and water for various droplet sizes.

Solvent	Data	V_{inj} (nL)	R_m (mm)	P (kPa)
Ethanol	P_o = 7.87 kPa	19.57	0.16717349	7.8700274
	γ = 22.39 dyn/cm	39.68	0.21158962	7.8700217
	M_w = 46.0688 g/mol	59.79	0.24257534	7.8700189
	ρ = 0.789 g/cm^3	79.98	0.26727865	7.8700171
	V_m = 58.3888 cm^3/mol	99.48	0.28744123	7.8700159
	T = 270°K	119.5	0.30555761	7.8700150
Water	P_o = 3.2 kPa	19.57	0.16717349	3.2000113
	γ = 72.94 dyn/cm	39.68	0.21158962	3.2000089
	M_w = 18.0152 g/mol	59.79	0.24257534	3.2000078
	ρ = 0.995 g/cm^3	79.98	0.26727865	3.2000070
	V_m = 18.1057 cm^3/mol	99.48	0.28744123	3.2000065
	T = 270°K	119.5	0.30555761	3.2000062

The vapor pressures shown in **Table 3-1** can be used along with Equation 3-c and Equation 3-d to calculate the number of solvent molecules that evaporate in a given period of time. The adjusted concentration of the solute can then be calculated based on the remaining volume of solvent. This calculation was performed for the injected volumes listed in **Table 3-1**, assuming a temperature of 270°K and estimating an elapsed time of three seconds between microinjections. The results are summarized in **Table 3-2** below.

Table 3-2 Concentrations of solutions of ^{14}C-iodoantipyrine in ethanol and ^{14}C-dextran in water adjusted for solvent evaporation due to curvature of droplets.

Solution	V_{inj} (nL)	P (kPa)	Adjusted Concentration (μCi/mL)
^{14}C-iodoantipyrine in ethanol	19.57	7.870027417	100.0009365
	39.68	7.870021662	100.0007399
	59.79	7.870018895	100.0006454
	79.98	7.870017148	100.0005857
	99.48	7.870015945	100.0005446
	119.5	7.870015	100.0005123
^{14}C-dextran in water	19.57	3.200011261	50.00009441
	39.68	3.200008897	50.00007459
	59.79	3.200007761	50.00006506
	79.98	3.200007044	50.00005905
	99.48	3.20000655	50.00005491
	119.5	3.200006161	50.00005165

The evaporation rate and corresponding increased concentrations of the droplets do not appear significant at these short times. The most obvious reason for this is that the vapor pressure calculations do not account for the continuing decrease in the size of a given droplet due to evaporation. As the droplet shrinks, the vapor pressure will increase, thereby further increasing the vapor pressure and hence the evaporation rate.

The simplifying assumption of a pendant droplet at the needle tip seems to be justified. In actuality there is no pendant drop and the solution simply fills the shaft of the needle up to the tip. The needle shaft has a smaller inner diameter (0.13 mm) than the droplets assumed in our calculations. This does not appear to significantly affect the calculated results, however. By using R = 0.13 mm in Equation 3-b, Equation 3-c, and Equation 3-d, the calculated adjusted concentrations are only 100.000936458 μCi/mL for ^{14}C-iodoantipyrine in ethanol, and 50.000096227 μCi/mL for ^{14}C-dextran in water, which are quite similar to the values obtained for the 19.57 nL injections shown in **Table 3-2**.

The calculated concentrations due to evaporation of the solvents do not fully explain the 20% increase in activity measured for the ^{14}C-iodoantipyrine samples. Additionally, the ^{14}C-dextran samples showed a lower measured activity than is expected, with a correspondingly smaller measured microinjected volume. One possible reason for this is that the temperature at the tip of the needle may be higher than the 270°K that was used in the calculations. The fiberoptic light source used with the stereomicroscope generates a noticeable amount of heat on the stage of the microscope, and the metal surface of the needle may act as a conductor of that heat. This would affect the vapor pressure of the ethanol solution to a greater degree than that of the water, as can be seen from Equation 3-b, perhaps further concentrating the solution than is indicated by **Table 3-2**.

The discrepancies in observed microinjected activities and calculated adjusted solution concentrations may also be partially explained by the surface tensions of the two solvents. First, the surface tension values may actually be lower than those used to calculate *P* and the adjusted concentrations in **Table 3-1** and **Table 3-2**, as we assumed the experimental setup was at 270°K and this may not be entirely accurate, as discussed above. Secondly, ethanol has a much lower surface tension at room temperature than water. The lower surface tension of the ethanol solution compared to water may have caused the ethanol solution to more fully wet the glass surface of the scintillation vial than the dextran solution. Slight bleeding of the solution from the microsyringe needle when it was touched to the surface of a glass slide has been observed in other studies in which ethanol solutions were used. Therefore, possible bleeding of the ethanol solution in this study may account for some of the observed increase in measured activity and microinjected volume compared to the predicted microinjected volume. Additionally, the presence of dextran in the water solution, while not exceedingly high, slightly increases the

viscosity (due to the high molecular weight chains) and thus the wetting angle of the solution on the surface of the glass scintillation vials into which the solutions were microinjected. The dextran solution may therefore have wetted the glass surfaces less than expected, resulting in a lower measured microinjected volume than expected.

3.3.1.2 Effect of Surface Geometry

A series of experiments was performed to determine the effect of surface geometry on the measured microinjected volume. Four different chemicals (fluorescein, fluorescein dextran, ^{14}C-dextran, and ^{14}C-iodoantipyrine) were injected onto the planar surface of poly(lactic acid) devices, as well as into the reservoirs of the devices. Injection volumes were 24.87 nL and 99.48 nL (with the exception of fluorescein dextran). As shown in **Table 3-3** and **Table 3-4**, the measured microinjected volumes on the surfaces of the devices were consistently larger than for injections into the reservoirs of the devices, with the exception of the 24.87 nL fluorescein injections. Additionally, the error (as indicated by the percentage of predicted volume that was measured) was larger for the 24.87 nL injections than for the 99.48 nL injections.

Table 3-3 Measured volume of fluorescein, fluorescein-dextran, ^{14}C-iodoantipyrine, and ^{14}C-dextran solutions microinjected onto the surface of **PLA** device substrates, calculated using concentrations of microinjected solutions.

Chemical	Type of injection	Predicted Microinjected Volume (nL)	Average Measured Volume (nL)	Standard Deviation (nL)	% of Predicted Volume Measured
fluorescein	surface	24.87	28.27	4.05	113.67
	surface	99.48	108.45	14.55	109.02
fluorescein dextran	surface	24.87	16.77	4.98	67.42
^{14}C-iodoantipyrine	surface	24.87	33.43	1.52	134.41
	surface	99.48	120.32	6.37	120.95
^{14}C-dextran	surface	24.87	30.99	7.93	124.62
	surface	99.48	86.09	25.52	86.54

Table 3-4 Measured volume of fluorescein, fluorescein-dextran, ^{14}C-iodoantipyrine, and ^{14}C-dextran solutions microinjected into reservoirs in **PLA** device substrates, calculated using concentrations of microinjected solutions.

Chemical	Type of injection	Predicted Microinjected Volume (nL)	Average Measured Volume (nL)	Standard Deviation (nL)	% of Predicted Volume Measured
fluorescein	reservoir	24.87	33.20	2.34	133.48
	reservoir	99.48	80.01	61.22	80.42
fluorescein dextran	reservoir	24.87	14.43	12.33	58.00
^{14}C-iodoantipyrine	reservoir	24.87	23.63	5.26	95.00
	reservoir	99.48	91.25	12.69	91.73
^{14}C-dextran	reservoir	24.87	28.11	1.38	113.02
	reservoir	99.48	67.73	20.39	68.08

The lower average volumes measured for the dextran solutions (both fluorescein and ^{14}C labeled) compared to the measured volumes of the fluorescein and ^{14}C-iodoantipyrine solutions are consistent with the hypothesis presented in section 3.3.1.1 that the dextran solutions have a higher viscosity and therefore do not wet the surface as thoroughly as the lower viscosity solutions of smaller molecules.

One possible explanation for the difference in results seen for the surface and reservoir topographies may be the minimization of surface free energy. In the case of the planar surface, the microinjected solution will form a spherical section on the surface of the device. This droplet will have only one surface in contact with air. The droplet that is microinjected into the reservoir, however, will form a conical frustum that has menisci instead of planar bases. This volume has two surfaces in contact with air. If we assume that it is more energetically favorable for the solution to form an interface with the polymer surface than with air, then it seems logical that the frustum is overall a less energetically favorable configuration than the spherical section, as it has two air-solution interfaces. When considering the surface free energy of the two systems as a whole (solution droplet on needle tip and droplet on polymer surface), the energetic minimum for the system with the conical frustum shape must necessarily require leaving a larger droplet remnant on the needle tip (in order to minimize the surface free energy of the system) than in the case of the spherical section on the planar surface.

Another possible explanation for the observed results is that there may be some residue within the reservoirs that is hydrophobic or otherwise unsuitable for wetting of the chemical solutions. More specifically, it is possible that some of the surface-functionalized fluorocarbon moieties (see section 2.2.2.1.2) detached from the aluminum mold during compression-molding of the device, and adhered to the inner walls of the reservoirs. This could make the reservoir walls more repulsive to the chemical solutions, leading to behavior that is more beading or nonwetting in nature.

Although the 24.87 nL injections of fluorescein show a larger measured volume for microinjections into the reservoir than on the planar surface of the device, the average measured volumes for surface and reservoir injections are within two standard deviations of each other. Therefore, this result does not seem significantly different from the trend shown by the other solutions.

As was discussed in section 3.3.1.1, evaporation of the solvent from the needle tip may affect the accuracy of the microinjector. This may also account for the fact that the 24.87 nL injections showed a consistently larger measured percentage of predicted volume than the 99.48 nL injections. The vapor pressure effects discussed above are more significant for smaller droplets and might cause greater concentration of the solution, which would appear as a greater measured percentage of predicted volume ("overinjected volume") compared to the larger droplets. Devices prepared for *in vitro* and *in vivo* release studies (presented in Chapters 4 and 9) were always filled with at least one injection of 90 nL or greater. Thus we would expect the device loading to be closer to the predicted amount than was seen for the smaller injections of 24.87 nL in this study.

Overall, the injections on the planar surfaces of the devices were on average 108% of the predicted volume, while the injections in the reservoirs were on average 91% if the predicted volume. While greater accuracy will be desired when loading devices for clinical use in a patient, the microinjection method provides a relatively easy and rapid way to load the microreservoir devices with small volumes of solution.

3.3.2 Device Sealing

A control experiment was performed to test the stability of the tape used to seal the devices. The results are shown in **Figure 3.4**.

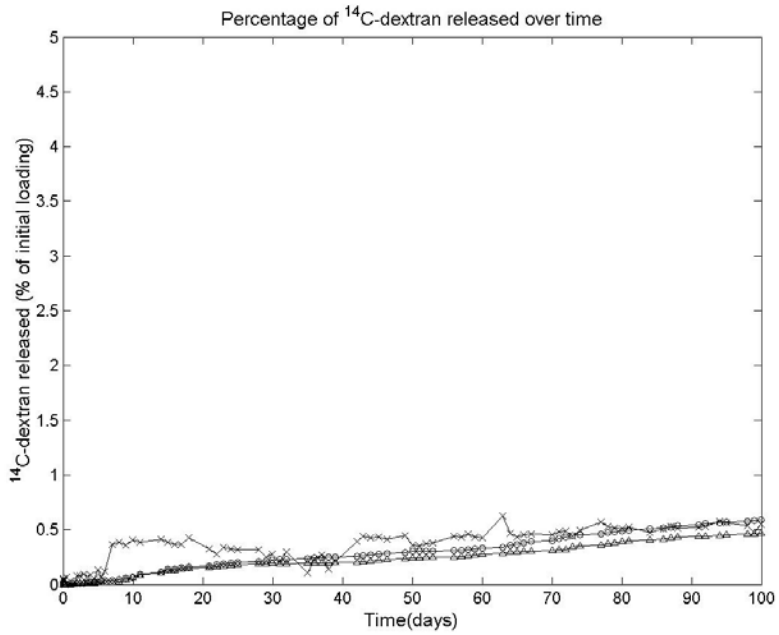

Figure 3.4 Cumulative percentage of initial loading of ^{14}C-dextran detected over 100 days from three unpolished control devices that had no reservoir membranes and that were sealed with 9144 masking tape. Note y-axis maximum is 5%.

The experiment indicated that a maximum of 0.5% of the total initial loading of approximately 0.073 μCi of ^{14}C-dextran (M_w = 70,000) was detected over 100 days from three unpolished **PLA** microchips having no membranes and having eight reservoirs loaded with ^{14}C-dextran. This suggests excellent stability of the seal under typical conditions and durations experienced during an *in vitro* release experiment.

3.4 Conclusions

The studies presented here clearly show that the microinjection method that is used to load the devices with chemicals is affected by several variables. The solvent vapor pressure and surface tension appear to affect the microinjected volume, with larger microinjected volumes measured for a solvent (ethanol) having high vapor pressure and low surface tension. Additionally, the geometry of the surface onto which the solutions are microinjected also appears to affect the measured microinjected volume, with larger amounts of solute measured for a given volume microinjected onto a planar surface as compared to into a reservoir, possibly due to wetting and minimization of surface free energy. However, as will be seen in Chapter 4, in general the amount of drug loading recovered from a given device over the course of a release study was relatively high (80–100% for ^{14}C-dextran and ^{3}H-heparin).

While these effects may simply be a nuisance for lab-scale production of *in vitro* prototypes, they become critical issues when considering scale-up for commercial production and end-stage clinical use. A more accurate, reproducible loading process is clearly needed in order to enable accurate dosing and quantitative recovery of drugs from the microreservoir device.

The technique that is used to seal the devices appears to be robust. Only 0.5% of the radiolabeled loading in test devices was detected after 100 days in saline solution at room temperature *in vitro*. While ultimately a completely sterile and hermetic sealing method will need to be developed for devices that will be used *in vivo*, the masking tape used for these studies appears to more than adequately fulfill the current performance requirements (no breakage, leakage, or diffusion).

3.5 References

1. Santini, J.T. Jr., "A Controlled Release Microchip," Ph.D. thesis, Massachusetts Institute of Technology, 1999, pp 50–53.

2. R. J. Jackman, D. C. Duffy, E. Ostuni, N. D. Willmore, and G. M. Whitesides, "Fabricating large arrays of microwells with arbitrary dimensions and filling them using discontinuous dewetting," *Anal. Chem.* 70 (1998) 2280–2287.

3. E. Sancaktar, "Polymer adhesion by ultrasonic welding," *J. Adhes. Sci. Technol.* 13 (1999) 179–201.

4. Y. H. Jeong, D. W. Kang, and H. J. Kang, "Adhesion strength of amorphous interfaces by solvent welding," *Polym-Korea* 24 (2000) 23–28.

5. M. N. Tolunay, P. R. Dawson, and K. K. Wang, "Heating and bonding mechanisms in ultrasonic welding of thermoplastics," *Polym. Eng. Sci.* 23 (1983) 726–733.

6. I. V. Mozgovoi, "The role played by shear strains in heat-generation in the ultrasonic welding of polymers," *Welding Production* 31 (1984) 11–14.

7. O.V. Tetslav and C. C. Volkov, "Study of the heat production process in the ultrasonic welding of lavsan fabrics," *Russian Ultrasonics* 30 (2000) 79–86.

8. A. W. Adamson and A. P. Gast, Physical Chemistry of Surfaces, 6th edition, John Wiley & Sons, Inc., New York, 1997.

4 *In Vitro* Release Experiments

4.1 Introduction and Motivation

Although a number of polymeric controlled drug delivery systems have been developed, tested, and commercialized, many of these devices can deliver only one or possibly two doses of drug. Additionally, pulsatile release from polymeric devices has traditionally been difficult in the absence of an externally applied stimulus, and thus most devices rely on stimuli such as ultrasound[1,2], a change in pH[3–5], temperature[6,7], analyte concentrations[8,9], and electric[10–12] or magnetic[13,14] fields to trigger drug release. Therefore, the goal of the experiments described here was to demonstrate the feasibility and reproducibility of achieving multiple pulsatile releases of model drugs from the polymeric microreservoir devices, without the application of a stimulus. We tested both single and double chemical releases to demonstrate the versatility of the device through multidosing.

4.2 Materials and Methods

4.2.1 Materials

Poly(L-lactic acid) (**PLA**, M_w 194 Kilodaltons (Kd), Medisorb® 100 L), poly(glycolic acid) (**PGA,** Medisorb® 100 PGA) and poly(D,L-lactic-*co*-glycolic acid) polymer powders of molecular weights (M_w) 4.4 Kd (**PLGA4.4**, Medisorb® 5050 DL 1A), 11 Kd (**PLGA11**, Medisorb® 5050 DL 2A), 28 Kd (**PLGA28**, Medisorb® 5050 DL 3A), and 64 Kd (**PLGA64**, Medisorb® 5050 DL 4A) were obtained from Alkermes (Cincinnati, Ohio). ^{14}C-carmustine (1,3-bis(2-chloroethyl)-1-nitrosourea, or BCNU) was purchased from Moravek Biochemicals (Brea, CA). ^{14}C-iodoantipyrine (^{14}C-IAP) was obtained from New England Nuclear (Boston, MA). ^{14}C-methylated dextran, M_w 70,000, was purchased from Sigma-Aldrich (St. Louis, MO). ^{125}I-human growth hormone (^{125}I-HGH), ^{125}I-Interleukin-2 (^{125}I-IL-2), and ^{3}H-heparin, sodium salt, were purchased from Perkin Elmer Life Sciences (Boston, MA). ScintiSafe Plus 50% was purchased from Fisher Scientific (Suwanee, GA). Ideal 9144 Masking Tape was obtained from American Biltrite, Inc. (Lowell, MA).

4.2.2 Selection of Release Chemicals

A number of factors were considered when selecting chemicals for these *in vitro* proof-of principle release studies. The small size of the reservoirs on the device (typically 120-130 nL) necessitates the use of a marker molecule that can be accurately quantitated at low concentrations in the aqueous release solution. While fluorescent markers are extremely attractive in this regard, with detection possible at concentrations as low as 0.1 nmol/L when using a spectrofluorometer, the instability of many common fluorescent labels makes them less than ideal for release studies that are longer than a few days. Photobleaching may become significant when precautions are not taken to isolate the experimental apparatus from ambient light (see Appendix A), which will make accurate quantitation of the released loading (as a percentage of the initial loading) quite difficult. Sodium fluorescein, which is widely used as a marker molecule and was used to quantitate microinjector performance (see Chapter 3), not only photobleaches but also has pH-dependent fluorescence. This makes it even more problematic for release studies from the polymeric microreservoir devices, as the degradation of the devices will generate acidic degradation products (see Chapter 5 for a more thorough discussion of the degradation processes of the PLGA membrane materials). Although buffered saline is typically used *in vitro* for release experiments, the pH change due to these acidic moieties can be significant over the course of a typical *in vitro* release experiment (see section 5.3.2), and this could affect the measured amount of fluorescence during the course of a typical release study.

Radiolabeled chemicals are a much more attractive alternative than fluorescently labeled chemicals for two reasons. First, the sensitivity of the detection method combined with the high specific activity of the molecules allows detection resolution in the range of tens of nanograms. For example, the ^{14}C-dextran that was used *in vitro* for release studies had a specific activity of 1.09 mCi/g (1090 μCi/mg) and a molecular weight of 70,000 g/mol. Assuming that the scintillation counter measures a background of approximately 25 disintegrations per minute (dpm), even 100 dpm in a 1 mL sample could easily be detected. Using the conversion factor of 2.2×10^6 dpm/μCi, we find that this corresponds to a concentration of:

$$\frac{\left(100 dpm \times \left(1 \times 10^9 \, nmol / mol\right)\right)}{\left(\left(2.2 \times 10^6 \, dpm / \mu Ci\right) \times \left(1090 \mu Ci / g\right) \times 70{,}000 g / mol \times 0.001 L\right)} = 0.5957 nmol / L$$

This detection limit compares favorably with that of the spectrofluorometer.

The second advantage of using radiolabeled molecules is that the change in activity over time can easily be quantified, unlike the changes in fluorescence due to photobleaching or pH. The half-life of the isotope (^{14}C, ^{3}H, or ^{125}I) can be used to determine the fraction of activity present after a specified amount of time has elapsed since the original concentration was assayed by the manufacturer. In the case of ^{14}C ($t_{1/2}$ = 5730 years) and ^{3}H ($t_{1/2}$ = 12.3 years) labeled moieties, decay is insignificant over the course of a typical release experiment (a few weeks to months). Although ^{125}I has a much shorter half-life ($t_{1/2}$ = 60 days), the raw data obtained from the scintillation counter (dpm) can quickly be corrected for decay and the amount of material released from a microreservoir device can be accurately quantitated.

The particular molecules that were used in these studies were selected based on a number of criteria. IL-2 and BCNU were selected due to their utility in chemotherapy. BCNU is currently used to treat glioblastoma mutiforme, a type of brain cancer[15,16]. Preliminary results from other studies in animals have shown efficacy of IL-2 in treating cancer[17–19]. Therefore, it might be of interest to deliver these molecules in a pulsatile manner. ^{14}C-iodoantipyrine was initially used in our release studies as a model chemical for BCNU, as they have similar molecular weights (214 for BCNU, 314 for iodoantipyrine) and partition coefficients (this is discussed in more detail in Chapter 6). Human growth hormone and heparin were both selected due to their biological activity, as well as because of an interest in trying to deliver both proteins and polysaccharides in a pulsatile fashion over extended periods of time from the microreservoir device. Dextran was selected as a model molecule due to the variety of molecular weights (later release studies in Chapter 7 look at the effect of drug molecular weight on the release characteristics from the devices) and labels (^{14}C and various fluorescent markers) that are available from chemical suppliers.

4.2.3 Methods

4.2.3.1 Device Fabrication

Devices were fabricated according to the procedures described in Chapter 2. Membranes were prepared in the reservoirs by injection of four different PLGA polymers in 1,1,1,3,3,3-hexafluoro-2-propanol solutions (12% by volume), as described in Chapter 3. The properties of

the polymers that were used are summarized in **Table 4-1** below. These polymers were chosen as suitable reservoir membrane materials based on previous release experiments (results not reported here) that used polymers having various molecular weights and ratios of lactic acid:glycolic acid as the membrane materials. Additionally, reports in the literature have shown that copolymers having a 50:50 ratio of lactic acid:glycolic acid have the fastest degradation rates[20,21], and therefore they were deemed appropriate for proof-of-principle release studies *in vitro*.

Table 4-1 Molecular weights, copolymer mole ratios, and approximate degradation times reported by the manufacturer for the **PLGA4.4**, **PLGA11**, **PLGA28**, and **PLGA64** poly(lactic-*co*-glycolic acid) copolymers used to make the reservoir membranes on the microreservoir devices.

Polymer designation	**M_w**	**L:G mole ratio**	**Chain End Group**	**Degradation time *in vitro* at 37°C**
PLGA4.4	4,400	51:49	-COOH	1-2 weeks
PLGA11	11,000	53:47	-COOH	2-3 weeks
PLGA28	28,000	54:46	-COOH	3-4 weeks
PLGA64	64,000	54:46	-COOH	3-4 weeks

Solutions of **PLGA4.4**, **PLGA11**, **PLGA28**, and **PLGA64** were used to make four different types of membranes in each device. Solutions were injected from a 1710RN 100 μL gas tight glass syringe with a 1" 31 gauge removable needle, blunt tip (part numbers 81030 and 0160831, both items from Hamilton Co., Reno, NV).

All reservoir membranes were designed to be approximately 150 μm thick in this study. The volume of membrane solution injected into each device varied due to the slight variations in thickness of the device and size of the reservoir openings. The volume of solution injected into each reservoir was calculated from the volume fraction of polymer in the solution, the specific geometry of each device, and the desired membrane thickness.

The devices were dried in a vacuum oven at 71–74°C and 6.7 kPa vacuum for approximately 48 hours after microinjection of the membrane solutions, with the exception of devices loaded with ^{14}C-iodoantipyrine. These devices had **PLGA28** and **PLGA64** membranes that were dried at 68°C for 16 hours, and **PLGA4.4** membranes that were subsequently dried at room temperature for five days. Devices were suspended on glass slides so that the truncated ends of the reservoirs in which the membranes were located faced the bottom of the vacuum oven, but were not touching the surface of the oven. The membranes were inspected for defects

after drying (such as air bubbles and pinholes) at 80X magnification using a PZMT Trinocular stereo microscope with 13338 Adapter Ring Light, R-8-8-WPI01 fiber optic ring light, and NOVA Novaflex fiber optic light source. Reservoirs having defect-free membranes were considered viable for use in release experiments, and selected reservoirs were loaded with the chemical(s) to be released.

The chemical solutions were allowed to dry in the reservoirs for approximately 24 hours at room temperature and pressure. The devices were sealed opposite the membranes and attached to glass microscope slides for stability with Ideal Masking Tape 9144.

4.2.3.2 *In Vitro* Release Studies

4.2.3.2.1 Single Chemical Release Studies

Devices were microinjected with solutions of ^{14}C-dextran, ^{3}H-heparin sodium salt, ^{125}I-HGH, ^{125}I-IL-2, ^{14}C-BCNU, or ^{14}C-IAP for release studies. The specific activities of the radiolabeled molecules, amount of drug loaded into the devices, and membrane materials and thicknesses are summarized in **Table 4-2** below. The maximum loading for these microreservoir devices is approximately 125 nL, or 125 μg for a drug having an approximate density of 1 g/mL. However, the device reservoirs were not completely filled with drug in these studies, as device loadings were selected based on the minimum amount of activity (μCi) required to be above the detection sensitivity of the scintillation counters. Multiple injections of smaller volumes were performed in cases where the volume of microinjected solution was larger than the volume of the reservoir (120–130 nL), allowing time in between injections for the solution to dry (evaporation of the solutions could be observed through the microscope when loading devices).

Table 4-2 Experimental parameters for *in vitro* release devices loaded with one of ^{14}C-dextran, ^{3}H-heparin, ^{125}I-HGH, ^{125}I-IL-2, ^{14}C-BCNU, or ^{14}C-IAP.

Device #'s	Radiolabel	Specific Activity of Radiolabeled Molecule (μCi/mg)	Loading Per Reservoir	# of Reservoirs Loaded	Total Loading Per Device	Reservoir Membrane Materials	Predicted Range Of Membrane Thicknesses (μm)
1–3	^{14}C-dextran	1.09	9.1 nCi 8.4 μg	4	36.4 nCi 33.4 μg	**PLGA4.4** **PLGA11** **PLGA28** **PLGA64**	153–155
4–6	^{3}H-heparin	320	18.0 nCi 0.06 μg	4	72.0 nCi 0.23 μg	**PLGA4.4** **PLGA11** **PLGA28** **PLGA64**	150–155
7–9	^{125}I-HGH	91023	8.8 nCi 9.7×10^{-5} μg	4	35.0 nCi 3.8×10^{-4} μg	**PLGA4.4** **PLGA11** **PLGA28** **PLGA64**	153–154
10–13	^{125}I-IL-2	36600	9.6 nCi 2.6×10^{-4} μg	4	38.5 nCi 1.1×10^{-3} μg	**PLGA4.4** **PLGA11** **PLGA28** **PLGA64**	152–153
14–17	^{14}C-BCNU	293	9.2 nCi 0.03 μg	4	36.6 nCi 0.12 μg	**PLGA4.4** **PLGA11** **PLGA28** **PLGA64**	151–153
18–21	^{14}C-IAP	161	17.9 nCi 0.11 μg	3	53.8 nCi 0.33 μg	**PLGA4.4** **PLGA28** **PLGA64**	145–156

Each device was placed in a screw-cap jar containing 20 mL stirred 1X phosphate-buffered saline (PBS) at 28–33°C after drying and sealing. One mL samples of the medium were pipetted from the jars twice daily, at eight- and sixteen-hour intervals, and fresh PBS was added to the release vessels to replace the volume of solution removed. ^{14}C-dextran, ^{3}H-heparin, ^{125}I-IL-2, ^{14}C-BCNU, and ^{14}C-IAP samples were pipetted into 7-mL glass scintillation vials, and five milliliters of Fisher Scientific ScintiSafe Plus 50% scintillation cocktail were added to each vial. The samples were analyzed on a Packard Tri-Carb liquid scintillation counter, Model U2200, using a ^{125}I, ^{14}C or ^{3}H counting protocol. ^{125}I-HGH samples were pipetted into 13 mm culture tubes, capped, and analyzed on a Packard Cobra II Auto Gamma scintillation counter.

4.2.3.2.2 Double Chemical Release Studies

Devices were loaded using the same procedure as described for the single chemical studies in the section above. Three devices were loaded with both ^{125}I-HGH and ^{14}C-dextran, while four devices were loaded with ^{3}H-heparin and ^{14}C-dextran. Experiments were conducted at 28–33°C. Representative results will be presented below for two devices from each batch. **Table 4-3** below summarizes the experimental matrix for the devices that will be discussed. Release media samples were analyzed on a Packard Tri-Carb liquid scintillation counter, Model U2200 using double label protocols to count both ^{14}C and ^{3}H. Devices loaded with ^{125}I-HGH and ^{14}C-dextran had two one-milliliter media samples removed and replaced at each time point. One sample was pipetted into a 7-mL glass scintillation vial and analyzed on the Packard Tri-Carb liquid scintillation counter, Model U2200 using a ^{14}C counting protocol, while one sample was pipetted into a 13 mm culture tube, capped, and analyzed on a Packard Cobra II Auto Gamma scintillation counter to quantify the ^{125}I label present.

Table 4-3 Experimental parameters for *in vitro* release devices loaded with ^{125}I-HGH and ^{14}C-dextran, or ^{3}H-heparin and ^{14}C-dextran.

Device #'s	Radiolabel	Specific Activity Of Radiolabeled Molecule (μCi/mg)	Loading per Reservoir	# of Reservoirs Loaded	Total Loading Per Device	Reservoir Membrane Materials	Predicted Range Of Membrane Thicknesses (μm)
22	^{125}I-HGH	91023	8.8 nCi 9.6×10^{-5} μg	2	17.5 nCi 1.9×10^{-4} μg	**PLGA4.4** **PLGA28**	151–152
	^{14}C-dextran	1.09	9.1 nCi 8.3 μg	2	18.2 nCi 16.7 μg	**PLGA11** **PLGA64**	151–152
23	^{125}I-HGH	91023	8.8 nCi 9.6×10^{-5} μg	2	17.5 nCi 1.9×10^{-4} μg	**PLGA11** **PLGA64**	149–150
	^{14}C-dextran	1.09	9.1 nCi 8.3 μg	2	18.2 nCi 16.7 μg	**PLGA4.4** **PLGA28**	149–150
24 and 25	^{3}H-heparin	320	18 nCi 0.06 μg	2	36.0 nCi 0.11 μg	**PLGA4.4** **PLGA28**	152–156
	^{14}C-dextran	1.09	9.1 nCi 8.3 μg	2	18.2 nCi 16.7 μg	**PLGA11** **PLGA64**	152–156

4.3 Results and Discussion

4.3.1 Device Design and Fabrication

Control over the release times was achieved in this study by varying the molecular weight of the materials from which the reservoir membranes were fabricated. Devices were fabricated and loaded with chemicals via two compression molding steps, and two microinjection steps, as detailed in Chapters 2 and 3. The devices were approximately 11.9 mm in diameter and between 470 and 645 μm thick (reservoir openings ranged in size from 389 to 259 μm in diameter, respectively). Membrane thicknesses (approximately 150 μm) and molecular weights (M_ws of 4,400, 11,000, 28,000, and 64,000 daltons) were chosen which would provide chemical releases from the devices over a period of approximately eight weeks, based on results from previous *in vitro* release studies that were performed.

4.3.2 *In Vitro* Release Studies

4.3.2.1 Single Chemical Release Studies

The objective of initial release experiments was to determine if pulsatile release of a single compound could be obtained from the microreservoir device. The following sections present the results obtained for devices loaded with one of the following radiolabeled chemicals: ^{14}C-dextran, ^{3}H-heparin, ^{125}I-HGH, ^{125}I-IL-2, ^{14}C-BCNU, or ^{14}C-IAP.

4.3.2.1.1 ^{14}C-dextran

The results for the three devices loaded with ^{14}C-dextran are shown in **Figure 4.1**. The first release was detected from the reservoirs having **PLGA4.4** membranes on the first day of the study. The reservoirs having **PLGA11** membranes showed the onset of release between 13 and 15 days. The reservoirs having **PLGA28** membranes showed release between 27 and 34 days, followed by the **PLGA64** membranes at 30 to 37 days.

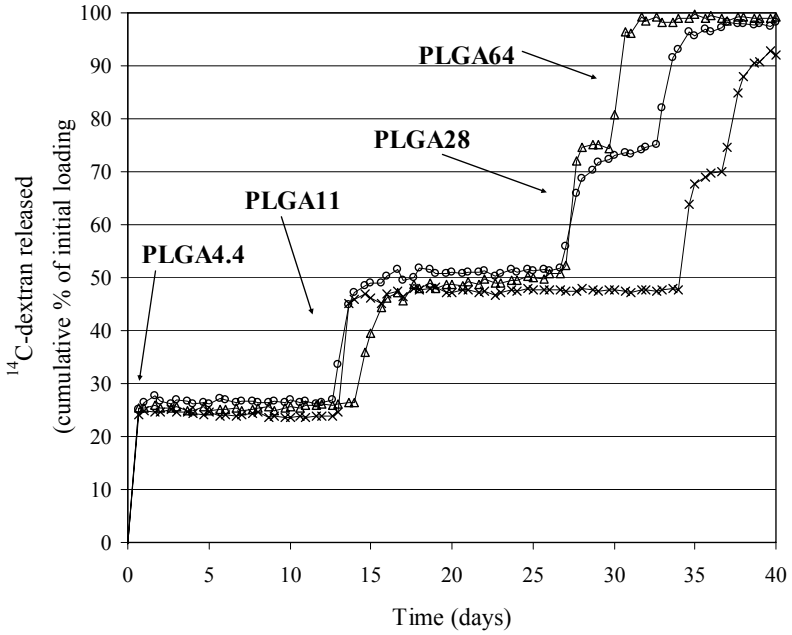

Figure 4.1 Cumulative percentage of initial ^{14}C-dextran loading released from three devices having **PLGA4.4**, **PLGA11**, **PLGA28**, and **PLGA64** reservoir membranes in saline solution at 28–33°C *in vitro*.

An interesting point of note is that although the **PLGA64** membrane had more than double the molecular weight of the **PLGA28** membrane (similar to the relation between the **PLGA11** and **PLGA4.4** membrane materials), the separation in release times was not as large as that seen for the lower molecular weight membranes. However, this is not a completely unexpected result, as the process of random chain scission by which the polymers are hydrolyzed and degraded will cause higher molecular weight polymers to end up with broader molecular weight distributions and consequent greater variation in the release time. The range of release times for the **PLGA28** and **PLGA64** membrane materials actually overlapped from 30 to 34 days. Similar results were obtained for the other experiments in this study, as will be discussed below. Further characterization of the *in vitro* degradation of the membrane polymers is presented in Chapter 5. All of the devices, however, clearly showed four pulses of ^{14}C-dextran, and the total cumulative amounts of loading recovered were 92–99% at 40 days.

4.3.2.1.2 ^{3}H-heparin

The three devices loaded with ^{3}H-heparin showed similar results to those loaded with ^{14}C-dextran, both in terms of release times and reproducibility.

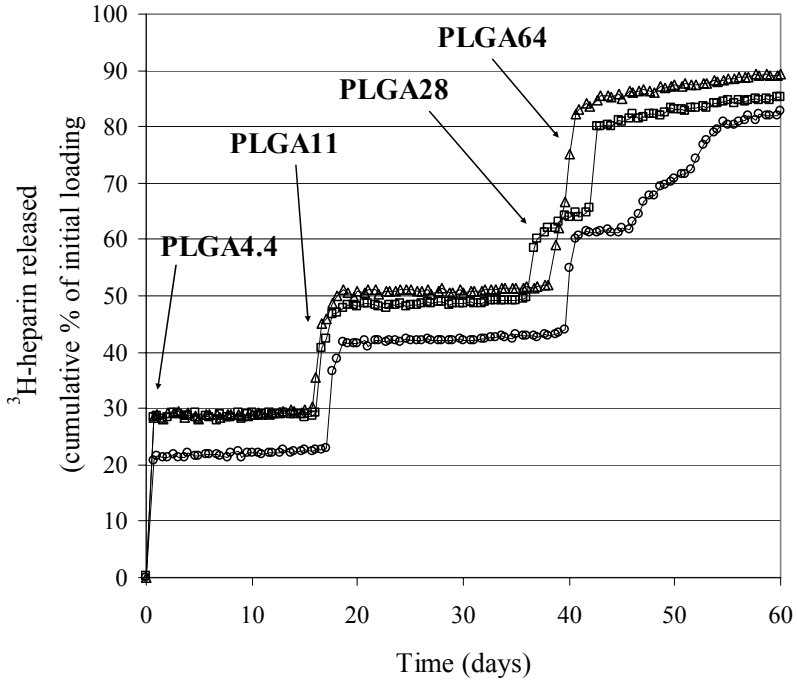

Figure 4.2 Cumulative percentage of initial ^{3}H-heparin loading released over time from three devices having **PLGA4.4**, **PLGA11**, **PLGA28**, and **PLGA64** reservoir membranes in saline solution at 28–33°C *in vitro*.

The reservoirs having membranes made from **PLGA4.4** showed release on the first day of the study, followed by the **PLGA11** membranes between 16 and 18 days. The reservoirs having **PLGA28** membranes showed release much later, between 37 and 40 days, followed closely by the **PLGA64** reservoir membranes at 40–47 days. The total cumulative amount of initial ^{3}H-heparin loading detected was 83–89% at 60 days. The slightly lower cumulative measured loading may be due to the lower counting efficiency of the scintillation counter for ^{3}H as compared to ^{14}C.

One of the ^{3}H-heparin loaded devices (△ symbol in **Figure 4.2**) did not show separate pulses for the reservoirs having **PLGA28** and **PLGA64** membranes. Additionally, a third device (○ symbol in **Figure 4.2**) showed a prolonged release for the reservoir with a **PLGA64** membrane, from approximately 46 to 56 days. It is not clear why this occurred, and this behavior was seldom seen for other large radiolabeled molecules. However, somewhat sustained release curves, similar to the curve in question, were seen for smaller radiolabeled molecules, and are discussed in sections 4.3.2.1.5 and 4.3.2.1.6 below.

4.3.2.1.3 ^{125}I-HGH

The results for three devices loaded with ^{125}I-HGH are shown in **Figure 4.3**. The first release occurred at day one, when the reservoirs having membranes made from **PLGA4.4** opened. Detection of the second release, from the reservoirs having **PLGA11** membranes, occurred between days six to ten. Greater variation was seen for the reservoirs having **PLGA28** (17 to 22 days) and **PLGA64** (20 to 30 days) membranes. The fluctuations in the release curve are most likely due to the high gamma radiation background, which decreases the detection sensitivity of the scintillation counter. This may also explain the high cumulative total percentages of the initial loading that were detected at day 40, which ranged from 108 to 134%.

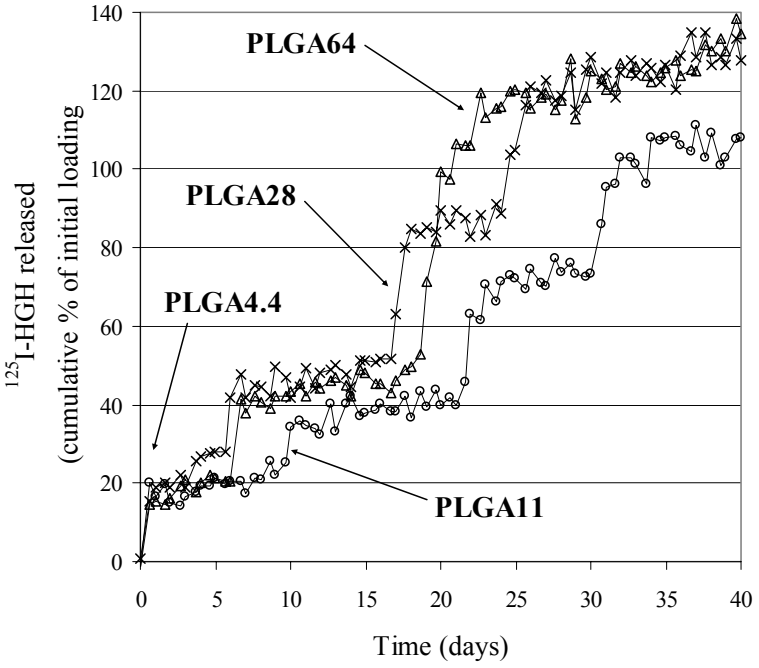

Figure 4.3 Cumulative percentage of initial ^{125}I-HGH loading released over time from three devices having **PLGA4.4**, **PLGA11**, **PLGA28**, and **PLGA64** reservoir membranes in saline solution at 28–33°C *in vitro*.

Overall, however, two out of the three devices showed four distinct pulses of ^{125}I-HGH. The third device (△ symbol in **Figure 4.3**) showed a large pulse starting at day 19 that appeared to be the release of ^{125}I-HGH from both of the reservoirs having **PLGA28** and **PLGA64** membranes. This result is similar to that seen for one of the devices loaded with ^{3}H-heparin, as discussed in section 4.3.2.1.2.

4.3.2.1.4 ^{125}I-IL-2

The results presented thus far clearly demonstrate the feasibility of using the polymeric microreservoir device for multi-pulse delivery of molecules. The possibility of delivering a number of other molecules, however, was also tested, based on the considerations presented in section 4.2.2. While the studies presented in the next three sections for ^{125}I-IL-2, ^{14}C-BCNU, and ^{14}C-IAP were not as successful in demonstrating pulsatile release as those previously presented for ^{14}C-dextran, ^{3}H-heparin, and ^{125}I-HGH, they are nevertheless important as they illustrate some of the limitations of the device, and therefore serve to delineate some of the factors that control device performance.

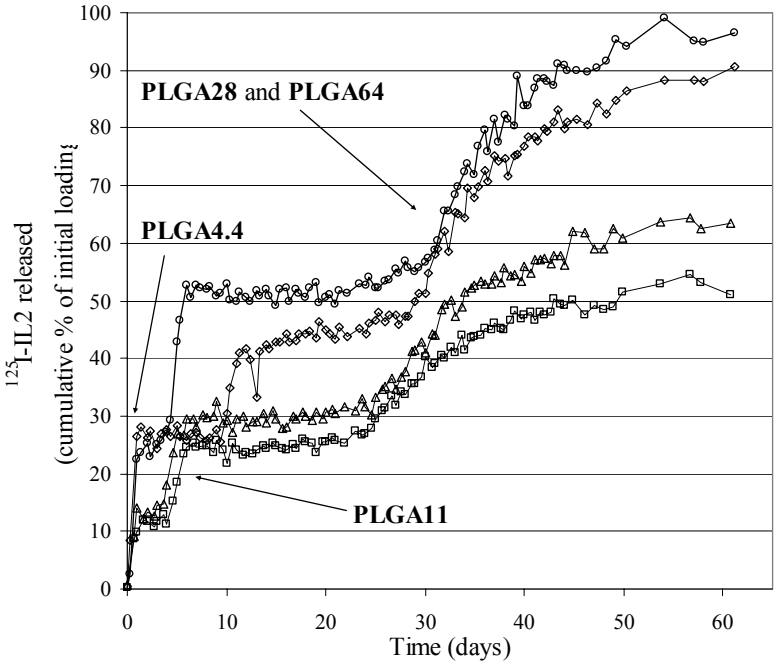

Figure 4.4 Cumulative percentage of initial ^{125}I-IL-2 loading released over time from four devices having reservoir membranes made from **PLGA4.4**, **PLGA11**, **PLGA28**, and **PLGA64** in saline solution at 28–33°C *in vitro*.

The cumulative release results for four devices loaded with ^{125}I-IL-2 are shown in **Figure 4.4** above. The release curves for these devices are more similar to those shown in **Figure 4.3** for ^{125}I-HGH than for either the ^{14}C-dextran or ^{3}H-heparin. This is not surprising, as both HGH and IL-2 are proteins, with similar molecular weights (~21,500 daltons for HGH, ~15,000 daltons for IL-2). The first two releases can be seen quite clearly in **Figure 4.4**, with the reservoirs having **PLGA4.4** membranes releasing their contents on the first day of the study, and the reservoirs

having **PLGA11** membranes opening between days four and ten. The releases for the reservoirs having the **PLGA28** and **PLGA64** membranes, however, appear to overlap so significantly that there is no discernible separation of the curves into two distinct pulses. This result is no doubt partially explained by the similar opening times of the **PLGA28** and **PLGA64** reservoir membranes, as was seen for the other devices in this study (^{14}C-dextran, ^{3}H-heparin, and ^{125}I-HGH loadings). In the case of ^{125}I-IL-2, however, the apparent merging of the third and fourth pulses from these devices may be the result of the fact that IL-2 adsorbs to glass and plastic[22]. Although the jars in which the experiments took place were silanized to prevent surface adsorption, the devices themselves, as well as the glass slides to which they were affixed and the pipet tips that were used to take the release samples, were not silanized. Therefore, it is likely that although there was not significant IL-2 loss due to sticking during the early portion of the experiments, at later times the amount lost may have become significant. This hypothesis is consistent with the clear pulses seen from the reservoirs having **PLGA4.4** and **PLGA11** membranes, as well as the lack of clear pulses from the reservoirs having **PLGA28** and **PLGA64** membranes, and the low total amount of ^{125}I-IL-2 detected (<100%).

4.3.2.1.5 ^{14}C-BCNU

The release results for four devices having **PLGA4.4**, **PLGA11**, **PLGA28**, and **PLGA64** reservoir membranes and loaded with ^{14}C-BCNU are shown in **Figure 4.5** below.

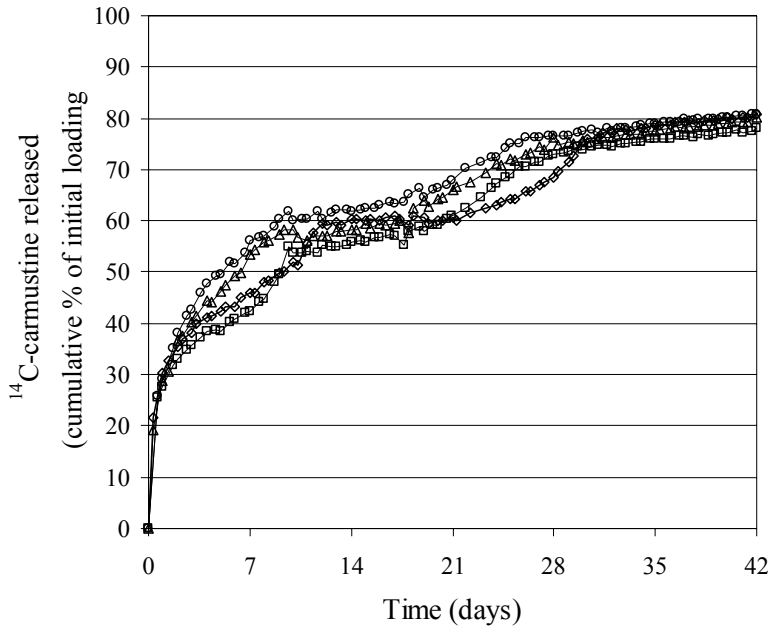

Figure 4.5 Cumulative percentage of initial ^{14}C-carmustine (BCNU) loading released over time from four devices having **PLGA4.4**, **PLGA11**, **PLGA28**, and **PLGA64** reservoir membranes in saline solution at 28–33°C *in vitro*.

In contrast to the other data presented thus far, the devices loaded with BCNU showed essentially no distinguishable pulses. However, it does not appear that all of the membranes opened immediately at the start of the experiment. If this had been the case, we would expect to see nearly 100% of the loading detected at day one. The shape of the curve, however, is very similar to that characteristic of diffusion curves ($\propto t^{1/2}$). The lipophilicity/hydrophobicity of this molecule, combined with its small molecular weight (see the chemical structure in **Figure 4.6** below), may have caused it to partition into and diffuse through the membranes. In fact, studies to determine the partition coefficient of this molecule in the membrane polymers (see Chapter 6) showed that it does indeed partition into the membranes, albeit less so for the **PLGA11**, **PLGA28**, and **PLGA64** materials than for the **PLGA4.4** polymer. Although the partitioning coefficient in the higher molecular weight polymers may be less significant than that in the **PLGA4.4**, diffusion of the molecule through the membranes may become more significant at the longer times scales on which the higher molecular weight polymers degrade, and this may explain the sustained release curve seen in **Figure 4.5**.

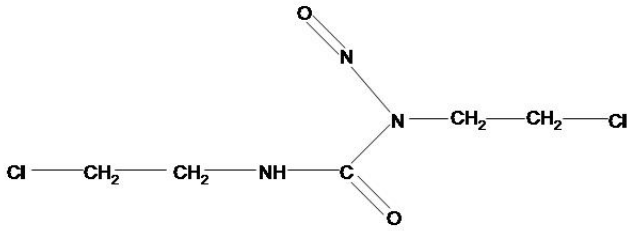

Figure 4.6 Chemical structure of 1,3-bis(2-chloroethyl)-1-nitrosourea (BCNU) or carmustine.

Another factor which may contribute to the atypical release behavior for this chemical is that BCNU is known to undergo hydrolysis in aqueous solutions, forming acetaldehyde, hydrochloric acid, nitrogen gas, and derivatives of 2-chloroethyl isocyanate[23]. Although later experiments (see Chapter 7) suggest that permeation of water into the reservoirs is minimal prior to membrane opening, the presence of some water in the reservoirs may cause degradation of the BCNU. Acidic products such as the hydrochloric acid might therefore cause more rapid degradation of the membrane materials, but it does not appear that this effect is significant, as the time to achieve nearly complete release of the drug from the reservoirs is comparable for these devices loaded with BCNU as for the other devices presented in this chapter.

4.3.2.1.6 ^{14}C-IAP

The release data for four devices having **PLGA4.4**, **PLGA28**, and **PLGA64** membranes and loaded with ^{14}C-IAP are shown in **Figure 4.7** below. These experiments were performed prior to the others presented here, and as such only three membrane polymers were used on the device. A comparison of the curves for ^{14}C-IAP in **Figure 4.7** with the ^{14}C-BCNU curves in **Figure 4.5**, however, clearly shows that the kinetics of release are quite similar. A relatively larger plateau is evident after the release of ^{14}C-IAP from the reservoirs having **PLGA4.4** membranes, due to the absence of a reservoir with a **PLGA11** membrane. The curve assumes a diffusion-type shape towards the end of the study, similar to that seen in **Figure 4.5** for the ^{14}C-

BCNU. Similar to BCNU, later experiments (see Chapter 6) determined that this molecule partitions into the membrane polymers, which might explain the results seen here. The chemical structure of this compound is shown in **Figure 4.8** below, and it is clear that the molecule is much smaller than the large proteins and polysaccharides that were used in the release studies presented previously. Optical microscopy of the devices after completion of the experiment showed that all of the reservoir membranes were open or ruptured.

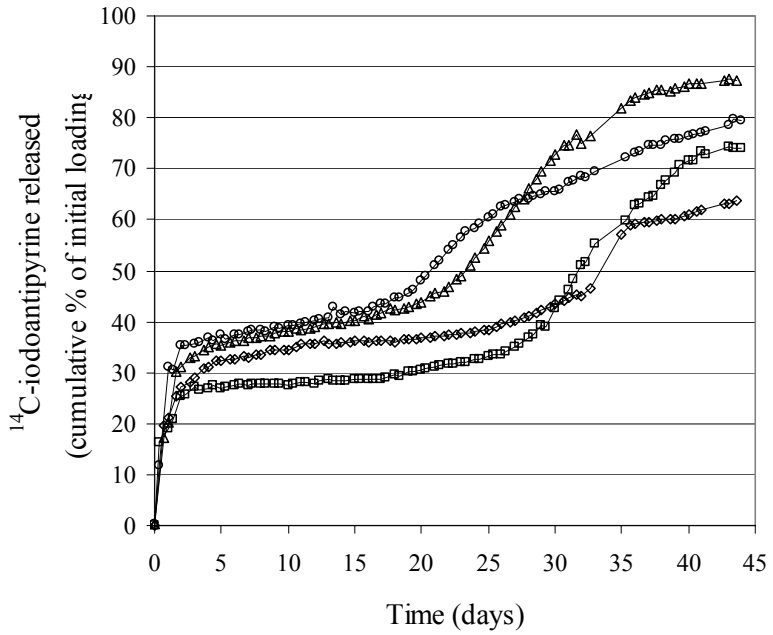

Figure 4.7 Cumulative percentage of initial ^{14}C-iodoantipyrine (IAP) loading released over time from four devices having **PLGA4.4**, **PLGA28**, and **PLGA64** reservoir membranes in saline solution at 28–33°C *in vitro*.

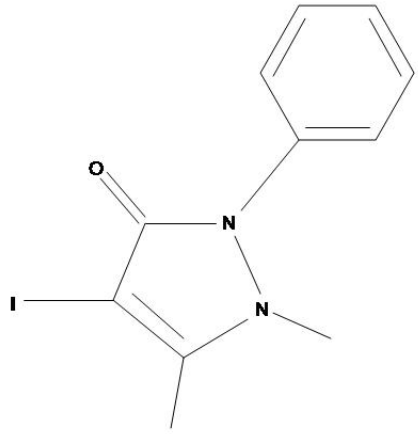

Figure 4.8 Chemical structure of iodoantipyrine (IAP).

The release results seem to indicate that the time and temperature of the drying step in the oven do not significantly affect the release characteristics of the device within the sensitivity of the analysis. Although the **PLGA28** and **PLGA64** reservoir membranes on these four devices were dried for only 16 hours at 68°C, instead of at 71–74°C for 48 hours as was the case for the other devices presented in this chapter, the release profiles of the ^{14}C-iodoantipyrine are quite similar to the profiles seen for ^{14}C-BCNU shown in **Figure 4.5**. Additionally, although the **PLGA4.4** membranes were not dried under vacuum, as they were microinjected into the device after the **PLGA28** and **PLGA64** reservoirs had been loaded with ^{14}C-IAP, this did not affect the release time from the reservoirs, as evidenced by the uniform release from the reservoirs having **PLGA4.4** membranes at day one in this as well as all of the other *in vitro* release studies presented in this thesis.

4.3.2.1.7 Discussion

The initial experiments presented here confirm that it is possible to release up to four pulses of a single chemical from the polymeric microreservoir devices. The larger molecules (^{14}C-dextran, ^{3}H-heparin, ^{125}I-HGH, and ^{125}I-IL-2) showed release that was more clearly pulsatile than the smaller molecules (^{14}C-BCNU and ^{14}C-IAP). The devices loaded with ^{14}C-dextran and ^{3}H-heparin had on average the best recovery of the initial loading, with 83–99% of the initial loading recovered over the course of the study.

The release times of the different chemicals are summarized in **Table 4-4** below. The release times are similar at relatively short elapsed times, but at longer time periods there is more variation in the release times of the reservoirs having **PLGA28** and **PLGA64** membranes for a device with a given chemical loading. Additionally, the release times for the reservoirs having **PLGA28** and **PLGA64** membranes showed greater variation when the chemical loading was changed than did the reservoirs with **PLGA4.4** and **PLGA11** membranes. These observations indicate that the degradation mechanisms of the membrane polymers are somewhat complex. A more in-depth study of the degradation of the membrane polymers is presented in Chapter 5.

Table 4-4 Average release times ± standard deviations (in days) from reservoirs on devices loaded with one of ^{14}C-dextran, ^{3}H-heparin, or ^{125}I-HGH and having membranes made from **PLGA4.4**, **PLGA11**, **PLGA28**, and **PLGA64**.

		Membrane Polymer			
Device #'s	Molecule (single chemical loading expts)	**PLGA4.4**	**PLGA11**	**PLGA28**	**PLGA64**
1-3	^{14}C-dextran	1±0	14±1	30±4	33±3
4-6	^{3}H-heparin	1±0	17±1	38±2	43±3
7-9	^{125}I-HGH	1±0	8±2	19±2	25±6

It is unlikely that the difference in release times between the devices loaded with different chemicals can be attributed to membrane material or fabrication variation, as the membranes were fabricated from the same materials and by the same operator in a single day. Further, the injected volume of membrane solution was adjusted to account for small variations in reservoir size in an effort to keep the membrane thicknesses constant. The results we obtained therefore suggest that the structure and chemistry of the molecules released from the devices may be an important component in explaining the disparity in their release times. Others have reported differences in release rates for neutral capped amino acids and positively-charged cyclic hexapeptides from PLGA microspheres, and have hypothesized that this is due to specific interactions between the molecules and the PLGA (adsorption on hydrophobic regions of the DL-PLGA)[24]. No effect on release kinetics was seen, however, as a result of changes in the size, charge, or conformational flexibility of the model peptides released from the microspheres. Evaluation of the interactions between the PLGA membranes and chemicals used in the

experiments reported here (as reflected by the partition coefficient), and the effects of molecule size on the observed release time and are more fully explored in Chapters 6 and 7, respectively.

Different molecular weights of PLGA (50:50) with carboxylic acid chain end groups were used to control the release time for these initial release experiments of a single compound loaded into a device. Changing the end group of the polymer, however, could change the degradation rate of the polymers and consequently modulate the release time. For example, in an experiment similar to the ones described here, ^{14}C-methylated dextran (M_w 70,000) was released from a device having reservoirs with membranes made from the PLGA 50:50 **PLGA4.4**, **PLGA11**, **PLGA28**, and **PLGA64** polymers. Additionally, one reservoir had a membrane made from PLGA 50:50, having a molecular weight of 7,500 daltons and ester end groups (**PLGA7.5e**). This device showed release from the reservoir having a **PLGA7.5e** membrane between the releases of reservoirs having **PLGA11** and **PLGA28** membranes (data not shown), even though the molecular weight of the **PLGA7.5e** was much smaller than that of the **PLGA11** or **PLGA28** polymers. The apparent slower degradation of the **PLGA7.5e** when compared to the **PLGA11** membrane is most likely due to the presence of ester end groups on the **PLGA7.5e** chains, which are less reactive and therefore are hydrolyzed more slowly. Although these ester groups represent only two bonds in the entire chain, the significantly less electrophilic nature of the ester end groups compared to typical carboxylic acid end groups causes the ester end groups to act as end caps on the chain, resulting in significantly slower degradation rate of the polymer. Other factors that may potentially be changed to tailor the observed release time of chemicals from the reservoirs on this device are the thicknesses of the membranes, copolymer composition, or membrane materials.

4.3.2.2 Double Chemical Release Studies

Subsequent release experiments were performed in order to determine if the independent release of multiple compounds from single devices could be achieved, as well as to further elucidate the behavior of the **PLGA28** and **PLGA64** membranes. These devices contained ^{14}C-dextran and ^{125}I-HGH, or ^{14}C-dextran and ^{3}H-heparin. On each device, a total of four reservoirs had PLGA membranes made from **PLGA4.4**, **PLGA11**, **PLGA28**, and **PLGA64**. In general, reservoirs having **PLGA11** and **PLGA64** membranes were loaded with ^{14}C-dextran, while

reservoirs having **PLGA4.4** and **PLGA28** membranes were usually loaded with either ^{125}I-HGH or ^{3}H-heparin.

4.3.2.2.1 ^{125}I-HGH and ^{14}C-dextran

The release results from a representative device loaded with ^{125}I-HGH and ^{14}C-dextran (device 22 from Table 4-3) are shown in **Figure 4.9** below. The reservoir having a **PLGA4.4** membrane and containing ^{125}I-HGH showed release at day one. The reservoir having a **PLGA11** membrane and loaded with ^{14}C-dextran opened on day 16. This was followed by the opening of the reservoir that had a **PLGA28** membrane and that was loaded with ^{125}I-HGH at day 23, and finally the reservoir with a **PLGA64** membrane that was loaded with ^{14}C-dextran at day 36.

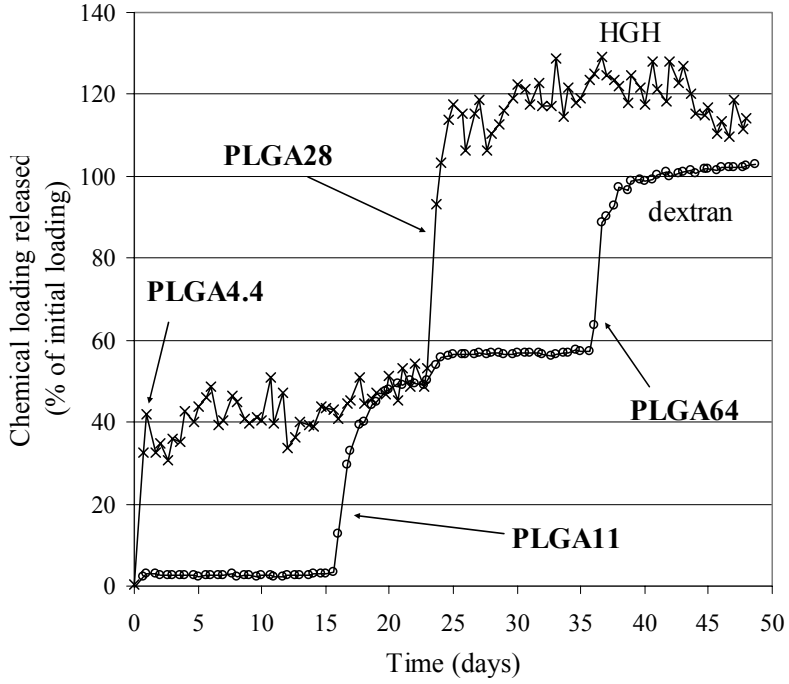

Figure 4.9 Cumulative percentages of initial ^{125}I-HGH (×) and ^{14}C-dextran (○) loadings released over time from a single device. ^{125}I-HGH released from reservoirs having **PLGA4.4** and **PLGA28** membranes. ^{14}C-dextran released from reservoirs having **PLGA11** and **PLGA64** membranes. Experiment performed in saline solution at 28–33°C *in vitro*.

Totals of 102% of the initial ^{14}C-dextran loading and 117% of the initial ^{125}I-HGH loading were measured after 45 days. The small plateaus (approximately 3% of the total loading for each plateau) in the ^{14}C-dextran curves beginning at days zero and 23, when the ^{125}I-HGH pulses occur, suggest a contribution to the ^{14}C counts from the ^{125}I present in the sample. Two

different scintillation counters were used to measure the ^{125}I (Packard Cobra II Auto Gamma) and ^{14}C (Packard Tri-Carb) counts. Although a ^{14}C only counting protocol was used for the samples analyzed on the Tri-Carb counter, the ^{125}I isotope emits gamma particles within the energy range used to detect the ^{14}C (from 0 to 156 keV). Therefore, the small plateaus in the ^{14}C-dextran curve starting at days zero and 23 are likely due to the presence of the ^{125}I-HGH in the release medium.

The large percentage of ^{125}I-HGH measured by the Cobra II Auto Gamma may be due to the low sensitivity of the scintillation counter at such small measured activities, which were on average between 0.1 and 0.2 nCi. The typical measured error was between 7 and 25%, and up to 40% for samples with readings similar to background. Further, although a standard curve was run with each batch of samples that were analyzed, the short half-life (60 days) of ^{125}I may have created additional uncertainty at the low activities that were used.

One out of three of the devices that were loaded with both ^{125}I-HGH and ^{14}C-dextran showed release from the reservoir having a **PLGA64** membrane earlier than from the reservoir having a **PLGA28** membrane. The release results for this device (device 23 from **Table 4-3**) are shown in **Figure 4.10** below. This device was slightly different than the other two that were loaded with both ^{125}I-HGH and ^{14}C-dextran, as the ^{125}I-HGH was loaded into the reservoirs that had **PLGA11** and **PLGA64** membranes, while the ^{14}C-dextran was loaded into the reservoirs that had **PLGA4.4** and **PLGA28** membranes. Therefore, we would expect the order of releases to be dextran (from the reservoir with a **PLGA4.4** membrane), followed by HGH (**PLGA11** membrane), then dextran again (**PLGA28** membrane), and finally HGH again (**PLGA64** membrane). As can be seen in **Figure 4.10**, however, the order of releases was dextran, then HGH, then the second HGH pulse, and finally the second dextran release, clearly indicating that the reservoir with the **PLGA64** membrane (loaded with HGH) released earlier than the reservoir with the **PLGA28** membrane (loaded with dextran).

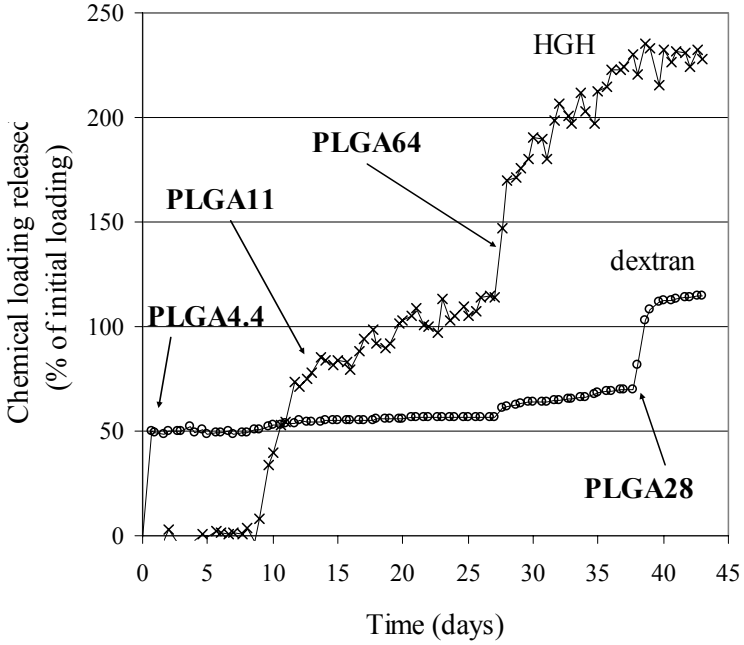

Figure 4.10 Cumulative percentages of initial ^{125}I-HGH (×) and ^{14}C-dextran (○) loadings released over time from a single device. ^{125}I-HGH released from reservoirs having **PLGA11** and **PLGA64** membranes. ^{14}C-dextran released from reservoirs having **PLGA4.4** and **PLGA28** membranes. The reservoir having a membrane made from the **PLGA64** polymer opened earlier than the reservoir having a membrane made from the **PLGA28** polymer on this device. Experiment performed in saline solution at 28–33°C *in vitro*.

Although the **PLGA64** polymer has a higher molecular weight than the **PLGA28** polymer, it does not always appear to take a longer time to degrade. It is unlikely that a difference in device manufacture, membrane fabrication, or device loading can account for the observed result of faster **PLGA64** degradation compared to the **PLGA28** degradation, as all of the devices in this batch (^{125}I-HGH and ^{14}C-dextran loading) were fabricated at the same time and in an identical manner. Additionally, analyses performed by the manufacturer to characterize the **PLGA28** and **PLGA64** polymers provide no explanation for the observed behavior. These two polymers were nearly identical in chemical composition; both were 54 mole% D,L-lactic acid and 46 mole% glycolic acid (confirmed by ^{1}H-NMR analysis), with 1.2% residual D,L-lactide monomer. The **PLGA28** had 0.2% residual glycolide monomer, while the **PLGA64** had 0.1% residual glycolide monomer. Given the nearly identical chemistries of the two polymers, we would expect the degradation rates to be controlled by the molecular weights of the two materials and that therefore the **PLGA64** material would take longer to degrade. However, the apparently faster degradation rate of the **PLGA64** polymer on some devices could perhaps be

explained by differing degrees of monomer block length within the polymer chains. While the PLGA polymers used to fabricate the membranes are supposed to be random copolymers (alternating, randomly sized blocks of lactic acid and glycolic acid units in the polymer chain backbones), the presence of longer blocks of lactic acid or particularly glycolic acid could cause the formation of crystallites as the oligomer blocks associate. Crystallites formed from PLA and PGA oligomers during the degradation of PLA[25–27] and PGA[28,29] homopolymers have been shown to be quite resistant to further hydrolysis and degradation. Additionally, greater reactivity of the glycolic acid during copolymerization has been hypothesized to cause formation of glycolide blocks within the copolymer backbone that are separated by single lactide units[30]. Larger monomer block size of the **PLGA28** might therefore explain the slower degradation rate that is sometimes observed compared to the **PLGA64**.

Similar to the release data shown in **Figure 4.9**, a slight increase in the measured amount of ^{14}C-dextran can be seen in **Figure 4.10** when the ^{125}I-HGH releases were detected from this device, most likely due to the contribution of the ^{125}I radiation to the scintillation counts for the ^{14}C isotope. The large cumulative amounts of ^{125}I-HGH measured over the course of the study may be due to the fact that this device was loaded first out of the three that had both ^{125}I-HGH and ^{14}C-dextran. If no test injections were done on a glass slide prior to loading of the first device, the solution may have been more concentrated at the needle tip due to evaporation (see section 3.3.1.1) and therefore more HGH may have been loaded into the reservoirs than was thought.

4.3.2.2.2 ^{3}H-heparin and ^{14}C-dextran

The release results for a representative device loaded with ^{3}H-heparin and ^{14}C-dextran (device 24 from **Table 4-3**) are shown in **Figure 4.11** below. The reservoir that had a **PLGA4.4** membrane and that was loaded with ^{3}H-heparin opened at day one. The reservoir that had a **PLGA11** membrane was loaded with ^{14}C-dextran, and opened on day 16. The reservoir that had a **PLGA28** membrane and was loaded with ^{3}H-heparin, showed release on day 33, and the reservoir having a **PLGA64** membrane and loaded with ^{14}C-dextran showed release on day 38.

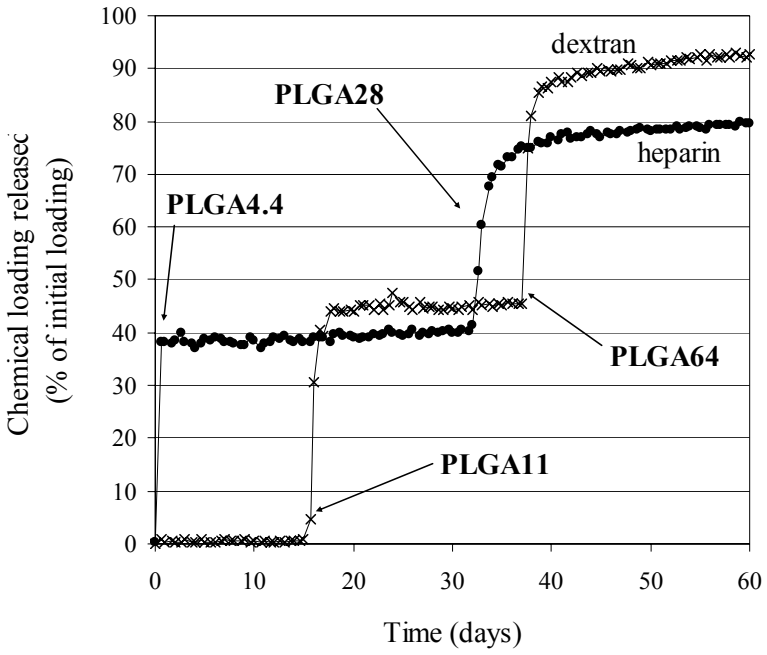

Figure 4.11 Cumulative percentages of initial ^{3}H-heparin (●) and ^{14}C-dextran (×) loadings released over time from a single device. ^{3}H-heparin released from reservoirs having **PLGA4.4** and **PLGA28** membranes, ^{14}C-dextran released from reservoirs having **PLGA11** and **PLGA64** membranes. Experiment performed in saline solution at 28–33°C *in vitro*.

Totals of 80% of the initial ^{3}H-heparin loading and 93% of the initial ^{14}C-dextran loading were measured after 60 days. Each chemical was released in two almost exactly equal pulses. The mathematical method used by the scintillation counter to separate the counts due to each isotope, as well as the calibration based on a quench curve, may account for the fact that the measured amount of each chemical released is less than 100%.

Similar to the devices that were loaded with ^{125}I-HGH and ^{14}C-dextran discussed in section 4.3.2.2.1, one out of four of these devices loaded with ^{3}H-heparin and ^{14}C-dextran showed release from the reservoir having a **PLGA64** membrane prior to the release from the reservoir having a **PLGA28** membrane. The results for this device (device 25 in **Table 4-3**) are shown in **Figure 4.12** below.

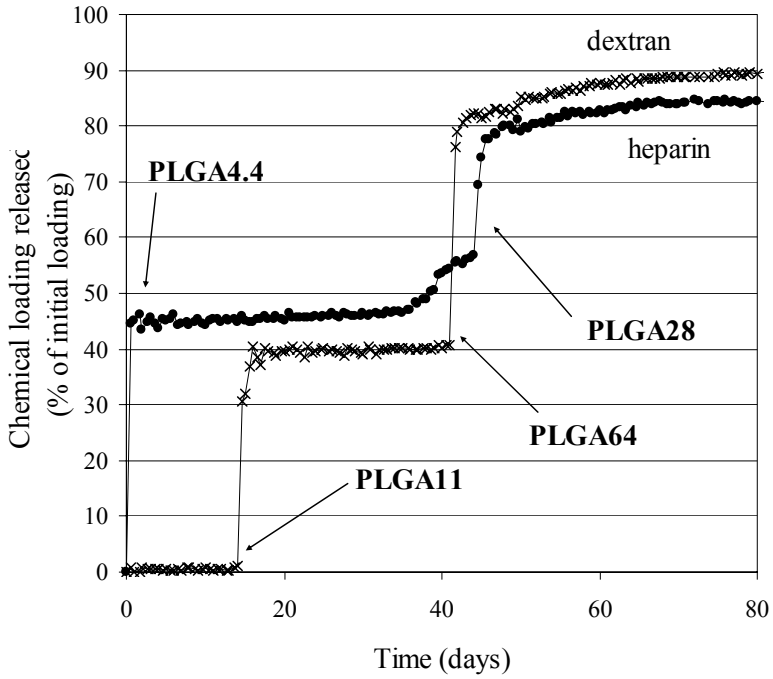

Figure 4.12 Cumulative percentages of initial ^{3}H-heparin (●) and ^{14}C-dextran (×) loadings released over time from a single device. ^{3}H-heparin released from reservoirs having **PLGA4.4** and **PLGA28** membranes, ^{14}C-dextran released from reservoirs having **PLGA11** and **PLGA64** membranes. The reservoir having a membrane made from the **PLGA64** polymer opened earlier than the reservoir having a membrane made from the **PLGA28** polymer on this device. Experiment performed in saline solution at 28–33°C *in vitro*.

The release of the ^{3}H-heparin was detected from the reservoir having a **PLGA4.4** membrane at day one, followed by the release of ^{14}C-dextran from the reservoir having a **PLGA11** membrane at 15 days. The ^{14}C-dextran was released from the reservoir having a **PLGA64** membrane at 42 days. The ^{3}H-heparin appeared to start releasing from the reservoir with a **PLGA28** membrane at around 37 days, but a large burst was not seen until 45 days.

4.3.2.2.3 Discussion

The release times for these studies showing release of multiple chemicals from single devices correlate well with those shown in the initial single chemical studies described in section 4.3.2.1 above. The average release times for the devices having a single chemical loading are reproduced below in **Table 4-5** for ease of comparison with the release times for the devices having double chemical loadings, which are summarized in **Table 4-6** below.

Table 4-5 Average release times ± standard deviations (in days) from reservoirs on devices loaded with one of ^{14}C-dextran, ^{3}H-heparin, or ^{125}I-HGH and having membranes made from **PLGA4.4**, **PLGA11**, **PLGA28**, and **PLGA64**. (Reproduced from **Table 4-4**)

		Membrane Polymer			
Device #'s	Molecule (single chemical loading expts)	**PLGA4.4**	**PLGA11**	**PLGA28**	**PLGA64**
1-3	^{14}C-dextran	1±0	14±1	30±4	33±3
4-6	^{3}H-heparin	1±0	17±1	38±2	43±3
7-9	^{125}I-HGH	1±0	8±2	19±2	25±6

Table 4-6 Range of observed release times (in days) from reservoirs on devices loaded with either ^{125}I-HGH and ^{14}C-dextran, or ^{3}H-heparin and ^{14}C-dextran, and having membranes made from **PLGA4.4**, **PLGA11**, **PLGA28**, and **PLGA64**.

		Membrane Polymer			
Device #	Molecule (double chemical Loading expts)	**PLGA4.4**	**PLGA11**	**PLGA28**	**PLGA64**
22	^{125}I-HGH	1		23	
	^{14}C-dextran		16		36
23	^{125}I-HGH		10		28
	^{14}C-dextran	1		38	
24	^{3}H-heparin	1		33	
	^{14}C-dextran		16		38
25	^{3}H-heparin	1		37-45	
	^{14}C-dextran		15		42

Devices 22 and 24 showed the expected order of release, while devices 23 and 25 showed release from the reservoirs having **PLGA64** membranes prior to release from the reservoirs

having **PLGA28** membranes. Comparison of the results in **Table 4-5** and **Table 4-6**, however, reveals that in the case of device 23, although the reservoir with a **PLGA64** membrane released earlier than the reservoir with a **PLGA28** membrane, the release times for these two reservoirs are fairly consistent with the results obtained for the devices loaded with a single chemical. For example, **Table 4-5** shows that ^{125}I-HGH was detected at 25±6 days from the reservoirs having membranes made from **PLGA64**. The release of ^{125}I-HGH at 28 days from the reservoir on device 23 having a **PLGA64** membrane is consistent with this result. Release of the ^{14}C-dextran from the reservoir having a **PLGA28** membrane on this device, however, occurred at 38 days, which is slightly longer than the range of 30±4 days seen for the devices in **Table 4-5** loaded with ^{14}C-dextran. Nevertheless, the fact that the ^{125}I-HGH release times were consistently earlier than those for the reservoirs loaded with ^{14}C-dextran on any of the devices explains why the results for this device show opening of the **PLGA28** reservoir membrane prior to that of the **PLGA64** reservoir membrane.

Similarly, the results obtained for device 25 are consistent with the results for the devices in **Table 4-5** that had single chemical loadings. The release time of 37–45 days for the **PLGA28** reservoir loaded with ^{3}H-heparin overlaps with the range of 38±2 days seen for devices in **Table 4-5**. The release time of 42 days for the ^{14}C-dextran from the **PLGA64** reservoir is only slightly later than the range of 33±3 days seen for devices in **Table 4-5**. Even if these reservoirs had released their contents within the time period observed for release from the devices with single chemical loadings, however (38±2 days for ^{3}H-heparin in **PLGA28** reservoir and 33±3 days for ^{14}C-dextran in **PLGA64** reservoir), the **PLGA64** reservoir would still have showed release earlier than the reservoir with a **PLGA28** membrane.

The results in **Table 4-5** clearly show that the release times from reservoirs with a membrane of a given polymer vary depending on the chemical that is loaded into the reservoir. Reservoirs loaded with ^{125}I-HGH showed the fastest release, while reservoirs loaded with ^{3}H-heparin showed the slowest release. These results suggest that the chemistry of the drug loaded into the reservoirs may affect the observed release time. This hypothesis is discussed further in Chapter 5, but can be grasped by the representation of data in **Figure 4.13** below. This graph shows the observed release times for each chemical from reservoirs having each of the different membrane polymers, and includes the results from both the single and double chemical release studies.

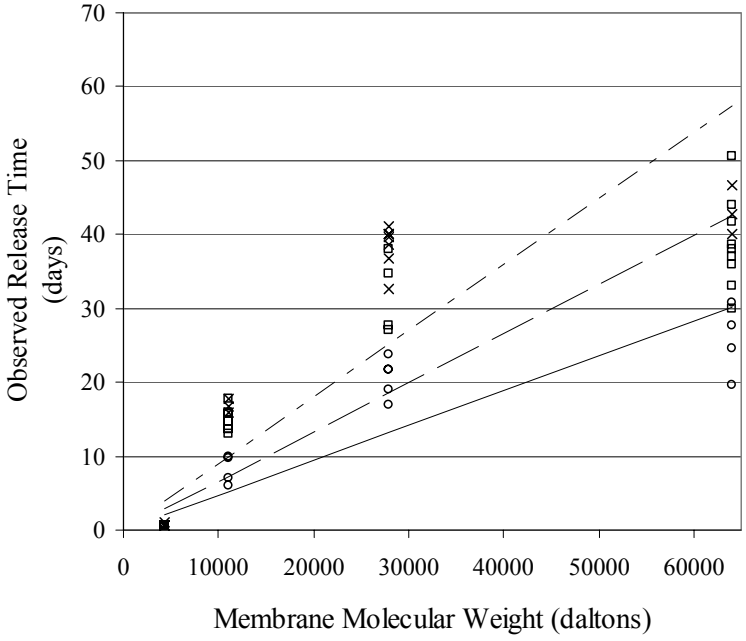

Figure 4.13 Compiled release times for single and double loaded devices having **PLGA4.4** (M_w 4400), **PLGA11** (M_w 11,000), **PLGA28** (M_w 28,000) and **PLGA64** (M_w 64,000) ~150 μm thick reservoir membranes. ^{125}I-HGH: ○ experimental data, solid line is linear least-squares fit. ^{14}C-dextran: □ experimental data, dashed line is linear least-squares fit. ^{3}H-heparin: × experimental data, dotted and dashed line is linear least-squares fit.

Linear least-squares fits were performed (solid, dashed, and dotted and dashed lines) for each molecule (^{125}I-HGH, ^{14}C-dextran, and ^{3}H-heparin, respectively) with the y-intercepts set to zero. The results clearly demonstrate that the ^{125}I-HGH (solid line) shows on average faster release than the other two radiolabeled molecules, as evidenced by the smaller slope of the trend line (0.402 days/Kd versus 0.516 days/Kd for the dashed line representing ^{14}C-dextran, and 0.760 days/Kd for the dashed and dotted line representing ^{3}H-heparin). **Figure 4.13** also clearly shows the overlap in release time ranges for the **PLGA28** and **PLGA64** membranes.

Overall, the devices exhibited better reproducibility of release times for the reservoirs having membranes of the lower molecular weight polymers (**PLGA4.4** and **PLGA11**). The key point, however, is that four pulses of one or two chemicals have been demonstrated from individual devices. This is the first time that such a result has been demonstrated from a polymeric system without the application of an external stimulus. Other reports in the literature of pulsatile release from programmable biodegradable implants have shown only one[31] or two[32] pulses from encapsulation-type compression molded devices having several concentric layers of

dye-loaded and dye-free polymer matrices. Devices having a polyanhydride dye-loaded core and PLGA 50:50 M_w 17,000 mantle that was tempered at 110°C showed onset of release between 14 and 17 days, but generally took between 6 and 13 days to release 80% of the loading, making these PLGA devices less useful for applications requiring pulsatile release. Devices fabricated in the same fashion but having PLGA 50:50 M_w 10,500 or PLA M_w 30,000 tempered mantles showed more pulsatile release (approximately one to two days elapsed between onset of release and achieving approximately 80% release), but the fabrication method may limit the ability deliver multiple pulses from these types of devices.

4.4 Summary and Conclusions

We have demonstrated the ability to reproducibly release four pulses of ^{14}C-dextran, ^{3}H-heparin, and ^{125}I-HGH from the polymeric microreservoir devices. We have also demonstrated two releases of each of two chemicals (^{125}I-HGH and ^{14}C-dextran, or ^{3}H-heparin and ^{14}C-dextran) from single devices. The observed release times for the lower molecular weight (**PLGA4.4** and **PLGA11**) membranes showed greater reproducibility and less variation than the release times for the higher molecular weight polymers (**PLGA28** and **PLGA64**), which actually showed overlap of their ranges of release times. Further discussion of the degradation of these membrane polymers will be presented in Chapter 5.

Although one out of three of the devices loaded with ^{125}I-HGH and ^{14}C-dextran, and one out of four of the devices loaded with ^{3}H-heparin and ^{14}C-dextran, showed release of the reservoir having a **PLGA64** membrane prior to release of the reservoir having a **PLGA28** membrane, this was most likely due to the different chemistries of the molecules, although unexpected variation in the polymer degradation rates may have been a contributing factor. The chemistries of the ^{14}C-BCNU and ^{14}C-IAP are also likely responsible for the absence of pulsatile releases from devices loaded with these chemicals.

The results obtained here clearly show that it is possible to deliver multiple (more than two) pulses of different chemicals from a polymeric device without the application of a stimulus or trigger, something which heretofore has not been demonstrated by others.

4.5 References

1. J. Kost, K. Leong, and R. Langer, "Ultrasound-enhanced polymer degradation and release of incorporated substances," *Proc. Natl. Acad. Sci. USA* 86 (1989) 7663–7666.

2. M. A. Wheatley, D. El-Sherif, R. Basude, R. Shimp, and P. Narayan, "Ultrasound-triggered drug delivery with contrast imaging: effect of microencapsulation method," *Mat. Res. Soc. Symp. Proc.* 550 (1999) 113–118.

3. A. M. Lowman, M. Morishita, M. Kajita, T. Nagai, and N. A. Peppas, "Oral delivery of insulin using pH-responsive complexation gels," *J. Pharm. Sci.* 88 (1999) 933–937.

4. J. Taillefer, M.-C. Jones, N. Brasseur, J. E. Van Lier, and J.-C. Leroux, "Preparation and characterization of pH-responsive polymeric micelles for the delivery of photosensitizing anticancer drugs," *J. Pharm. Sci.* 89 (2000) 52–62.

5. O. V. Gerasimov, J. A. Boomer, M. M. Qualls, and D. H. Thompson, "Cytosolic drug delivery using pH- and light-sensitive liposomes," *Adv. Drug Deliv. Rev.* 38 (1999) 317–338.

6. D. Needham and M. W. Dewhirst, "The development and testing of a new temperature-sensitive drug delivery system for the treatment of solid tumors," *Adv. Drug Deliv. Rev.* 53 (2001) 285–305.

7. L. E. Bromberg and E. S. Ron, "Temperature-responsive gels and thermogelling polymer matrices for protein and peptide delivery," *Adv. Drug Deliv. Rev.* 31 (1998) 197–221.

8. X. Cao, S. Lai, and L. J. Lee, "Design of a self-regulated drug delivery device," *Biomedical Microdevices* 3 (2001) 109–118.

9. T. Miyata, T. Uragami, and K. Nakamae, "Biomolecule-sensitive hydrogels," *Adv. Drug Deliv. Rev.* 54 (2002) 79–98.

10. M. J. Tierney and C. R. Martin, "New electrorelease systems based on microporous membranes," *J. Electrochem. Soc.* 137 (1990) 3789–3793.

11. S. Kagatani, T. Shinoda, Y. Konno, M. Fukui, T. Ohmura, and Y. Osada, "Electroresponsive pulsatile depot delivery of insulin from poly(dimethylaminoproplyacrylamide) gel in rats," *J. Pharm. Sci* 86 (1997) 1273–1277.

12. S. H. Yuk, S. H. Cho, and H. B. Lee, "Electric current-sensitive drug delivery systems using sodium alginate/polyacrylic acid composites," *Pharm. Res.* 9 (1992) 955–957.

13. E. R. Edelman, J. Kost, H. Bobeck, and R. Langer, "Regulation of drug release from polymer matrices by oscillating magnetic fields," *J. Biomed. Mater. Res.* 19 (1985) 67–83.

14. J. Kost, J. Wolfrum, and R. Langer, "Magnetically enhanced insulin release in diabetic rats," *J. Biomed. Mater. Res.* 21 (1987) 1367–1373.

15. P. Sampath and H. Brem, "Implantable slow-release chemotherapeutic polymers for the treatment of malignant brain tumors," *Journal of the Moffitt Cancer Center* 5 (1998) 130–137.

16. H. Brem, R. J. Tamargo, A. Olivi, M. Pinn, J. D. Weingart, M. Wharam, and J. I. Epstein, "Biodegradable polymers for the controlled delivery of chemotherapy with and without radiation therapy in the monkey brain," *J. Neurosurg.* 80 (1994) 283–290.

17. S. E. Ettinghaus and S. A. Rosenberg, "Immunotherapy of murine sarcomas using lymphokine activated killer cells: optimization of the schedule and route of administration of recombinant Interleukin-2," *Cancer Res.* 46 (1986) 2784–2792.

18. S. A, Rosenberg, J. J. Mulé, P. J. Speiss, C. M. Reichert, and S. L. Schwarz, "Regression of established pulmonary metastases and subcutaneous tumor mediated by the systemic administration of high-dose recombinant Interleukin-2," *J. Exp. Med.* 161 (1985) 1169–1188.

19. P. Perrin, E. Cassagnau, C. Burg, Y. Patry, F. Vavasseur, J. Harb, J. Le Pendu, J.-Y. Douillard, J.-P. Galmiche, F. Bornet, and K. Meflah, "An Interleukin-2/sodium butyrate combination as immunotherapy for rat colon cancer peritoneal carcinomatosis," *Gastroenterology* 107 (1994) 1697–1708.

20. L. Lu, S. J. Peter, M. D. Lyman, H.-L. Lai, S. M. Leite, J. A. Tamada, S. Uyama, J. P. Vacanti, R. Langer, and A. G. Mikos, "In vitro and in vivo degradation of porous poly(DL-lactic-*co*-glycolic acid) foams," *Biomaterials* 21 (2000) 1837–1845.

21. J. M. Anderson and M. S. Shive, "Biodegradation and biocompatibility of PLA and PLGA microspheres," *Adv. Drug Deliv. Rev.* 28 (1997) 5–24.

22. PerkinElmer Life Sciences Technical Data Certificate of Analysis, "NEX229 [^{125}I]-Interleukin-2, (human, recombinant) [^{125}I]-rIl-2."

23. J. A. Montgomery, R. James, G. S. McCaleb, and T. P. Johnston, "The modes of decomposition of 1,3-bis(2-chloroethyl)-1-nitrosourea and related compounds," *J. Med. Chem.* 10 (1967) 668–674.

24. F. W. Okumu, J. L. Cleland, and R. T. Borchardt, "The effect of size, charge, and cyclization of model peptides on their in vitro release from DL-PLGA microspheres," *J. Controlled Release* 49 (1997) 133–140.

25. S. Li, H. Garreau, and M. Vert, "Structure-property relationships in the case of the degradation of massive poly(α-hydroxy acids) in aqueous media. Part 3: Influence of the morphology of poly(L-lactic acid)," *J. Biomed. Mater. Res.* 1 (1990) 198–206.

26. S. Li, A. Girard, H. Garreau, and M. Vert, "Enzymatic degradation of polylactide stereocopolymers with predominant D-lactyl contents," *Polym. Degrad. Stab.* 71 (2001) 61–67.

27. S. Li and M. Vert, "Crystalline oligomeric stereocomplex as an intermediate compound in racemic poly(DL-lactic acid) degradation," *Polym. Int.* 33 (1994) 37–41.

28. R. M. Ginde and R. K. Gupta, "In vitro chemical degradation of poly(glycolic acid) pellets and fibers," *J. Appl. Polym. Sci.* 33 (1987) 2411–2429.

29. S. Hurrell and R. E. Cameron, "The effect of initial polymer morphology on the degradation and drug release from polyglycolide," *Biomaterials* 23 (2002) 2401–2409.

30. D. K. Gilding and A. M. Reed, "Biodegradable polymers for use in surgery—polyglycolic/poly(lactic acid) homo- and copolymers:1," *Polymer* 20 (1979) 1459–1464.

31. W. Vogelhuber, P. Rotunno, E. Magni, A. Gazzaniga, T. Spruß, G. Bernhardt, A. Buschauer, and A. Göpferich, "Programmable biodegradable implants," *J. Controlled Release* 73 (2001) 75–88.

32. A. Göpferich, "Bioerodible implants with programmable drug release," *J. Controlled Release* 44 (1997) 271–281.

5 Poly(Lactic-co-Glycolic Acid) Dimension and Temperature-Dependent Degradation

5.1 Introduction and Motivation

5.1.1 Introduction

A key goal in the design and commercialization of drug delivery devices is the ability of the manufacturer to achieve reliable, reproducible performance from the device of interest. It is nearly impossible to achieve this goal without a thorough understanding of the mechanisms and phenomena that control device performance. In the case of the microreservoir devices that we have developed, it is quite clear that the membranes which seal the drug-containing reservoirs are the most important component of the device for controlling device performance. Changing the membrane material, molecular weight, copolymer ratio, crosslink density, or thickness, for example, will change the time at which the reservoirs release their contents. The release studies presented in Chapter 4 also suggest that the chemical that is loaded into the reservoirs may slightly affect the time at which the drug is observed to be released from the reservoirs. It is vitally important to understand the mode(s) by which the membranes open in order to achieve reproducible performance of these devices. Characterizing the factors that influence the membrane degradation is thus an important endeavor.

The degradation mechanisms and molecular weight change over time of PLGA copolymers have been reported on quite thoroughly in the literature. Poly(lactic acid), poly(glycolic acid), and their copolymers undergo heterogeneous degradation, possibly as a result of the fact that several processes occur simultaneously in the *in vitro* and *in vivo* environments (water uptake, swelling, ester hydrolysis, diffusion of oligomers and degradation products, and local pH drop)[1–3]. Some evidence has been presented for the theory that the rate of PLGA degradation is dependent on the size of the polymer object being studied[1,4,5]. The diffusion of degradation products out of large polymer objects and into the surrounding medium is hindered. The accumulation of acidic degradation products within the polymer object causes a local drop in pH inside the object, which catalyzes further degradation[6]. Thus, larger objects degrade more rapidly in the center than at the edges, and the overall degradation rate is faster

than that observed for small objects. This phenomenon is of particular interest for the microreservoir devices that we have developed, because of our interest in controlling the degradation rates of the reservoir membranes and hence the release of drugs from the reservoirs.

The temperature dependence of PLGA degradation rate has not been extensively studied, but some authors have reported faster degradation of polylactide and polyglycolide homo- and co-polymers at elevated temperature[4,7–9]. While some of our studies of the microreservoir devices are performed at 37°C, others have been at lower temperatures. Correlation of the membrane degradation rates at these two different temperatures was desired in order to fully characterize the effect of temperature on device performance.

5.1.2 Motivation

The goal of the studies reported here was to characterize the degradation behavior of the reservoir membrane materials used in our devices, both to determine whether or not the size-dependent degradation phenomenon was observed at size scales typical for membranes on a microreservoir device if we increased the membrane thickness, and also to quantify the size and temperature dependence of the degradation rate. Specifically, we wanted to determine whether the observed "release time" of a reservoir (time at which the release of a given reservoir's contents is detected) is correlated with 1) the initial membrane thickness, 2) the initial molecular weight of the membrane material, 3) the mass loss and molecular weight change of the membrane material, and 4) the temperature at which the membranes are degraded. These parameters were chosen based upon the accepted methods in the literature of characterizing the degradation of polyesters, as well as consideration of the environment that the devices will be exposed to *in vivo*.

5.2 Materials and Methods

5.2.1 Materials

Poly(L-lactic acid) (**PLA**, M_w 194 Kilodaltons (Kd), Medisorb® 100 L), and poly(D,L-lactic-*co*-glycolic acid) polymer powders of molecular weights (M_w) 4.4 Kd (**PLGA4.4**, Medisorb® 5050 DL 1A), 11 Kd (**PLGA11**, Medisorb® 5050 DL 2A), 28 Kd (**PLGA28**, Medisorb® 5050 DL 3A), and 64 Kd (**PLGA64**, Medisorb® 5050 DL 4A) were obtained from

Alkermes (Cincinnati, Ohio). Each PLGA copolymer had approximately a 50:50 mole ratio of lactic acid:glycolic acid units. Reagent grade dichloromethane, 1,1,1,3,3,3-hexafluoro-2-propanol (HFIP), HPLC grade methyl alcohol, and ^{14}C-dextran (M_w = 70,000) were purchased from Sigma-Aldrich (St. Louis, MO). HPLC reagent grade chloroform was purchased from J.T. Baker (Phillipsburg, NJ). Ideal 9144 Masking Tape was obtained from American Biltrite, Inc. (Lowell, MA). Polystyrene standards for GPC analysis were obtained from PolySciences, Inc. (Warrington, PA). ScintiSafe Plus 50% was purchased from Fisher Scientific (Suwanee, GA). Mylar® sheets were donated from the laboratory of Dr. James Anderson at Case Western Reserve University.

5.2.2 Methods

5.2.2.1 *In vitro* measurement of release time as a function of membrane thickness

Twenty devices were fabricated as described in Chapter 2. Devices were loaded with ^{14}C-dextran or ^{3}H-heparin. Devices that were loaded with ^{14}C-dextran had four reservoirs on each device loaded and sealed with a different PLGA membrane (**PLGA4.4**, **PLGA11**, **PLGA28**, or **PLGA64**). Two devices had membranes that were approximately 175 μm thick, while the other two had membranes that were approximately 250 μm thick. Nine nCi of ^{14}C-dextran were loaded into each reservoir having a membrane. The devices that were loaded with ^{3}H-heparin (72 nCi per reservoir) had one reservoir filled on each device. Four devices were fabricated with each type of membrane material (**PLGA4.4**, **PLGA11**, **PLGA28**, or **PLGA64**), two of the devices having membrane thicknesses of approximately 150 μm, and two having membrane thicknesses of approximately 250 to 275 μm. The heparin devices only had one membrane per device, as when this study was conducted the release times from reservoirs loaded with ^{3}H-heparin had not been fully investigated, and it was unknown whether the **PLGA64** membrane might release earlier than the **PLGA28** membranes, as discussed in Chapter 4. In order to ensure accurate correlation of an observed release with the correct membrane polymer, the ^{3}H-heparin devices therefore each had only one membrane. In contrast, the release times for ^{14}C-dextran had been fairly well characterized, and therefore the devices loaded with dextran had four reservoir membranes (one of each type of polymer) on each device.

The devices were sealed and affixed to the bottom of polystyrene 6-well tissue culture plates using American Biltrite 9144 masking tape, and 5 mL of 1X phosphate buffered saline (PBS, prepared with milliQ deionized water) was added to each well. The 6-well plates were placed on an orbital shaker (Thermolyne Rotomix Type 50800) at 60 rpm and room temperature (approximately 22–25°C). Typically, 200 μL of the medium in each well was pipetted into 7-mL glass scintillation vials at 8- and 16-hour intervals daily. Five milliliters of ScintiSafe Plus 50% were added to each sample vial and the samples were analyzed on a Packard Tri-Carb liquid scintillation counter using either a ^{14}C or ^{3}H protocol. Confirmation of reservoir opening was obtained by optical microscopy of the devices at the conclusion of the study.

5.2.2.2 *In vitro* degradation: GPC characterization and mass loss of membrane polymers

Films of each membrane polymer (**PLGA4.4**, **PLGA11**, **PLGA28**, and **PLGA64**) were cast from HFIP solutions (volume fractions of the polymer in solution ranged from 7 to 15%) onto Mylar® sheets. The total weight and volume of polymer as well as volume of solvent were calculated in order to give the desired film thicknesses (either approximately 50 μm or 150 μm) when cast over a specified area. The solutions were allowed to become homogenous (dissolution of the polymers) over the course of a few hours before being cast onto Mylar® film, approximately 130 μm thick, which had been cleaned with acetone and Kimwipes®. The desired area of each film was marked on the Mylar® and then enclosed by placing several layers of VWR brand time tape onto the Mylar®. The solutions were poured onto the Mylar® areas in several layers. The cast polymer solutions were typically left to dry in a chemical hood for one to two hours. They were then dried in a Napco Vacuum Oven Model 5831 for either 24 or 48 hours at between 76 and 81°C under 6.7 kPa (28 in Hg VAC, 93.5% vacuum) house vacuum. After the oven heaters were turned off, the oven was left to cool for at least one hour before removing the films. Film thicknesses were measured with a Fowler micrometer. The 50 μm films were cut into 1×1.5 cm^2 samples, while the 150 μm films were cut into 1×1 cm^2 samples (a smaller area was required in order to obtain adequate polymer mass for the GPC characterization due to the larger thicknesses of these films). Each film was weighed and placed in a micro-centrifuge (microfuge) tube. One and one-half milliliters of PBS made with milliQ water (resistivity ~18 MΩ) were added to each tube before it was capped, and the tubes were agitated on Thermolyne Rotomix Type 50800 orbital shakers at 60 rpm.

The experimental matrix is shown in **Table 5-1** below. The goals of this study were to investigate the effect of temperature, film thickness, and media conditions on the degradation rate of the films, as characterized by molecular weight, polydispersity index (PDI), pH of the media surrounding the samples, and mass loss measurements. The samples that had the media changed were designed to mimic the experimental conditions that reservoir membranes are subjected to during an *in vitro* release experiment. Typically 1/20 of the release medium volume is changed at each time point (twice daily) in a release experiment. This corresponds to a complete volume change every ten days, which is similar to the media changes that occurred on average every seven days in this degradation study. The samples that did not have the media changed were designed to investigate what effect the local accumulation of degradation products would have on the pH and degradation rate of the films. Each sample group typically consisted of three films of each material at each time point.

Table 5-1 Experimental matrix for *in vitro* degradation study.

	50 μm	150 μm
25°C, no medium change	X	X
25°C, with medium change		X
37°C, with medium change		X

Batches of samples were removed from the microfuge tubes at 7, 14, 21, 28, 35, 42, and 49 days (some groups had additional samples at three, four, or ten days), rinsed with deionized water, dried under 6.7 kPa (28 in Hg VAC, 93.5%) vacuum at room temperature for 48 hours, and weighed. pH measurements were taken using colorpHast pH paper at 4, 7, 14, 21, 28, 35, 42, and 49 days for the 150 μm thick films as they were removed from the media for analysis. After drying, the samples were placed in 7-mL glass vials, and one milliliter of chloroform was added with a B-D polypropylene 1-mL syringe in order to dissolve the PLGA off of the Mylar® film. The vials were wrapped with ParaFilm M® to prevent evaporation of the chloroform. The samples were left to dissolve in chloroform for between six and 72 hours and then vortexed until no PLGA was visibly remaining on the Mylar® films. The solutions were transferred to 1-mL glass GPC vials (Waters Corporation) using 1-mL polypropylene syringes and 0.2 μm PTFE syringe filters. GPC analysis was performed on the polymer solutions in chloroform at 1 mL/min flow rate on a Waters GPC system consisting of a 515 HPLC Pump, 717_{plus} Autosampler, Styragel Guard Column, two Styragel HR 4 columns or one each of Styragel HR 4 and HR 3

columns, and 2410 refractive index detector. Polymer molecular weights were calculated relative to selected polystyrene standards of molecular weights 400,000, 300,000, 200,000, 50,000, 25,000, 20,000, 17,500, 9,000, 4,000, 2,000, and 1,000 daltons. Data was analyzed using Millenium v.3.20 software.

5.3 Results and Discussion

5.3.1 *In vitro* measurement of release time as a function of membrane thickness

The observed release times according to the membrane materials and thicknesses for the devices loaded with ^{14}C-dextran or ^{3}H-heparin are summarized in **Table 5-2** below.

Table 5-2 Summary of observed release times (in days) of devices having PLGA reservoir membranes of various thicknesses and molecular weights, loaded with ^{14}C-dextran or ^{3}H-heparin.

		Reservoir Membrane Material			
Chemical	Reservoir Membrane Thickness (μm)	**PLGA4.4**	**PLGA11**	**PLGA28**	**PLGA64**
^{14}C-dextran	175	0.9	25-26	63-92	100-121
	250	0.6-0.9	27-36	56-60	66-69
^{3}H-heparin	150	0.6	23-32	58-59	66-71
	275	0.6	23-24	45	51-52

5.3.1.1 ^{14}C-dextran

Figure 5.1 and **Figure 5.2****Figure 5.2** show the release data for devices loaded with ^{14}C-dextran. For the two lowest molecular weight membranes (**PLGA4.4** and **PLGA11**), the devices showed very similar release times. The **PLGA4.4** membranes uniformly released on day 1 for all four devices, while the **PLGA11** reservoirs released between 25 to 36 days for all four devices. However, the higher molecular weight membrane materials showed greater variation. The devices that had 175 μm thick membranes showed, on average, release at later times than the devices that had 250 μm thick membranes. The 250 μm thick **PLGA28** membranes showed release between 56 and 60 days, while the 175 μm thick membranes of the same material showed release between 63 and 92 days.

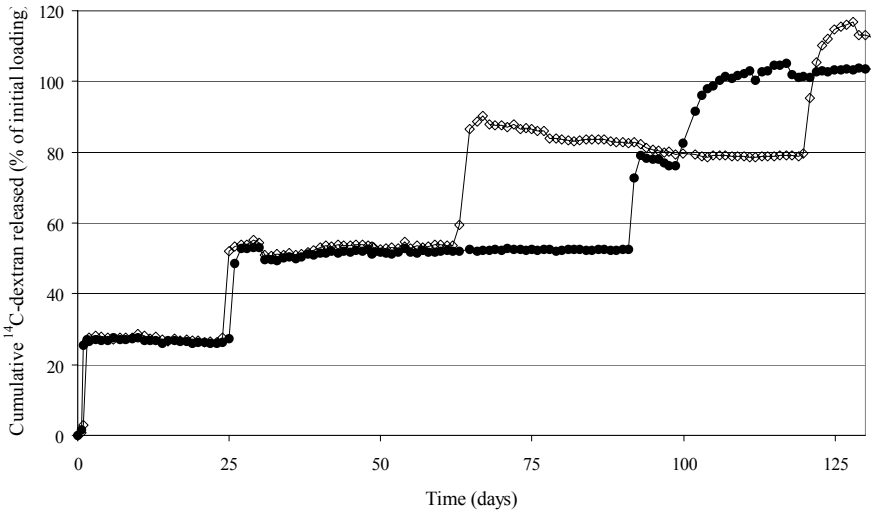

Figure 5.1 Cumulative percentage of initial ^{14}C-dextran loading released over time *in vitro* at 25°C from two devices having ~175 μm thick membranes made from **PLGA4.4**, **PLGA11**, **PLGA28**, and **PLGA64**.

Similarly, the 250 μm thick **PLGA64** membranes showed release at approximately 66 to 69 days, while their 175 μm counterparts showed release between 100 and 121 days. The thicker membranes show faster degradation as evidenced by the earlier release times, as well generally more uniform release times (smaller variation in release times).

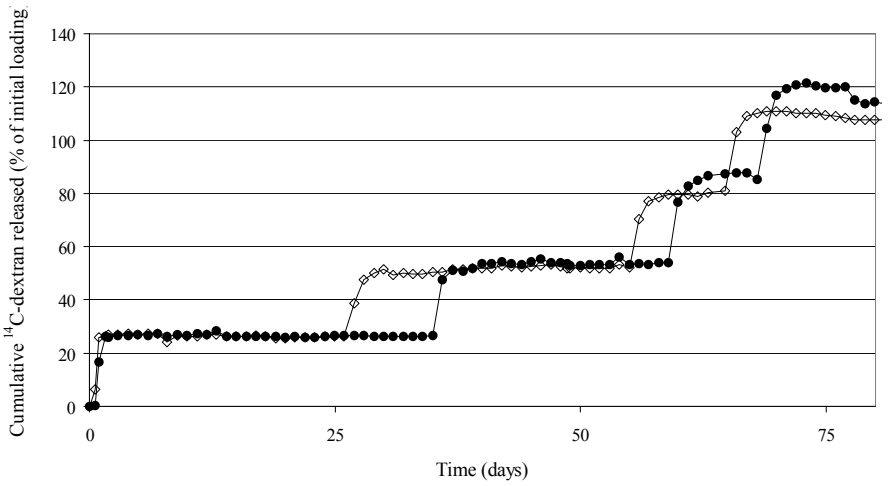

Figure 5.2 Cumulative percentage of initial ^{14}C-dextran loading released over time *in vitro* at 25°C from two devices having ~250 μm thick membranes made from **PLGA4.4**, **PLGA11**, **PLGA28**, and **PLGA64**.

The high cumulative percentages indicated on the graphs (>100%) are most likely due to the fact that it was extremely difficult to prevent evaporation of the PBS media over the course of the study from the wells in which the devices were situated. It is likely that evaporation of the media caused subsequently higher concentrations of the radiolabel to be measured. Small aliquots of the media were used for the measurements of the ^{14}C-dextran present, and the error introduced by the mathematical calculations, combined with the difficulty in keeping the volume of PBS constant, most likely caused the high measured percentages.

5.3.1.2 ^{3}H-heparin

The results for the devices loaded with ^{3}H-heparin are shown in **Figure 5.3** and **Figure 5.4**. Similar to the ^{14}C-dextran devices, we see for the ^{3}H-heparin that the devices with thicker reservoir membranes exhibited earlier release of their contents as well as less variation in release times than those having thinner membranes. Although the differences in release times were not as dramatic for the devices loaded with ^{3}H-heparin as for the ones loaded with ^{14}C-dextran in this study, they were nevertheless quite notable. Similar to the results obtained for the ^{14}C-dextran, the **PLGA4.4** and **PLGA11** membranes did not show very different release times as a function of membrane thickness. However, we again see that the **PLGA28** ~275 μm membranes showed release earlier (day 45) than the **PLGA28** ~150 μm membranes (days 58 to 59). Similarly, the **PLGA64** ~275 μm membranes showed release at 51 to 52 days, while their thinner counterparts showed release at between 66 and 71 days.

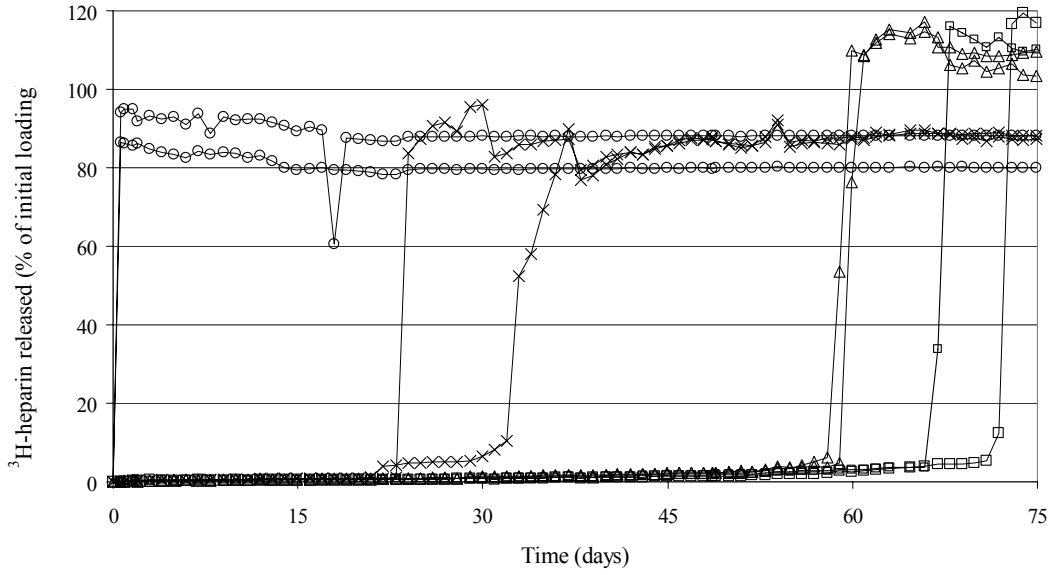

Figure 5.3 Cumulative percentage of initial ^{3}H-heparin loading released over time *in vitro* at 25°C from devices having 150 μm thick membranes: ○ **PLGA4.4**, × **PLGA11**, △ **PLGA28**, and □ **PLGA64**.

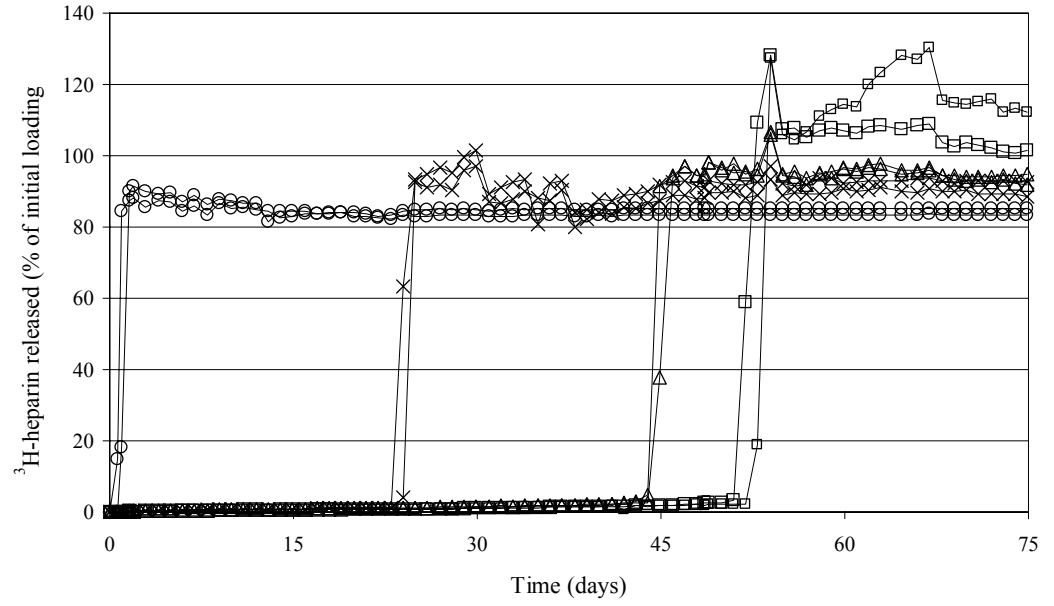

Figure 5.4 Cumulative percentage of initial ^{3}H-heparin loading released over time *in vitro* at 25°C from devices having 275 μm thick membranes: ○ **PLGA4.4**, × **PLGA11**, △ **PLGA28**, and □ **PLGA64**.

Similar to the devices that were loaded with ^{14}C-dextran, the >100% cumulative release detected for the devices that released the ^{3}H-heparin towards the end of the study is most likely due to evaporation of the release media and subsequent concentration of the remaining radiolabel, which gave rise to an artificially high quantitative value when the cumulative amount of release was calculated.

Overall, the **PLGA4.4** and **PLGA11** reservoir membranes did not appear to show significant differences in release time as the membrane thickness was changed. However, the release times were faster and showed less variation for the thicker **PLGA28** and **PLGA64** reservoir membranes. Additionally, the release times observed for the different membrane polymers appeared to vary depending on the chemical that was loaded into the reservoirs. The reservoirs having 150–175 μm thick **PLGA64** membranes, for example, showed release between 66–71 days when loaded with ^{3}H-heparin, and between 100–121 days when loaded with ^{14}C-dextran. While the molecular weight of the chemical loaded into the reservoir may affect the opening time of the membrane (see Chapter 7 for further discussion), it also appears that the chemistry of the molecule may affect the release time.

5.3.2 *In vitro* degradation: GPC characterization and mass loss of membrane polymers

Although the studies described above have given us quantitative data correlating the observed release time with the initial membrane thickness, our ultimate goal is to thoroughly understand the mechanisms and factors that determine the opening of the membranes in order to better control device performance. A more thorough characterization of the molecular weight, mass loss, and polydispersity index (PDI = M_w/M_n) of the membrane polymers over time *in vitro*, as well as the pH of the release media, was therefore performed. The molecular weight of the membrane materials and pH of the media can provide us with information about the degradation rate of the materials, while the PDI can indicate whether or not size-dependent degradation is taking place. A high PDI is due to a broad distribution of molecular weights, which may indicate that size-dependent degradation is occurring (both extremely low molecular weight oligomers and higher molecular weight chains are present). Conversely, a low PDI indicates a narrow distribution of chain molecular weights, which is more likely in the case where oligomers can diffuse out of the polymer objects (no size-dependence of degradation rate). Most importantly, however, characterization of the molecular weight and mass loss can give us a

better understanding of whether or not the membrane opening is correlated with either a threshold molecular weight or percentage of membrane mass remaining.

5.3.2.1 **PLGA4.4**

The weight-average molecular weight (M_w) reported by the manufacturer for this polymer is approximately 4,400 daltons, with a polydispersity index (PDI) of 2. Undegraded polymer powder (stored dry at –4°C since receipt from the manufacturer) that was analyzed on the GPC along with various sample batches showed a molecular weight ranging from 3,660 to 5,220 daltons and PDI values from 1.73–2.59.

The results of the *in vitro* degradation study of the **PLGA4.4** materials are shown in **Figure 5.5** to **Figure 5.9**. **Figure 5.5** shows the change in molecular weight over time for the **PLGA4.4** films.

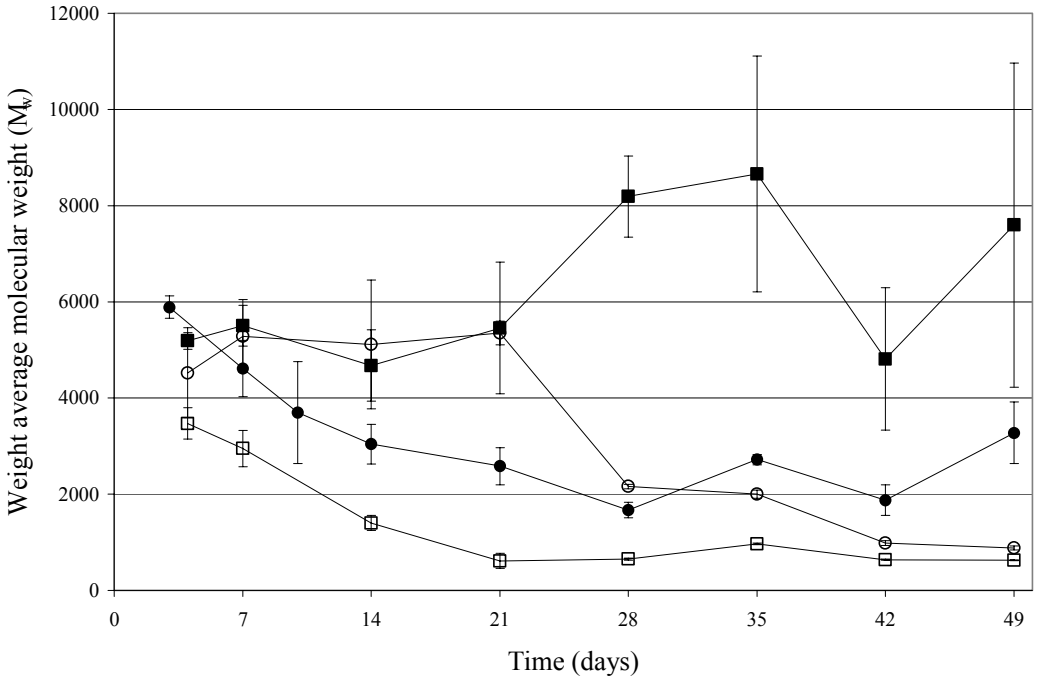

Figure 5.5 M_w over time of **PLGA4.4** film samples degraded *in vitro*: ● 50 μm films at 25°C with no media change, ○ 150 μm films at 25°C with no media change, ■ 150 μm films at 25°C with media change, □ 150 μm films at 37°C with media change.

As is expected, the samples that were kept at 37°C (□ symbols) showed the most rapid drop in molecular weight. Faster degradation of PLGA copolymers at higher temperatures has

been reported elsewhere[4,7,8]. The 150 μm films at 25°C with no media change (○ symbols) show a lower molecular weight at 49 days than both the 50 μm films at 25°C with no media change (● symbols) and the 150 μm thick films at 25°C with media change (■ symbols). This suggests that the thicker films undergo more rapid degradation, and that the local accumulation of the acidic degradation products helps to autocatalyze further degradation of the polymer, in the case of the samples that did not have the media changed. A comparison of the 150 μm films at 25°C (■ symbols) and 37°C (□ symbols) clearly shows that the samples at 37°C undergo more rapid degradation and molecular weight decrease.

The pH results in **Figure 5.6** confirm the hypothesis presented above based on the molecular weight data, namely that local accumulation of the degradation products was occurring in the case of the samples that did not have the media changed. The pH values obtained for 150 μm thick samples at 25°C that did not have the media changed (○ symbols) were much lower than that of the samples that did have the medium changed (■ symbols). All sample groups showed an initial drop in the measured pH value, most likely due to the rapid onset of degradation of the polymer. The 37°C sample group (□ symbols) showed a large drop in pH at day 14, with subsequent recovery to pH 7.4 at days 35 to 49. The lower pH seen for this sample group over the first days of the study can be attributed to the faster degradation rate of the material at elevated temperature.

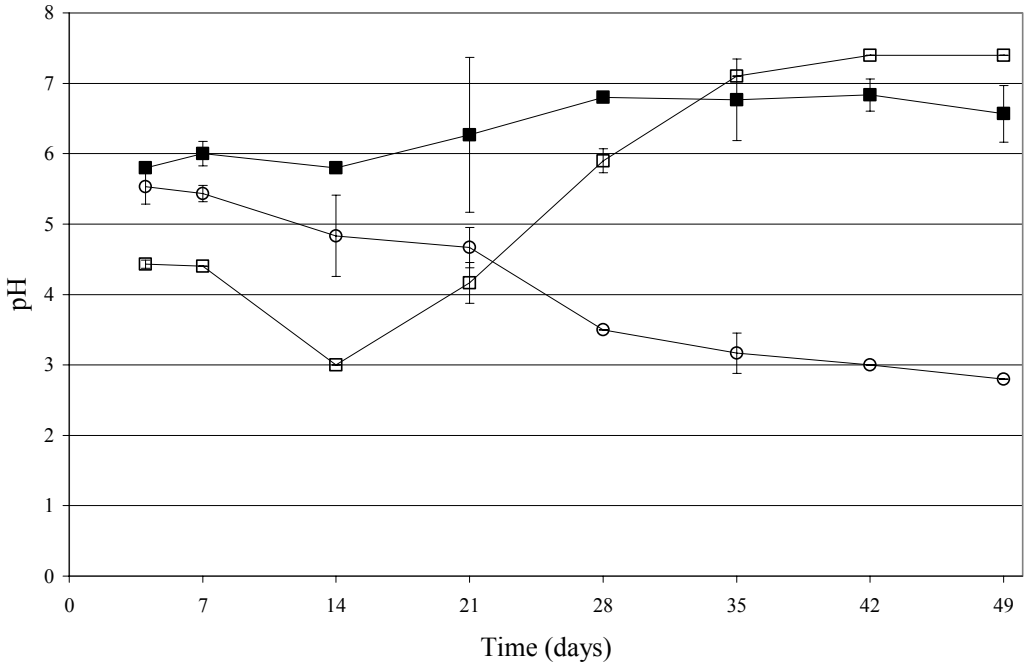

Figure 5.6 pH over time of media surrounding **PLGA4.4** film samples degraded *in vitro*: ○ 150 μm films at 25°C with no media change, ■ 150 μm films at 25°C with media change, □ 150 μm films at 37°C with media change.

The change in mass of the samples over time is shown in **Figure 5.7**. The samples at 37°C showed the largest drop in the sample mass, with nearly complete loss of the material after 21 days. Although the 37°C samples appeared to have no sample remaining after this time, there may have been a very small amount of material remaining that was difficult to quantify using our microbalance, but which was sufficient to be analyzed on the GPC. However, many of these samples showed exceedingly small peaks on the GPC chromatograms.

Reservoirs having membranes made from the **PLGA4.4** polymer have shown universal release times between zero and one days in release studies performed *in vitro* (as discussed in Chapter 4). Although the mass lost from the **PLGA4.4** polymers was not characterized in this study at day one, the results presented here show that 60–80% of the **PLGA4.4** mass remained at three or four days. This suggests that either a very high threshold of remaining mass (or alternatively a very small mass loss) is correlated with the observed opening of the **PLGA4.4** membranes, or that no threshold of remaining mass exists, and that the opening of the reservoir is correlated with some other parameter, such as molecular weight.

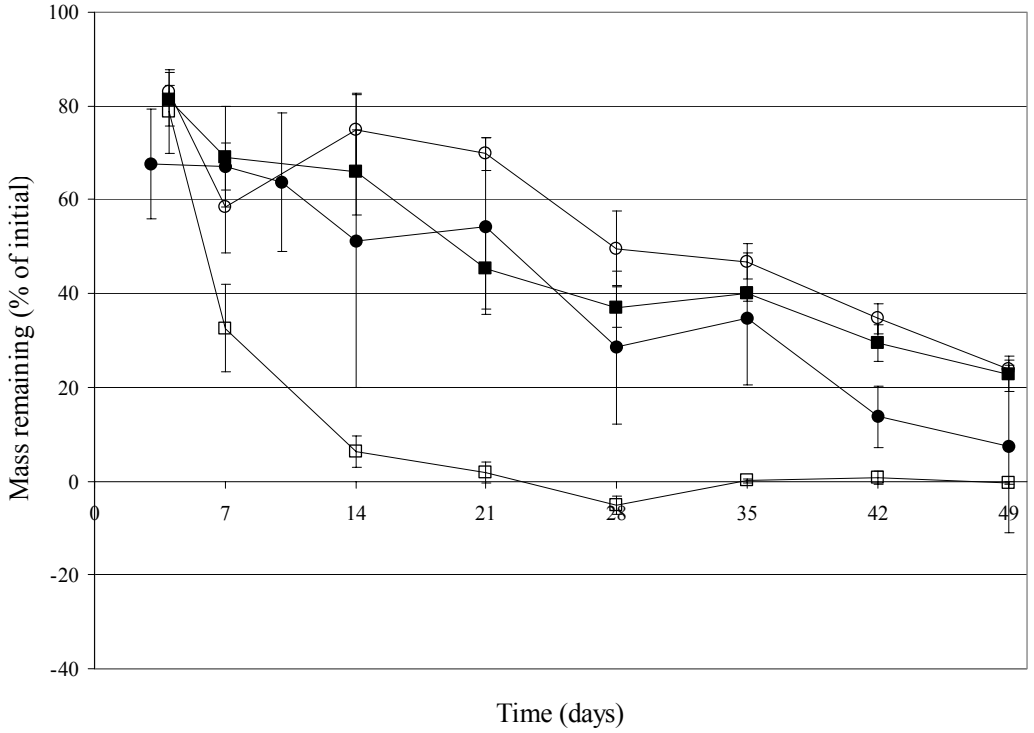

Figure 5.7 Mass remaining over time of **PLGA4.4** film samples degraded *in vitro*: ● 50 μm films at 25°C with no media change, ○ 150 μm films at 25°C with no media change, ■ 150 μm films at 25°C with media change, □ 150 μm films at 37°C with media change.

The calculated mass loss in mg/cm^2 is shown in **Figure 5.8** below for the **PLGA4.4** films in various degradation conditions. Normalization of the mass loss by the film area (the 50 μm thick films had a larger surface area) highlights the much larger mass loss for the 150 μm thick films at all time points compared to the 50 μm thick films (● symbols).

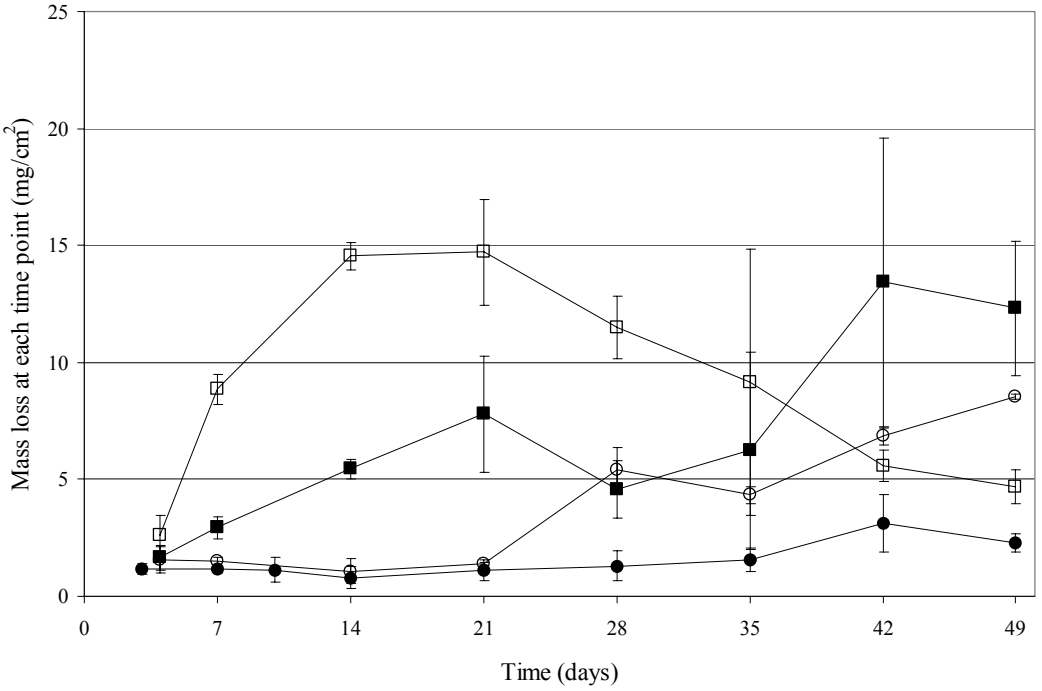

Figure 5.8 Mass loss (mg/cm^2) at each time point for **PLGA4.4** films degraded in PBS *in vitro*: ● 50 μm films at 25°C with no media change, ○ 150 μm films at 25°C with no media change, ■ 150 μm films at 25°C with media change, □ 150 μm films at 37°C with media change.

The polydispersity indices (PDI) of the **PLGA4.4** samples under different degradation conditions are shown in **Figure 5.9**. In general, the 150 μm films at 25°C (both without media change, ○ symbols, and with media change, ■ symbols) showed a higher PDI value than the 50 μm films at 25°C. This could be due to size-dependent degradation, which would cause faster and slower degrading regions of the films to have lower and higher molecular weights, respectively, and a correspondingly higher PDI value. The 150 μm films at 37°C (□ symbols) had consistently low values of PDI for the entire course of the study. This is most likely due to the extremely rapid degradation of the **PLGA4.4** at 37°C, as reflected by both the molecular weight (**Figure 5.5**) and mass loss (**Figure 5.7**) results. The increase in PDI for most of the samples at days 42 and 49 may be due to the extremely low molecular weight values obtained. The lowest molecular weight cutoff of the GPC columns used was either 500 or 5,000 daltons, and at the later time points of this study, the **PLGA4.4** material had reported M_n and M_w results that approached or were below these values. Therefore, the accuracy of the PDI values at days 42 and 49 may not be very high.

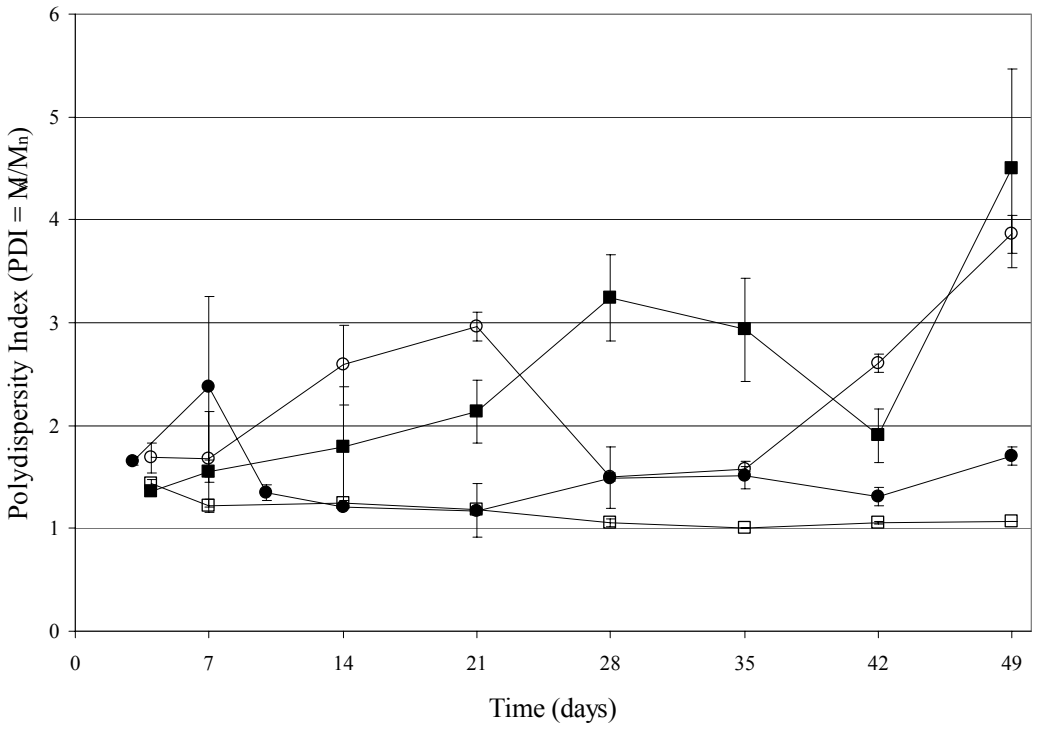

Figure 5.9 PDI over time of **PLGA4.4** film samples degraded *in vitro*: ● 50 μm films at 25°C with no media change, ○ 150 μm films at 25°C with no media change, ■ 150 μm films at 25°C with media change, □ 150 μm films at 37°C with media change.

5.3.2.2 **PLGA11**

The weight-average molecular weight (M_w) reported by the manufacturer for this polymer is approximately 11,000 daltons, with a polydispersity index (PDI) of 2.5. Undegraded polymer powder (stored dry at –4°C since receipt from the manufacturer) that was analyzed on the GPC along with various sample batches showed a molecular weight ranging from 8,550 to 12,700 daltons and PDI values of 1.73–2.83.

The **PLGA11** material showed degradation behavior that was similar to that seen for the **PLGA4.4** material, although the degradation rate was slower. The results are summarized in **Figure 5.10** to **Figure 5.14**. The molecular weight results for this material are shown in **Figure 5.10**. Similar to the **PLGA4.4** results, the samples that were kept at 37°C showed the most rapid drop in molecular weight, and the lowest molecular weight at the end of the study. The other three sets of samples showed similar trends in both the change in molecular weight over the course of the study, and the final molecular weight at day 49, although the 150 μm films at 25°C

with media change (■ symbols) showed an overall flatter curve and higher molecular weight at day 49 than the other two sample groups at 25°C. This may be due simply to the effect of the media change, which may have maintained the pH at a higher value and therefore slowed the degradation of these samples. A comparison of the two sample groups that did not have the media changed (● 50 μm films and ○ 150 μm films) shows that the degradation rate and change in molecular weight over time appear to be similar for these sample groups.

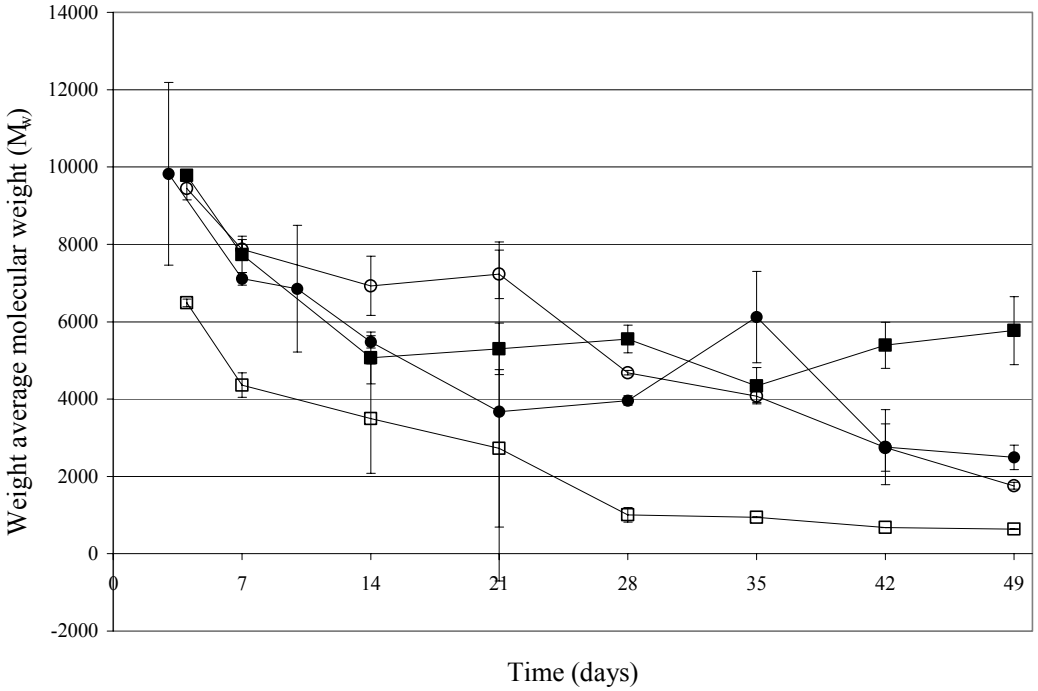

Figure 5.10 M_w over time of **PLGA11** film samples degraded *in vitro*: ● 50 μm films at 25°C with no media change, ○ 150 μm films at 25°C with no media change, ■ 150 μm films at 25°C with media change, □ 150 μm films at 37°C with media change.

The measured pH of the media surrounding the **PLGA11** samples is shown in **Figure 5.11**. Similar to the **PLGA4.4** results, the samples at 37°C showed a much lower pH value during the initial part of the study. Again, this is not surprising since the higher temperature appears to cause more rapid degradation of the polymer. The 150 μm samples at 25°C with no media change (○ symbols) showed a similar trend initially as that presented by the 150 μm samples at 25°C with media change (■ symbols). However, after day 35, the samples that did not have the media changed showed a continuing drop in the pH compared to those samples that did have the media changed. These results are loosely similar to the molecular weight data shown in

Figure 5.10, where the samples that did not have the media changed (○ symbols) show a continued drop in molecular weight after day 35, while the samples that had fresh media (■ symbols) showed a decrease in the rate of molecular weight drop. This is consistent with sustained faster degradation of the sample groups that did not have the media changed.

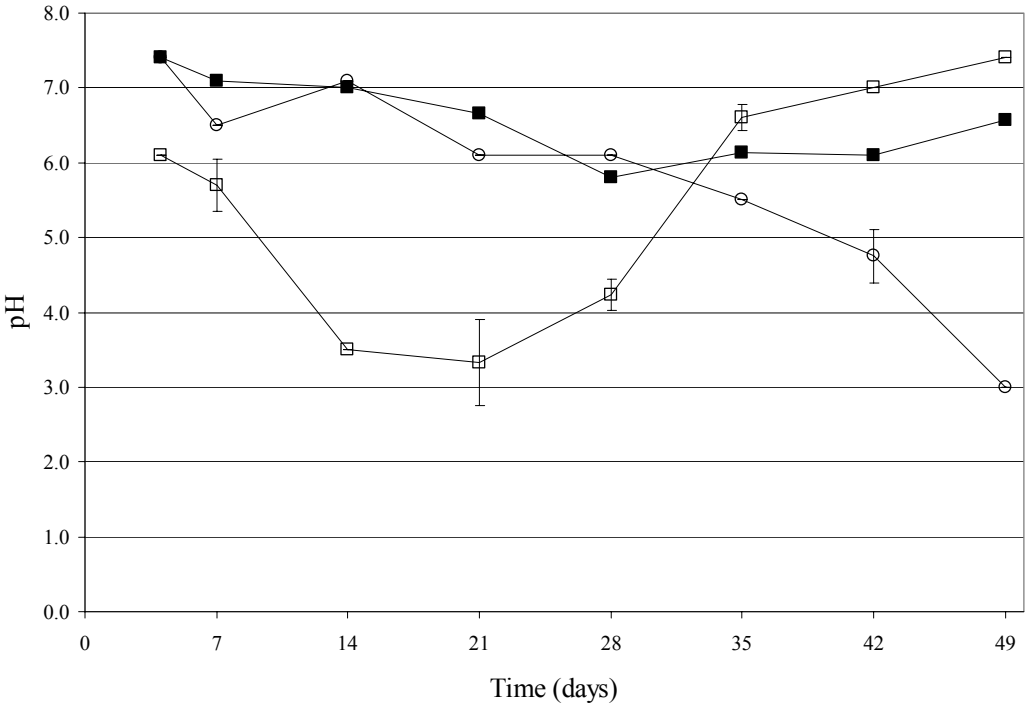

Figure 5.11 pH over time of medium surrounding **PLGA11** film samples degraded *in vitro*: ○ 150 μm films at 25°C with no media change, ■ 150 μm films at 25°C with media change, □ 150 μm films at 37°C with media change.

The **PLGA11** samples showed significantly more mass remaining over the course of the study (**Figure 5.12**) compared to the **PLGA4.4** samples, as is expected. The samples at 37°C (□ symbols) show the largest drop in mass remaining, with essentially all of the material lost after 28 days. This is confirmed by the mass loss per unit area calculations shown in **Figure 5.13**. The other three sample groups had consistent results, with approximately 50% of the initial mass remaining on the Mylar® substrate after 49 days of *in vitro* degradation. This compares favorably with the molecular weight results (**Figure 5.10**), which showed much greater degradation of the 37°C samples than the other three groups. Interestingly, the molecular weight and pH results suggest that the 150 μm films at 25°C with no media change (○ symbols) undergo more rapid degradation towards the end of the study than the other 25°C sample groups, while

the mass data in **Figure 5.12** indicate that all three of the sample groups have roughly the same amount of polymer remaining on the substrate after 49 days. These two results suggest that although the 150 μm films at 25°C with no media change may have the same amount of polymer remaining on the Mylar® substrates, on average, as the other sample groups at 25°C, the remaining polymer material in this sample group is of a lower molecular weight.

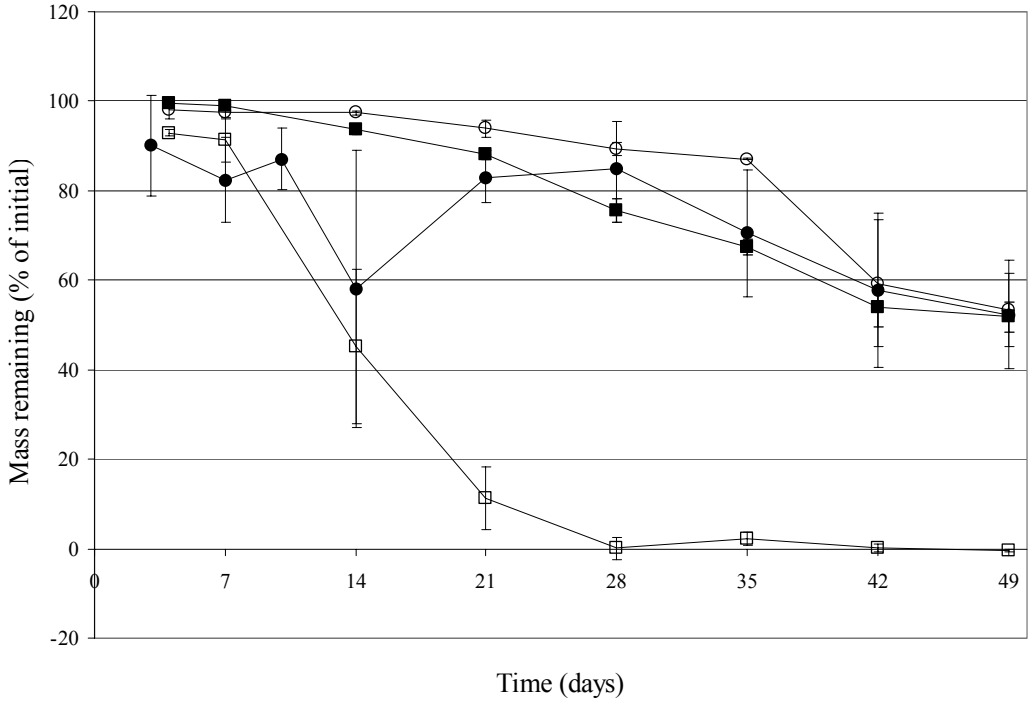

Figure 5.12 Mass remaining over time of **PLGA11** film samples degraded *in vitro*: ● 50 μm films at 25°C with no media change, ○ 150 μm films at 25°C with no media change, ■ 150 μm films at 25°C with media change, □ 150 μm films at 37°C with media change.

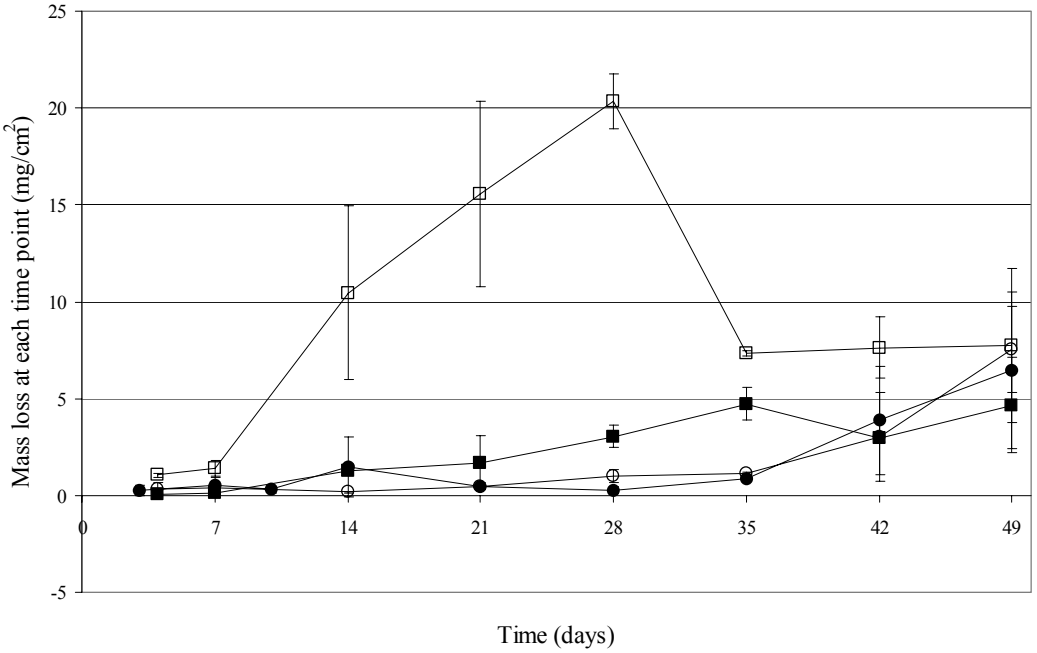

Figure 5.13 Mass loss (mg/cm^2) at each time point for **PLGA11** films degraded in PBS *in vitro*: ● 50 μm films at 25°C with no media change, ○ 150 μm films at 25°C with no media change, ■ 150 μm films at 25°C with media change, □ 150 μm films at 37°C with media change.

The PDI results for the **PLGA11** sample groups are shown in **Figure 5.14**. With the exception of the 150 μm films at 25°C with no media change (○ symbol), which showed a peak at day 42, the PDI values obtained for the **PLGA11** samples were similar to those obtained for the **PLGA4.4** materials. The 37°C sample group showed the lowest PDI, most likely due to the rapid degradation of the **PLGA11** at that temperature. The 150 μm films at 25°C with no media change (○ symbols) showed slightly higher PDI values than the 50 μm films at 25°C with no media change (● symbols). This result suggests that the 150 μm films are degrading more rapidly, supporting the hypothesis that size-dependent degradation occurs at the thicknesses investigated here.

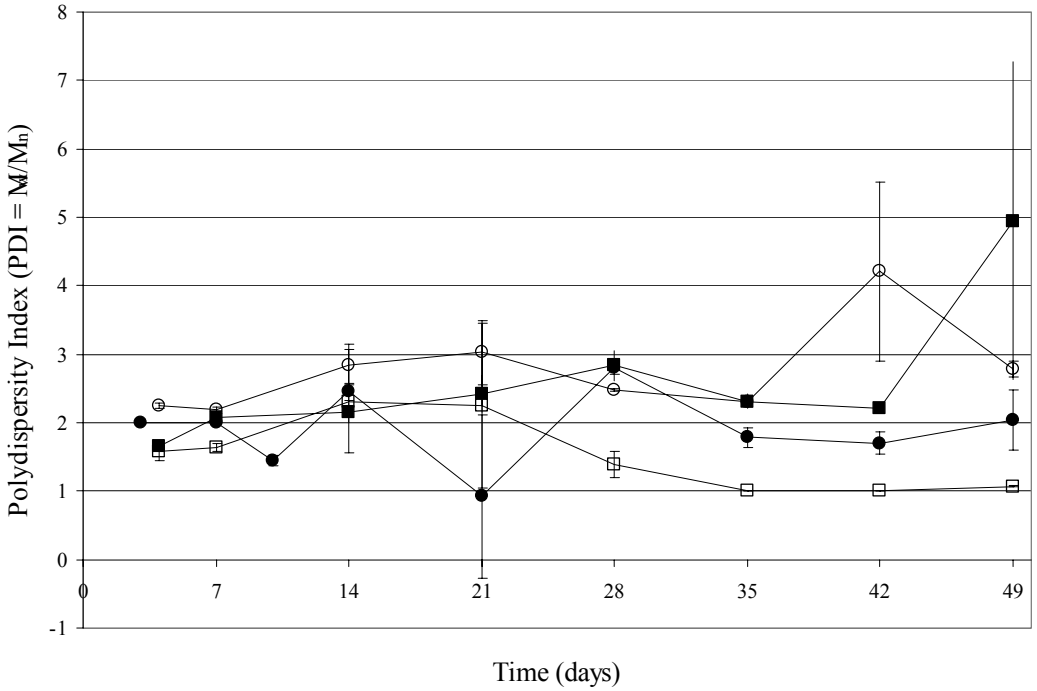

Figure 5.14 PDI over time of **PLGA11** film samples degraded *in vitro*: ● 50 μm films at 25°C with no media change, ○ 150 μm films at 25°C with no media change, ■ 150 μm films at 25°C with media change, □ 150 μm films at 37°C with media change.

5.3.2.3 **PLGA28**

The weight-average molecular weight (M_w) reported by the manufacturer for this polymer is approximately 28,000 daltons, with a polydispersity index (PDI) of 6.6. Undegraded polymer powder (stored dry at –4°C since receipt from the manufacturer) that was analyzed on the GPC along with various sample batches showed a molecular weight ranging from 23,900 to 49,000 daltons and PDI values from 1.29–6.12.

Figure 5.15 to **Figure 5.19** summarize the results obtained for the **PLGA28** sample groups. The molecular weight results for the **PLGA28** material are shown in **Figure 5.15**. Similar to the **PLGA4.4** and **PLGA11** materials, again we see that the sample group at 37°C (□ symbols) showed the most rapid degradation and the lowest molecular weight after 49 days. The 50 μm films at 25°C with no media change (● symbols) initially showed a more rapid drop in molecular weight compared to the remaining sample groups, but then seemed to slow down. The 150 μm films at 25°C with no media change (○ symbols) had a slightly higher initial molecular

weight than the 50 μm thick films, and a slightly lower molecular weight at day 49. Thus although there was a peak in the curve at day 28, the overall degradation rate of the 150 μm thick films seems to be slightly more rapid than the 50 μm films under the same degradation conditions. Comparing the 150 μm films at 25°C with (■) and without (○) media change, it appears that the molecular weight changed similarly over time, but that the act of changing the media slightly slowed down the degradation of the polymer, resulting in a higher measured molecular weight at day 49. The effect of temperature on the degradation rate is quite obvious when the 150 μm samples at 25°C (■) and 37°C (□) are compared in **Figure 5.15**. The samples at 25°C still showed a measured molecular weight of approximately 15,000 daltons at day 49, while the samples degraded at 37°C were just 500 daltons, on average.

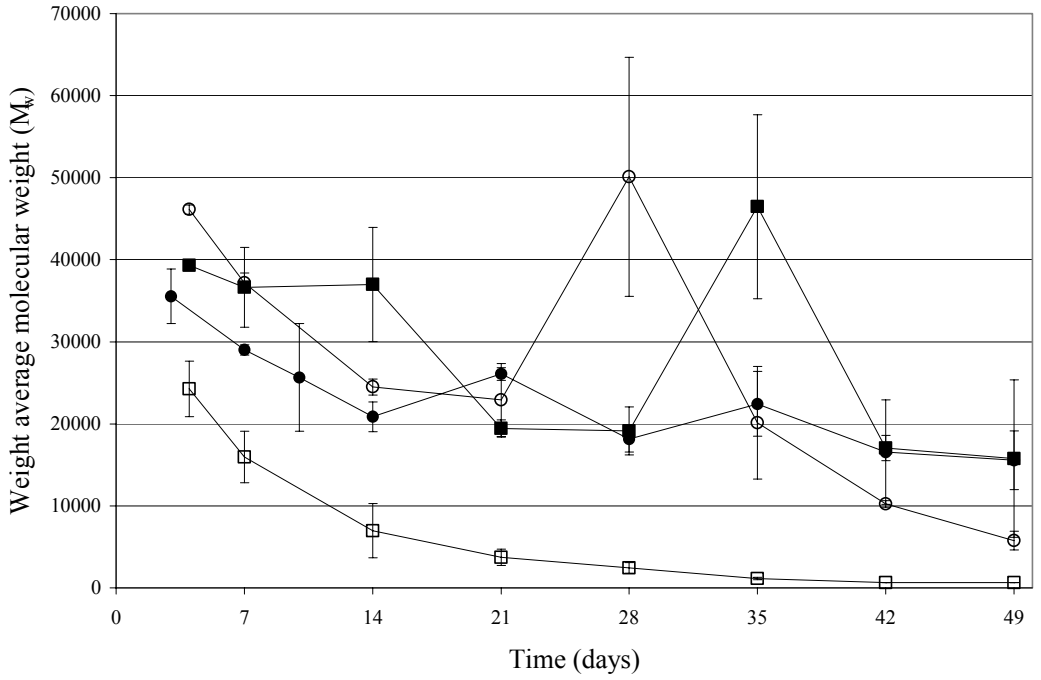

Figure 5.15 M_w over time of **PLGA28** film samples degraded *in vitro*: ● 50 μm films at 25°C with no media change, ○ 150 μm films at 25°C with no media change, ■ 150 μm films at 25°C with media change, □ 150 μm films at 37°C with media change.

The measured pH values for the media surrounding the **PLGA28** samples are shown in **Figure 5.16**. Only the **PLGA28** samples maintained at 37°C (□ symbols) showed a change in the measured pH over time. The pH value for this sample group reached a minimum of approximately 3 on day 28, and then recovered to pH 6.8 at day 49. The minimum pH value

measured for this sample group was similar to that measured for 37°C sample groups of other materials (**PLGA4.4** and **PLGA11**), as well as the **PLGA4.4** 150 μm sample group at 25°C with no media change, which all showed significant mass losses and decreases in their molecular weights.

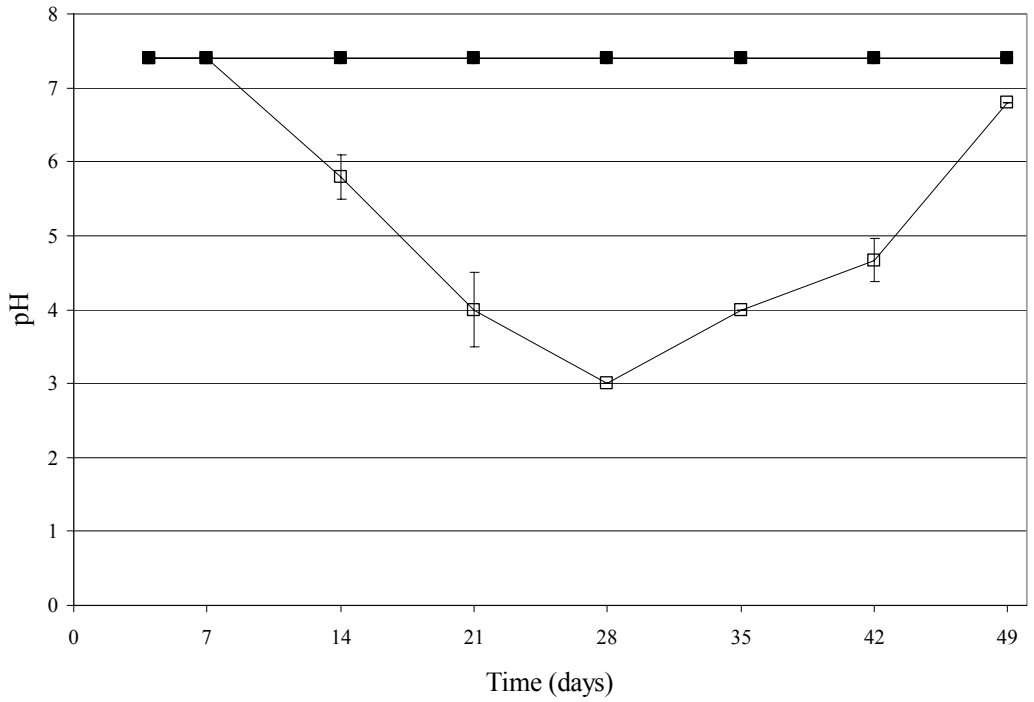

Figure 5.16 Measured pH over time of media surrounding **PLGA28** film samples degraded *in vitro*: ○ 150 μm films at 25°C with no media change, ■ 150 μm films at 25°C with media change, □ 150 μm films at 37°C with media change.

The characterization of mass remaining for the **PLGA28** sample groups is shown in **Figure 5.17**. Similar to the other materials investigated in this study, the **PLGA28** samples maintained at 37°C (□ symbols) show the most rapid and complete mass loss. This sample group appeared to have completely lost all polymer from the surface of the Mylar® substrates after 35 days *in vitro*. The other three sample groups, however, were in striking contrast to the 37°C samples. They showed almost no mass lost over the entire 49 days of the degradation study.

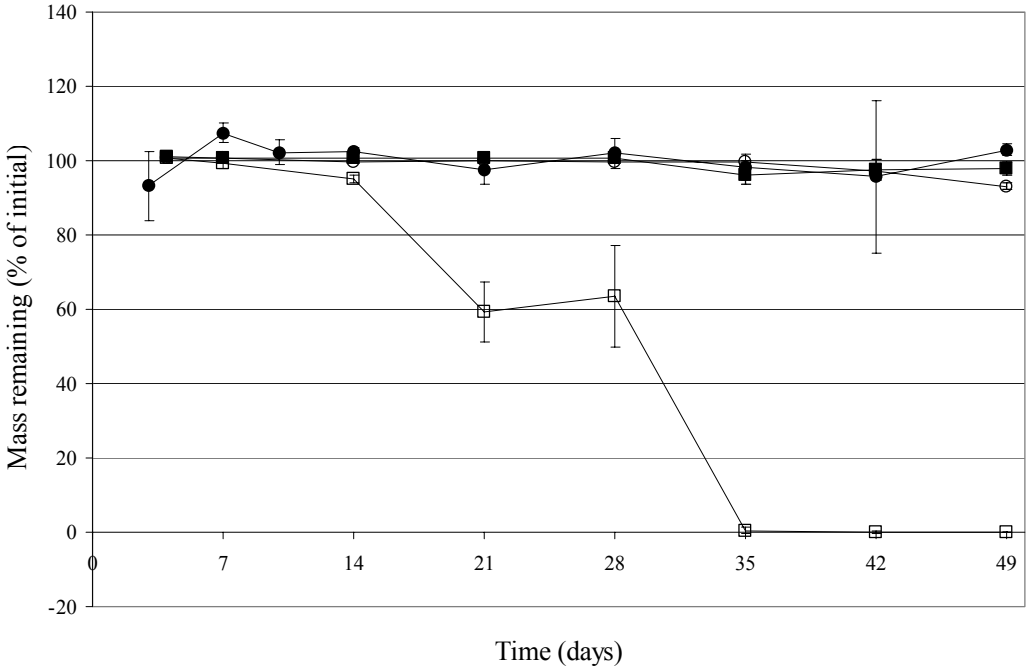

Figure 5.17 Mass remaining over time of **PLGA28** film samples degraded *in vitro*: ● 50 μm films at 25°C with no media change, ○ 150 μm films at 25°C with no media change, ■ 150 μm films at 25°C with media change, □ 150 μm films at 37°C with media change.

The mass loss per unit area values for the different **PLGA28** sample groups are shown in **Figure 5.18** below. These results also show, as expected, that the samples maintained at 37°C had much greater mass loss per unit area than the other three sample groups at all time points.

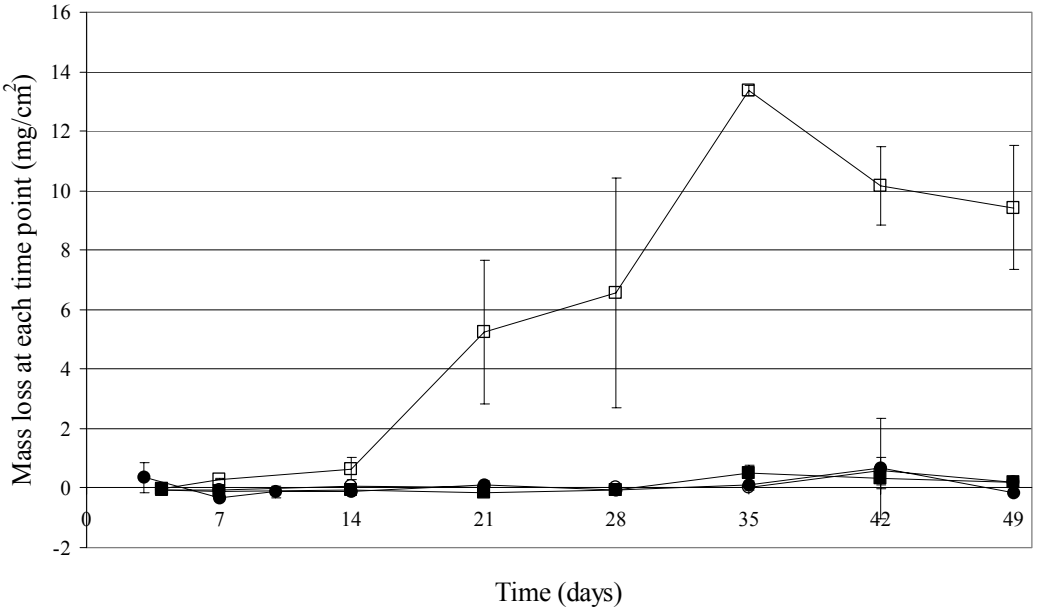

Figure 5.18 Mass loss (mg/cm^2) at each time point for **PLGA28** films degraded in PBS *in vitro*: ● 50 μm films at 25°C with no media change, ○ 150 μm films at 25°C with no media change, ■ 150 μm films at 25°C with media change, □ 150 μm films at 37°C with media change.

The PDI results for the **PLGA28** sample groups are shown in **Figure 5.19**. The 150 μm thick samples at 25°C with no media change (○) showed an increasing trend in PDI starting at day 14 and continuing to day 49. When comparing the 50 μm (●) and 150 μm (○) thick films at 25°C with no media change, the 150 μm thick films show a higher PDI than the 50 μm films at most time points, supporting the hypothesis of size-dependent degradation effects. The 150 μm thick samples at 25°C with media change (■) also showed an increase in PDI to greater than a value of 3 beginning at day 21 and continuing to increase up to day 49, at which time the measured PDI value was 10. When comparing the effect of media change on the 150 μm films at 25°C (○ = no media change, and ■ = media change), the samples that did not have the media changed showed an earlier increase in PDI and higher PDI values at most time points, again supporting the theory that changing the media helps to remove the acidic degradation products, thereby slowing the degradation rate. When comparing the 150 μm samples at 25°C (■) and 37°C (□), it is evident that the 37°C samples did not show a large increase in PDI over the course of the study, while the 25°C samples showed a delayed increase in the measured PDI. This result, along with the M_w, mass loss, and pH results, suggests that the 37°C samples degraded

quite rapidly. Overall, the PDI results for the **PLGA28** samples appear to correlate well with the molecular weight results.

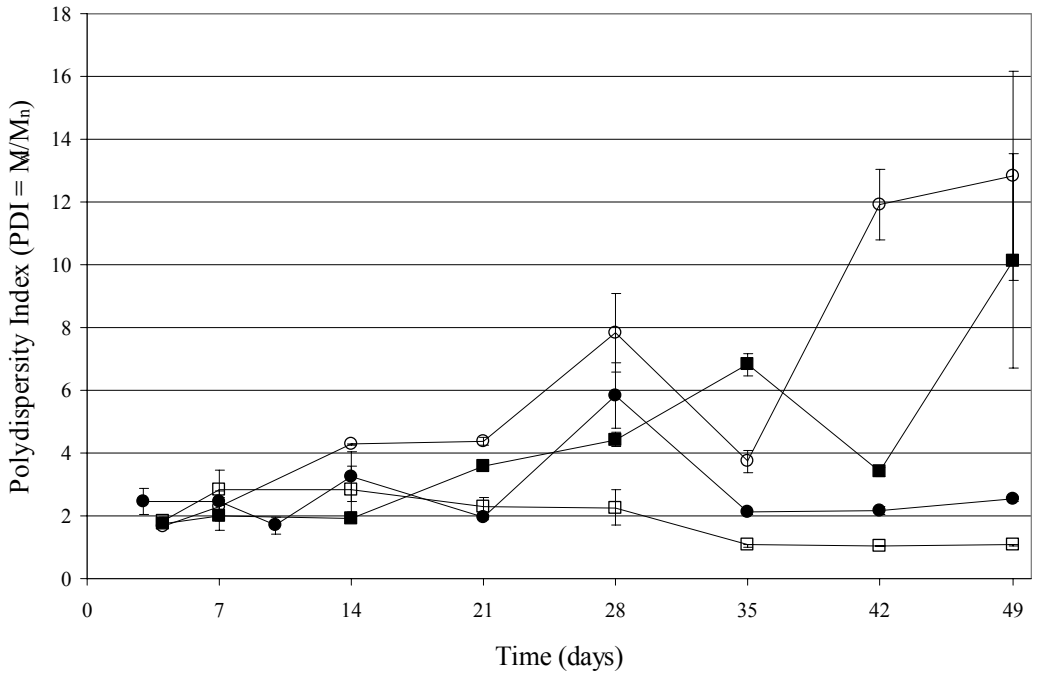

Figure 5.19 PDI over time of **PLGA28** film samples degraded *in vitro*: ● 50 μm films at 25°C with no media change, ○ 150 μm films at 25°C with no media change, ■ 150 μm films at 25°C with media change, □ 150 μm films at 37°C with media change.

5.3.2.4 **PLGA64**

The weight-average molecular weight (M_w) reported by the manufacturer for this polymer is approximately 64,000 daltons, with a polydispersity index (PDI) of 1.9. Undegraded polymer powder (stored dry at –4°C since receipt from the manufacturer) that was analyzed on the GPC along with various sample batches showed a molecular weight ranging from 40,280 to 61,500 daltons and PDI values of 1.09–2.05.

The results for the **PLGA64** sample groups are summarized in **Figure 5.20** to **Figure 5.24**. The molecular weights of the **PLGA64** sample groups are shown in **Figure 5.20**.

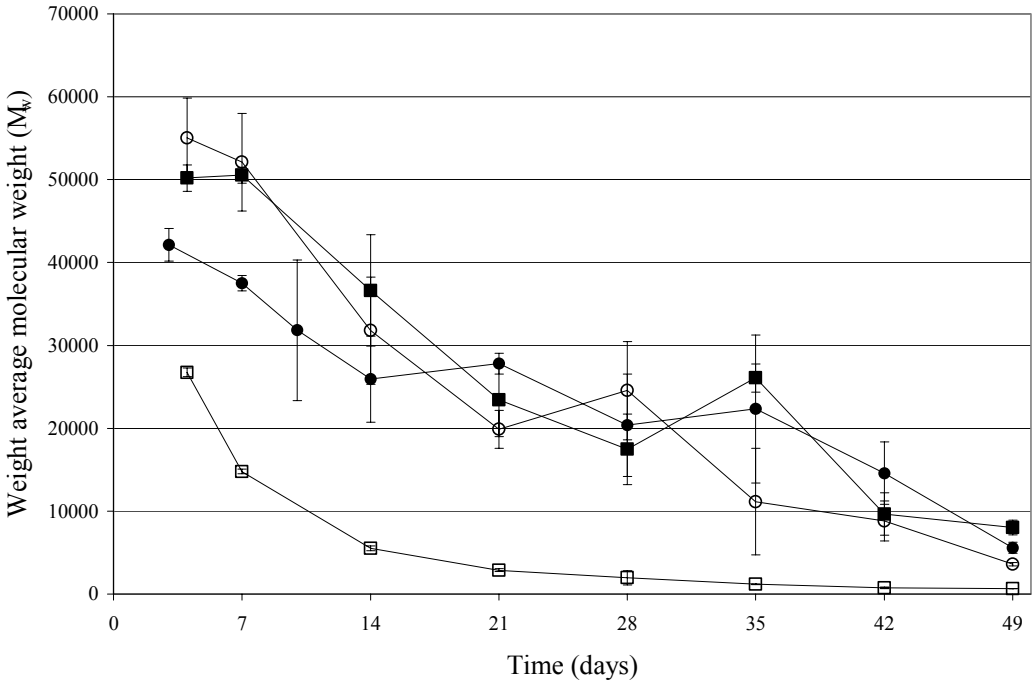

Figure 5.20 M_w over time of **PLGA64** film samples degraded *in vitro*: ● 50 μm films at 25°C with no media change, ○ 150 μm films at 25°C with no media change, ■ 150 μm films at 25°C with media change, □ 150 μm films at 37°C with media change.

A comparison of the curves for the 50 μm films (●) and 150 μm films (○) at 25°C with no media change shows that the initial degradation rates (slopes of the curves) for the two materials are similar. However, the 150 μm films initially had a higher measured molecular weight, but had a lower molecular weight at the conclusion of the study on day 49. This seems to support the size dependent degradation rate theory, with the thicker films showing faster degradation overall than the thinner ones. A comparison of the curves for the 150 μm films at 25°C with (○) and without (■) media change shows very similar behavior for the samples in these two groups. Changing the media does not appear to significantly affect the molecular weight change of this polymer, although the 150 μm films at 25°C without media change (○) show a slightly lower molecular weight at 49 days compared to the films with media change (■). The effect of temperature can clearly be seen in a comparison of the curves for the 150 μm thick films at 25°C (■) and at 37°C (□). Similar to the other polymers examined in this study, the **PLGA64** showed a much faster drop in molecular weight for the samples that were maintained at 37°C.

The measured pH of the media surrounding the different samples groups is shown in **Figure 5.21**. Similar to the results obtained for the **PLGA28** materials (see **Figure 5.16**), the 150 μm films at 37°C were the only group to show a significant change in pH over the course of the study. Interestingly, however, the 150 μm films at 25°C with no media change (○) showed a small drop in pH at day 49, which was not observed for **PLGA28** films under the same conditions (see **Figure 5.16**).

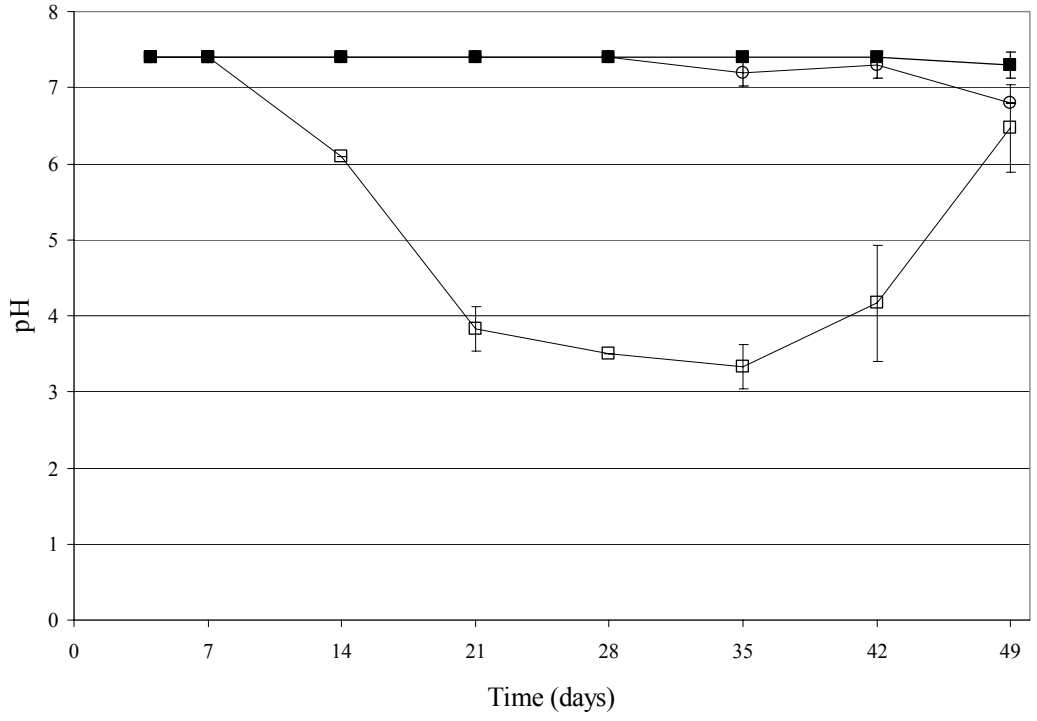

Figure 5.21 Measured pH over time of medium surrounding **PLGA64** film samples degraded *in vitro*: ○ 150 μm films at 25°C with no media change, ■ 150 μm films at 25°C with media change, □ 150 μm films at 37°C with media change.

The masses remaining of the various samples groups are shown in **Figure 5.22**. Similar to the results obtained for all of the other polymers investigated in this study, the **PLGA64** material showed the greatest mass loss for the films maintained at 37°C (□ symbols). Both the 50 μm and 150 μm thick films at 25°C with no media change (● and ○ symbols, respectively) showed slight mass loss over the course of the study, but the 150 μm films at 25°C with media change (■ symbols) did not appear to show any significant mass loss. This confirms the molecular weight results in **Figure 5.20**, which indicated that the 150 μm PLGA films at 25°C

with media change (■ symbols) showed less degradation and a higher molecular weight than the samples without media change (● and ○ symbols).

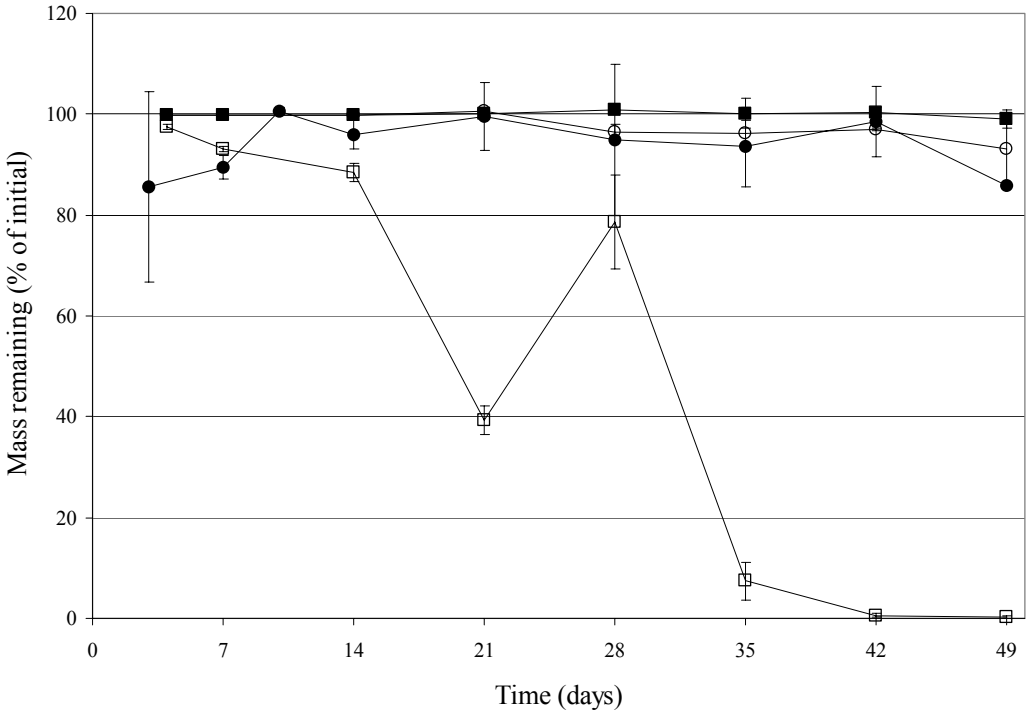

Figure 5.22 Mass remaining over time of **PLGA64** film samples degraded *in vitro*: ● 50 μm films at 25°C with no media change, ○ 150 μm films at 25°C with no media change, ■ 150 μm films at 25°C with media change, □ 150 μm films at 37°C with media change.

The normalized mass loss per unit area (shown in Figure 5.23) is much larger at each time point over the course of the study for the samples maintained at 37°C than for any of the other sample groups, which is consistent with the results obtained for the other polymers that were investigated in this study.

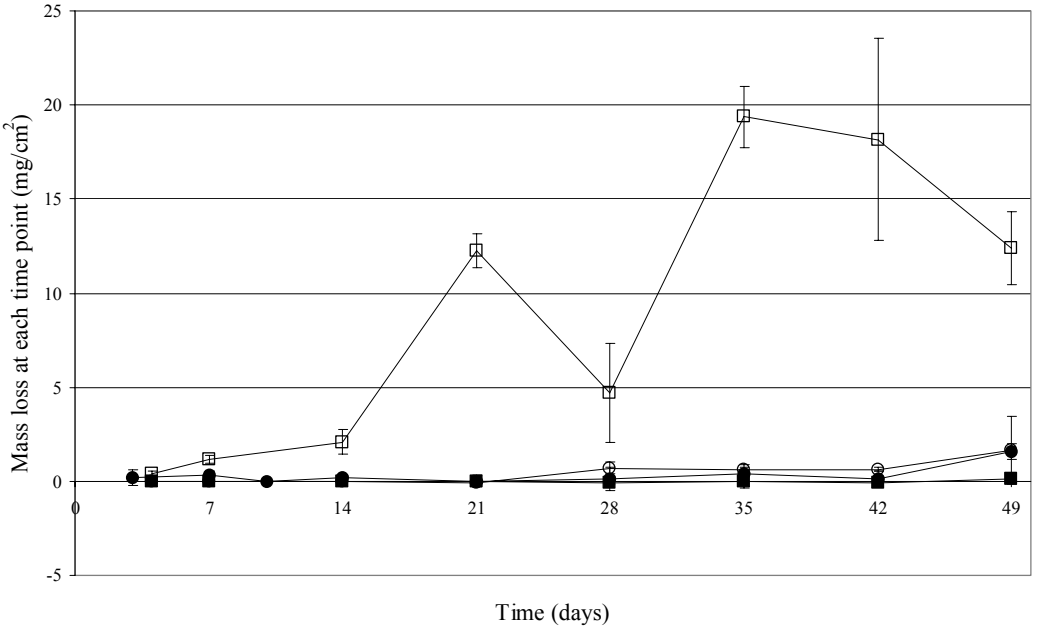

Figure 5.23 Mass loss (mg/cm^2) at each time point for **PLGA64** films degraded in PBS *in vitro*: ● 50 μm films at 25°C with no media change, ○ 150 μm films at 25°C with no media change, ■ 150 μm films at 25°C with media change, □ 150 μm films at 37°C with media change.

The PDI of the various **PLGA64** sample groups are shown in **Figure 5.24**. Overall, the 150 μm films at 25°C with no media change (○ symbols) showed the highest measured PDI, followed by the 150 μm films with media change at 25°C (■ symbols), the 50 μm films at 25°C with no media change (● symbols), and the 150 μm films at 37°C (□ symbols). The low PDI measured for the samples at 37°C is not surprising, considering the rapid loss of molecular weight seen in **Figure 5.20**. The slightly higher PDI of the 150 μm samples (○) compared to the 50 μm films (●) at 25°C with no media change suggests that this polymer may be exhibiting size-dependent degradation. The larger PDI value may be attributed to the presence of a wider range of molecular weight chains, with perhaps lower molecular weight chains existing in the interior of the film, and higher molecular weight chains towards the outside of the film.

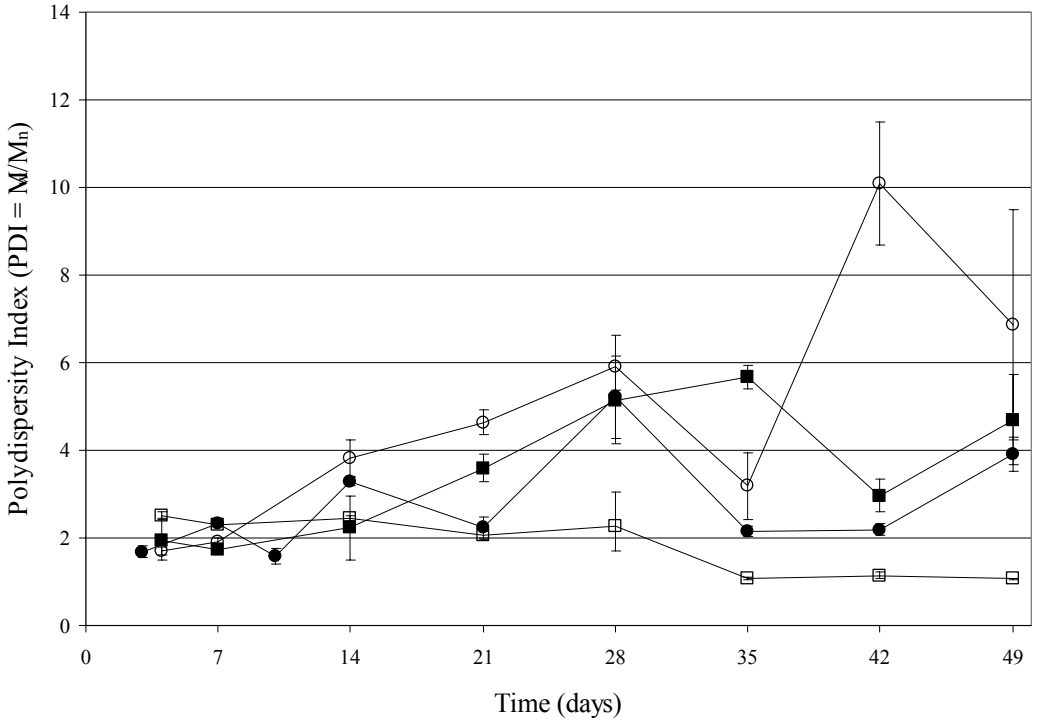

Figure 5.24 PDI values over time of **PLGA64** film samples degraded *in vitro*: ● 50 μm films at 25°C with no media change, ○ 150 μm films at 25°C with no media change, ■ 150 μm films at 25°C with media change, □ 150 μm films at 37°C with media change.

5.3.2.5 Discussion

A half-life ($t_{½}$, time at which the molecular weight is half of the initial molecular weight) was calculated for each sample group. The experimentally obtained molecular weight data were fit to the following equation:

$$M_w = bm^t$$

Equation 5-a

where M_w = molecular weight at time t, and b and m are constants determined using the LOGEST function in Windows Excel 2002, which uses regression analysis to fit an exponential curve to the data. The half-life was therefore found by using Equation 5-a with the experimentally calculated values of b and m, and setting $M_w = 0.5 \times M_w^{t=0}$. The calculated half-lives for each sample group are summarized in **Table 5-3** below.

Table 5-3 Calculated half-lives (time in days at which molecular weight is predicted to be one-half the initial molecular weight) for 50 and 150 μm thick **PLGA4.4**, **PLGA11**, **PLGA28**, and **PLGA64** films degraded *in vitro* under various conditions.

Polymer	50 μm films at 25°C, no media change	150 μm films at 25°C, no media change	150 μm films at 25°C, with media change	150 μm films at 37°C, with media change
PLGA4.4	46	26	NA (∞)	9
PLGA11	19	20	29	6
PLGA28	74	36	54	7
PLGA64	12	14	16	NA (<4)

Overall, the degradation rates of the four different polymers (**PLGA4.4**, **PLGA11**, **PLGA28**, and **PLGA64**) generally exhibited the expected behavior, with the lowest molecular weight material (**PLGA4.4**) showing the most rapid degradation rate as measured by the experimentally obtained values for M_w, PDI, pH, and mass loss.

In general, the 150 μm thick films showed more rapid degradation than the 50 μm films. This is evidenced by the $t_{1/2}$ values in **Table 5-3** for the **PLGA4.4** and **PLGA28** samples, as well as by the experimental results. The 150 μm films typically had higher PDI values than the 50 μm films at 25°C, and the 150 μm films at 25°C always had an average molecular weight at 49 days that was lower than that of the 50 μm films at 25°C after 49 days. Both of these results indicate that the 150 μm films undergo size dependent degradation, with a resulting wider range of chain molecular weights (high PDI values) and greater drop in molecular weight over the course of the study. Further evidence for the more rapid degradation of the thicker membranes is provided by the figures which show the mass loss per unit area, particularly **Figure 5.8** and **Figure 5.13**. Although some authors have speculated that the critical thickness above which the hydrolytic degradation of PLGA polymers becomes heterogeneous is 200 to 300 μm[1], others have reported differential rates of degradation for samples having dimensions from 100 μm to as small as 0.53 μm[4,14]. Faster degradation, as characterized by gel permeation chromatography of polymer molecular weights, has been reported for poly(lactide-co-glycolide) microspheres 22.5 μm in diameter compared to both 6.87 and 0.53 μm diameter microspheres[4]. Similarly, 100 μm thick films of poly(D,L-lactic-*co*-glycolic acid) had both faster mass loss and a faster decrease in

molecular weight than ten μm thick films when degraded over a period of ten weeks in PBS at 37°C *in vitro*[14]. Our results tend to support these studies, as we observed a difference in degradation rates between the 50 and 150 μm thick films.

The 150 μm films at 25°C that had the media changed typically showed an increase in PDI values at later times than the 150 μm films at 25°C that did not have the media changed. **Error! Reference source not found.** also shows longer $t_{1/2}$ values for 150 μm thick films that had media changed than for 150 μm thick films that did not have the media changed. This indicates that the accumulation of acidic degradation products (confirmed by the pH measurements) contributed to the faster degradation of the sample groups that did not have the media changed.

The effect of temperature on the degradation rate was clearly visible for all four of the materials studied. The sample groups at 37°C showed much more rapid decreases in molecular weight, faster drops in pH, earlier onset of mass loss, and lower PDI values compared to the samples at 25°C. The difference in degradation rates between the samples maintained at 37°C and at 25°C is quite dramatic when comparing the $t_{1/2}$ values in **Table 5-3**. These results all suggest extremely rapid degradation at this temperature.

The **PLGA64** material shows a surprisingly steep decrease in the molecular weight over time compared to the **PLGA28** material, as evidenced by the smaller $t_{1/2}$ values for the **PLGA64** compared to the $t_{1/2}$ values for the **PLGA28** in **Table 5-3**. In fact, the **PLGA64** polymer had a lower measured molecular weight after 49 days than the **PLGA28** in all sample groups. Additionally, when comparing the pH results for these two materials for the groups of 150 μm films at 25°C with no media change (○ symbols) in **Figure 5.16** and **Figure 5.21**, the **PLGA64** sample group shows a slight drop in the pH at day 49, while the **PLGA28** sample group does not. This result also indicates faster degradation of the **PLGA64** material. As was discussed in section 4.3.2.2.1 (^{125}I-HGH and ^{14}C-dextran *in vitro* release studies), these two polymers were nearly identical in chemical composition: both polymers were 54 mole % D,L-lactic acid and 46 mole % glycolic acid, with 1.2% residual D,L-lactide monomer. The **PLGA28** had 0.2% residual glycolide monomer, while the **PLGA64** had 0.1% residual glycolide monomer. Thus although it is unlikely that any chemistry difference can account for the faster degradation rate of the **PLGA64** in some cases, greater blockiness of the **PLGA28** could explain the unexpected degradation behaviors. X-ray diffraction of these two materials, however, did not show any

significant crystallinity. Additionally, the observation of a lower molecular weight of the **PLGA64** polymer compared to the **PLGA28** polymer at day 49 offers an explanation for the observed opening of reservoirs having **PLGA64** membranes prior to those having **PLGA28** membranes in some instances, as discussed in Chapter 4.

The molecular weight results for the **PLGA28** correlate well with data at short times from the literature[10], which indicate a molecular weight of 22,500 daltons after 10 days in pH 7.4 PBS at 37°C for a similar polymer of 29,270 M_w. However, at longer times, the 29,270 M_w polymer was reported to show a continually rapid decrease in molecular weight with a final molecular weight of less than 2,500 after 40 days, while the **PLGA28** polymer samples in our study had a molecular weight of nearly 600 after 42 days *in vitro* at 37°C. Another study reported a final M_w close to 500 daltons for a polymer having an initial M_w of 18,000 daltons after 14 days in deionized water at 37°C[11]. The comparable polymer in our study, **PLGA11**, showed an average molecular weight of ~3,500 daltons after 14 days. The faster apparent degradation of the M_w 18,000 polymer may be due to the larger size of the specimens studied (300 μm thick films) in the reported investigation, as well as the fact that the media in which the samples were immersed was not refreshed over the course of the study, in contrast to the **PLGA11** samples maintained at 37°C in our study, which did have the media replaced once per week. The molecular weight of the **PLGA4.4** material was difficult to reliably characterize over the entire course of our study due to its rapid degradation and the lower molecular weight limits of the GPC columns.

In general, most of the sample groups studied exhibited a drop in molecular weight followed by mass loss. In the specific example of the 150 μm films at 37°C, the **PLGA11** films did not begin to lose mass until after day 7, at which time the M_w had already dropped to approximately 4,400 daltons. Similarly, the **PLGA28** and **PLGA64** did not show appreciable mass loss until after 14 days, at which point the measured molecular weights were between 5,000 to 7,000 daltons. An initial drop in molecular weight followed by mass loss has been reported elsewhere for degradation studies of PLA and PGA homo- and co-polymers[1,2,7–10,12]. It is hypothesized that although the PLGA objects show a decrease in their molecular weights as soon as hydrolytic scission of the chains begins (when the samples come into contact with water), the polymer chains are still too large to diffuse out of the polymer object. Only at longer degradation times, after continued chain scission, will the chains become short enough to diffuse out of the

object and cause a subsequent loss in mass[8]. For example, poly(lactide-*co*-glycolide) having an initial molecular weight of 29,270 daltons had a measured molecular weight around 5,000 to 10,000 daltons after 30 days in pH 7.4 PBS at 37°C *in vitro*, at which point mass loss began and was complete by 50 to 60 days[10]. These results are very similar to the molecular weight and mass loss results that were obtained for the **PLGA28** material, shown in **Figure 5.15** and **Figure 5.17**. Data reported in the literature for polymers of 65,000 to 67,000 daltons (degraded in PBS at 37°C *in vitro*), however, are slightly different from the results we obtained. PLGA 50:50 copolymers having an initial M_w of 65,000 show a delay of 7 weeks before mass loss began[2]. Other studies have reported a 5–6% initial weight loss for M_w 67,000 PLGA 50:50 copolymers, followed by no further weight loss until 25 weeks[1]. However, the discrepancy between these results and the results obtained for our **PLGA64** are consistent with the fact that the **PLGA64** appears to degrade more rapidly than expected (i.e. faster than the **PLGA28** polymer in this study). Finally, for PLGA 50:50 copolymers with a molecular weight of 94,500 that were studied for 6 weeks, the maximum erosion rate appears to occur between 18 and 20 days[13]. Our results are in agreement with the general trend shown by others, that the polymers having lower initial molecular weights have an earlier onset of mass loss, and that mass loss is preceded by a decrease in the measured molecular weight.

Finally, comparison of results from release studies with the molecular weight data obtained in the degradation study of the 150 μm films (**Figure 5.5**, **Figure 5.10**, **Figure 5.15**, and **Figure 5.20**) suggest that perhaps a threshold molecular weight might exist that is correlated with release of the reservoir contents due to mechanical weakness of the membranes. **Table 5-4** below shows the observed release times for the devices that were loaded with ^{14}C-dextran and that had 150–175 μm thick membranes (release results are shown in **Figure 5.1** and discussed in section 5.3.1.1). The **PLGA4.4** and **PLGA11** samples in the degradation study had a molecular weight near 4,400 during the time period in which release was detected from reservoirs on the ^{14}C-dextran loaded devices that had membranes made from those two polymers. The 150 μm thick **PLGA28** and **PLGA64** polymer samples had average molecular weights of 15,770 and 8,040, respectively, at the conclusion of the *in vitro* degradation study, while release of ^{14}C-dextran was detected from reservoirs having **PLGA28** and **PLGA64** membranes from 58–92 and 66–121 days, respectively. Although a direct comparison of the molecular weight data from the degradation study with the observed release times from the release study cannot be made due to

conclusion of the *in vitro* degradation study prior to observed release, the overall results nevertheless suggest that the release of chemicals from the devices may be correlated with a critical membrane molecular weight of around 5,000 daltons.

Table 5-4 Release times *in vitro* at 25°C for devices loaded with ^{14}C-dextran and having ~150-175 μm thick **PLGA4.4**, **PLGA11**, **PLGA28**, and **PLGA64** membranes compared with molecular weight results from *in vitro* degradation study of 150 μm thick films at 25°C with media change.

Membrane Polymer	Time to Release (days)	Measured M_w of film samples
PLGA4.4	<1	4,400 @ 0 days
PLGA11	25-32	4,400 @ 28 days
PLGA28	58-92	15,770 @ 49 days
PLGA64	66-121	8,040 @ 49 days

Similarly, comparison of release results at 37°C *in vitro* from devices having 150 μm thick **PLGA11** and **PLGA64** membranes and loaded with ^{14}C-mannitol (experimental methods are presented in Chapter 9) show excellent agreement with results obtained for the 150 μm thick films at 37°C with media change in the *in vitro* degradation study presented in this chapter. The compiled data are shown in **Figure 5.25** below. ^{14}C-mannitol was released from the reservoirs having **PLGA11** membranes around four to six days, and the **PLGA11** films in the degradation study had an average molecular weight in the range of 5,000 to 7,000 during this time period. Similarly, ^{14}C-mannitol was released from the reservoirs having **PLGA64** membranes between days 12 to 15, at which time the **PLGA64** films in the degradation study had an average molecular weight close to the range of 5,000 to 7,000.

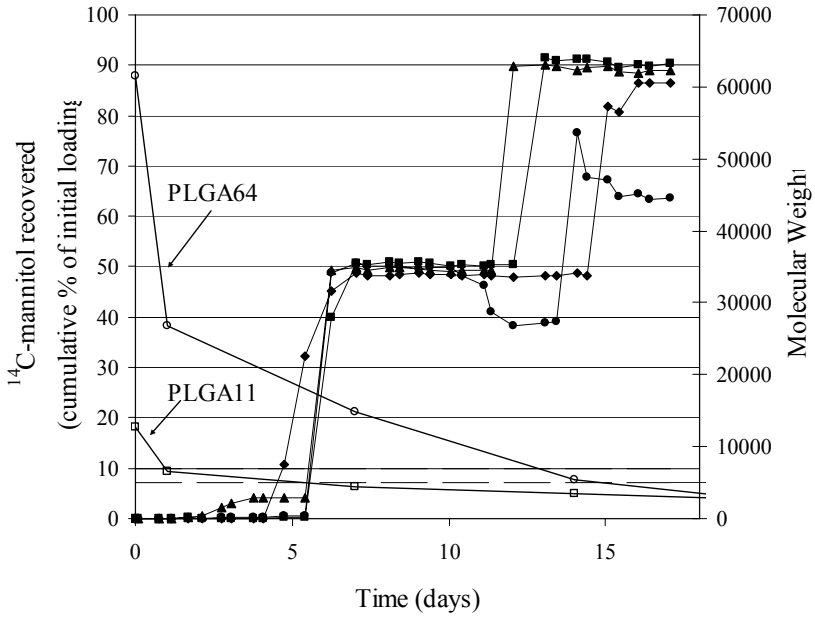

Figure 5.25 Comparison of release results obtained *in vitro* at 37°C for four devices (▲■●♦) loaded with ^{14}C-mannitol and having 150 μm thick **PLGA11** and **PLGA64** reservoir membranes with molecular weight data obtained for 150 μm thick **PLGA11** (□) and **PLGA64** (○) film samples degraded at 37°C *in vitro* with media change. Horizontal dashed lines indicate range of 5,000 to 7,000 molecular weight on right y-axis.

These results suggest that perhaps once the molecular weight of the membrane material drops below a critical value, in the range of 4,000 to 7,000 daltons, the membrane becomes so mechanically weak that it ruptures and releases the contents of the reservoir. It seems unlikely that the membrane opens due to simple dissolution of the low molecular weight chains, as others have reported a critical weight average molecular weight of 1,050 to 1,150 for water solubility of poly(D,L-lactic acid) oligomers[15], which is much lower than the 4,000–7,000 molecular weight that seems to be significant for membrane opening in the studies reported here.

5.4 Conclusions

The results obtained for the *in vitro* release studies presented here clearly show a dimension-dependence of the membrane degradation rate with consequent changes in the release times of chemicals from the microreservoir device. This is confirmed by the results of the degradation study that was conducted. Higher environmental temperatures appear to cause faster degradation of the materials, but changing the media in which the samples are maintained appears to slow the degradation process, as the removal of the acidic degradation products tends

to maintain the pH of the medium at a higher value. Perhaps most significantly, comparison of the results of release studies with the degradation study suggest that a threshold molecular weight for the reservoir membranes may exist which is correlated with drug release from the reservoir. Further study of the mechanical properties of the membrane materials may aid in elucidating the exact relationship between membrane molecular weight and reservoir release time.

5.5 Acknowledgements

The experiments reported here were conducted in part by Rebecca Griffiths and Casey Dwyer as part of the UROP program at MIT.

5.6 References

1. I. Grizzi, H. Garreau, S. Li, and M. Vert, "Hydrolytic degradation of devices based on poly (DL-lactic acid) size-dependence," *Biomaterials*, 16 (1995) 305–311.

2. S. M. Li, H. Garreau, and M. Vert, "Structure-property relationships in the case of the degradation of massive aliphatic poly-(α-hydroxy acids) in aqueous media, Part 1: Poly (DL-lactic acid)," *Journal of Materials Science: Materials in Medicine*, 1 (1990) 123–140.

3. S. Hurrell and R. E. Cameron, "Polyglycolide: degradation and drug release. Part I: Changes in morphology during degradation," *Journal of Materials Science: Materials in Medicine*, 12 (2001) 811–816.

4. M. Dunne, O. I. Corrigan, and Z. Ramtoola, "Influence of particle size and dissolution conditions on the degradation properties of polylactide-*co*-glycolide particles," *Biomaterials* 21 (2000) 1659–1668.

5. L. Lu, S. J. Peter, M. D. Lyman, H.-L. Lai, S. M. Leite, J. A. Tamada, J. P. Vacanti, R. Langer and A. G. Mikos, "*In vitro* degradation of porous poly(L-lactic acid) foams," *Biomaterials* 21 (2000) 1595–1605.

6. K. Fu, D. W. Pack, A. M. Klibanov, and R. Langer, "Visual evidence of acidic environment within degrading poly (lactic-co-glycolic acid) (PLGA) microspheres," *Pharmaceutical Research* 17 (2000) 100–106.

7. M. Hakkarainen, A.-C. Albertsson, and S. Karlsson, "Weight losses and molecular weight changes correlated with the evolution of hydroxyacids in simulated *in vivo* degradation of homo- and copolymers of PLA and PGA," *Polymer Degradation and Stability* 52 (1996) 283–291.

8. C. M. Agarwal, D. Huang, J. P. Schmitz, and K. A. Athanasiou, "Elevated temperature degradation of a 50:50 copolymer of PLA-PGA," *Tissue Eng.* 3 (1997) 345–352.

9. A. M. Reed and D. K. Gilding, "Biodegradable polymers for use in surgery — poly(glycolic)/poly(lactic acid) homo and copolymers: 2. *In vitro* degradation," *Polymer* 22 (1981) 494–498.

10. C. Witt, K. Mäder, and T. Kissel, "The degradation, swelling and erosion properties of biodegradable implants prepared by extrusion or compression moulding of poly (lactide-co-glycolide) and ABA triblock copolymers," *Biomaterials* 21 (2000) 931–938.

11. C. G. Pitt, Y. Cha, S. S. Shah, and K. J. Zhu, "Blends of PVA and PGLA: control of the permeability and degradability of hydrogels by blending," *J. Control. Release* 19 (1992) 189–200.

12. J. E. Bergsma, F. R. Rozema, R. R. M. Bos, G. Boering, C. A. P. Joziasse, and A. J. Pennings, "*In vitro* predegradation at elevated temperatures of poly(lactide)," *Journal of Materials Science: Materials in Medicine* 6 (1995) 642–646.

13. J. A. Tamada and R. Langer, "Erosion kinetics of hydrolytically degradable polymers," *Proc. Natl. Acad. Sci. U. S. A.* 90 (1993) 552–556.

14. L. Lu, C. A. Garcia, and A. G. Mikos, "In vitro degradation of thin poly(DL-lactic-co-glycolic acid) films," *Journal of Biomedical Materials Research* 46 (1999) 236–244.

15. T. G. Park, "Degradation of poly(D,L-lactic acid) microspheres: effect of molecular weight," *J. Controlled Release* 30 (1994) 161–173.

6 Calculation of Partition Coefficients

6.1 Introduction and Motivation

6.1.1 Introduction

The reliability and reproducibility of drug delivery devices is a vital factor when considering end-stage application and use in human patients. In the case of our biodegradable microreservoir devices, there are numerous factors that may affect the performance of the devices, including the degradation behavior of the reservoir membranes as discussed in Chapter 5. However, the performance of the device may also be affected by the characteristics of the drugs that are released from the reservoirs. The results obtained in Chapter 4 showed different release times for reservoirs having the same polymer membranes but different chemicals loaded into the reservoirs. One possible reason for this is that the partitioning of the drug into the membrane itself may affect the observed release kinetics. The complex mechanisms by which the PLGA membrane materials undergo degradation (swelling, diffusion of oligomers, and production of a porous structure[1]) may mean that partitioning of the chemicals into the membranes could affect the observed release times and kinetics. In the case of 1,3-bis(2-chloroethyl)-1-nitrosourea (BCNU), the release kinetics may be further complicated by the formation of hydrolysis products, which might themselves diffuse through the reservoir membranes or affect the degradation rate of the membrane materials. Understanding the chemistry and physics of the interactions between the drug of interest and the membrane materials is essential in order to reliably predict and control device performance. Thus, our long-term goal is to design our microreservoir drug delivery system such that the release characteristics and device performance are either a) independent of the drug being released, or b) vary according to the properties of the drugs in a predictable and well-understood manner.

6.1.2 Motivation

Previous release experiments suggested that the release times for various reservoir membrane materials might be partially controlled by the molecule of interest that is released from the reservoirs, but it is not clear that this is solely either a size or chemistry effect. In Chapter 4, for example, reservoirs loaded with ^{14}C-labeled 1,3-bis(2-chloroethyl)-1-nitrosourea

(BCNU) showed much different release kinetics than reservoirs loaded with ^{14}C-dextran or ^{3}H-heparin, even when the reservoir membranes were fabricated from the same PLGA copolymer. The goal of the experiments reported in this chapter was to determine whether the observed kinetic behavior of chemicals that have been investigated in prior release studies could be systematically explained by their molecular chemistry or size. Specifically, we desired to determine the partition coefficients of various molecules in four membrane materials of interest, and compare and contrast our results with release data obtained in prior experiments.

6.2 Materials and Methods

6.2.1 Materials

Poly(L-lactic acid) (**PLA**, M_w 194 Kilodaltons (Kd), Medisorb® 100 L) and poly(D,L-lactic-*co*-glycolic acid) polymer powders of molecular weights (M_w) 4.4 Kd (**PLGA4.4**, Medisorb® 5050 DL 1A), 11 Kd (**PLGA11**, Medisorb® 5050 DL 2A), 28 Kd (**PLGA28**, Medisorb® 5050 DL 3A), and 64 Kd (**PLGA64**, Medisorb® 5050 DL 4A) were obtained from Alkermes (Cincinnati, Ohio). Reagent grade dichloromethane, 1,1,1,3,3,3-hexafluoro-2-propanol (HFIP), HPLC grade methyl alcohol, and ^{14}C-dextran (M_ws = 40,000 and 70,000) were purchased from Sigma-Aldrich (St. Louis, MO). ^{14}C-carmustine (1,3-bis(2-chloroethyl)-1-nitrosourea, or BCNU) was purchased from Moravek Biochemicals (Brea, CA). ^{3}H-heparin sodium salt and ^{125}I-interleukin-2 (IL-2) were purchased from PerkinElmer Life Sciences (Boston, MA). ^{14}C-iodoantipyrine (IAP) was purchased from New England Nuclear Life Science Products (Boston, MA). Ideal 9144 Masking Tape was obtained from American Biltrite, Inc. (Lowell, MA). Mylar® sheets were donated from the laboratory of Dr. James Anderson at Case Western Reserve University.

6.2.2 *In vitro* measurement of partition coefficients

Solutions of **PLA**, **PLGA4.4**, **PLGA11**, **PLGA28**, and **PLGA64** were prepared in HFIP. The solutions were cast onto Mylar® sheets that had been cleaned with Kimwipes® and acetone, and that had 3.5 × 3 cm^2 areas marked off with several layers of VWR time tape. Films were designed to be 50 μm thick. After casting, the films were dried at 93.5% vacuum (6.7 kPa, 28 in HgVAC) and approximately 80°C for 48 hours. After drying, the films were cut into samples

having an area of approximately 1 × 0.5 cm^2 and placed in microcentrifuge (microfuge) tubes. Mylar® control samples with no cast polymer films, 1 × 0.5 cm^2 in area, were also prepared and placed in microfuge tubes. Aliquots of the stock radiolabeled solutions (^{14}C-BCNU, ^{14}C-IAP, ^{14}C-dextran M_w 40,000, ^{14}C-dextran M_w 70,000, ^{3}H-heparin, and ^{125}I-IL-2) were analyzed on a Packard Tri-Carb Liquid Scintillation Analyzer, model U2200, using either a ^{14}C, ^{3}H, or ^{125}I counting protocol to verify the specific activities of the solutions (μCi/mL). One and one-half milliliters of a given stock solution were added to a microfuge tube containing one of the polymer films. Samples were prepared in triplicate. The experimental matrix is summarized in **Table 6-1** below.

Table 6-1 Sample labels for partition coefficient experiment.

Polymer / Chemical	**PLA**	**PLGA4.4**	**PLGA11**	**PLGA28**	**PLGA64**	**Mylar control**
^{14}C-dextran, 40K	L40K1	140K1	240K1	340K1	440K1	M40K1
	L40K2	140K2	240K2	340K2	440K2	M40K2
	L40K3	140K3	240K3	340K3	440K3	M40K3
^{14}C-dextran, 70K	L70K1	170K1	270K1	370K1	470K1	M70K1
	L70K2	170K2	270K2	370K2	470K2	M70K2
	L70K3	170K3	270K3	370K3	470K3	M70K3
^{14}C-IAP	LIAP1	1IAP1	2IAP1	3IAP1	4IAP1	MIAP1
	LIAP2	1IAP2	2IAP2	3IAP2	4IAP2	MIAP2
	LIAP3	1IAP3	2IAP3	3IAP3	4IAP3	MIAP3
^{14}C-BCNU	LB1	1B1	2B1	3B1	4B1	MB1
	LB2	1B2	2B2	3B2	4B2	MB2
	LB3	1B3	2B3	3B3	4B3	MB3
^{3}H-heparin	LHEP1	1HEP1	2HEP1	3HEP1	4HEP1	MHEP1
	LHEP2	1HEP2	2HEP2	3HEP2	4HEP2	MHEP2
	LHEP3	1HEP3	2HEP3	3HEP3	4HEP3	MHEP3
^{125}I-IL-2	LIL1	1IL1	2IL1	3IL1	4IL1	MIL1
	LIL2	1IL2	2IL2	3IL2	4IL2	MIL2
	LIL3	1IL3	2IL3	3IL3	4IL3	MIL3

The microfuge tubes were placed on an orbital shaker (Thermolyne Rotomix Type 50800) at 60 rpm and room temperature. After 48 hours, 100 μL aliquots of the solutions were pipetted from each microfuge tube into 7-mL scintillation vials. Five mL of ScintiSafe Plus 50% scintillation cocktail (Fisher Scientific, Suwanee, GA) were added to each vial, and the activities were measured on the Scintillation Analyzer using either a ^{14}C, ^{3}H, or ^{125}I counting protocol. Each film was then removed from the microfuge tube using tweezers, rinsed with milliQ deionized water, and placed in a 7-mL glass scintillation vial along with 5 mL of fresh milliQ deionized water. The films were left in the deionized water for a total of 30 days. At two, four,

seven, 18, and 30 days, aliquots of solution (one mL at each time point except 0.5 mL at 30 days) were pipetted from each microfuge tube into scintillation vials and assayed following the procedure described above. The measured activity (μCi) and the specific activity (μCi/μg) of the radiolabeled molecules were used to calculate the amount of radiolabel released from the films into the solution at each of the time points.

The partition coefficients (K_p) were calculated according to the following relation[2]:

$$K_p = \frac{C_{film}}{C_{solution}} = \frac{C_2 V_2}{V_m C_1}$$

Equation 6-a

where C_{film} = concentration of solute in the polymer film of interested, $C_{solution} = C_1$ = initial concentration of solute in which the membrane is equilibrated for 48 hours, C_2 = concentration of solute released into volume V_2 after desorption equilibrium has been reached, and V_m = volume of the polymer membrane or film of interest. The amount of solute in the solution in which the membrane was equilibrated for 48 hours was much larger than the amount of solute extracted from the films.

6.3 Results and Discussion

6.3.1 Stock Solution Activities and Film Characterization

The measured stock solution concentrations are summarized in **Table 6-2** below.

Table 6-2 Specific activities of radiolabeled stock solutions used to determine partition coefficients.

Chemical	Stock Solution Specific Activity (μCi/mL)
^{14}C-dextran, 40k	1.04
^{14}C-dextran, 70k	3.42
^{14}C-IAP	3.96
^{14}C-BCNU	0.61
^{3}H-heparin	3.17
^{125}I-IL-2	1.23

The area of each film was individually measured using a ruler. Film widths varied from 0.4 to 0.55 cm, while film lengths ranged from 0.85 to 1.05 cm. The partition coefficients for the various chemicals in each of the polymers were calculated according to Equation 6-a at each of the time points (two, four, seven, 18, and 30 days), taking into account the media that was

removed at previous time points. Partition coefficients for the various radiolabeled molecules were calculated including the contribution from the Mylar® backing. Scintillation measurements for iodine labeled samples were corrected for half-life decay of the isotope.

6.3.2 Small molecules (^{14}C-iodiantipyrine and ^{14}C-carmustine)

The partition coefficients calculated after 30 days for the small molecules of interest (^{14}C-IAP and ^{14}C-BCNU) are shown in **Figure 6.1** below.

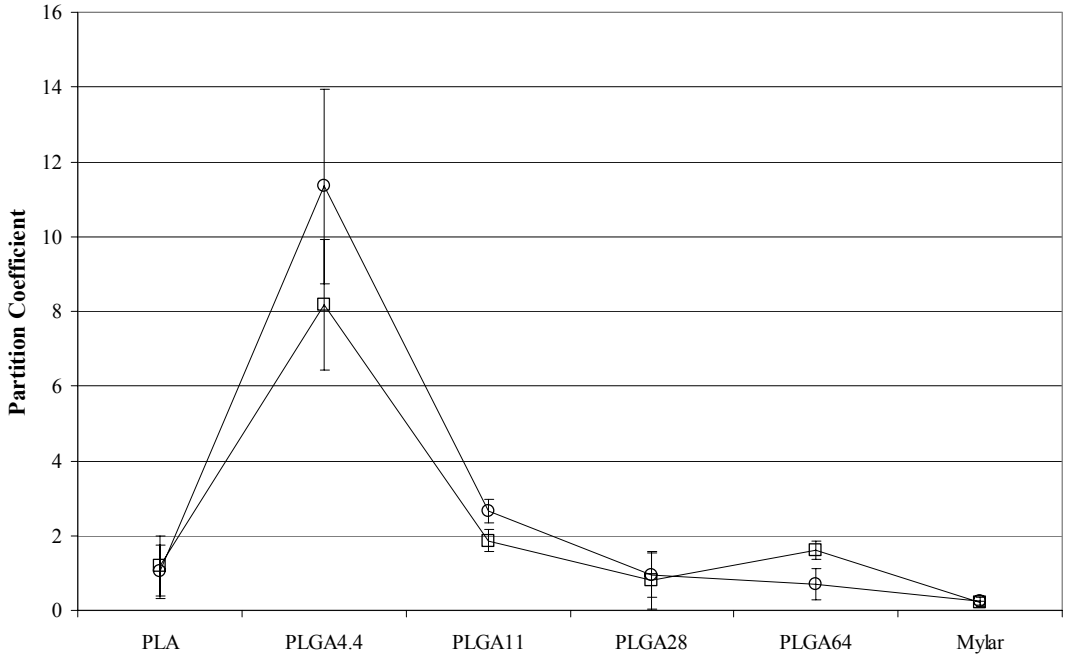

Figure 6.1 Partition coefficients of small molecules in various polymers: □ ^{14}C-IAP, ○ ^{14}C-BCNU.

Figure 6.1 clearly shows that the small molecules have a much higher partition coefficient in the lowest molecular weight PLGA (**PLGA4.4**) than any of the other polymers investigated. Although all of the PLGA materials have essentially the same chemical composition, the larger partitioning of the lower molecular weight molecules in the **PLGA4.4** may be due to the shorter polymer chain length and therefore greater free volume available in which the solute can reside. The free volume of a polymer is closely correlated with its glass transition temperature according to the following relation[3]:

$$f = f_g + (T - T_g)\alpha_f$$

Equation 6-b

where f = fractional free volume at temperature T above the glass transition temperature T_g, f_g = free volume at or below T_g (a constant for a given polymer), and α_f = thermal expansion coefficient. Given this relation between the glass transition temperature and free volume of a polymer, it is therefore not surprising that the **PLGA4.4** polymer, which has the lowest T_g of all the materials investigated here (**PLGA4.4** T_g = 31.4°C, **PLGA11** T_g = 37.8°C, **PLGA28** T_g = 45.2°C, **PLGA64** T_g = 47.7°C, **PLA** T_g = 45–50°C as reported by the manufacturer, Mylar® T_g = 99–102°C, determined experimentally – see section 10.3.3.1), showed the largest partitioning of these small molecules. A study reported in the literature of the permeability of homo- and copolymers of poly(ε-caprolactone) and poly(DL-lactic acid) provides further evidence for this theory, as the poly(DL-lactic acid) (T_g = 57°C) showed a much lower partition coefficient of progesterone compared to poly(ε-caprolactone) (T_g = –65°C)[4,5].

Although the octanol-water partition coefficient reported for BCNU (carmustine) in the literature[6] is much larger (approximately 33.8, log $P_{o:w}$ = 1.53) than the value measured here, this is not unexpected since our study measured the partitioning into a solid substrate, rather than into another liquid.

Sorption of BCNU (carmustine) to polymer surfaces has been reported elsewhere[7,8]. The lipophilicity and low molecular weight of this molecule have been cited as contributing factors to its sorption to plastic surfaces. A loss of approximately 80% of carmustine concentration over 120 minutes was seen when the molecule was retained in solution in polyurethane infusion sets[7]. Similar results were obtained in ethylenevinyl acetate copolymer (EVA, approximately 60% loss) and polyvinyl chloride (PVC, approximately 65% loss) infusion sets.

Iodoantipyrine (IAP) has a slightly lower octanol-water partition coefficient (18.62, log $P_{o:w}$ = 1.27)[9] than BCNU, meaning that it is slightly more hydrophilic. Thus we would expect slightly less partitioning of the IAP into the polymers when compared to the BCNU. Although the results shown in **Figure 6.1** actually show slightly greater partitioning of the IAP into the polymers compared to the BCNU, the results are within one standard deviation of each other and therefore the difference is not statistically significant.

6.3.3 Polysaccharides (^{14}C-dextrans and ^{3}H-heparin)

The calculated partition coefficients of various polysaccharides (^{14}C-dextran of 40,000 and 70,000 dalton molecular weights, as well as ^{3}H-heparin) are shown in **Figure 6.2**.

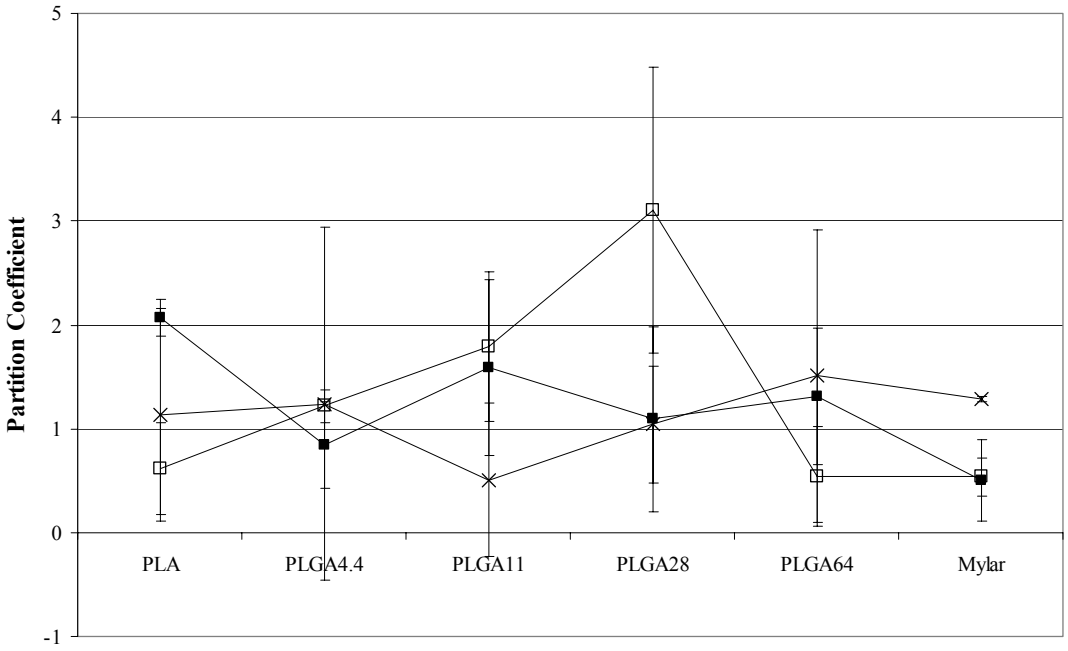

Figure 6.2 Partition coefficients of polysaccharides in various polymers: □ ^{14}C-dextran M_w~40,000, ■ ^{14}C-dextran M_w~70,000, × ^{3}H-heparin.

The behavior of the polysaccharides appears significantly different from that of the small molecules in several respects. The first is that the partition coefficients do not exhibit a maximum for the **PLGA4.4** polymer. While the **PLGA28** polymer showed the greatest absorption of the 40,000 molecular weight ^{14}C-dextran, however, this result was not significant due to the large standard deviation. In fact, the differences in calculated partition coefficients for both the ^{14}C-dextrans (40,000 and 70,000 molecular weights) as well as the ^{3}H-heparin were not significantly different (greater than one standard deviation) for any of the membrane polymers (**PLGA4.4**, **PLGA11**, **PLGA28**, and **PLGA64**) or the **PLA**. This result suggests that perhaps these molecules are above a threshold size at which permeation into the polymer films can occur. This hypothesis is supported by the fact that the partition coefficient values are generally equal to or less than those calculated for the small molecules shown in **Figure 6.1**. Additionally, partitioning of these molecules into the Mylar® films was small but non-zero (K_p values of 0.5 to 1.28), and the values obtained for the partition coefficients in the other polymers were typically within one standard deviation of the K_p values obtained in the Mylar®. This suggests that some of the adsorption of these molecules may have been due to their interactions with the Mylar®

substrate. This is a surprising result, since Mylar® is known to be relatively chemically inert, and partially crystalline. In the case of the heparin molecule that was used in this study, however, this result could be explained by the fact that the heparin sulfate was in the form of an ammonium salt. Hydrogen bonding or other ionic association of the sulfate groups on the heparin polysaccharide with the carbonyl in the Mylar® backbone or the ammonium ions with the benzyl ring in the Mylar® backbone could explain the larger apparent partitioning of the ^{3}H-heparin (× symbols in **Figure 6.2**) into the Mylar® compared to the other polymers in this study.

6.3.4 Proteins (^{125}I-IL-2)

The calculated partition coefficients for ^{125}I-IL-2 are shown in **Figure 6.3** below.

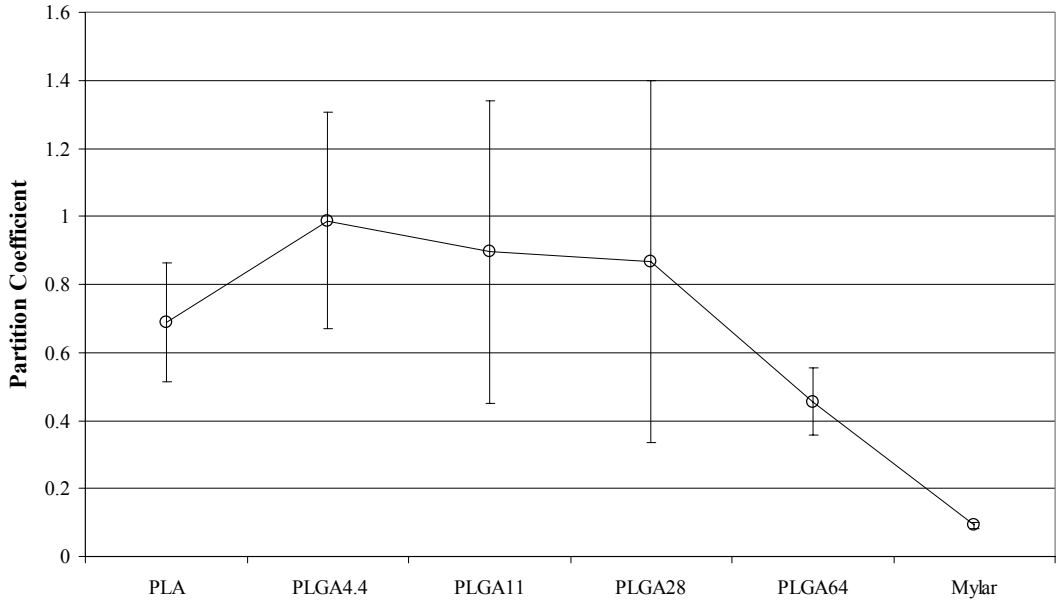

Figure 6.3 Partition coefficients of ^{125}I-IL-2 in various polymers.

The calculated partition coefficients for the ^{125}I-IL-2 are quite low, showing a maximum of only 0.4 for the **PLGA4.4** films. This is not surprising, given the high molecular weight of the protein (approximately 15,000 daltons) and its relative hydrophobicity. Another factor that may contribute to the low measured absorption by the polymers of IL-2 is that the recombinant IL-2 that was used in this study is known to stick to glass and plastics[10]. Sticking of IL-2 to the surface of the microfuge tube during the initial equilibration phase of the study would cause the

concentration of the molecule in solution to be less than expected. Thus the solution concentration C_1 in the denominator of Equation 6-a used to calculate the partition coefficients would be larger than the actual value, resulting in an artificially low value of K_p for this molecule. Further, sticking of the IL-2 to the surface of the polymer film during the desorption phase of the study would result in an artificially low value of C_2 (concentration of the solute released into the medium after desorption equilibrium was reached), which would also result in a lower value of K_p according to Equation 6-a.

6.3.5 Discussion

The values of partition coefficients obtained for the various chemicals in this study help to explain, to some extent, the sustained release that was observed for ^{14}C-BCNU and ^{14}C-IAP in some of the release experiments reported (see Chapter 4). The high partition coefficients of the ^{14}C-BCNU and ^{14}C-IAP in the **PLGA4.4** may partially explain the diffusional release seen in Chapter 4 for devices loaded with both ^{14}C-BCNU and ^{14}C-IAP, although the reservoirs having **PLGA11**, **PLGA28**, and **PLGA64** membranes also showed diffusional release. This suggests that perhaps the driving force for diffusion due to the concentration gradient across the reservoir membranes on a microreservoir device may be responsible for the observed diffusional release, rather than just the partitioning of the molecule. In the case of our partitioning study reported here, the system is allowed to come to equilibrium in order to determine the partition coefficient. An actual release study, in contrast, is not in equilibrium due to the high concentration gradient of the drug across the reservoir membrane. Although the equilibrium partitioning of the drug into the membrane may not necessarily be large, if the driving force for diffusion is large there will be a continual flux of the drug through the membrane, and consequently diffusional release of the drug from the device will be observed. In contrast, we would expect that although the concentration gradient across the membranes may be comparable for the large molecules investigated here (^{14}C-dextrans, ^{3}H-heparin, and ^{125}I-IL-2), the diffusion coefficients are likely much smaller due to the large sizes of the molecules, and this may be the reason that no diffusional release of these molecules was seen in our release studies presented in Chapter 4 over the time period of interest.

While the partition coefficients obtained here are small but non-zero for all of the polymers that were investigated, it is important to keep in mind that the experimental conditions

that were used here are dissimilar to those that would be experienced by a drug for either *in vitro* or *in vivo* release. The circumstances of interest for chemicals partitioning into the reservoir membranes in a release study will be the situation in which chemical solids are dried on the inside of the device reservoir and are in contact with the cast (or microinjected) polymer film membrane at 37°C. It is expected that the partitioning and diffusion would be much lower in that case than in the studies reported here, as the reservoir membranes would not be as hydrated and swollen on the inside of the reservoirs as they presumably were in the study reported here. In the absence of an experimental setup that exactly mimics that of an *in vitro* or *in vivo* release study, however, a qualitative evaluation of the partition coefficients can simply be deduced from the shape of the release curves for a given microreservoir device. In the case of the large molecules investigated (^{14}C-dextran having a molecular weight of 70,000, ^{3}H-heparin, and ^{125}I-IL-2 at short times), pulsatile release without significant diffusion is clearly achievable and demonstrable as was shown in Chapter 4.

None of the chemicals studied showed significant partitioning into the **PLA** films over the course of the study. This suggests that permeation of drugs from the reservoir chambers into the substrate of the device will not be significant over the first 30 days of device usage. However, the microreservoir device substrate is hot compression molded rather than solvent cast, as was the case for the **PLA** films used in this study, so these results should be extrapolated with care.

6.4 Conclusions

While most of the chemicals investigated did not appear to undergo significant partitioning into the various membrane materials, both ^{14}C-BCNU and ^{14}C-IAP showed large K_p values for both the **PLGA4.4** and **PLGA11** membrane materials. This is generally consistent with results reported in the literature for other polymers having low glass transition temperatures that showed significant permeability of solutes. These results are also consistent with release data obtained and reported in Chapter 4 that show no significant burst or diffusional release of chemicals from the reservoirs prior to membrane opening, except in the cases of ^{14}C-BCNU or ^{14}C-IAP loaded reservoirs. This result bodes well for device scale up and commercialization for large molecules, as the release kinetics of the chemicals appear to be dictated only by the

degradation times of the reservoir membrane materials and not by the partitioning and/or diffusion of these large molecules into and through the reservoir membranes.

6.5 References

1. S. M. Li, H. Garreau, and M. Vert, "Structure-property relationships in the case of the degradation of massive aliphatic poly-(α-hydroxy acids) in aqueous media, Part 1: Poly(DL-lactic acid), *Journal of Materials Science: Materials in Medicine* 1 (1990) 123–130.

2. L. LeBrun, and G.-A. Junter, "Diffusion of sucrose and dextran through agar gel membranes," *Enzyme Microb. Technol*. 15 (1993) 1057–1062.

3. R. J. Young and P. A. Lovell, Introduction to Polymers, 2nd edition, Chapman and Hall, London, 1991, pg. 295.

4. C. G. Pitt, A. R. Jeffcoat, R. A. Zweidinger, and A. Schindler, "Sustained drug delivery systems. I. The permeability of poly(ε-caprolactone), poly(DL-lactic acid), and their copolymers," *J. Biomed. Mater. Res.* 13 (1979) 497–507.

5. C. G. Pitt, M. M. Gratzl, A. R. Jeffcoat, R. Zweidinger, and A. Schindler, "Sustained drug delivery systems II: factors affecting release rates from poly(ε-caprolactone) and related biodegradable polyesters," *J. Pharm. Sci.* 68 (1979) 1534–1538.

6. L. K. Fung, M. G. Ewend, A. Sills, E. P. Sipos, R. Thompson, M. Watts, O. M. Colvin, H. Brem, and W. M. Saltzman, "Pharmacokinetics of interstitial delivery of carmustine, 4-hydroperoxycyclophosphamide, and paclitaxel from a biodegradable polymer implant in the monkey brain," *Cancer Res.* 58 (1998) 672–684.

7. K. Fredriksson and P. Lundgren, "Stability of carmustine – kinetics and compatibility during administration," *Acta Pharm. Suec.* 23 (1986) 115–124.

8. M.-F. Hadjii-Minaglou-Gonzalvez, A. Gayte-Sorbier, C. B. Airaudo, and M. Verdier, "Effects of temperature, solution composition, and type of container on the stability and absorption of carmustine," *Clin. Ther.* 14 (1992) 821–824.

9. http://esc.syrres.com/interkow/webprop.exe?CAS=129-81-7

10. PerkinElmer Life Sciences Technical Data Certificate of Analysis, NEX229 [^{125}I]-Interleukin-2, (Human, recombinant).

11. J. Tong and J. L. Anderson, "Partitioning and diffusion of proteins and linear polymers in polyacrylamide gels," *Biophysical J.* 70 (1996) 1505–1513.

7 Chemical Release: Characterization of Membrane Swelling and Dependence of Chemical Release on Osmotic Pressure and Molecular Chemistry

7.1 Introduction and Motivation

7.1.1 Introduction

Thus far we have seen that a number of factors can affect the performance of our drug delivery microreservoir devices. The chemistry and size of the drug molecule may play a role in the observed release kinetics, and changing the molecular weight of the membrane polymer can control the release time of the drug. Although it is well known that PLGA copolymers are subject to a complex degradation process, one of the least studied aspects is the swelling of the polymer prior to the commencement of hydrolysis. While PLGA swelling seems to be of minor interest when studying most PLGA implants, such as microspheres, in the case of our devices the swelling may cause or be related to the time at which the reservoir membranes open. Thus the water uptake and swelling behaviors of the reservoir membranes on our device are of great interest. Further, although no diffusion of the drug has been observed through the reservoir membranes on our microreservoir devices in most cases (with the exceptions of BCNU and IAP), it is possible that water may diffuse into the reservoir from the surrounding environment. This might cause a loading-dependent osmotic pressure within the reservoir. In order to reliably predict device operation it is vital to know whether or not such an osmotic pressure effect exists.

While the degradation of PLGA copolymers has been fairly extensively studied and reported on in the literature[1], the changes in their mechanical properties over time in both the *in vitro* and *in vivo* environments are less well understood. This may be due to the fact that these polymers are largely used in drug-delivery[2–8] and tissue engineering[9–11] applications rather than in load-bearing applications, with the exception of some types of orthopedic implants[12–16]. However, the mechanical properties and behavior over time of these PLGA copolymers are extremely important when considering their use as membrane materials in our polymeric microreservoir devices, as the ultimate failure of the membrane and release of the drug from the reservoir may depend on the loss of mechanical strength of the membrane polymer.

7.1.2 Motivation

The experiments presented here were designed to achieve several goals. First, we desired to quantify the extent of swelling of the membranes during a typical release experiment. Second, we wanted to correlate the membrane swelling with the observed release time of molecules from the reservoirs. Third, we wanted to determine whether or not the observed swelling varied depending on the molecule that was loaded into the reservoirs. Lastly, we wanted to determine whether the loading of the reservoir affected the extent of membrane swelling that was observed. A correlation between these two phenomena would suggest that the observed membrane swelling is at least partially due to an osmotic pressure effect within the reservoir, rather than solely due to water uptake, and that therefore the reservoir loading could affect the observed release time.

7.2 Materials and Methods

7.2.1 Materials

Poly(L-lactic acid) (**PLA**, M_w 194 Kilodaltons (Kd), Medisorb® 100 L), and poly(D,L-lactic-*co*-glycolic acid) polymer powders of molecular weights (M_w) 4.4 Kd (**PLGA4.4**, Medisorb® 5050 DL 1A) and 11 Kd (**PLGA11**, Medisorb® 5050 DL 2A) were obtained from Alkermes (Cincinnati, Ohio). Each PLGA copolymer had approximately a 50:50 mole ratio of lactic acid:glycolic acid units. Reagent grade 1,1,1,3,3,3-hexafluoro-2-propanol (HFIP), and ^{14}C-dextran (M_ws = 10,000, 40,000, and 70,000) were purchased from Sigma-Aldrich (St. Louis, MO). ^{14}C-glucose, ^{14}C-glycerol, ^{14}C-glycerol 3-phosphate (ammonium salt), and ^{14}C-glycerol trioleate were purchased from Amersham Pharmacia Biotech (Buckinghamshire, England). Ideal 9144 Masking Tape was obtained from American Biltrite, Inc. (Lowell, MA). Hexamethyldisilazane was purchased from Polysciences, Inc. (Warrington, PA). Ethyl alcohol, 200 proof, was purchased from Pharmco (Brookfield, CT).

7.2.2 Methods

Twenty-two devices were fabricated as described in Chapter 2. On each device, one reservoir was sealed with a membrane of **PLGA4.4**, and one reservoir was sealed with a **PLGA11** membrane. Predicted membrane thicknesses ranged from 151 to 161 μm. One control device had no chemical loaded into the reservoirs. The devices were loaded with a calculated

amount of ^{14}C-glucose, ^{14}C-dextran (M_w~10,000, or 40,000 daltons), ^{14}C-glycerol, ^{14}C-glycerol 3-phosphate, or ^{14}C-glycerol trioleate that corresponded to an osmotic pressure of approximately 40 kPa. Three identical devices were fabricated for each chemical. Devices loaded with ^{14}C-dextran (M_w~70,000) had a loading that corresponded to osmotic pressures of 20, 40, or 80 kPa.

The loading of each chemical, with the exception of the dextrans of various molecular weights, corresponded to a specified osmotic pressure and was calculated using the equation:

$$\Pi = MRT$$

Equation 7-a

where Π = osmotic pressure (in atmospheres), M = molarity of the solution, R = the ideal gas constant, and T = temperature (K), assumed to be 270°K. The molarity of the solution was understood to be the molarity of the solution if the reservoir were completely filled with water. In this case, the molarity M can be found from the following relation:

$$M = \frac{W}{M_w V}$$

Equation 7-b

where W = the weight of solute in the reservoir in grams, M_w = the molecular weight of the solute in grams per mole, and V = the total volume of the reservoir, taken to be 126 nL based on the geometry of the device (see Chapter 2).

The osmotic pressure due to the dextran molecules cannot be accurately calculated using Equation 7-a, as the polymeric nature of the chains causes nonlinear behavior. Equations for calculating osmotic pressure effects in the case of dextran are thus often determined experimentally. The osmotic pressure Π (in dynes/cm^2) due to dextran in solution can be found using the following equation[17]:

$$\log \Pi = a + b \cdot (W_p)^c$$

Equation 7-c

where a, b, and c are experimentally determined constants, and W_p = weight percent of the dextran in solution. This equation is applicable over the range of 14–34% solutions by weight for dextran having a molecular weight of 10,000 daltons, and the constants have the following values: a = 4.52, b = 0.28, and c = 0.60[17]. The constants have values of a = 3.009, b = 0.97602, and c = 0.393 and the equation is applicable for 0.4% < W_p < 20%[17] for dextran having a molecular weight of 40,000 daltons. The parameters a, b, and c are not reported in the case of 70,000 molecular weight dextran, but they are reported for dextran having a molecular weight of 110,000 daltons (a = 1.385, b = 2.185, c = 0.2436 for W_p < 10%). Therefore, interpolation of osmotic pressure data reported elsewhere for 40,000 and 110,000 dalton dextran was used to determine the parameters a, b, and c for 70,000 molecular weight dextran as follows:

$$a_{70k} = \frac{4}{7}(a_{110k} - a_{40k}) + a_{40k} = 2.07$$

Equation 7-d

$$b_{70k} = \frac{3}{7}(b_{110k} - b_{40k}) + b_{40k} = 1.5$$

Equation 7-e

$$c_{70k} = \frac{3}{7}(c_{110k} - c_{40k}) + c_{40k} = 0.33$$

Equation 7-f

It was found that using the ratio of 3/7 in Equation 7-d produced osmotic pressure values for the 70,000 molecular weight dextran that were larger at a given weight percentage than for dextran having a molecular weight of 40,000, which is not consistent with the trends observed for increasing molecular weights of dextran. The ratio of 4/7 was therefore used instead.

The devices were sealed and affixed to glass slides for stability using American Biltrite 9144 masking tape after they were loaded with the calculated amounts of radiolabeled molecules. Each device was then put in a screw-cap jar containing 20 mL stirred 1X phosphate-buffered saline (PBS). A magnetic stir bar was also added to each jar, and the jars were placed on a magnetic stir plate at room temperature. One mL samples of media were taken from the jars once per day and pipetted into 7-mL glass scintillation vials. One milliliter of fresh PBS was added to the jars to keep the volume of release medium constant. The amount of radiolabel present in the

scintillation vials was quantified using a ^{14}C-protocol on a Packard Tri-Carb liquid scintillation counter (Model U2200). Also once per day, one device from each sample group was removed from its jar, carefully blotted dry with a paper towel, and viewed under an Olympus BH2 microscope using either an Olympus TH3 light source (Olympus, Melville, NY), or Series 180 Fiber-Lite high intensity illumination source (Dolan-Jenner Industries, Inc., Lawrence, MA). The maximum height of the membrane surface was measured relative to the surface of the substrate by observing the locations of the numerically marked fine focus knob for each surface, and multiplying the numerical difference between the two numbers by two μm/mark. The average and standard deviation at each time point were found by combining the measurements at the two magnifications. Digital photos were taken with a Pixera digital camera using Pixera Viewfinder software on a Dell Dimension L566cx computer.

An estimation of the percentage (by weight) of water uptake can be found by performing a series of calculations as follows. The percentage of water uptake can be calculated based on the mass of water absorbed (M_w) and the initial mass of the membrane polymer ($M_{p.}$):

$$\%uptake = \frac{M_w}{M_p} \times 100$$

Equation 7-g

The mass of water absorbed was not measured, but it can be estimated based on the change in volume of the membrane. If we assume that the portion of the membrane above the surface of the device swells in the shape of a spherical section, having a radius r_1 = radius of the reservoir opening, and height h = measured maximum membrane height, then the volume of the swollen region V_s can be found as follows:

$$V_s = \frac{\pi}{6}\left(3r_1^2 + h^2\right)h$$

Equation 7-h

We assume that the actual membrane itself does not swell inside the reservoir, but that the membrane swells perpendicular to the surface of the device, and that all of the swelling is reflected in the measured increase in membrane height. Additionally, we make the simplifying

assumption that the polymer itself does not undergo any change in density or swelling due to solvent interactions, but that all of the observed change in volume is solely due to the absorption of a volume of water. Then the percentage of water uptake can be calculated as:

$$\%uptake = \frac{V_s \times \rho_w}{V_p \times \rho_p}$$

Equation 7-i

where ρ_w = density of water, V_p = volume of polymer in membrane, and ρ_p = density of the membrane polymer. One additional simplifying assumption that is used in calculating the percentage of water uptake is to assume that, for devices in which the height of the membrane was initially below the surface of the device, the difference in swollen volume is negligible whether calculated as the frustum of a cone or as a spherical section. Therefore, for devices in which this was the case, the maximum height of the membrane *h* used in Equation 7-h was the measured maximum membrane height minus the initial membrane height.

The devices were dehydrated in a series of ethanol washes of increasing concentrations (50%, 75%, 90%, 100%, and 100%) after completion of the release experiments. The devices were then removed from the glass slides to which they were affixed, and placed in 12-well polystyrene tissue culture plates. One milliliter of hexamethyldisilazane (HMDS), a dehydrating agent that is purported to preserve the structure of tissue and other organic materials, was added to each well. The HMDS was left in each well for one to two minutes before being pipetted out and replaced with fresh HMDS for another one to two minutes. The second volume of HMDS was then pipetted out of the wells, and the devices were left in a hood until they were dry. The devices were sputter coated with gold for 60 seconds at 24 mA (Pelco SC-6 sputter coater), and imaged in a scanning electron microscope (SEM, Hitachi model S-530) at two keV. Digital photos were taken using Oxford Instruments Link ISIS software.

7.3 Results and Discussion

7.3.1 *In vitro* release and swelling measurements of radiolabel loaded devices

7.3.1.1 Control device

The swelling measurements for the membranes on the control device are shown in **Figure 7.1**. The arrows on the figure indicate when the membrane appeared to be "open" when viewed under the microscope. Large holes were seen in the centers of the reservoir membranes in the case of this control device.

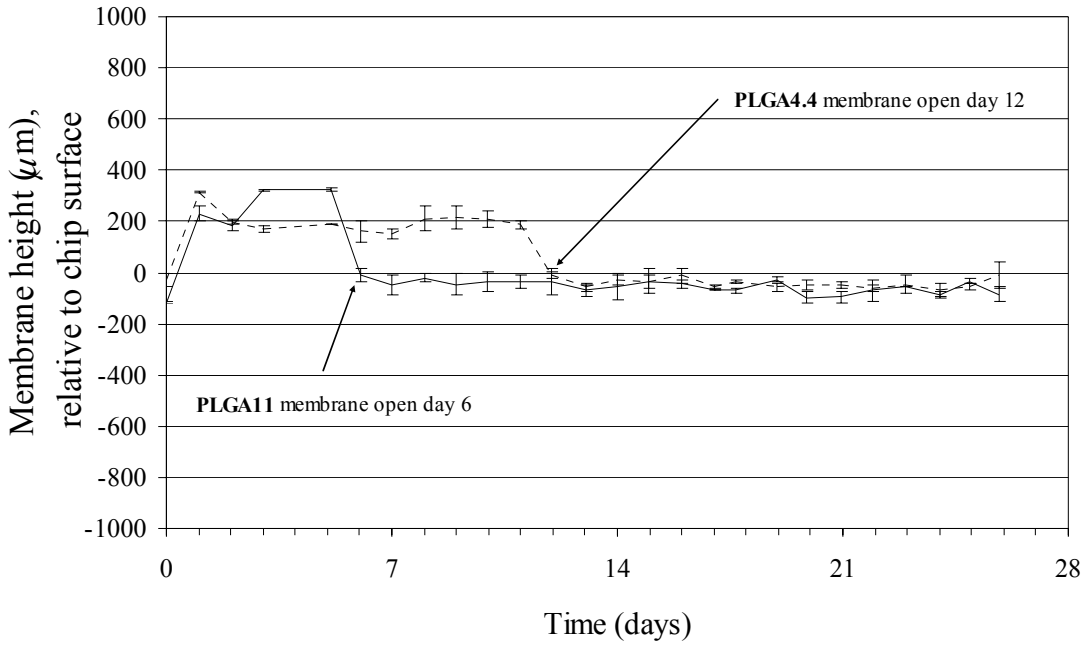

Figure 7.1 Maximum measured membrane height relative to device surface for ~150 μm thick **PLGA4.4** (dotted line) and **PLGA11** (solid line) membranes on unloaded control device.

This device exhibited large decreases in the maximum membrane heights on the same days that the reservoirs appeared open when viewed under the microscope. This result was also observed for some of the other devices that will be discussed.

Figure 7.2 shows photographs of the two reservoir membranes taken at various times during the experiment.

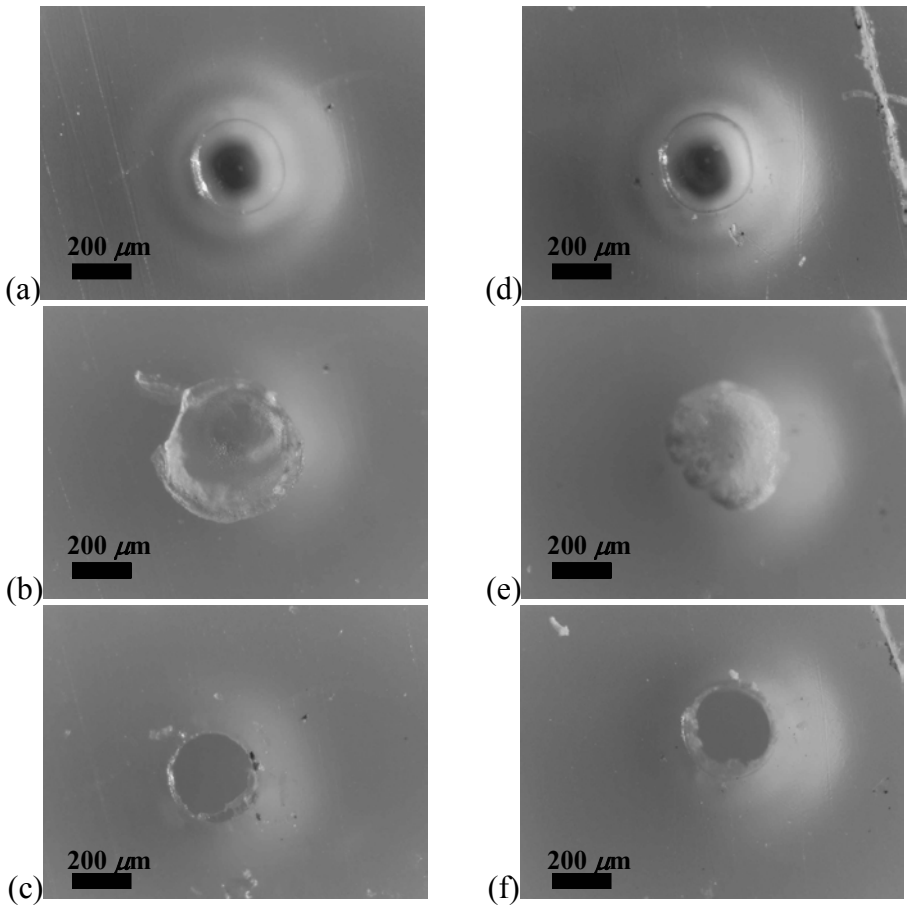

Figure 7.2 ~150 μm thick membranes on control (unloaded) device, viewed under optical microscope: (a) **PLGA4.4** membrane at day zero, (b) **PLGA4.4** membrane at day five, (c) **PLGA4.4** membrane at day 12, (d) **PLGA11** membrane at day zero, (e) **PLGA11** membrane at day five, (f) **PLGA11** membrane at day six.

The membranes initially were transparent and planar, as can be seen in **Figure 7.2**(a) and (d). However, the membranes began to swell within a few days of being immersed in the saline solution, as can be seen in **Figure 7.2**(b) and (e) for the **PLGA4.4** and **PLGA11** membranes, respectively. In the case of both the **PLGA4.4** and **PLGA11** membranes, the time at which a hole appeared in the reservoir membrane (shown in **Figure 7.2**(c) and (f)) corresponded with a drop in the maximum height of the membrane. The **PLGA4.4** membrane showed a sudden drop in height between days 11 and 12, and the membrane exhibited a large hole at day 12. Similarly, the **PLGA11** membrane showed a large drop in height between days five and six, and had a large hole at day six as shown in **Figure 7.2**(f). It is hypothesized that the region of the membrane that underwent the maximum swelling was most likely to be under the largest amount of stress. This large stress may have ultimately caused that swollen region of the membrane to fail and detach

from the device. Measurement of the maximum membrane height during subsequent examination under the microscope would therefore result in a smaller measured membrane height relative to previous measurements, as borne out by our results.

One unexpected result was that the opening time for the **PLGA11** membrane was earlier than that for the **PLGA4.4** membrane. This result was not seen for any of the other devices in this study. Although it is possible that the **PLGA11** actually degraded faster than the **PLGA4.4**, thus causing the membrane to fail earlier, this is highly unlikely given the difference in molecular weights of the two materials, as well as the observed changes in molecular weights over time for these two materials (see sections 5.3.2.1 and 5.3.2.2 for GPC characterization of 150 μm films of these materials). One possible explanation for the observed results may be the limited depth of field of the microscope. Due to the large vertical swelling of the membranes, viewing the entire surface of the membranes in the field of view was difficult to achieve. Features such as crevices or flaps that have a large variation in three-dimensional topography are thus difficult to see under the optical microscope. Therefore, although the **PLGA11** membrane exhibited a large hole earlier than the **PLGA4.4** membrane, it is possible that a crack or other break in the surface of the **PLGA4.4** membrane may have occurred earlier than the observed hole in the **PLGA11** membrane. In the case of these control devices, no chemical was loaded into the reservoirs and therefore confirmation of reservoir opening via a pinhole or crack could not be obtained from detection of chemical release.

The **PLGA4.4** membrane showed a difference in height of approximately 350 μm (315 μm maximum on day one and –31 μm on day zero) over the course of the experiment, while the **PLGA11** membrane showed a difference in height of approximately 440 μm (324 μm maximum on day five and –117 μm minimum on day zero). These correspond to 230 and 290% approximate increases in membrane height, respectively, from the initial ~150 μm membrane thickness.

7.3.1.2 ^{14}C-glucose

The release data for the three devices loaded with ^{14}C-glucose are shown in **Figure 7.3**. The swelling data for one of these devices that was inspected under the microscope (solid line in **Figure 7.3**) is shown in **Figure 7.4**.

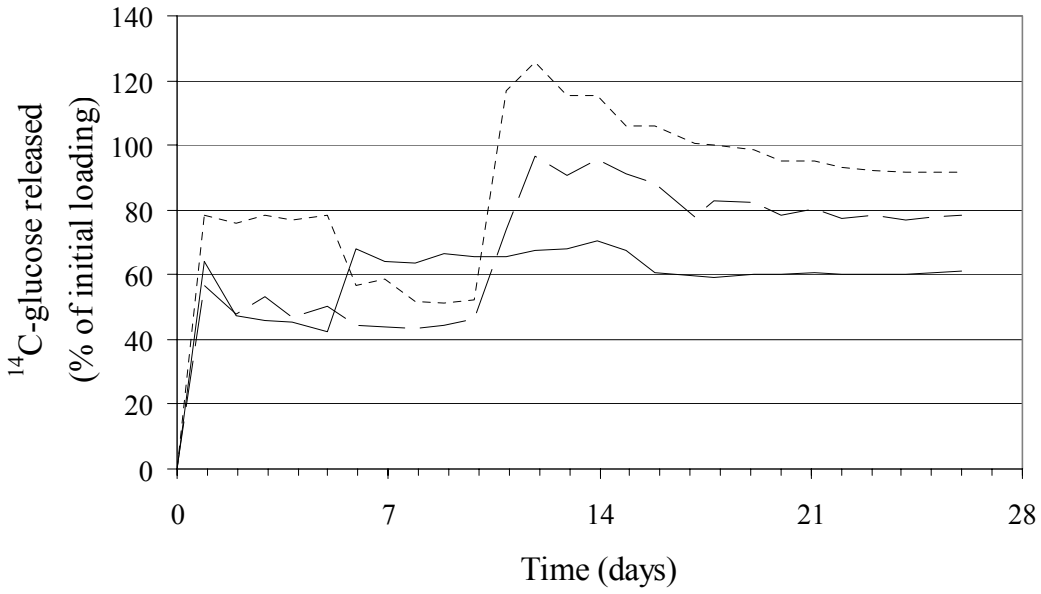

Figure 7.3 Cumulative percentage of ^{14}C-glucose loading released over time from three devices having ~150 μm thick **PLGA4.4** and **PLGA11** reservoir membranes.

All three of the devices that were loaded with ^{14}C-glucose showed release from the reservoirs having **PLGA4.4** membranes on day one, consistent with results seen in other *in vitro* studies (see sections 5.3.1 and 4.3.2). Larger variation was seen in the release times for the **PLGA11** membranes. Two of the devices (dotted and dashed lines in **Figure 7.3**) showed release from the **PLGA11** reservoirs between 11–12 days, while the third device (solid line, device that was viewed on the microscope) showed much earlier release at approximately six days. Additionally, the total amount of radiolabel recovered for the three devices showed a large variation. The device viewed under the microscope showed only approximately 60% release of the ^{14}C-glucose, while between 100 and 120% of the initial loading was detected from the other two devices. The variation in amount of radiolabel detected may be due to several factors. In the case of the device that was viewed under the microscope, the device was blotted with a paper towel prior to microscopy in order to eliminate any water on the surface of the device so that

clear photographs could be obtained. Some of the radiolabeled glucose may have been removed from the surface of the device during this procedure. In the case of the other two devices that were not photographed, the variation in the amount of radiolabel detected may be due to the evaporation from and subsequent addition of saline solution to the vessel in which the experiments were conducted. Although efforts were made to maintain the volume of saline solution (the release medium) constant at 20 mL, some variation undoubtedly occurred, and the solution would have become more concentrated when evaporation occurred. This may have caused the variations seen in **Figure 7.3** when the cumulative amount of ^{14}C-glucose released was calculated.

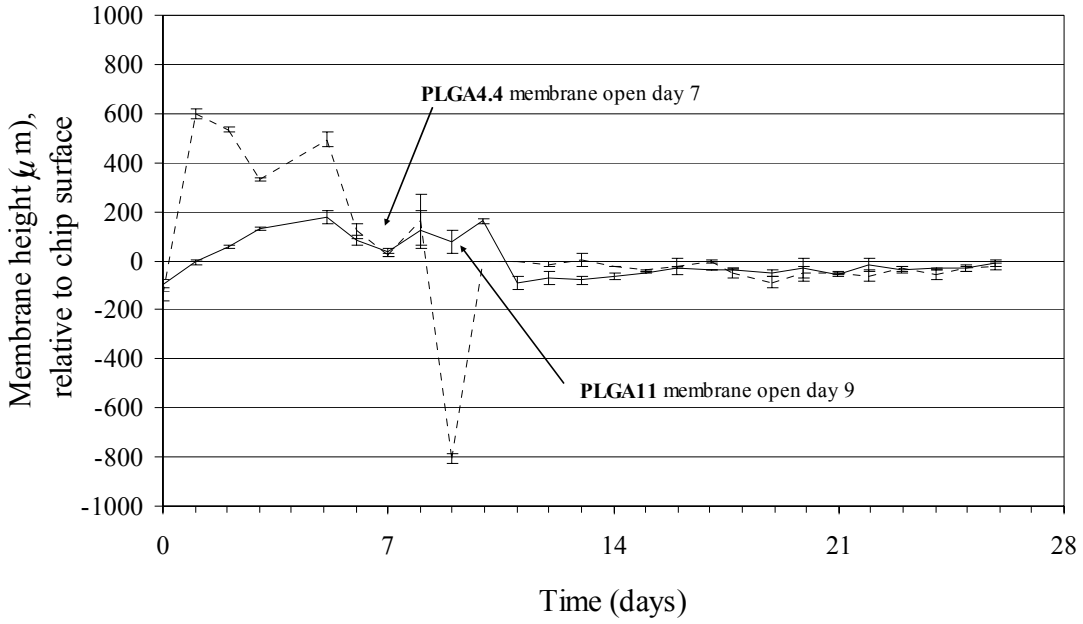

Figure 7.4 Maximum measured membrane height relative to device surface for ~150 μm thick **PLGA4.4** (dotted line) and **PLGA11** (solid line) membranes on device loaded with ^{14}C-glucose.

The maximum measured membrane heights for one of the devices loaded with ^{14}C-glucose are shown in **Figure 7.4** above. Optical microscopy photographs taken over the course of the study, as well as SEM photos of the reservoirs at the conclusion of the experiment (after 30 days in saline solution) are shown in **Figure 7.5** below. A crack in the surface of the **PLGA4.4** membrane appeared at day seven, as indicated by the arrow in **Figure 7.5**(c). Surprisingly, ^{14}C-glucose was detected from this device at day one, but a decrease in the maximum measured membrane height was observed between days five and six. These three pieces of seemingly conflicting evidence do not seem to support our theory that the drop in

membrane height is indicative of or correlated with membrane opening. In the case of this **PLGA4.4** membrane, it may be likely that a small fissure on the side of the membrane began at day one, causing the radiolabel release, and that the swelling continued after release of the ^{14}C-glucose had already begun.

In the case of the **PLGA11** membrane, the radiolabel data in **Figure 7.3** for this device (solid line) indicate that release from the reservoir occurred between days five and six. The measurements of membrane height in **Figure 7.4**, however, show a drop in membrane height between days ten and 11, and optical microscopy of the device revealed the appearance of a hole in the membrane at day nine. Interestingly, the maximum membrane height occurred on day five (a photograph of the **PLGA11** reservoir membrane at day five is shown in **Figure 7.5**(f)). These results suggest that the time at which the maximum membrane height is measured may correspond with the time at which release from the reservoir occurs. Although no large hole was visible in the **PLGA11** membrane until day nine, it is possible that a fissure on the side of the membrane or some other type of breach in the structure that was not visible at the magnification we used occurred between days five and six, which would have caused release of the radiolabel from the reservoir.

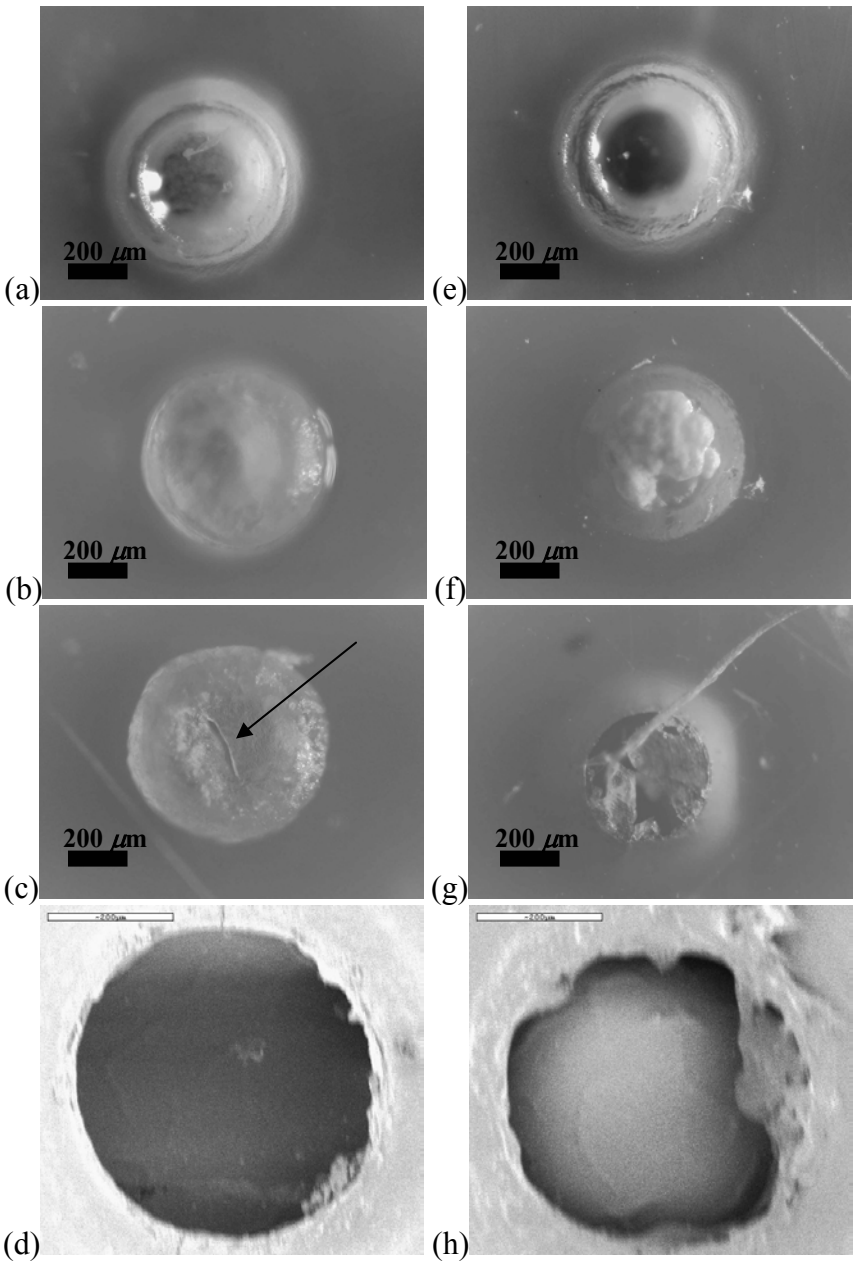

Figure 7.5 ~150 μm thick membranes on device loaded with ^{14}C-glucose, viewed under optical microscope or viewed under SEM: (a) **PLGA4.4** membrane at day zero, (b) **PLGA4.4** membrane at day five, (c) **PLGA4.4** membrane at day seven, (d) SEM of **PLGA4.4** membrane after 30 days in saline solution, (e) **PLGA11** membrane at day zero, (f) **PLGA11** membrane at day five, (g) **PLGA11** membrane at day nine, (h) SEM of **PLGA11** membrane after 30 days in saline solution.

The maximum measured increase in height for the **PLGA4.4** membrane was approximately 740 μm, corresponding to a 490% increase in the membrane thickness. The **PLGA11** membrane height increased by approximately 280 μm, or approximately 190%.

7.3.1.3 ^{14}C-dextran: M_w~10,000

The radiolabel release data for the three devices loaded with ^{14}C-dextran having a molecular weight of ~10,000 daltons are shown in **Figure 7.6** below. Again we see that the reservoirs sealed with the **PLGA4.4** material uniformly released on day one. The **PLGA11** membranes show much greater consistency in release times (days 10–12) compared to the results obtained for the ^{14}C-glucose devices (6–12 days, **Figure 7.3**).

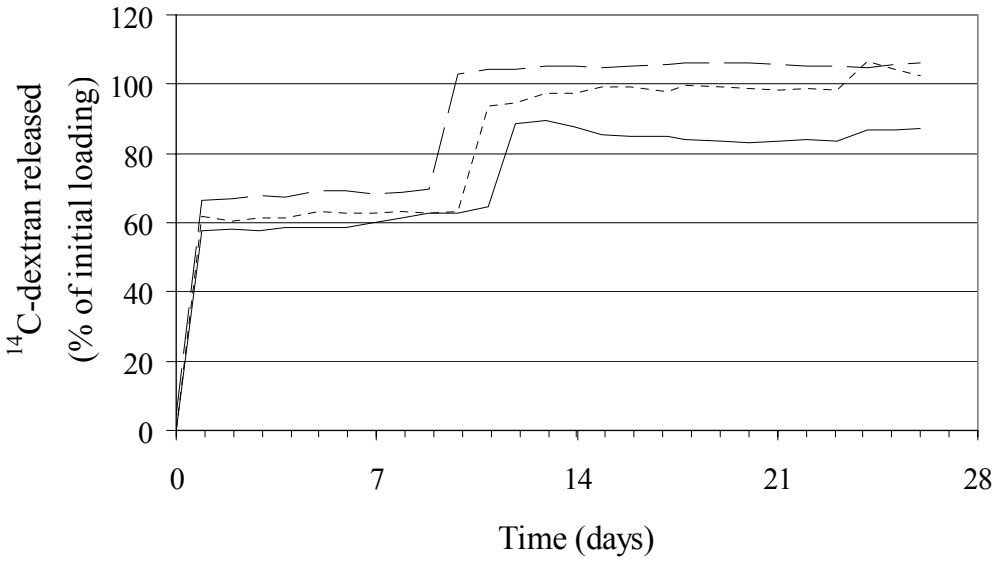

Figure 7.6 Cumulative percentage of ^{14}C-dextran (M_w~10,000) loading released over time from three devices having ~150 μm thick **PLGA4.4** and **PLGA11** membranes.

The maximum measured membrane heights for one of these devices (solid line in **Figure 7.6**) are shown in **Figure 7.7** below. The swelling data in **Figure 7.7** indicate a decrease in the maximum measured **PLGA4.4** membrane height between days two and three. Optical and SEM photographs of this reservoir are shown in **Figure 7.8**. The opening in the **PLGA4.4** membrane at day two can be seen as a crack in the center of the membrane in **Figure 7.8**(b). Similar to the results obtained for the ^{14}C-glucose loaded device, detection of the radiolabel released from the

reservoir sealed with a **PLGA4.4** membrane occurred prior to the membrane appearing open under the microscope.

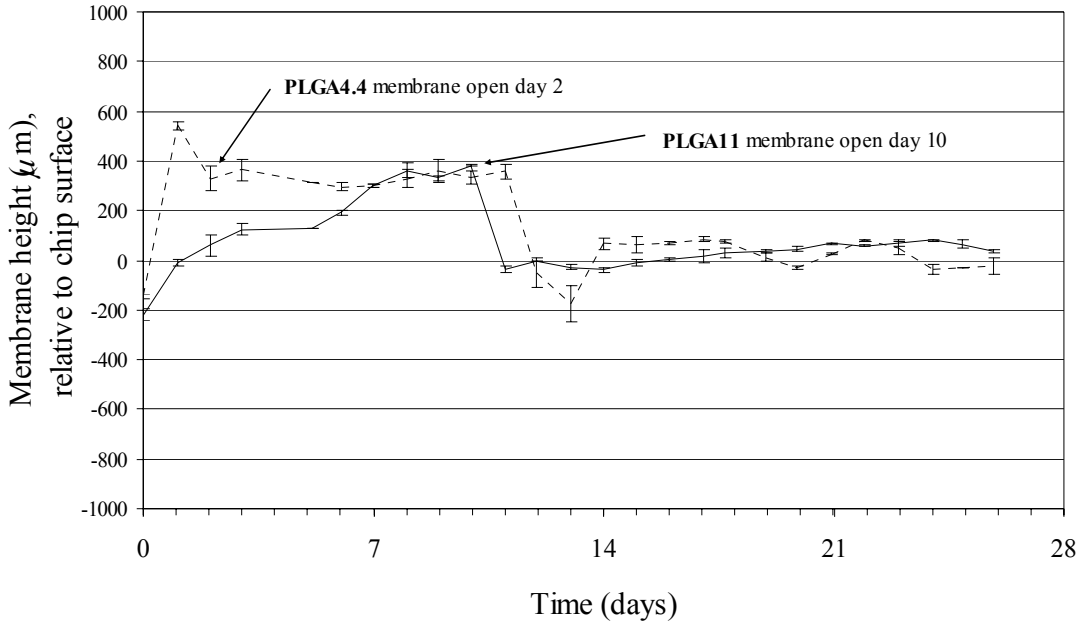

Figure 7.7 Maximum measured height of reservoir membranes relative to device surface for ~150 μm thick **PLGA4.4** (dotted line) and **PLGA11** (solid line) membranes on device loaded with ^{14}C-dextran (M_w~10,000).

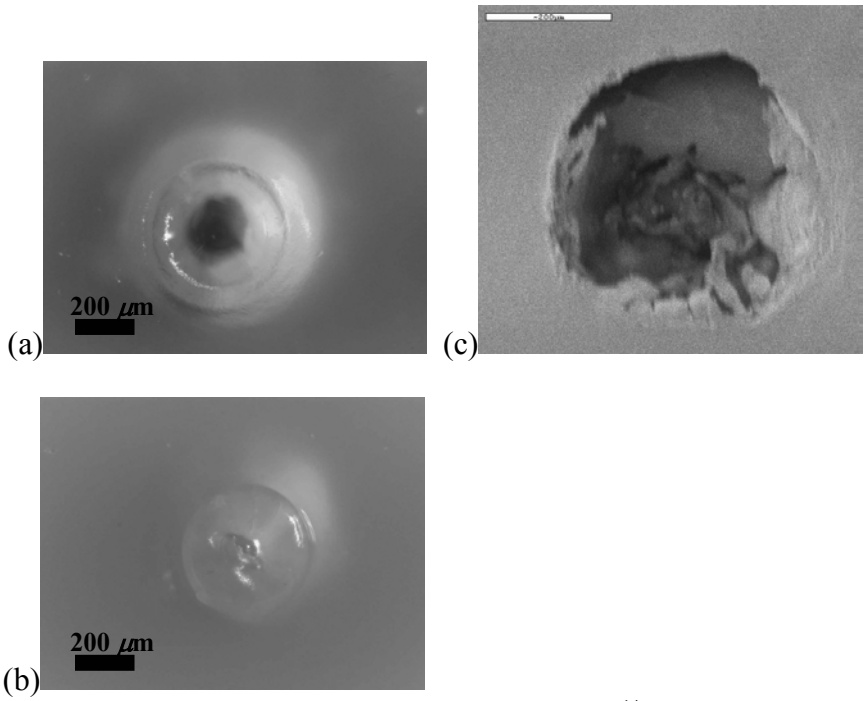

Figure 7.8 ~150 μm thick **PLGA4.4** membrane on device loaded with ^{14}C-dextran (M_w~10,000) viewed under optical microscope or viewed under SEM: (a) **PLGA4.4** membrane at day zero, (b) **PLGA4.4** membrane at day two, (c) SEM of **PLGA4.4** membrane after being in saline solution for 30 days.

The swelling data in **Figure 7.7** indicate a large decrease in the **PLGA11** membrane height between days ten and 11. However, radiolabel release was not detected from this reservoir until day 12, as shown by the solid line in **Figure 7.6**. Additionally, optical microscopy showed what appeared to be a small pinhole in this membrane and a fissure near the reservoir perimeter at day ten, as indicated by the arrows in **Figure 7.9**(d), although a large hole did not appear in the membrane until day 11, as shown in **Figure 7.9**(e). One possible coherent explanation for these seemingly disparate data is that the pinhole may not have penetrated completely through the **PLGA11** membrane at day ten, but may in fact just have been a dimple in the surface of the membrane. Depth of field limitations of the microscope made it difficult to resolve how deep the feature was and whether it penetrated completely through the membrane. Additionally, the large molecular weight of the dextran may have slowed the dissolution of the molecule within the reservoir. Thus even if the pinhole may have completely penetrated through the membrane, it may have taken some time for the dextran to dissolve, diffuse out of the reservoir, and be measured. Further, the media aliquots that were used for scintillation measurements of the radiolabel were removed from the release vessel prior to microscopy of the devices at any give time point. Thus it is possible that although no radiolabel was detected at the day 11 time point, perhaps the membrane was dislodged from the surface of the reservoir between the time at which the media aliquot was taken and the subsequent microscopy, during which a hole appeared in the membrane. This would be consistent with the radiolabel detection that was observed at day 12.

The maximum measured height for the **PLGA4.4** membrane was approximately 690 μm greater than the initial membrane height, corresponding to a 460% increase in the membrane thickness. The **PLGA11** membrane exhibited a height change of 600 μm at ten days, corresponding to a 400% increase in the membrane thickness.

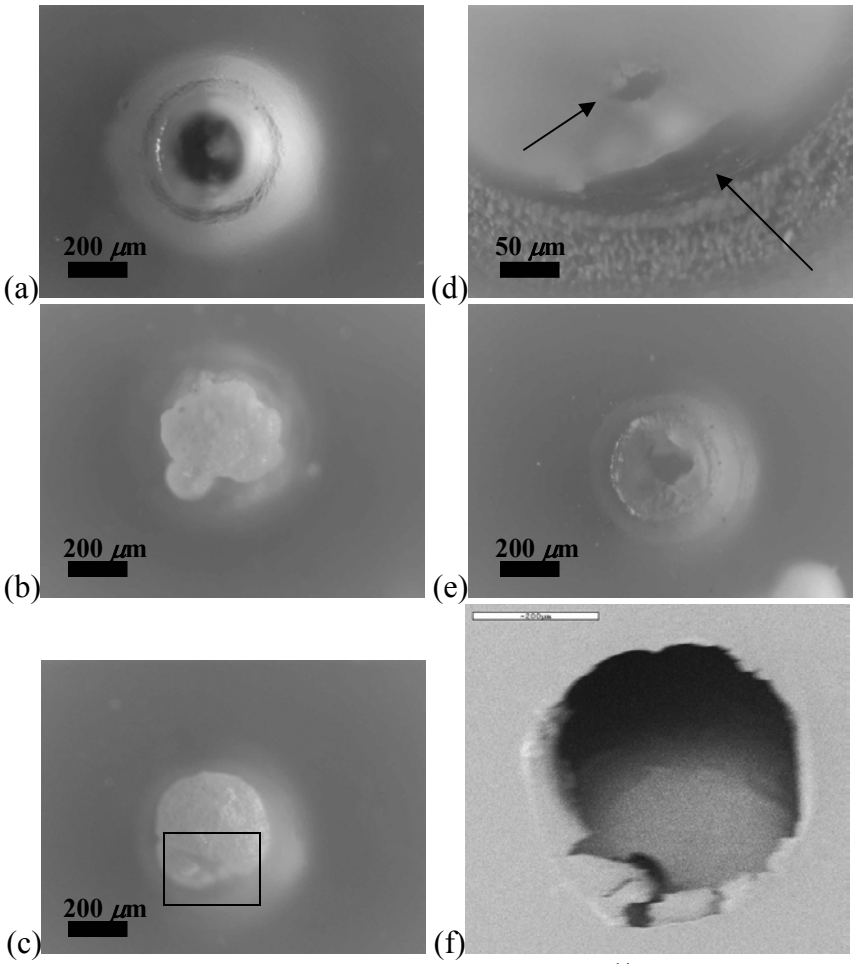

Figure 7.9 ~150 μm thick **PLGA11** membrane on device loaded with ^{14}C-dextran (M_w~10,000) viewed under optical microscope or viewed under SEM: (a) **PLGA11** membrane at day zero, (b) **PLGA11** membrane at day eight, (c) **PLGA11** membrane at day ten, box indicates region enlarged in (d) showing pinhole and fissure in **PLGA11** membrane at day ten, (e) **PLGA11** membrane at day 11 showing large hole in membrane, (f) SEM of **PLGA11** membrane after 30 days in saline solution.

7.3.1.4 ^{14}C-dextran: M_w~40,000

The release results for three devices loaded with ^{14}C-dextran having a molecular weight of 40,000 daltons are shown in **Figure 7.10**. The device indicated by a solid line in **Figure 7.10** was viewed under the microscope, and the measured membrane heights relative to the device surface are plotted in **Figure 7.11**.

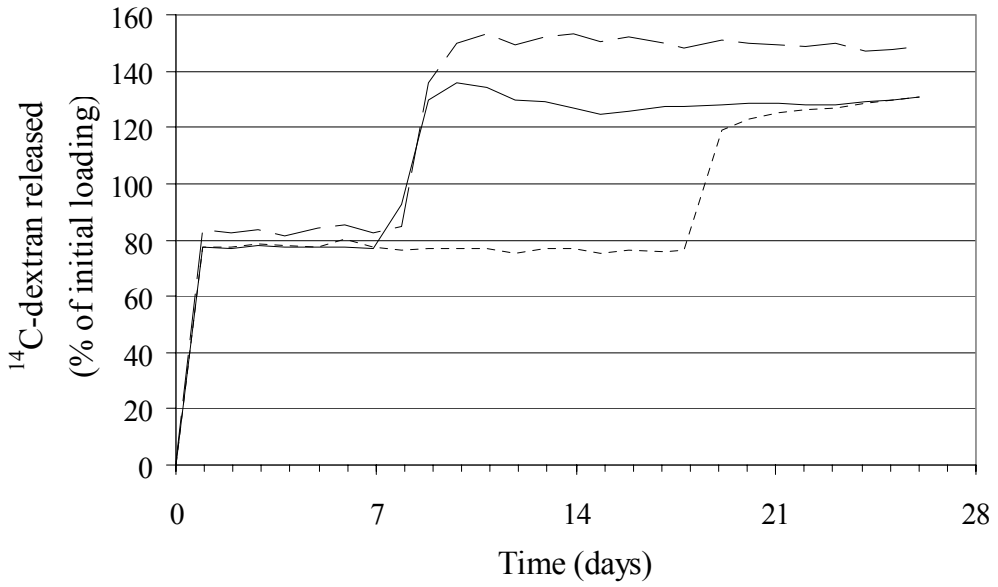

Figure 7.10 Cumulative percentage of ^{14}C-dextran (M_w~40,000) loading released over time from three devices having ~150 μm thick **PLGA4.4** and **PLGA11** membranes.

The reservoirs having membranes made from **PLGA4.4** uniformly released on day one. The reservoirs having **PLGA11** membranes showed more variation in release times than was seen for the devices loaded with either ^{14}C-glucose or ^{14}C-dextran having a molecular weight of 10,000 daltons. With the exception of the device that showed release from the **PLGA11** reservoir at 19 days, however, these devices showed similar release times (eight to nine days) to those loaded with ^{14}C-glucose (six to 12 days) and ^{14}C-dextran having a molecular weight of 10,000 daltons (ten to 12 days).

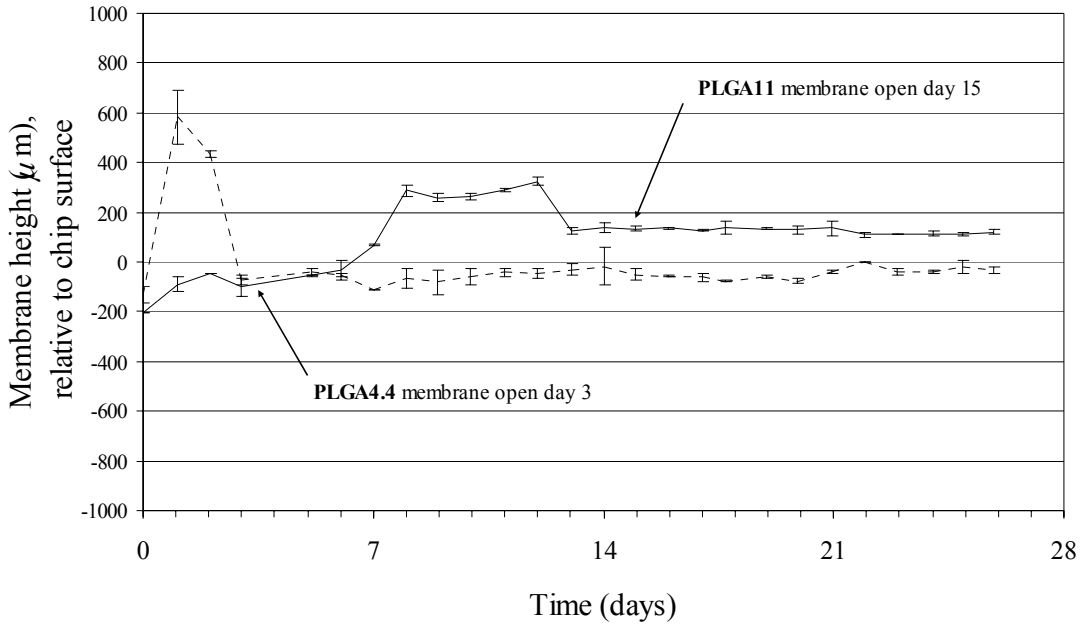

Figure 7.11 Maximum measured membrane height relative to device surface for ~150 μm **PLGA4.4** (dotted line) and **PLGA11** (solid line) membranes on device loaded with ^{14}C-dextran (M_w~40,000).

The measured membrane heights for the device represented by the solid line in **Figure 7.10** are shown in **Figure 7.11** above, and photographs of the membranes over the course of the experiment are shown in **Figure 7.12** and **Figure 7.13**. The **PLGA4.4** membrane did not appear open until day three (**Figure 7.12(**c)), and showed a sudden decrease in the maximum measured membrane height between days two and three. However, the radiolabel was detected from this reservoir on day one. These results are similar to those obtained for the devices loaded with ^{14}C-glucose and ^{14}C-dextran having a molecular weight of 10,000 daltons. The **PLGA11** membrane showed a decrease in membrane height between days 12 and 13, but the membrane did not appear open until a very small pinhole appeared at day 15 (indicated by the arrow in **Figure 7.13**(c) below). Radiolabel release was detected from this reservoir starting at day eight (solid line in **Figure 7.10** above).

It is somewhat surprising that radiolabel release was detected from both of these reservoirs before opening of the membranes was seen, that is to say that there did not appear to be a correlation between the observed opening time (via microscopy) and the actual opening time (via scintillation measurements). Again this may be explained by the consideration that the membranes were highly swollen and that it is quite difficult to obtain an accurate image of them given the limited depth of field of the microscope. Further, the **PLGA11** membrane on this

device never exhibited a large hole similar to that seen for some of the devices. Even after 28 days (see **Figure 7.13**(d)), most of the membrane was still present within the reservoir opening. Although some swelling of the central region was evident, it was very difficult to determine the existence of holes or ruptures in the membrane even at this late time point, although radiolabel release had already been detected.

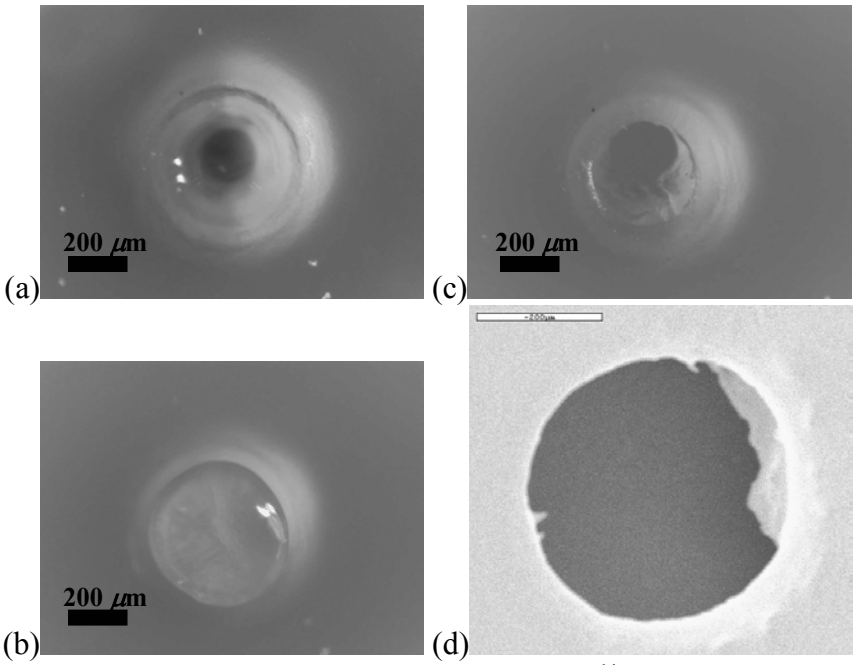

Figure 7.12 ~150 μm thick **PLGA4.4** membrane on device loaded with ^{14}C-dextran having a molecular weight of 40,000 daltons, viewed under optical microscope or viewed under SEM: (a) **PLGA4.4** membrane at day zero, (b) **PLGA4.4** membrane at day one, (c) **PLGA4.4** membrane at day three, (d) SEM of **PLGA4.4** membrane after being in saline solution for 30 days.

The maximum swelling measured of the **PLGA4.4** membrane was approximately 710 μm on day one (**Figure 7.12**(b)), or approximately a 470% increase in membrane thickness, similar to that seen for the devices loaded with both ^{14}C-glucose (490%) and ^{14}C-dextran having a molecular weight of 10,000 daltons (460%). The **PLGA11** membrane attained a maximum swelling of approximately 530 μm at day 12 (**Figure 7.13**(b)), corresponding to an increase of approximately 350% in membrane thickness, slightly less than that seen for the device loaded with ^{14}C-dextran having a molecular weight of 10,000 daltons (400%).

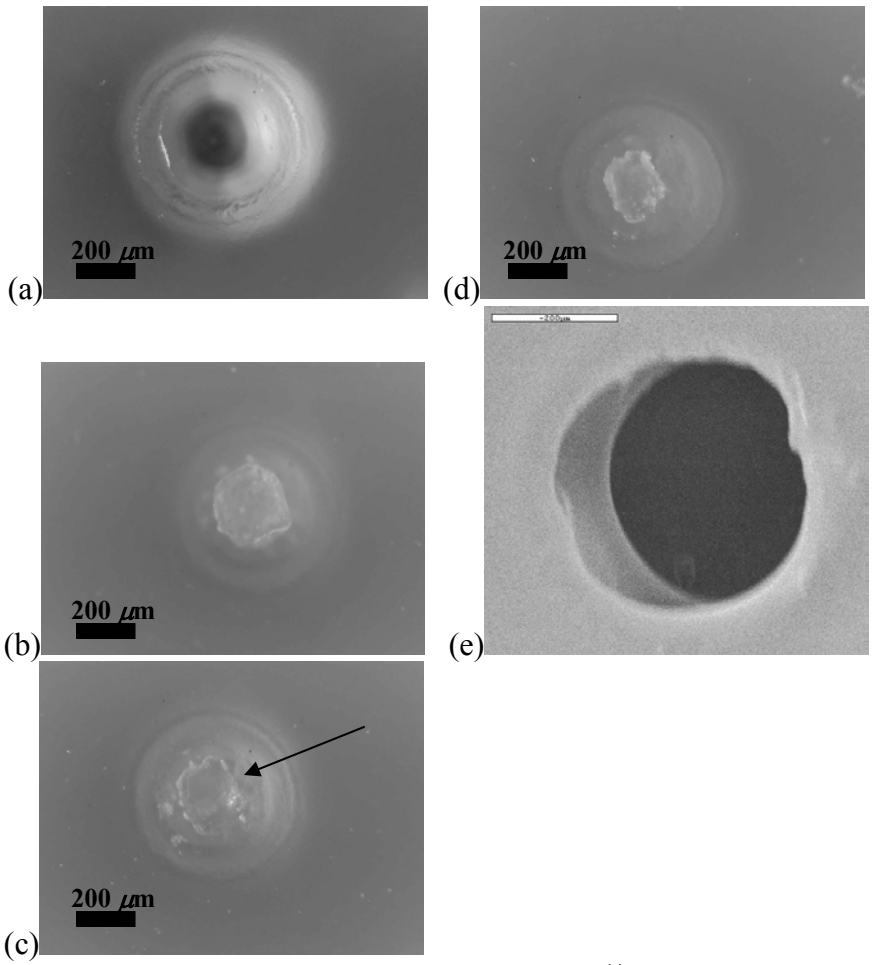

Figure 7.13 ~150 μm thick **PLGA11** membrane on device loaded with ^{14}C-dextran having a molecular weight of 40,000 daltons, viewed under optical microscope or viewed under SEM: (a) **PLGA11** membrane at day zero, (b) **PLGA11** membrane at day 12, (c) **PLGA11** membrane at day 15 with arrow indicating location of pinhole, (d) **PLGA11** membrane at day 28, (e) SEM of **PLGA11** membrane after being in saline solution for 30 days.

7.3.1.5 ^{14}C-dextran: M_w~70,000

The release results for devices loaded with ^{14}C-dextran having a molecular weight of 70,000 daltons are shown in **Figure 7.14** below. Three different loadings of ^{14}C-dextran were used, corresponding to osmotic pressures of 20 (low loading, solid line in **Figure 7.14**), 40 (intermediate loading, dashed line), and 80 (high loading, dotted line) kPa if the remaining volume of the reservoirs were to fill with water.

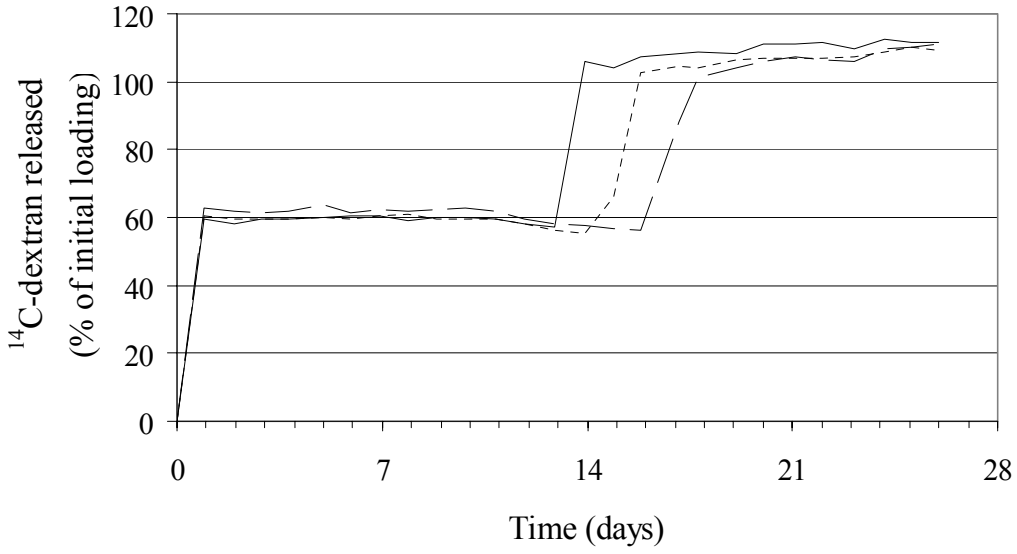

Figure 7.14 Cumulative percentage of ^{14}C-dextran (M_w~70,000) released from three devices having ~150 μm thick **PLGA4.4** and **PLGA11** membranes. Solid line = 20 kPa loading, dashed line = 40 kPa loading, dotted line = 80 kPa loading.

The reservoirs sealed with **PLGA4.4** membranes appeared to uniformly release their contents on day one. The reservoirs sealed with **PLGA11** membranes showed surprisingly little variability in release times. The device with the lowest loading showed release on day 14, while the device with the highest loading showed release between days 15–16, and the device with intermediate loading between 17 and 18 days. In comparison, the devices loaded with ^{14}C-dextran having a molecular weight of 10,000 daltons (same loading for all three devices, see **Figure 7.6** in section 7.3.1.3) showed variation in the release time from the **PLGA11** reservoirs of only ±1 day. In contrast, devices loaded with ^{14}C-glucose (same loading for all three devices, see **Figure 7.3** in section 7.3.1.2) showed release times from six to 12 days, or a variation of ±3 days, from reservoirs having **PLGA11** membranes. Devices loaded with ^{14}C-dextran having a molecular weight of 40,000 daltons showed even greater variation, with release times from the **PLGA11** reservoirs ranging from six to 19 days (see **Figure 7.10** in section 7.3.1.4). The fact that no greater variation in release times was seen for the devices loaded with different amounts of 70,000 molecular weight ^{14}C-dextran compared to devices loaded with other radiolabels suggests that the amount of drug that is loaded into the reservoir does not noticeably affect the release time over the range of different loadings that were investigated. More specifically, it is

evidence that there is no osmotic pressure effect on the rupturing of the membrane. If such an osmotic pressure effect were to exist, we would expect that the device with the highest loading (dotted line in **Figure 7.14**) would show the earliest release, due to higher pressure within the reservoir, while the device with the lowest loading (solid line in **Figure 7.14**) would show the latest release time. The device with the lowest loading, however, showed the earliest release at day 14, followed next by the device with the highest loading at 15 days, and finally the device with intermediate loading at day 17. The lack of an apparent loading or osmotic pressure effect suggests that diffusion of water through the **PLGA11** membrane into the reservoir is not significant on the time scale at which the membrane fails, and that therefore the membranes are completely dense.

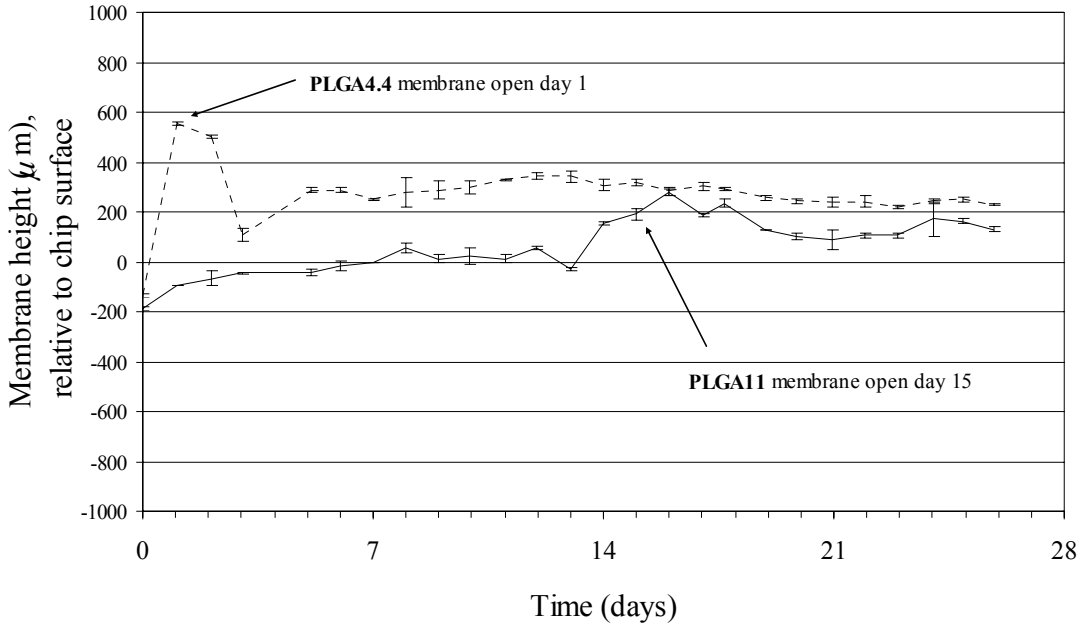

Figure 7.15 Maximum measured membrane height relative to device surface for ~150 μm thick **PLGA4.4** (dotted line) and **PLGA11** (solid line) membranes on device loaded with ^{14}C-dextran (M_w~70,000) corresponding to osmotic pressure of 20 kPa.

The maximum measured membrane heights for the device with a loading of 70,000 molecular weight ^{14}C-dextran corresponding to Π = 20 kPa (low loading) are shown in **Figure 7.15** above, while photographs of the **PLGA4.4** and **PLGA11** membranes at various times are shown in **Figure 7.16** below.

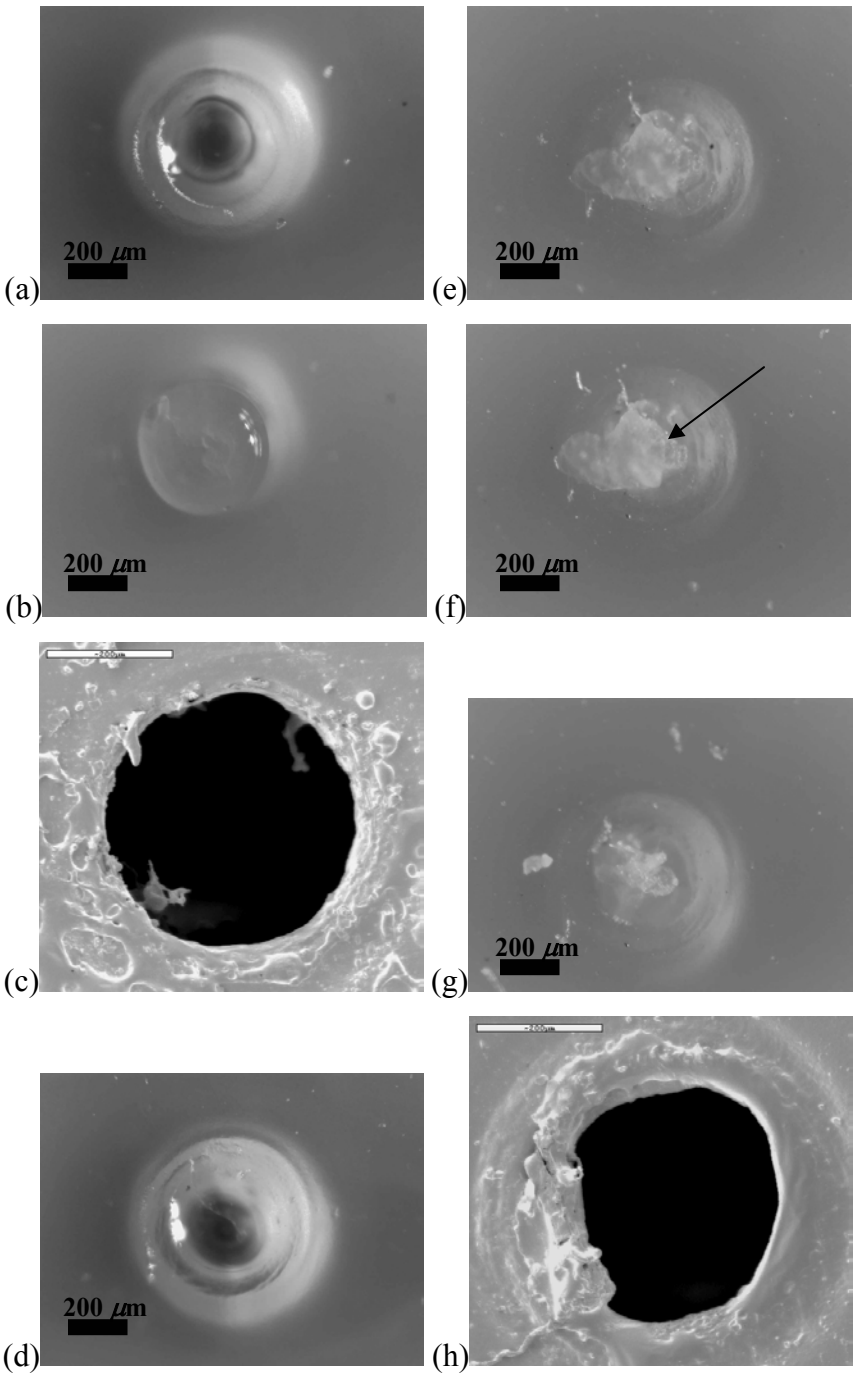

Figure 7.16 ~150 μm thick membranes on device loaded with ^{14}C-dextran having a molecular weight of 70,000 daltons (loading corresponds to an osmotic pressure of 20 kPa), membranes viewed under optical microscope or viewed under SEM: (a) **PLGA4.4** membrane at day zero, (b) **PLGA4.4** membrane at day one, (c) SEM of **PLGA4.4** membrane after 30 days in saline solution, (d) **PLGA11** membrane at day zero, (e) **PLGA11** membrane at day 14, (f) **PLGA11** membrane at day 15, (g) **PLGA11** membrane at day 21, (h) SEM of **PLGA11** membrane after 30 days in saline solution.

The **PLGA4.4** membrane showed a rapid increase in height at day one (see **Figure 7.16**(b)), followed by a decrease at day two and an even larger decrease between days two and three, as was observed for devices loaded with other radiolabeled compounds. After the reservoir appeared to open, the membrane continued to swell as indicated by the slow drift upwards in the measured membrane height plotted in **Figure 7.15**. The **PLGA11** membrane, on the other hand, showed a fairly steady increase in the measured membrane height up to day 13, when it increased more rapidly. Radiolabel release was detected from this reservoir on day 14, followed by the appearance of a hole in the membrane on day 15 (indicated by the arrow in **Figure 7.16**(f)). A large decrease in the **PLGA11** membrane height was not seen for this device. The most likely reason for the absence of a large drop in the **PLGA11** membrane height after chemical release from the reservoir is that the membrane was not very smooth and most of the membrane remained attached to the reservoir after release was detected from the reservoir (see **Figure 7.16**(g) showing the **PLGA11** membrane after 21 days, for example). No large hole appeared in the membrane, similar to the **PLGA11** membrane on the device loaded with dextran having a molecular weight of 40,000 daltons. For many of the other devices inspected during this study, formation of a hole in the membrane was concurrent or followed by detachment of a large portion of the membrane from the edge of the reservoir. However, in some cases large remnants of the membrane remained attached to the surface of the device and continued to swell even after the membrane had opened. This phenomenon was observed in the case of this device having a 20 kPa loading of 70,000 molecular weight ^{14}C-dextran.

The maximum swelling measured for the **PLGA4.4** membrane on this device was approximately 690 μm (460% swelling) at day one, shown in **Figure 7.16**(b). This membrane showed a similar amount of swelling as was observed for **PLGA4.4** membranes on other devices loaded with different chemicals. The **PLGA11** membrane exhibited a maximum swelling of 470 μm (approximately 310% increase in membrane height) at day 16. Similar swelling percentages were seen for other **PLGA11** membranes in this study.

The maximum measured membrane heights for the device with an intermediate loading of 70,000 molecular weight ^{14}C-dextran are shown in **Figure 7.17** below, and photos of the reservoir membranes at various times are shown in **Figure 7.18** and **Figure 7.19** below. Similar to results obtained for other devices, the radiolabel was detected from the reservoir having a **PLGA4.4** membrane on day one, and a hole was clearly visible in the membrane after two days,

as shown in **Figure 7.18**(a). The membrane height showed a large decrease between days two and three, as shown by the dotted line in **Figure 7.17**. Although release of the radiolabel from the reservoir having a **PLGA11** membrane was detected on days 17 and 18 (dashed line in **Figure 7.14**), no hole was seen in the membrane until day 20 (**Figure 7.19**(d)). The maximum membrane height was seen at day 17 (a photograph of the membrane at day 17 is shown in **Figure 7.19**(e)), and was followed by a decrease in membrane height.

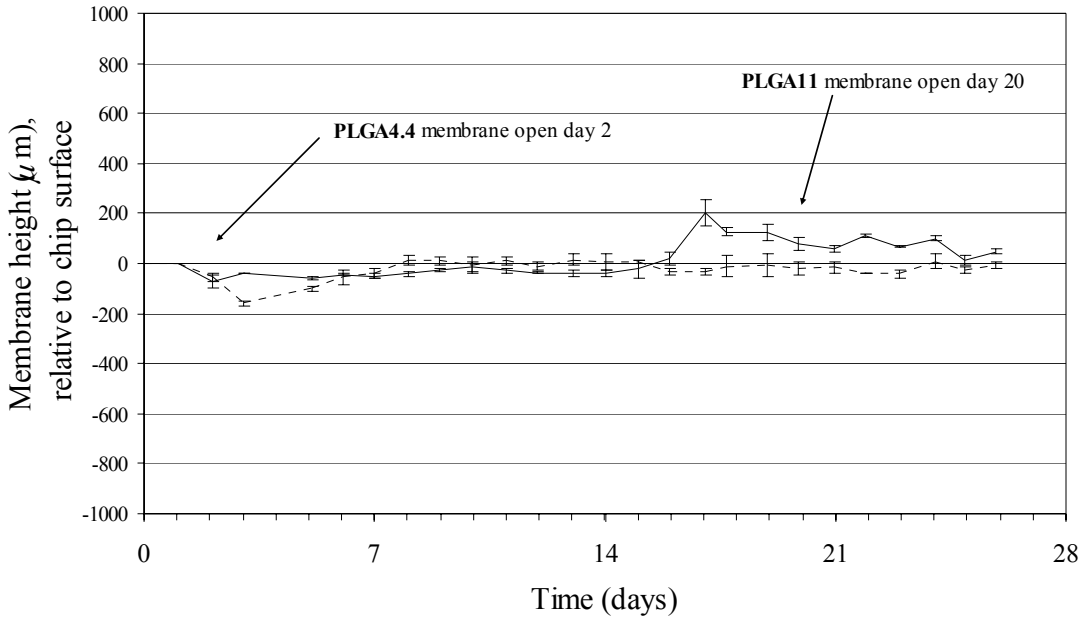

Figure 7.17 Maximum measured membrane height relative to device surface for ~150 μm thick **PLGA4.4** (dotted line) and **PLGA11** (solid line) membranes on device loaded with ^{14}C-dextran (M_w~70,000) corresponding to an osmotic pressure of 40 kPa.

The **PLGA11** membrane on this device only exhibited a small drop in membrane height after a hole appeared. A significant portion of the **PLGA11** membrane remained visible within the reservoir even after the radiolabel was detected from the reservoir, as can be seen in **Figure 7.19**(d) and (e). Most likely these portions of the membrane detached from the perimeter of the reservoir over time, giving rise to the gradual decrease in measured membrane height seen in **Figure 7.17**. The absence of a hole in the **PLGA11** membrane in the SEM photographs is explained by the continued presence of the **PLGA11** membrane within the reservoir even up to day 28, just prior to dehydration of the samples and preparation for SEM analysis.

The maximum measured increase in membrane height for the **PLGA4.4** membrane on this device was approximately 170 μm at day 13, corresponding to a 110% increase in membrane

thickness. The **PLGA11** membrane had a maximum increase in membrane height of approximately 270 μm, or a 180% increase in membrane thickness relative to the initial 150 μm thickness.

(a) 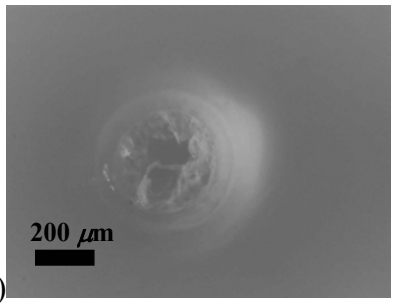

(b) 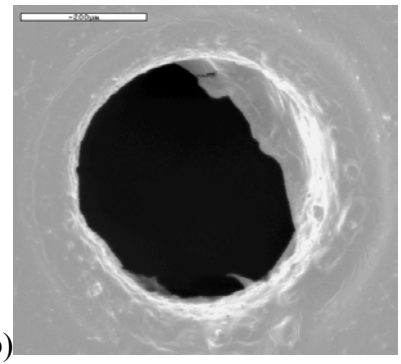

Figure 7.18 ~150 μm thick **PLGA4.4** membranes on device loaded with ^{14}C-dextran having a molecular weight of 70,000 daltons (loading corresponding to 40 kPa osmotic pressure), viewed under optical microscope or viewed under SEM: (a) **PLGA4.4** membrane at day two, (b) SEM of **PLGA4.4** membrane after 30 days in saline solution.

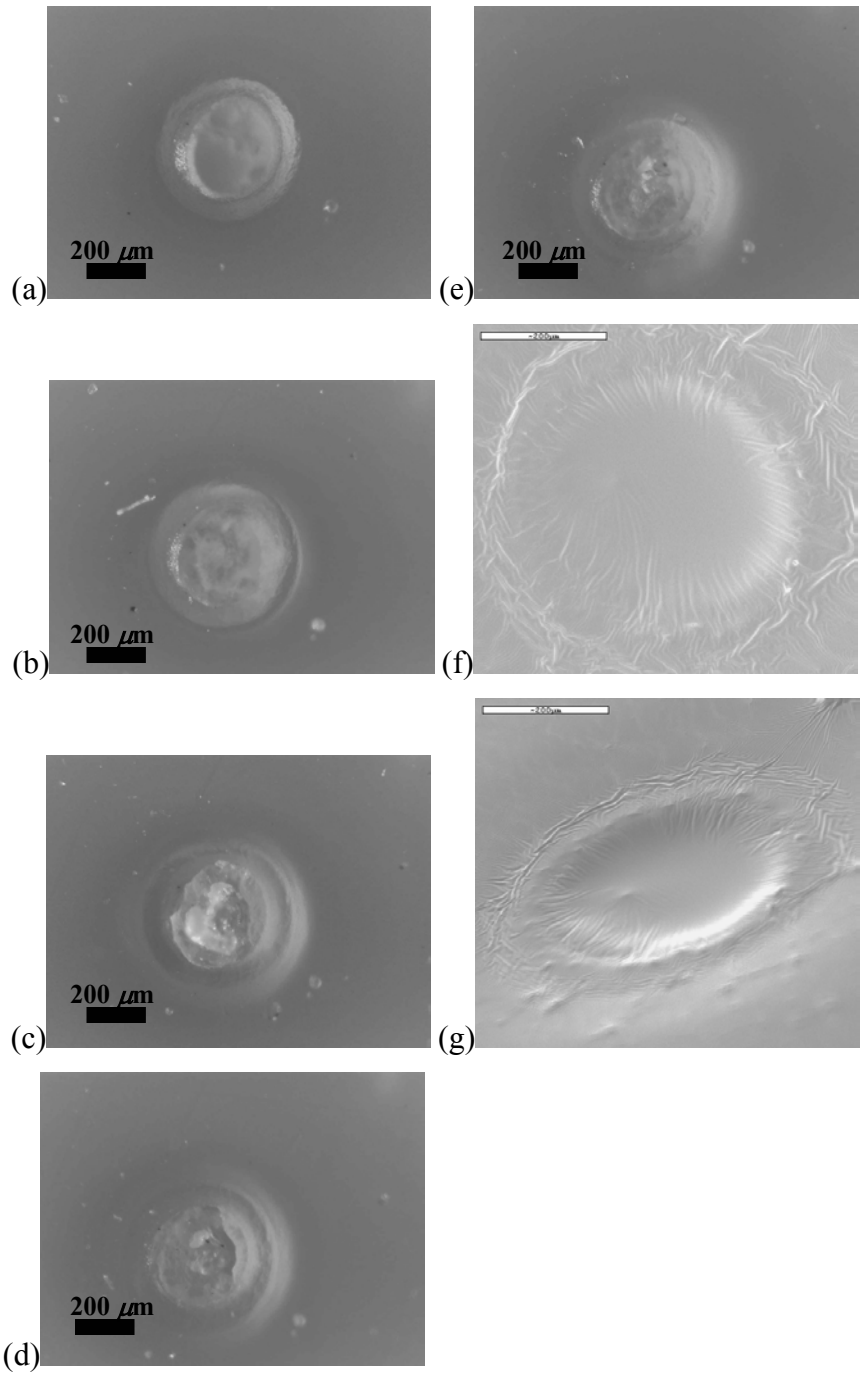

Figure 7.19 ~150 μm thick **PLGA11** membranes on device loaded with ^{14}C-dextran having a molecular weight of 70,000 daltons (loading corresponding to 40 kPa osmotic pressure), viewed under optical microscope or viewed under SEM: (a) **PLGA11** membrane at day two, (b) **PLGA11** membrane at day ten, (c) **PLGA11** membrane at day 17, (d) **PLGA11** membrane at day 20, (e) **PLGA11** membrane at day 28, (f) SEM of **PLGA11** membrane after 30 days in saline solution, (g) SEM of **PLGA11** membrane after 30 days in saline solution, stage tilted 66°.

The maximum measured membrane heights for the device having a loading of 70,000 molecular weight ^{14}C-dextran corresponding to Π = 80 kPa (high loading) are plotted in **Figure 7.20** below, while photographs of the reservoir membranes over time are shown in **Figure 7.21** and **Figure 7.22** below.

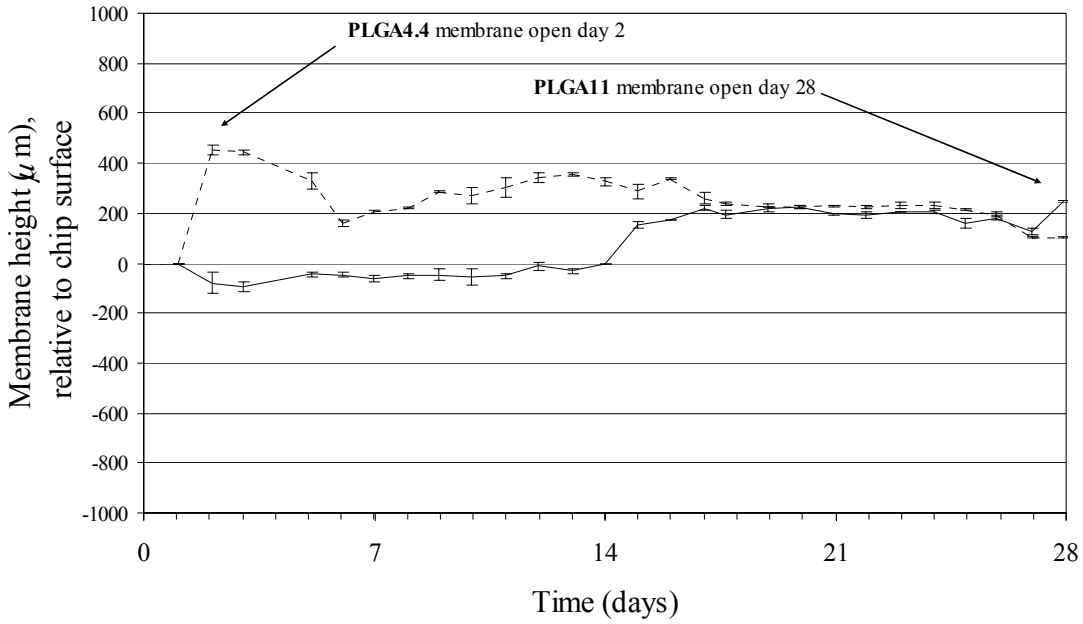

Figure 7.20 Maximum measured membrane height relative to chip surface for ~150 μm thick **PLGA4.4** (dotted line) and **PLGA11** (solid line) membranes on device loaded with ^{14}C-dextran (M_w~70,000) corresponding to osmotic pressure of 80 kPa.

The **PLGA4.4** membrane appeared open at day two, as shown in Figure 7.21 (a)-(c). The membrane height decreased slightly between days two and three as shown in **Figure 7.20**, and then dropped more sharply between days five and six. Radiolabel release was detected from this reservoir on day one. Radiolabel release was detected from the reservoir having a **PLGA11** membrane starting at day 15 (see dotted line in **Figure 7.14** above), but surprisingly the membrane did not appear open until day 28, as indicated by the arrow in **Figure 7.22**(d). However, the membrane swelling showed a large increase between days 14 and 15, and remained at a plateau value for essentially the rest of the study. This membrane had a very rough surface, with several large protrusions which can clearly be seen in **Figure 7.22**(b)-(d). This is most likely the reason why no hole or rupture was seen in the membrane until such a late time during the experiment. The topography of the membrane surface would make it quite difficult to observe any features that were underneath or on the side of the protrusions. This may also

explain why no decrease in the membrane height was observed when the radiolabel release was detected. If it is the case that the membrane rupture occurred on the side of the membrane, or underneath a protruding feature, this would not be reflected in a decrease in the measured maximum membrane height.

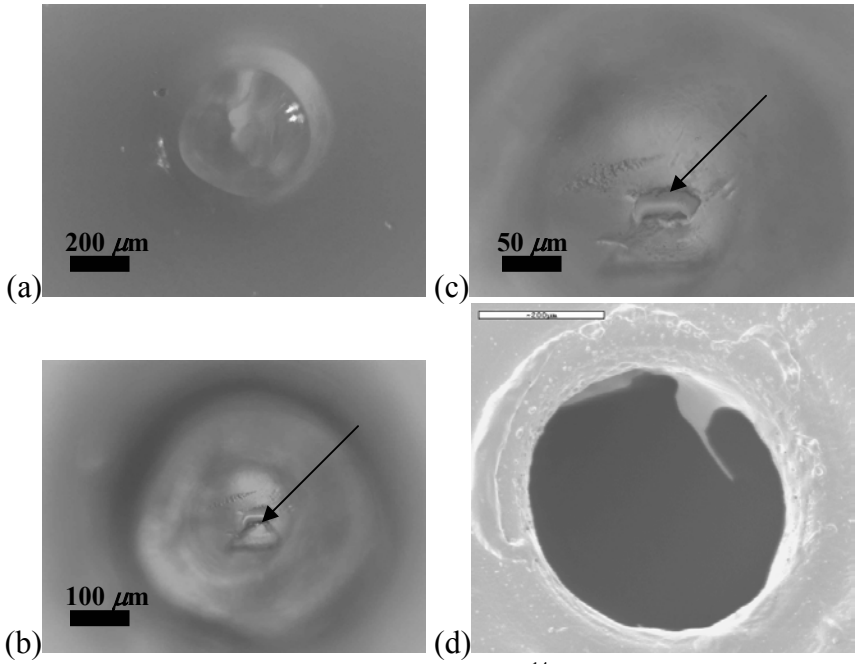

Figure 7.21 ~150 μm **PLGA4.4** membranes on device loaded with ^{14}C-dextran having a molecular weight of 70,000 daltons (loading corresponds to 80 kPa osmotic pressure), viewed under optical microscope or viewed under SEM: (a) **PLGA4.4** membrane at day two, (b) **PLGA4.4** membrane at day two shown at higher magnification, arrow indicates hole in membrane, (c) **PLGA4.4** membrane at day two viewed at yet higher magnification, arrow indicates hole in membrane, (d) SEM of **PLGA4.4** membrane after 30 days in saline solution.

The **PLGA4.4** membrane showed a maximum increase in height of approximately 450 mm, or a 300% increase in the membrane thickness relative to the initial thickness of 150 μm. The **PLGA11** membrane showed a maximum swelling of approximately 320 μm at day 20, or approximately a 210% increase in the membrane thickness.

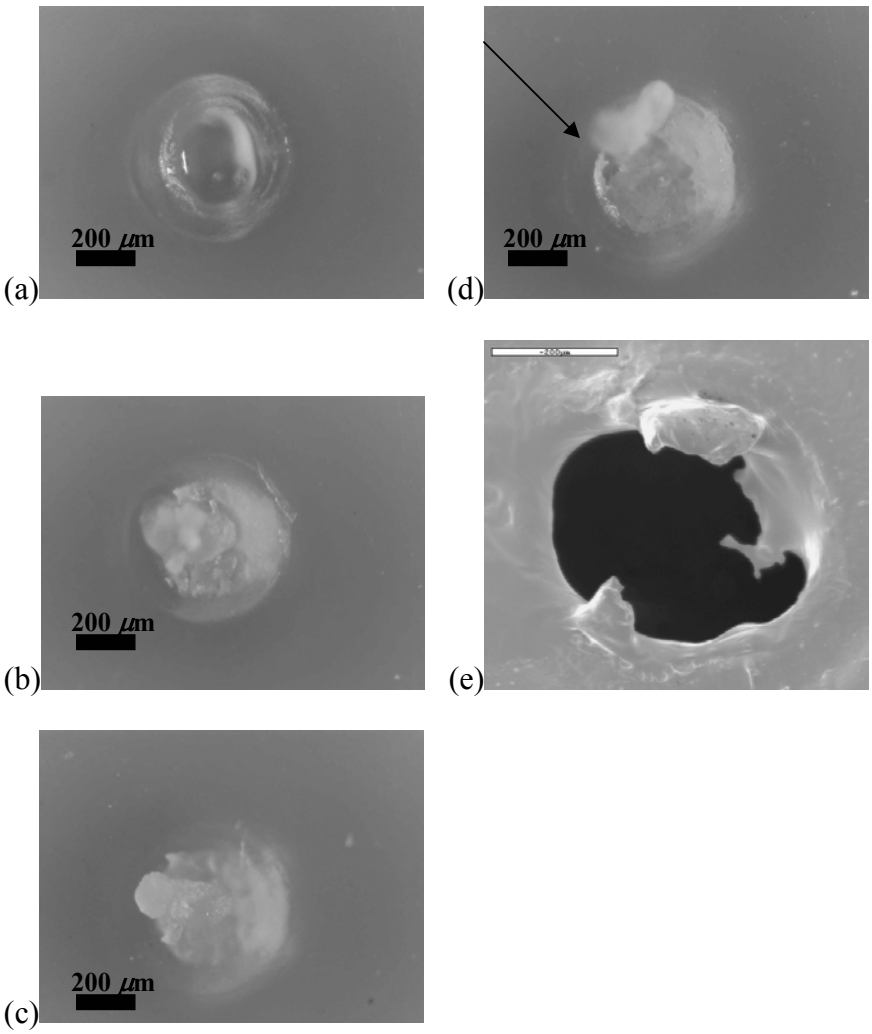

Figure 7.22 ~150 μm **PLGA11** membranes on device loaded with ^{14}C-dextran having a molecular weight of 70,000 daltons (loading corresponds to 80 kPa osmotic pressure), viewed under optical microscope or viewed under SEM: (a) **PLGA11** membrane at day two, (b) **PLGA11** membrane at day 15, (c) PLGA11 membrane at day 22, (d) **PLGA11** membrane at day 28, (e) SEM of **PLGA11** membrane after 30 days in saline solution.

7.3.1.6 ^{14}C-glycerol

The release results for three devices loaded with ^{14}C-glycerol are shown in **Figure 7.23**. The device represented by the solid line in **Figure 7.23** was viewed under the microscope in order to measure the height of the reservoir membranes over time. The maximum measured membrane heights for this device are shown in **Figure 7.24**, and photographs of the reservoir membranes at different times are shown in **Figure 7.25** and **Figure 7.26**. The cumulative amounts of ^{14}C-glycerol measured and plotted in **Figure 7.23** are much lower than those reported

for the other molecules discussed up to this point. This is somewhat surprising, as glycerol is readily soluble in water.

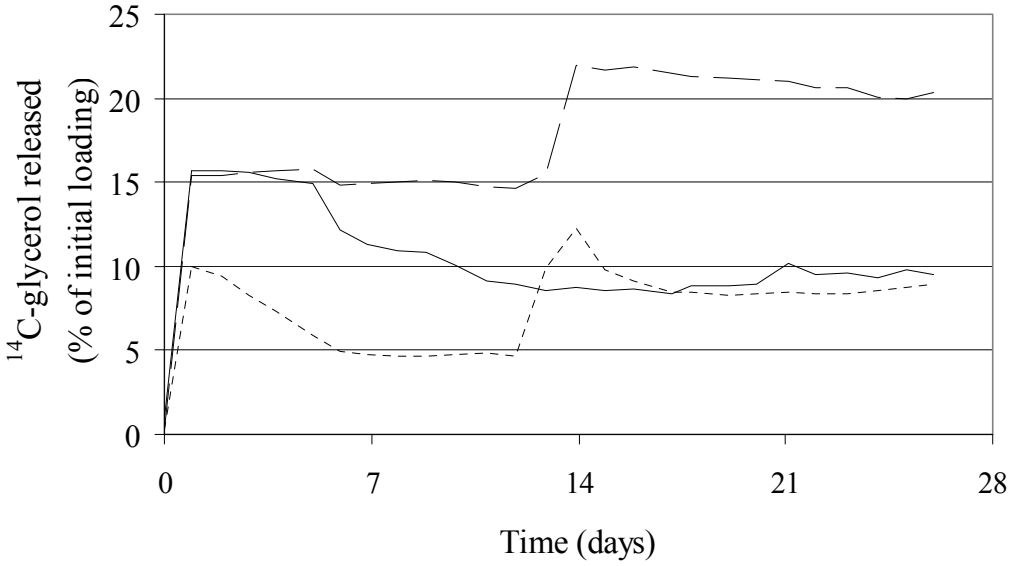

Figure 7.23 Cumulative percentage of ^{14}C-glycerol released from three devices having ~150 μm thick **PLGA4.4** and **PLGA11** membranes.

Figure 7.23 shows that the reservoirs having membranes made from the **PLGA4.4** material all showed release on day one. Two of the devices appeared to show release from the reservoirs having **PLGA11** membranes on day 14. However, the third device (solid line in **Figure 7.23**) did not appear to show release of any radiolabel from the **PLGA11** reservoir. Microscopy of this device, however, clearly showed that the reservoir membrane was open on day 10, as can be seen in **Figure 7.26**(c). It is possible that the amount of ^{14}C-glycerol that was released from the reservoir having the **PLGA11** membrane was so small that blotting of the device with a paper towel prior to microscopy removed any excess ^{14}C above the background concentration. Alternatively, the decrease in the cumulative amount of ^{14}C-glycerol measured suggests that there may be an additional loss of the material from the release vessel other than that removed by pipetting the solution aliquots. Adsorption of the glycerol to the pipet tips, device surface, or surface of the glass release vessel might account for the decrease in the measured amount of glycerol over time.

The measured membrane heights for both the **PLGA4.4** and **PLGA11** membranes on the device that was viewed under the microscope (indicated by the solid line in **Figure 7.23**) showed

a large increase in the first few days of the study before reaching a plateau up to day nine. Both membranes showed a large drop in the measured maximum membrane height between days nine and ten. The decrease in membrane height for the **PLGA11** membrane at day ten is consistent with some of the other results discussed in this chapter, which correlate a decrease in membrane height with the opening of the membrane.

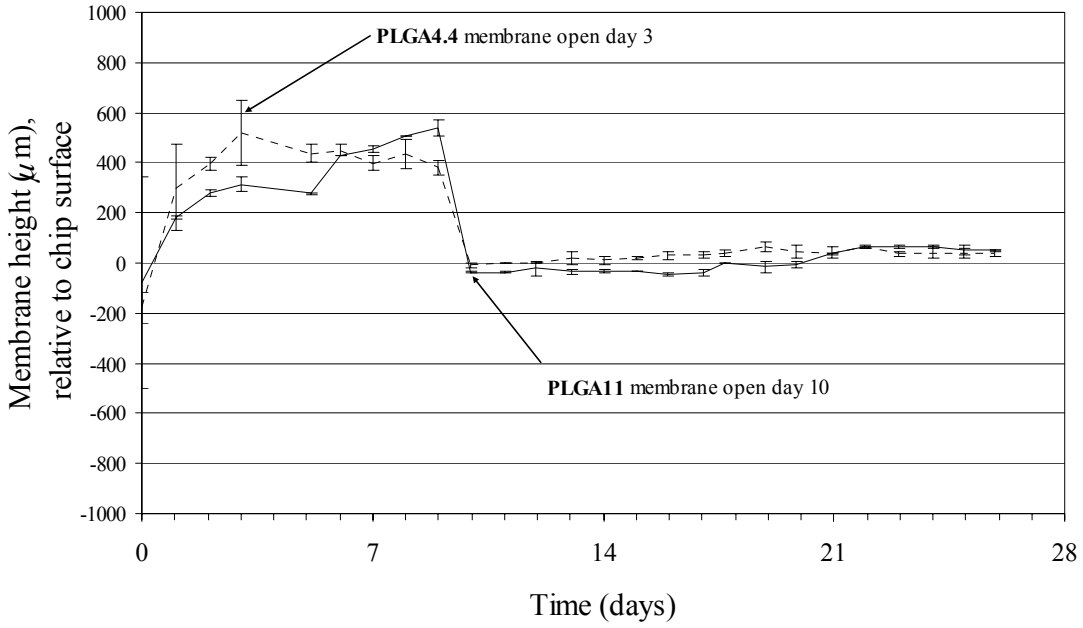

Figure 7.24 Maximum measured height of membranes relative to chip surface for ~150 μm thick **PLGA4.4** (dotted line) and **PLGA11** (solid line) membranes on device loaded with ^{14}C-glycerol.

The **PLGA4.4** membrane showed a maximum change in height of approximately 700 μm (a 470% increase in the membrane thickness) at day nine, while the **PLGA11** membrane showed a maximum change in height of approximately 620 μm (representing a 410% increase in membrane thickness) at day eight (a photograph of this membrane at day eight is shown in **Figure 7.26**(b)). These swelling percentages are consistent with the range of values seen for the other devices in this study.

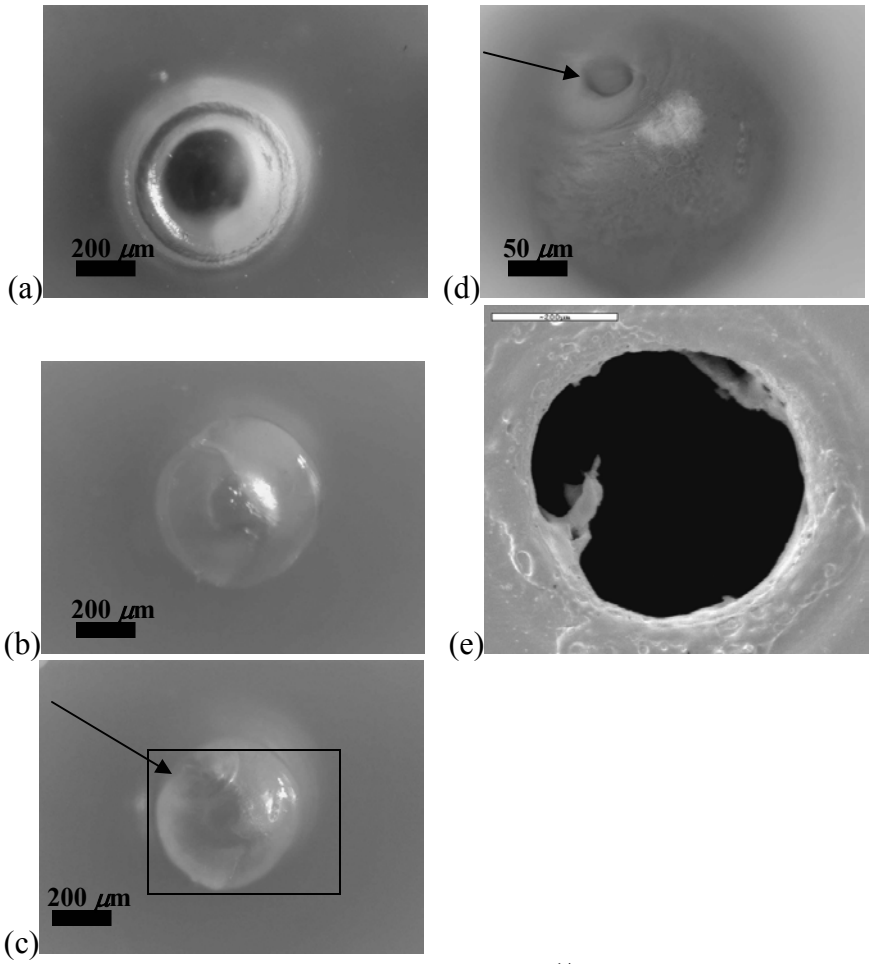

Figure 7.25 ~150 μm **PLGA4.4** membranes on device loaded with ^{14}C-glycerol, viewed under optical microscope or viewed under SEM: (a) **PLGA4.4** membrane at day zero, (b) **PLGA4.4** membrane at day one, (c) **PLGA4.4** membrane at day three, arrow indicates location of hole, which can be seen in the enlargement of boxed region in (d) showing **PLGA4.4** membrane at day three with the hole in the membrane clearly visible as indicated by the arrow, (e) SEM of **PLGA4.4** membrane after 30 days in saline solution.

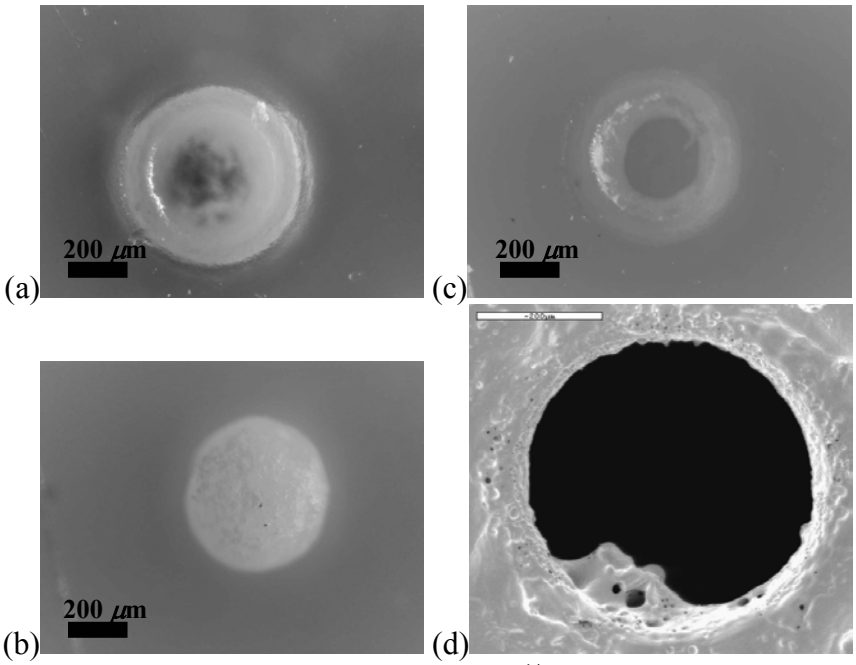

(a) (c)

(b) (d)

Figure 7.26 ~150 μm **PLGA11** membranes on device loaded with ^{14}C-glycerol, viewed under optical microscope or viewed under SEM: (a) **PLGA11** membrane at day zero, (b) **PLGA11** membrane at day eight, (c) **PLGA11** membrane at day ten, (d) SEM of **PLGA11** membrane after 30 days in saline solution.

7.3.1.7 ^{14}C-glycerol 3-phosphate

The release plots for three devices loaded with ^{14}C-glycerol 3-phosphate are shown in **Figure 7.27**. While the amounts of radiolabel detected for the three devices are slightly higher than those seen for the ^{14}C-glycerol loaded devices, they are still quite low in comparison to the results obtained for the glucose and dextran molecules.

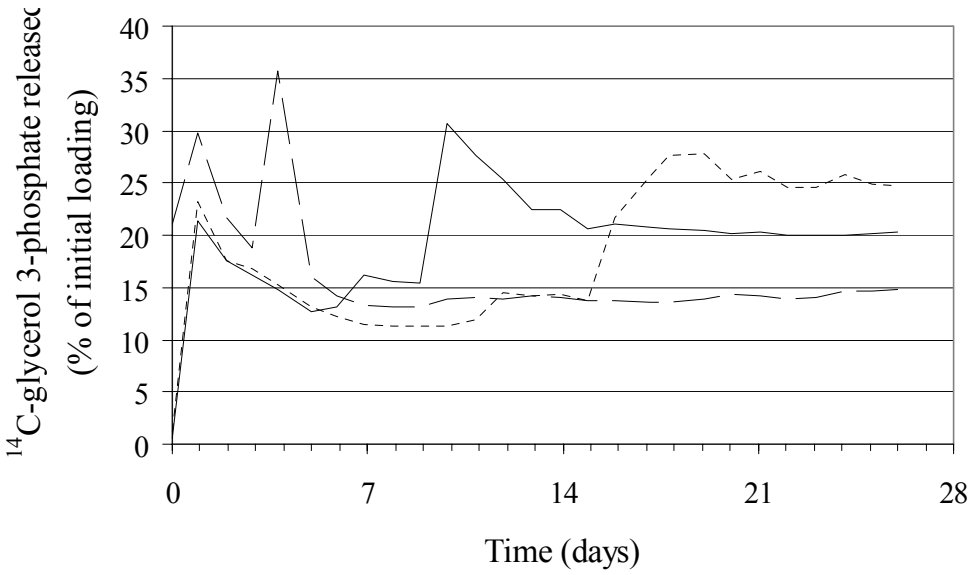

Figure 7.27 Cumulative percentage of ^{14}C-glycerol 3-phosphate released over time from three devices having ~150 μm thick **PLGA4.4** and **PLGA11** membranes.

Glycerol-3-phosphate is readily soluble in water, similar to glycerol, so it is surprising that such low amounts were detected over the course of the experiment. The only reasonable explanations for this result might be adhesion or adsorption of the molecule to the surface of the device, the pipet tips, or glass release vessel. One device showed release on day zero from the reservoir having a membrane made of the **PLGA4.4** polymer, while the other two devices showed release on day one for reservoirs having **PLGA4.4** membranes. Greater variation was seen in the release times of the reservoirs having **PLGA11** membranes. One device (solid line in **Figure 7.27**) showed release at day ten, and another (dotted line) showed release at 16–18 days. The third device (dashed line) appeared to have a large spike at day four, which may indeed have been when the **PLGA11** membrane opened, but the cumulative amount of radiolabel measured after day four dropped back down to approximately 15% of the initial loading and did not show any further increase during the course of the study.

The maximum measured membrane height for each of the **PLGA4.4** and **PLGA11** membranes on one of the devices (device represented by a solid line in **Figure 7.27**) are shown in **Figure 7.28**, and photographs of the membranes over the course of the study are shown in **Figure 7.29** and **Figure 7.30**.

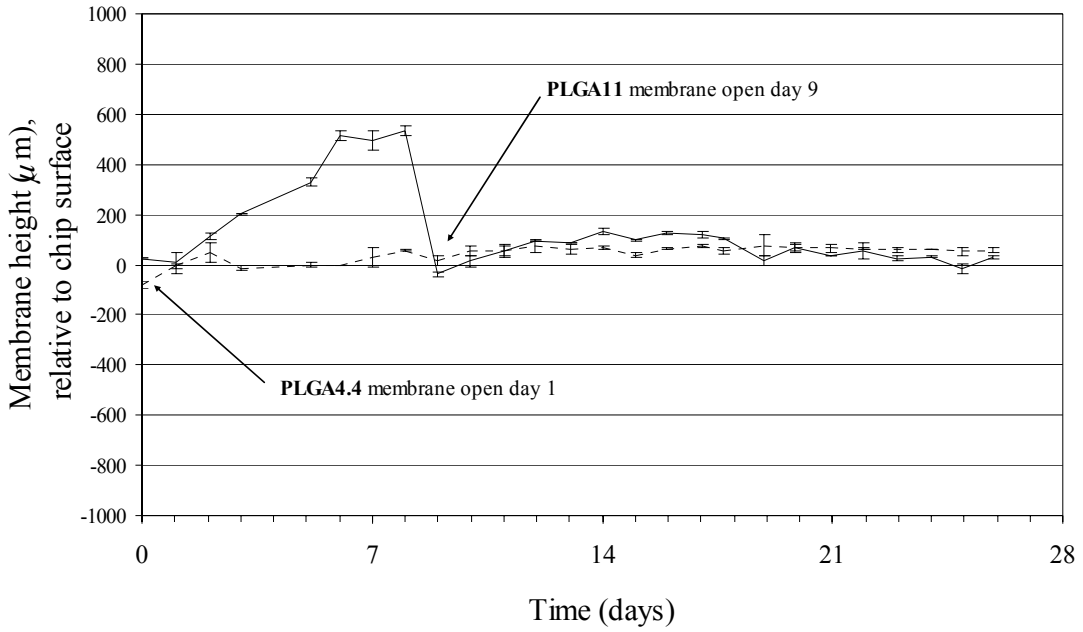

Figure 7.28 Maximum measured membrane height relative to chip surface for ~150 μm thick **PLGA4.4** (dotted line) and **PLGA11** (solid line) membranes on device loaded with ^{14}C-glycerol 3-phosphate.

The **PLGA4.4** membrane (dotted line in **Figure 7.28**) showed only a very small amount of swelling, reaching a maximum swelling of approximately 160 μm (110% increase in membrane thickness) on day 19. No large decrease in membrane height was seen on day one, when a large hole appeared in the membrane as shown in **Figure 7.29**(b). The **PLGA11** membrane, however, attained a maximum swelling of approximately 510 μm (340% increase in membrane thickness) on day eight (a photograph of the membrane at day eight is shown in **Figure 7.30**(b)), which was followed by a sharp drop in membrane height at day nine, at which time a hole appeared in the center of the membrane as shown in **Figure 7.30**(c). Release of the radiolabel from this reservoir was detected at day ten, as shown in **Figure 7.27** above, even though the reservoir membrane appeared open a day earlier, at day nine. This result is similar to that obtained for the reservoir having a **PLGA11** membrane that was loaded with 10,000 molecular weight ^{14}C-dextran, as discussed in section 7.3.1.3. Photographs of the devices were always taken after an aliquot of the media was removed, thus agitation of the media as the device was transferred from the incubator to the microscope may have dislodged the membrane after the day nine scintillation aliquot was removed (which did not show any release of radiolabel) but before the day nine photographs were taken (which showed a hole in the membrane).

Interestingly, it appeared as though the **PLGA11** membrane was still intact in the device reservoir when SEM was performed after the experiment was completed. Although the hole in the membrane was clearly visible at day nine when the device was viewed on the optical microscope, a large portion of the membrane remained visible even after 28 days, as shown in **Figure 7.30**(d). Thus it is possible that accretion of gold at the edges of the membrane hole during the sputter coating process prior to SEM analysis may have caused the formation of a gold plug or layer within the membrane hole, thus causing the smooth surface seen in the SEM photos in **Figure 7.30**(e) and (f).

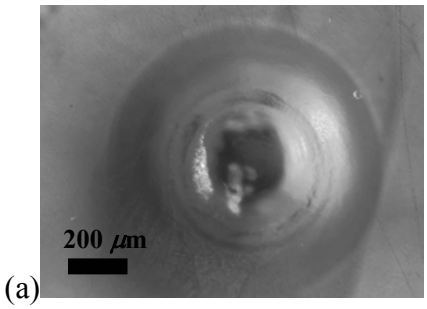

(a)

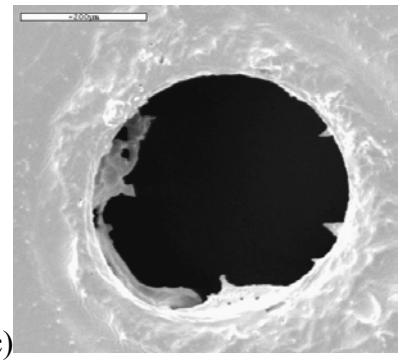

(c)

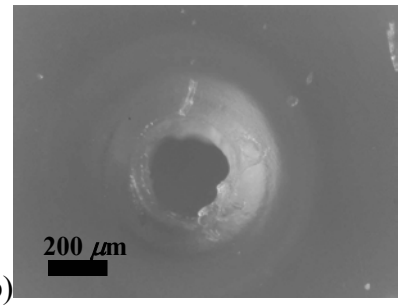

(b)

Figure 7.29 ~150 μm thick **PLGA4.4** membranes on device loaded with ^{14}C-glycerol 3-phosphate viewed under optical microscope or viewed under SEM: (a) **PLGA4.4** membrane at day zero, (b) **PLGA4.4** membrane at day one, (c) SEM of **PLGA4.4** membrane after 30 days in saline solution.

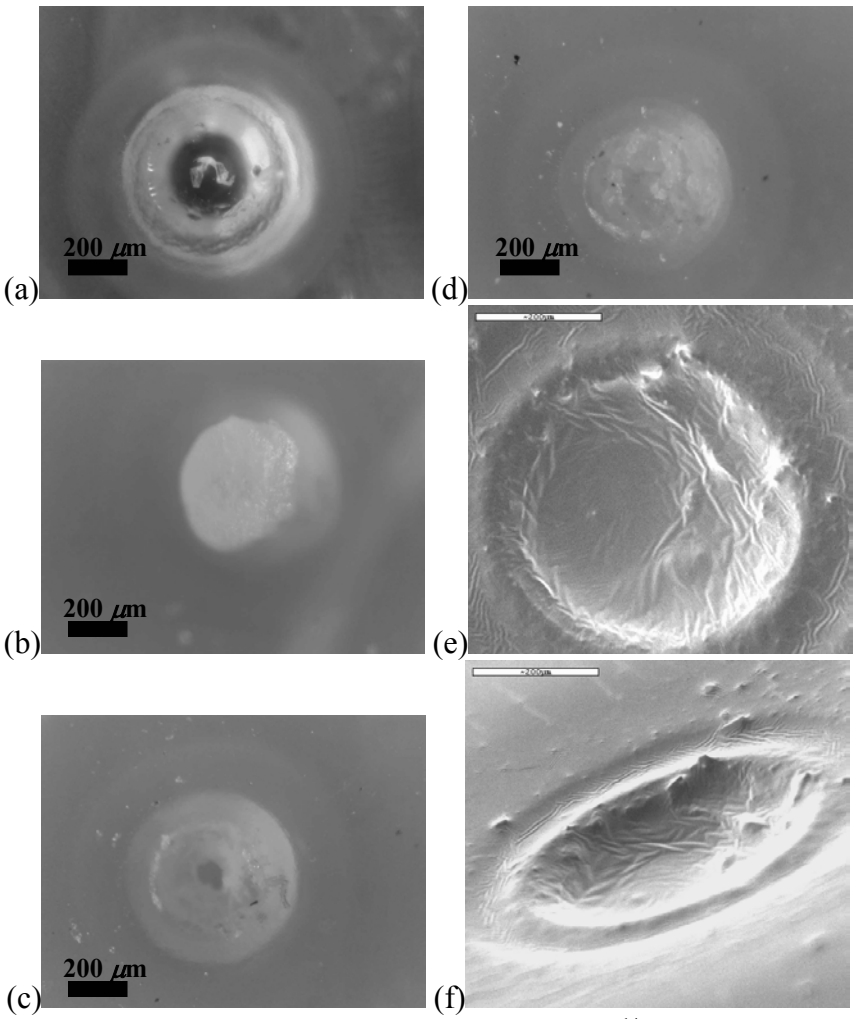

Figure 7.30 ~150 μm thick **PLGA11** membranes on device loaded with ^{14}C-glycerol 3-phosphate viewed under optical microscope or viewed under SEM: (a) **PLGA11** membrane at day zero, (b) **PLGA11** membrane at day eight, (c) **PLGA11** membrane at day nine, (d) PLGA11 membrane at day 28, (e) SEM of **PLGA11** membrane after 30 days in saline solution, (f) SEM of **PLGA11** membrane after 30 days in salt solution, stage tilted 66°.

7.3.1.8 ^{14}C-glycerol trioleate

The release results for three devices loaded with ^{14}C-glycerol trioleate are shown in **Figure 7.31**. The cumulative amounts of ^{14}C-glycerol trioleate detected from the three different devices are even lower than the amounts measured for the devices loaded with ^{14}C-glycerol and ^{14}C-glycerol 3-phosphate discussed in sections 7.3.1.6 and 7.3.1.7, respectively. This is not surprising, as glycerol trioleate is not very soluble in water (it is shipped from the manufacturer in toluene). Additionally, only one of the devices showed a significant release pulse over the entire course of the study, over the first three days after the device was immersed in the PBS.

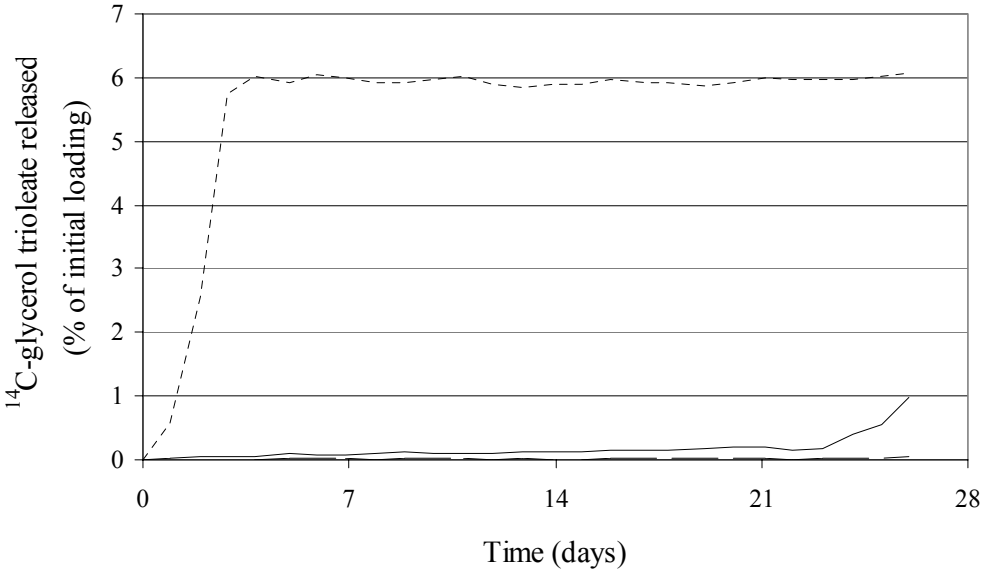

Figure 7.31 Cumulative percentage of ^{14}C-glycerol trioleate released over time from three devices having ~150 μm thick **PLGA4.4** and **PLGA11** membranes.

Significant membrane swelling was measured for the device indicated by the solid line in **Figure 7.31**. The maximum measured membrane heights for this device are shown in **Figure 7.32**. Photographs of the **PLGA4.4** and **PLGA11** membranes on this device are shown in **Figure 7.33** and **Figure 7.34**. The **PLGA4.4** membrane appeared open after only one day, as shown in **Figure 7.33**(b). The **PLGA4.4** membrane height reached a maximum on day one, and then decreased slowly until day eight, at which time the membrane height began to decrease more sharply. The maximum swelling measured for this membrane at day one was approximately 405 μm, or 270% of the initial membrane thickness of 150 μm.

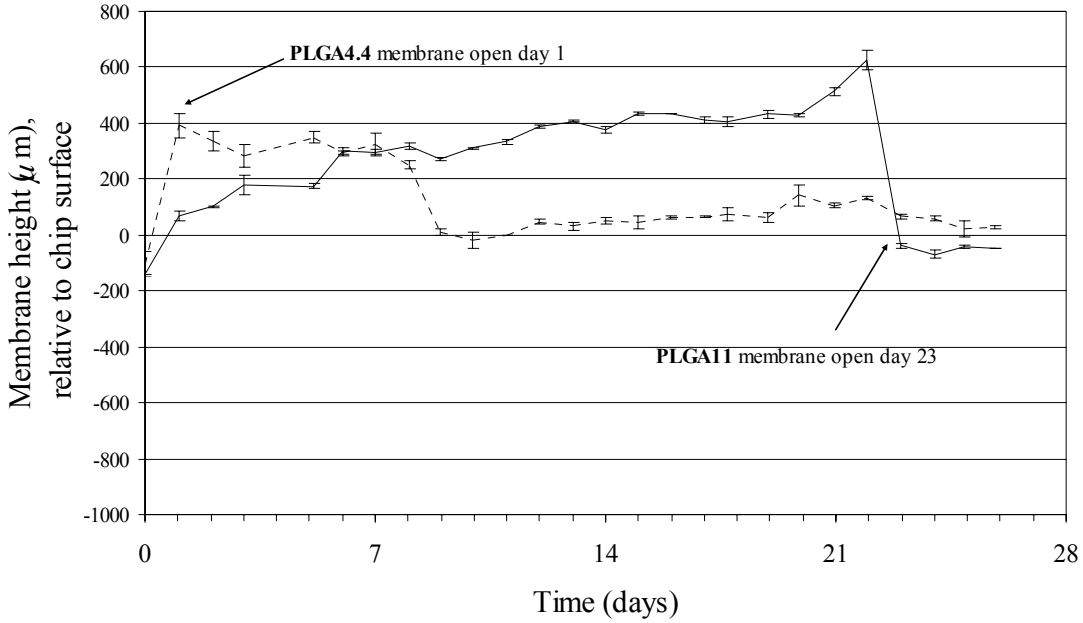

Figure 7.32 Maximum measured membrane height relative to chip surface for ~150 μm thick **PLGA4.4** (dotted line) and **PLGA11** (solid line) membranes on device loaded with ^{14}C-glycerol trioleate.

The **PLGA11** membrane also showed a large amount of swelling, with the membrane height increasing steadily over approximately the first three weeks of the study before reaching a maximum on day 22. The maximum membrane height at that time was approximately 770 μm greater than at day zero (626 μm above the surface at day 22, versus 141 μm below the surface of the device at day zero), corresponding to a 510% increase in membrane thickness compared to the initial thickness of 150 μm. Although no significant amount of ^{14}C-glycerol trioleate appeared to be released from this device based on scintillation measurements, **Figure 7.33**(b) and **Figure 7.34**(e) clearly show holes in the centers of the membranes on days one and 23, respectively. Thus it appears that although the membrane opened, perhaps the relative insolubility of the ^{14}C-glycerol trioleate in water might explain the fact that no radiolabel was detected in the medium.

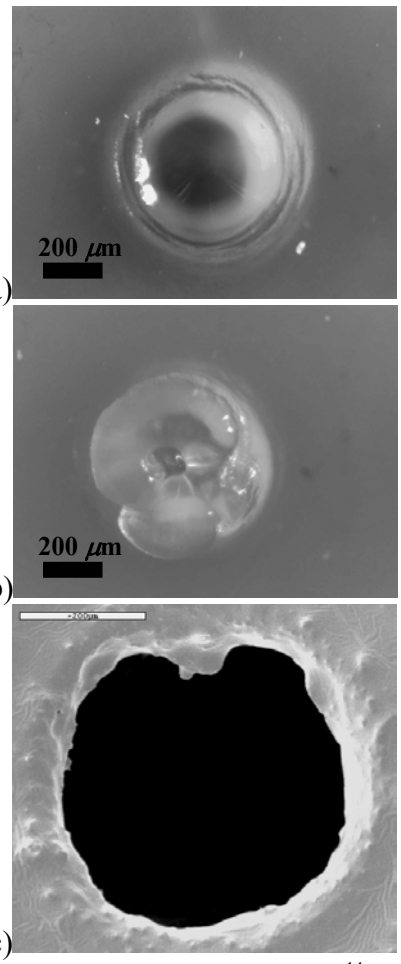

Figure 7.33 ~150 μm thick **PLGA4.4** membrane on device loaded with ^{14}C-glycerol trioleate, viewed under optical microscopy or viewed under SEM: (a) **PLGA4.4** membrane at day zero, (b) **PLGA4.4** membrane at day one, (c) SEM of **PLGA4.4** membrane after 30 days in saline solution.

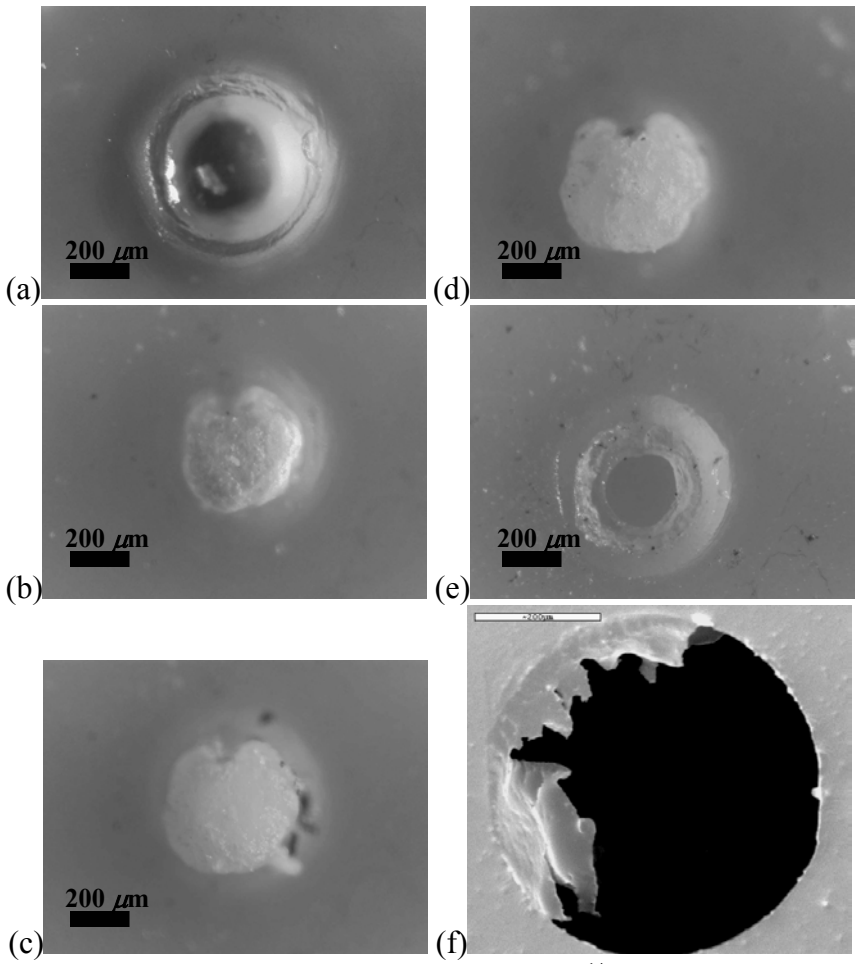

Figure 7.34 ~150 μm thick **PLGA11** membrane on device loaded with ^{14}C-glycerol trioleate, viewed under optical microscope or viewed under SEM: (a) **PLGA11** membrane at day zero, (b) **PLGA11** membrane at day seven, (c) **PLGA11** membrane at day 14, (d) **PLGA11** membrane at day 21, (e) **PLGA11** membrane at day 23, (f) SEM of **PLGA11** membrane after 30 days in saline solution.

7.3.1.9 Discussion

Three characteristic times were determined from the data collected in these studies. The time at which the maximum measured increase in membrane height occurred is designated as $t_{max\ swelling}$. The corresponding water uptake (as a percentage of the initial mass of membrane polymer) was calculated at $t_{max\ swelling}$ using Equation 7-h and Equation 7-i. The characteristic release time, $t_{release}$, is the time at which detection of the radiolabel from a reservoir occurred. Finally, the time at which the reservoir membrane appeared open when viewed under the optical microscope is designated as t_{open}. These characteristic times for devices loaded with ^{14}C-glucose, ^{14}C-dextran (M_w 10,000 and 40,000), as well as the unloaded control device, are summarized in **Table 7-1** and **Table 7-2** below.

Table 7-1 Maximum measured membrane height, calculated % water uptake, $t_{max\ swelling}$, $t_{release}$, and t_{open} for **PLGA4.4** membranes on unloaded control device, as well as devices loaded with ^{14}C-glucose and ^{14}C-dextran having molecular weights of 10,000 and 40,000.

Device Loading	max Δh (PLGA4.4 membrane height) (μm)	water uptake (% of initial membrane weight)	$t_{max\ swelling}$	$t_{release}$	t_{open}
none (control)	350	190	1	NA	12
glucose	740	680	1	1	7
10k dextran	690	750	1	1	2
40k dextran	710	680	1	1	3

Table 7-2 Maximum measured membrane height, calculated % water uptake, $t_{max\ swelling}$, $t_{release}$, and t_{open} for **PLGA11** membranes on unloaded control device, as well as devices loaded with ^{14}C-glucose and ^{14}C-dextran having molecular weights of 10,000 and 40,000.

Device Loading	max Δh (PLGA11 membrane height) (μm)	water uptake (% of initial membrane weight)	$t_{max\ swelling}$	$t_{release}$	t_{open}
none (control)	440	330	5	NA	6
glucose	280	80	5	6	9
10k dextran	600	520	10	12	10-11
40k dextran	530	340	12	8	15

The fact that swelling was observed for the control device, although perhaps to a slightly lesser degree than for the other devices having a chemical loaded into the reservoirs, is evidence that at the very least, the membrane swelling cannot be solely attributed to a loading or osmotic pressure effect of the chemical in the reservoirs. Additionally, the molecular weight of the chemical that was loaded into the reservoirs did not appear to have a significant effect on either the maximum measured membrane height or $t_{release}$, as the devices loaded with ^{14}C-glucose or either of the ^{14}C-dextran molecules showed comparable swelling and release times. This is an important result, as it suggests that for the drugs investigated in this study, the performance of the device is independent of the size of the drug that is to be delivered from the device. Although previous release studies presented in Chapter 4 showed more continuous release of small molecules such as BCNU and IAP, ^{14}C-glucose showed pulsatile release in the studies presented here. This suggests that the hydrophobicity or hydrophilicity of the drug may be a more important factor than the molecule size in determining the release characteristics of the drug from the microreservoir device. Other researchers have also shown little effect of protein or peptide molecular weight on the release kinetics from PLGA microspheres[18,19], which supports the results obtained here for the devices loaded with glucose and dextran.

The characteristic times, maximum membrane height, and water uptake for the devices loaded with dextran having a molecular weight of 70,000 are summarized in **Table 7-3** and **Table 7-4** below.

Table 7-3 Maximum measured membrane height, calculated % water uptake, $t_{max\ swelling}$, $t_{release}$, and t_{open} for **PLGA4.4** membranes on devices having three different loadings of 70,000 molecular weight ^{14}C-dextran.

Device Loading	max Δh (PLGA4.4 membrane height) (μm)	water uptake (% of initial membrane weight)	$t_{max\ swelling}$	$t_{release}$	t_{open}
70k dex low	690	640	1	1	1
70k dex intermediate	170	40	13	1	2
70k dex high	450	220	2	1	2

Table 7-4 Maximum measured membrane height, calculated % water uptake, $t_{max\ swelling}$, $t_{release}$, and t_{open} for **PLGA11** membranes on devices having three different loadings of 70,000 molecular weight ^{14}C-dextran.

Device Loading	max Δh (PLGA11 membrane height) (μm)	water uptake (% of initial membrane weight)	$t_{max\ swelling}$	$t_{release}$	t_{open}
70k dex low	470	250	16	14	15
70k dex intermediate	270	90	17	17	20
70k dex high	320	110	20	15	28

There was no correlation between the loading and the maximum membrane height, water uptake, $t_{release}$, or t_{open} for the different loadings of 70,000 molecular weight ^{14}C-dextran which were investigated. The devices loaded with different amounts of 70,000 molecular weight ^{14}C-dextran showed surprisingly little variation (14–18 days) in $t_{release}$ from the reservoirs sealed with **PLGA11** membranes, even though the loading was increased by nearly a factor of two. Although $t_{max\ swelling}$ for the **PLGA11** membranes (**Table 7-4**) appears to occur at later times for higher loadings, this is opposite to the trend we would expect if the osmotic pressure due to the solute were a contributing factor to the membrane opening. The absence of a correlation between the release times and the reservoir loadings is an important result for two reasons. The first is that it suggests that no water penetrates into the reservoir. Our other release results support this theory as well, especially those obtained for small molecules that might be able to diffuse through small fissures or pores in the membranes. The apparent hermeticity of the reservoirs once they are sealed with the polymer membranes indicates that a) no leakage of the drug through the membrane will occur, barring significant diffusion or permeation into the membrane itself (see Chapter 6 for further discussion), and b) compounds that are unstable or prone to degradation in aqueous environments will stay dry and therefore active until the reservoir membrane ruptures and the drug is delivered from the device. The second reason that the results of the 70,000 molecular weight dextran devices are important is that they are further evidence for the independence of device performance from the drug loading. These results show that for the chemical loadings we investigated, changing the loading of the chemical within the reservoir does not affect the release time of the drug from the device. If this result is borne out for other

chemicals and loadings, it could allow the device to be loaded with dosages of varying sizes, without having to change the membrane characteristics according to the reservoir loading. This is in contrast to other PLGA based systems reported in the literature, such as microspheres, that exhibit loading-dependent drug release kinetics[20].

The characteristic times, maximum membrane height, and water uptake for the devices that were loaded with different glycerol moieties are summarized in **Table 7-5** and **Table 7-6** below.

Table 7-5 Maximum measured membrane height, calculated % water uptake, $t_{max\ swelling}$, $t_{release}$, and t_{open} for **PLGA4.4** membranes on devices loaded with ^{14}C-glycerol, ^{14}C-glycerol 3-phosphate, and ^{14}C-glycerol trioleate.

Device Loading	max Δh (PLGA4.4 membrane height) (μm)	water uptake (% of initial membrane weight)	$t_{max\ swelling}$	$t_{release}$	t_{open}
glycerol	700	570	3	1	3
glycerol 3-phosphate	160	40	19	1	1
glycerol trioleate	490	240	1	not observed	1

Table 7-6 Maximum measured membrane height, calculated % water uptake, $t_{max\ swelling}$, $t_{release}$, and t_{open} for **PLGA11** membranes on devices loaded with ^{14}C-glycerol, ^{14}C-glycerol 3-phosphate, and ^{14}C-glycerol trioleate.

Device Loading	max Δh (PLGA11 membrane height) (μm)	water uptake (% of initial membrane weight)	$t_{max\ swelling}$	$t_{release}$	t_{open}
glycerol	620	430	9	not observed	10
glycerol 3-phosphate	510	380	8	10	9
glycerol trioleate	770	740	22	not observed	23

The results for the devices that were loaded with the glycerol moieties clearly show that the hydrophilicity or hydrophobicity of the molecule that is loaded into the reservoir does not appear to affect the amount of maximum measured membrane swelling. Other researchers have suggested that the observed water uptake of PLA may be due to osmotic pressure driving the buffer solution (media) into the polymer matrix to neutralize the acidic end groups of the polymer chains[23]. This theory would explain the similar swelling seen for the membranes on reservoirs that had different chemical loadings, as the concentration of acidic end groups would be the essentially the same in all membranes made from a given polymer, no matter with what chemical the reservoir was loaded. Although the more hydrophilic molecules (glycerol and glycerol 3–phosphate) appeared to show earlier release (as indicated by t_{open}) than the glycerol trioleate from the reservoirs having **PLGA11** membranes, this is not conclusive due to the small number of devices in the study, as well as the fact that no confirmation of release ($t_{release}$) was

obtained by scintillation measurements for the devices loaded with ^{14}C-glycerol or ^{14}C-glycerol trioleate due to apparent chemical insolubility.

Although $t_{release}$ was not observed for the **PLGA11** membranes on devices loaded with glycerol and glycerol trioleate (**Table 7-6**), the device that was loaded with glycerol 3-phosphate showed good agreement between the three characteristic times. This is consistent with the results obtained for the devices that were loaded with other chemicals.

Overall, approximately 50% of the devices that were viewed under the microscope showed a correlation between $t_{max\ swelling}$ and $t_{release}$. Some devices also showed a correlation between t_{open} and $t_{release}$. One difficulty with drawing a parallel or correlation between these two phenomena, however, is that the failure mode of the membranes seemed to vary. Specifically, some devices suddenly exhibited a large hole in the membrane that corresponded temporally to the detection of radiolabel from the reservoir, while other membranes showed only small pinholes, some membranes stayed quite smooth and bulbous during the swelling process, and others showed a very nonuniform surface texture. Still other membranes never appeared to completely open, and large portions of the membrane remained in the reservoirs throughout the entire course of the study. Membranes that did not exhibit a large hole or catastrophic failure often did not show a large drop in the measured maximum membrane height when release of the radiolabel was detected from the reservoir. The fact that approximately half of the devices in this study, however, showed a correlation between $t_{max\ swelling}$ and $t_{release}$ suggests that the mechanical behavior of the membranes may be an important factor in drug release from the devices, in addition to the threshold molecular weight discussed in Chapter 5.

Slightly more of the devices (six out of ten devices) showed greater swelling for the **PLGA4.4** membranes than for the **PLGA11** membranes (four out of ten devices). One explanation for this observed behavior might be that the shorter polymer chains in the **PLGA4.4** membrane may provide greater free volume due to the higher concentration of polymer chain ends. The larger amount of free volume present might allow for greater water uptake, which is reflected as a larger amount of swelling. This mechanism has been proposed by others, who observed greater water uptake for PLA copolymers having increasing ratios of D:L lactide monomer, and proposed that the lower T_g of those polymers reflects greater chain mobility and consequently greater water uptake[21]. Alternatively, some researchers have proposed that plasticization of PLGA copolymers occurs when the T_g of the polymer drops below 37°C after

hydration[22]. This theory has been advanced in order to explain the observation of partial collapse of PLGA microspheres, with the hypothesis that as the T_g of the polymer drops below the ambient temperature, the polymer chains become more mobile and seal off pores and channels that were originally present in the microspheres. A nonporous but completely dense microsphere was the result of this process. In the case of the membranes studied here, swelling of the membranes instead of collapse might be observed if the membranes were initially fabricated as nonporous, since in the absence of densification the morphological changes would be dictated by the enthalpic driving force for swelling. Greater morphological changes might be observed for the **PLGA4.4** membranes due to their initially lower T_g compared to the **PLGA11** membranes.

Water absorption and swelling of PLA and PLGA polymers have been studied, to a limited extent, by others. While quantitative measurements of the volume change (swelling) are not typically performed, the change in weight due to water uptake is more routinely characterized. Compression molded parallelepiped PLA samples ($15 \times 10 \times 2$ mm^3) having an initial M_w of 65,000 had a linear increase in water absorption up to approximately 50% at seven weeks, when aged in saline or PBS at 37°C[24]. PLA M_w 67,000 film samples 0.3 mm in thickness absorbed up to 50% water in one week in phosphate buffer at 37°C[25]. The amount of water absorption remained relatively constant until between 24 and 29 weeks, when the water absorption increased to 300%. However, for PLA M_w 43,000 compression molded plates ($15 \times 10 \times 2$ mm^3), initial water uptake was only 10% at four weeks, but rapidly increased between 11 and 18 weeks to over 400%. A study of PLGA M_w 29,270 extruded samples showed 15% (by volume) swelling at just two days[26]. In contrast, solid PGA disks were found to have an increase in diameter of only approximately 1–2% over 15 days, with a measured water content of approximately 20%[27]. In general, we expect the membranes in our study, which are fabricated from PLGA, to exhibit more water uptake than the PLA objects reported in the literature, due to the more hydrophilic nature of the PGA in the copolymer membranes. Additionally, the lower molecular weight of the membrane materials investigated in our study most likely causes them to degrade more rapidly than the materials reported on in the literature, which may also explain the larger water uptake seen for the materials in the study presented here, as compared to the results reported in the literature.

7.4 Conclusions

Both the **PLGA4.4** and **PLGA11** membranes showed a large amount of swelling and water uptake that did not appear to depend on the chemistry or molecular weight of the molecule that was loaded into the reservoirs. The calculated values of percentage of water uptake for the different membrane materials were larger in general than those reported in the literature for other PLA and some PLGA polymers. This may be explained by both the lower molecular weight of the membrane materials in our study, as well as the greater hydrophilicity of the 50:50 PLGA copolymers that were used to fabricate the membranes compared to the materials reviewed in the literature. **PLGA4.4** membranes showed very uniform release behavior, similar to the release results presented in Chapters 4 and 5, while greater variation in release time was seen for **PLGA11** membranes. Approximately 50% of the devices that were viewed under the optical microscope showed a correlation between $t_{max\ swelling}$ and $t_{release}$. The loading of the molecules in the reservoirs did not appear to affect the observed release times, indicating that no water penetrates into the reservoirs to cause an osmotic pressure effect. These results indicate that the device performance is independent of the chemistries and dosages of the drugs investigated here. The ability to change the amount of drug loaded into a reservoir, without affecting the release time or release kinetics of the drug from the device, may provide great flexibility in device design for a variety of applications.

7.5 References

1. J. M. Anderson and M. S. Shive, "Biodegradation and biocompatibility of PLA and PLGA microspheres," *Advanced Drug Delivery Reviews* 28 (1997) 5–24.

2. M. Ramchandani and D. Robinson, "*In vitro* and *in vivo* release of ciprofloxacin from PLGA 50:50 implants," *Journal of Controlled Release* 54 (1998) 167–175.

3. M. J. Blanco-Príeto, K. Besseghir, O. Zerbe, D. Andris, P. Orsolini, F. Heimgartner, H. P. Merkle, and B. Gander, "*In vitro* and *in vivo* evaluation of a somatostatin analogue released from PLGA microspheres," *Journal of Controlled Release* 67 (2000), 19–28.

4. C. Mallard, J. Coudane, I. Rault, and M. Vert," The use of additives to modulate the release of a sparingly water soluble drug entrapped in PLA50 microparticles: *in vivo* investigation," *J. Microencapsulation* 17 (2000) 95–110.

5. R. Herrero-Vanrell, L. Ramirez, A. Fernandez-Carballido, and M. F. Refojo, "Biodegradable PLGA microspheres loaded with Ganciclovir for intraocular administration. Encapsulation technique, *in vitro* release profiles, and sterilization process," *Pharmaceutical Research* 17 (2000) 1323–1328.

6. H. Eroğlu, H.S. Kaş, L. Oner, Ö. F. Türkoğlu, N. Akalan, M. F. Sargon, and N. Özer, "The *in-vitro* and *in-vivo* characterization of PLGA:L-PLA microspheres containing dexamethasone sodium phosphate," *J. Microencapsulation* 18 (2001) 603–612.

7. J. H. Jeong and T. G. Park, "Novel polymer-DNA hybrid polymeric micelles composed of hydrophobic poly(D,L-lactic-*co*-glycolic acid) and hydrophilic oligonucleotides," *Bioconjugate Chem.* 12 (2001) 917–923.

8. T. Hickey, D. Kreutzer, D. J. Burgess, and F. Moussy, "*In vivo* evaluation of a dexamethasone/PLGA microsphere system designed to suppress the inflammatory tissue response to implantable medical devices," *J. Biomed. Mater. Res.* 61 (2002) 180–187.

9. G. Shi, Q. Cai, C. Wang, N. Lu, S. Wang, and J. Bei, "Fabrication and biocompatibility of cell scaffolds of poly(L-lactic acid) and poly(L-lactic-co-glycolic acid)," *Polym. Adv. Technol.* 13 (2002) 227–232.

10. P. X. Ma and R. Langer, "Degradation, structure and properties of fibrous nonwoven poly(glycolic acid) scaffolds for tissue engineering," *Mat. Res. Soc. Symp. Proc.* 394 (1995) 99–104.

11. J. Gao, L. Niklason, and R. Langer, "Surface hydrolysis of poly(glycolic acid) meshes increases the seeding density of vascular smooth muscle cells," *J. Biomed Mater. Res.* 42 (1998) 417–424.

12. S. Santavirta, Y. T. Kontinnen, T. Saito, M. Grönblad, E. Partio, P. Kemppinen, and P. Rokkanen, "Immune response to polyglycolic acid implants," *The Journal of Bone and Joint Surgery* 72-B (1990), 597–600.

13. K. A. Athanasiou, G. G. Niederauer, and C. M. Agarwal, "Sterilization, toxicity, biocompatibility and clinical applications of polylactic acid/polyglycolic acid copolymers," *Biomaterials* 17 (1996) 93–102.

14. K. A. Athanasiou, J. P. Schmitz, and C. M. Agarwal, "The effects of porosity on *in vitro* degradation of polylactic acid-polyglycolic acid implants used in repair of articular cartilage," *Tissue Engineering* 4 (1998) 53–63.

15. K. Anselme, B. Flautre, P. Hardouin, M. Chanavaz, C. Ustariz, and M. Vert, "Fate of bioresorbable poly(lactic acid) microbeads implanted in artificial bone defects for cortical bone augmentation in dog mandible," *Biomaterials* 14 (1993) 44–50.

16. H. Winet and J. Y. Bao, "Comparative bone healing near eroding polylactide-polyglycolide implants of differing crystallinity in rabbit tibial bone chambers," *J. Biomater. Sci. Polymer Edn.* 8 (1997) 517–532.

17. http://aqueous.labs.brocku.ca/osfile.html

18. F. W. Okumu, J. L. Cleland, and R. T. Borchardt, "The effect of size, charge, and cyclization of model peptides on their in vitro release from DL–PLGA microspheres," *J. Controlled Release* 49 (1997) 133–140.

19. M. Sandor, D. Enscore, P. Weston, E. Mathiowitz, "Effect of protein molecular weight on release from micron-sized PLGA microspheres," *J. Controlled Release* 76 (2001) 297–311.

20. J. F. Fitzgerald and O. I. Corrigan, "Investigation of the mechanisms governing the release of levamisole from poly-lactide-co-glycolide delivery systems," *Journal of Controlled Release* 42 (1996) 125–132.

21. S. Li, A. Girard, H. Garreau, and M. Vert, "Enzymatic degradation of polylactide stereocopolymers with predominant D-lactyl contents," *Polym. Degrad. Stab.* 71 (2001) 61–67.

22. N. B. Viswanathan, S. S. Patil, J. K. Pandit, A. K. Lele, M. G. Kulkarni, and R. A. Mashelkar, "Morphological changes in degrading PLGA and P(DL)LA microspheres: implications for the design of controlled release systems," *J. Microencapsulation* 18 (2001) 783–800.

23. S. Li and S. McCarthy, "Further investigation on the hydrolytic degradation of poly (DL-lactide)," *Biomaterials* 20 (1999) 35–44.

24. S. M. Li, H. Garreau, and M. Vert, "Structure-property relationships in the case of the degradation of massive aliphatic poly-(α-hydroxy acids) in aqueous media, Part 1: Poly(DL-lactic acid), *Journal of Materials Science: Materials in Medicine* 1 (1990) 123–130.

25. I. Grizzi, H. Garreau, S. Li, and M. Vert, "Hydrolytic degradation of devices based on poly(DL-lactic acid) size-dependence," *Biomaterials* 16 (1995) 305–311.

26. C. Witt, K. Mader, and T. Kissel, "The degradation, swelling, and erosion properties of biodegradable implants prepared by extrusion or compression moulding of poly(lactide-*co*-glycolide) and ABA triblock copolymers," *Biomaterials* **21** (2000) 931–938.

27. S. Hurrell and R. E. Cameron, "Polyglycolide: degradation and drug release. Part I: Changes in morphology during degradation," *Journal of Materials Science: Materials in Medicine* 12 (2001) 811–816.

8 Measured Biological Activity of Heparin After Release from Microreservoir Devices

8.1 Introduction and Motivation

8.1.1 Introduction

The feasibility of delivering multiple chemicals from biodegradable microreservoir devices *in vitro* has been demonstrated by experiments presented in Chapter 4. An important consideration, however, is whether or not chemicals will be biologically active after they are released from the device. A device that is capable of releasing multiple pulses of drugs will be rendered useless if the drugs are no longer effective after delivery to the patient.

Biological activity can be measured in a number of different ways, depending on the molecule that is of interest. Proteins, for example, can be tested for activity via a variety of methods, including antibody binding and cell proliferation assays. However, these tests may be difficult to perform *in vitro* due to the associated complications of cell culture, antibody integrity, and difficulty in finding an appropriate clinical model system. Interleukin-2, for example, which we have shown to be released from the microreservoir devices (see section 4.3.2.1.4), can be assayed for activity via a lymphocyte proliferation assay[1,2]. However, this molecule is hydrophobic[3] and has a propensity to adsorb to glass and plastic surfaces[4], making it difficult to obtain quantitative results *in vitro*. Measurements of interleukin-2 activity *in vivo* are complicated by the fact that the molecule has a short half-life in the human body.

Biological activity measurements of other types of molecules such as polysaccharides are simpler due to the obviation of the need for cell-based assays. We chose to investigate the biological activity of heparin during an *in vitro* release experiment from the microreservoir devices using a colorimetric anti-Factor XA assay. This assay contains excesses of both antithrombin III and Factor XA. In the presence of excesses of these two molecules, the inhibition of Factor XA is proportional to the heparin concentration present. The use of a chromogenic Factor XA substrate allows the spectrophotometric measurement of the residual Factor XA activity, which is inversely proportional to the heparin concentration[5].

8.1.2 Motivation

The goal of these experiments was twofold. First, it was desired to characterize the release times of heparin from devices having reservoir membranes made from **PLGA4.4**, **PLGA11**, **PLGA28**, and **PLGA64** polymers. The second goal was to demonstrate that heparin retains its biological activity after it has been released from the microreservoir devices *in vitro*. Although heparin is and has been widely used therapeutically as an anticoagulant, its stability has not been extensively studied. However, we hypothesized that its polysaccharide nature would provide reasonable stability over the course of our *in vitro* release experiments.

8.2 Materials and Methods

8.2.1 Materials

Poly(L-lactic acid) (**PLA**, M_w 194 Kilodaltons (Kd), Medisorb® 100 L), and poly(D,L-lactic-*co*-glycolic acid) polymer powders of molecular weights (M_w) 4.4 Kd (**PLGA4.4**, Medisorb® 5050 DL 1A), 11 Kd (**PLGA11**, Medisorb® 5050 DL 2A), 28 Kd (**PLGA28**, Medisorb® 5050 DL 3A), and 64 Kd (**PLGA64**, Medisorb® 5050 DL 4A) were obtained from Alkermes (Cincinnati, Ohio). ^{3}H-heparin, sodium salt, was purchased from Perkin Elmer Life Sciences (Boston, MA). Heparin sodium salt, fetal bovine serum (FBS), and ACCUCOLOR™ kits (heparin activity assays) were purchased from Sigma-Aldrich (St. Louis, MO). ScintiSafe Plus 50% was purchased from Fisher Scientific (Suwanee, GA). Ideal 9144 Masking Tape was obtained from American Biltrite, Inc. (Lowell, MA).

8.2.2 Methods

8.2.2.1 Device Fabrication

Devices with reservoir membranes were fabricated according to the procedures described in Chapter 2. All reservoir membranes were designed to be approximately 150 μm thick in this study. The membranes were inspected for defects after drying (such as air bubbles and pinholes) at 80X magnification using a PZMT Trinocular stereomicroscope. Reservoirs having defect-free membranes were considered viable for use in release experiments, and selected reservoirs were loaded with the heparin to be released. The heparin solutions were allowed to dry in the

reservoirs for approximately 24 hours at room temperature and pressure before the devices were sealed opposite the membranes with Ideal Masking Tape 9144 (American Biltrite, Inc.).

8.2.2.2 *In Vitro* Release and Activity Measurements

Devices were affixed to the bottom of 6-well polystyrene tissue culture plates using 9144 Masking Tape, and four milliliters of phosphate buffered saline (PBS, Roche, pH~7.4) were added to each well. The plates were agitated on a Thermolyne Rotomix Type 50800 orbital shaker at 60 rpm and 25°C. Once daily, a 200 μL aliquot of the release medium from each was pipetted into a 7-mL glass scintillation vial, and 200 μL of fresh PBS were added to each well to keep the volume of release medium in the wells constant at approximately four milliliters. Five mL of Fisher Scientific ScintiSafe Plus 50% scintillation cocktail were added to each scintillation vial. The samples were analyzed on a Packard Tri-Carb liquid scintillation counter, Model U2200, using a ^{3}H counting protocol. Detection of ^{3}H above background levels was assumed to be indicative of the opening of a reservoir membrane (release of ^{3}H-heparin from a reservoir). The amount of therapeutic heparin was quantitated using a Sigma Diagnostics ACCUCOLOR™ heparin kit after a reservoir release was detected. Heparin standard dilutions of 0.1, 0.2, 0.4, and 0.8 USP/mL concentrations were prepared from a stock solution of unlabeled heparin in deionized milliQ water (8 USP/mL), and mixed with equal volumes of FBS prior to assay in 96 well plates. Aliquots of 100 μL of the media surrounding each device were mixed with equal volumes with FBS for performing the ACCUCOLOR™ assay on release samples. Optical density was measured on a spectrophotometer microplate reader (Dynatech MR5000 or Molecular Devices Spectramax 384 Plus) at 405 nm. A plot of measured optical density versus heparin concentration was obtained for the standard dilutions. A linear standard curve was assumed in the region of 0.1 to 0.8 USP/mL. Microsoft Excel LINEST function was used to calculate the slope (m) and intercept (A_0, the extrapolated value for the absorbance at 0 USP/mL concentration of heparin) using a least squares method. The concentration of heparin in the release samples, C, was then quantitated according to the following relation:

$$A_{405} = mC + A_0$$

Equation 8-a

where A_{405} = measured absorbance at 405 nm for a given sample. The standards and samples were analyzed in quadruplicate.

8.3 Results and Discussion

8.3.1 Device Fabrication

The thicknesses of the devices after polishing ranged from 516 to 534 μm, with corresponding reservoir openings ranging from 352 to 340 μm in diameter. Predicted membrane thicknesses were 153 to 154 μm, based on the volume of membrane polymer injected into each reservoir.

Each device had three reservoirs loaded with heparin, one sealed with a membrane made from **PLGA4.4**, one sealed with a membrane made from **PLGA11**, and one sealed with a membrane made from either **PLGA28** (three devices) or **PLGA64** (three devices). Prior release experiments (see Chapter 4) have shown that reservoirs having **PLGA28** and **PLGA64** membranes may show similar release times. **PLGA28** and **PLGA64** membranes were therefore used on separate devices in order to eliminate any uncertainty in correlating detection of released ^{3}H-heparin with the opening of a **PLGA28** or **PLGA64** membrane. Reservoirs were loaded with a combination of ^{3}H-heparin sodium salt (0.2924 mCi/mg) and unlabeled heparin sodium salt. Total loading was 24.78 nCi of ^{3}H-heparin and 8.79 USP heparin per device, accounting for 3.45% loss of activity on drying.

8.3.2 *In Vitro* Release

The objective of these release experiments was to determine the release profiles and characterize the biological activity of heparin *in vitro* from prototype microreservoir devices. The cumulative amounts of ^{3}H-heparin detected from the two sets of devices are shown in **Figure 8.1** and **Figure 8.2** below.

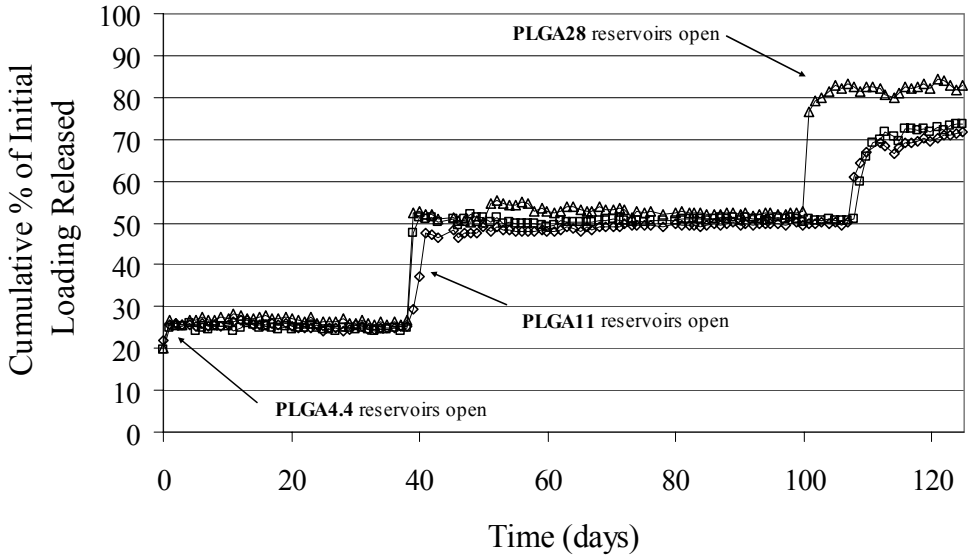

Figure 8.1 Cumulative percentage of ^{3}H-heparin loading released over time from three devices having **PLGA4.4**, **PLGA11**, and **PLGA28** reservoir membranes. Experiments conducted at 25°C.

For all six devices, the reservoirs having membranes fabricated from the **PLGA4.4** polymer uniformly released their contents within the first two days of the start of the experiment. Between 22 and 28% of the total initial loading was detected from these reservoirs. Similarly, the **PLGA11** reservoir membranes showed release between days 40 and 48 for all six devices, and the cumulative percentage of the initial loading detected ranged from 41 to 52% at day 50. The **PLGA28** reservoir membranes showed release between days 100 and 108 (**Figure 8.1**, 72 to 83% cumulative of total loading released at 125 days), while the **PLGA64** reservoir membranes showed onset of release between 132 and 139 days (**Figure 8.2**, a range of 68 to 77% cumulative of total initial loading released at 143 days).

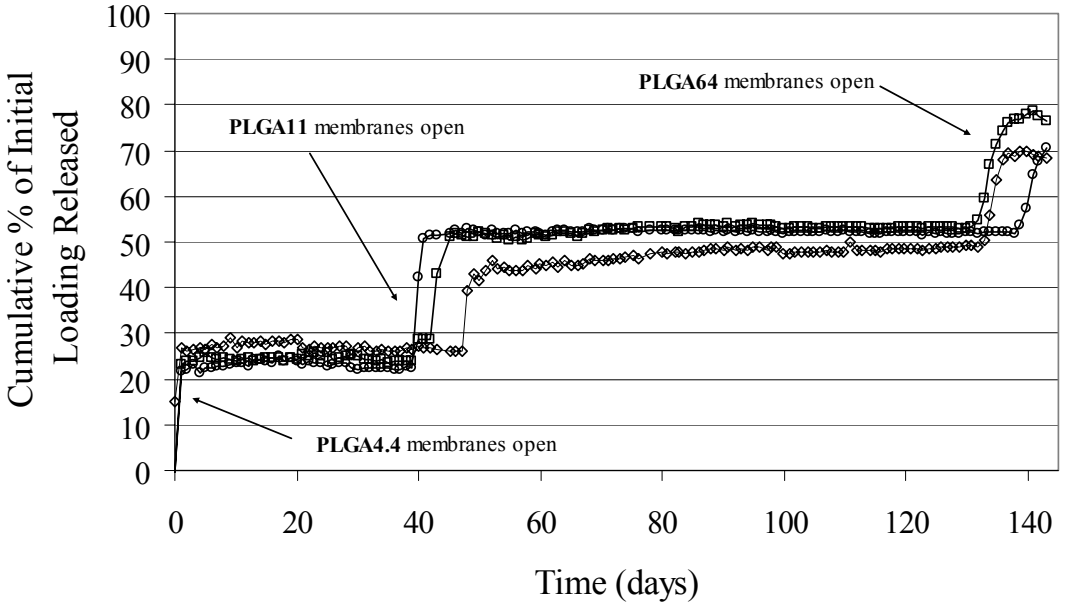

Figure 8.2 Cumulative percentage of ^{3}H-heparin loading released over time from three devices having **PLGA4.4**, **PLGA11**, and **PLGA64** reservoir membranes. Experiments conducted at 25°C.

The devices in each batch showed excellent agreement of release times, with each type of reservoir membrane opening within an 11-day window. Further, the devices appeared to release approximately equal pulses of heparin as each reservoir membrane opened, and there appeared to be no significant diffusional release of heparin from the reservoirs. This is in sharp contrast to the behavior typically seen with microspheres[6].

8.3.3 *In Vitro* Activity Measurements

The results of the heparin activity assays are summarized in **Table 8-1**, which shows the percentage of heparin that was present in the release media that still retained biological activity, including a correction for 3.45% loss of activity upon drying when the solution was loaded into the reservoirs. The activity assays indicated that essentially all of the heparin that was released from the reservoirs having **PLGA4.4** membranes was biologically active. Measured heparin activity was 105±16% of the material present in the PBS after opening of the **PLGA11** reservoirs. 80±30% of the heparin present in the PBS was active after the reservoirs having **PLGA28** membranes opened, while 96±20% of the heparin present in the PBS was active after the reservoirs having **PLGA64** membranes opened. A stock solution (8 USP/mL) was prepared

at the beginning of the experiment and stored at 4°C for the duration of the study as a control. The stock solution was assayed after 147 days and found to have retained 95% of its original activity.

Table 8-1 Measured biological activity of heparin released from polymeric microreservoir devices having reservoir membranes made from **PLGA4.4**, **PLGA11**, **PLGA28**, or **PLGA64**.

	PLGA4.4 reservoirs			PLGA11 reservoirs			PLGA28 reservoirs		
Device	**Release Day(s)**	**Assay Day(s)**	**Measured heparin activity, % of heparin present**	**Release Day(s)**	**Assay Day(s)**	**Measured heparin activity, % of heparin present**	**Release Day(s)**	**Assay Day(s)**	**Measured heparin activity, % of heparin present**
040202-05	0	0	***106***	41-43	43	***114***	107	109	***60***
040202-07	0	0	***105***	41	41	***107***	108	109	***65***
040202-08	0	0	***96***	41	41	***107***	100	102	***114***
	PLGA4.4 reservoirs			**PLGA11 reservoirs**			**PLGA64 reservoirs**		
040302-04	1	0	***NA***	43	43	***129***	132-136	136	***110***
040302-06	1	0	***NA***	40-41	41	***85***	139-143	142	***73***
040302-07	0	0	***151***	48-52	49	***91***	133-136	136	***106***

The relatively long-term stability of heparin seen in these experiments agrees with findings by other authors[7]. Stability studies of heparin at 30°C in 0.1 N hydrochloric acid and 0.1 N sodium hydroxide showed a decrease in the molecular weight of the heparin chains over time, as well as β-elimination of uronic acid residues in basic conditions, and desulfation in acidic conditions. At neutral pH (7.0) and elevated temperature (100°C) in these studies, however, the heparin remained stable over approximately 500 hours (21 days), retaining 80–90% of its activity as measured by anti-Factor XA (the same method as was used in the studies reported here) and anti-Factor IIA amidolytic methods. However, the measured activity showed an extremely large drop at 1000 hours to just ~6% of the initial activity. While the conditions of our release studies were much milder than the conditions in the reported study, it is expected that the pH decreased at least slightly over time as the PLGA membranes degraded and released their acidic degradation products into the PBS. The fact that the heparin retained its activity over an extended period of time suggests that the pH change was not significant enough to cause the desulfation and loss of activity seen by others.

8.4 Conclusions

Microreservoir devices fabricated from PLA demonstrated release of heparin in three separate pulses over a period of 108 days for devices having **PLGA4.4**, **PLGA11**, and **PLGA28** membranes, and over a period of 143 days for devices having **PLGA4.4**, **PLGA11**, and **PLGA64** membranes. Further, the heparin retained an average of 80 % of its activity over 102 to 109 days for devices having **PLGA28** membranes, and an average of 96 % of its activity over

136 to 142 days for devices having **PLGA64** membranes. The conditions to which the heparin was exposed during the course of the study were not severe enough to cause uniform or complete loss of activity, as exhibited by the retention of biological activity through an anti-Factor XA assay.

8.5 References

1. S. Gillis, M. M. Ferm, W. Ou, and K. A. Smith, "T-cell growth factor: parameters of production and a quantitative microassay for activity," *J. Immunol.* 120 (1978) 2027–2032.

2. J. Watson, "Continuous proliferation of murine antigen-specific helper T-lymphocytes in culture," *J. Exp. Med.* 150 (1979) 1510–1519.

3. M. S. Hora, R. K. Rana, J. H. Nunberg, T. R. Tice, R. M. Gilley, and M. E. Hudson, "Controlled release of interleukin-2 from biodegradable microspheres," *Biotechnology* 8 (1990) 755–758.

4. PerkinElmer Life Sciences Technical Data Certificate of Analysis, "NEX229 [^{125}I]-Interleukin-2, (human, recombinant) [^{125}I]-rIl-2."

5. Sigma Diagnostics HEPARIN procedure No. CRS106, Revised 2001-03.

6. M. R. Kreitz, J. A. Domm, and E. Mathiowitz, "Controlled delivery of therapeutics from microporous membranes. II. *In vitro* degradation and release of heparin-loaded poly(D,L-lactide-co-glycolide)," *Biomaterials* 18 (1997) 1645–1651.

7. K. A. Jandik, D. Kruep, M. Cartier, and R. J. Linhardt, "Accelerated stability studies of heparin," *J. Pharm. Sci.* 85 (1996) 45–51.

9 *In Vivo* Release Studies

9.1 Introduction and Motivation

Although a number of polymeric drug-delivery implants have been designed and tested *in vitro*, reproducible performance *in vitro* is rarely a guarantee of *in vivo* operation. Several factors may contribute to the variable performance of drug-delivery implants *in vivo*, including (in the case of PLA, PGA, and their copolymers) their hydrolysis rate and degradation by biological entities such as enzymes that are not present during *in vitro* studies. Additionally, devices that are implanted for periods longer than a few weeks begin to be encapsulated by fibrous tissue. Different drug delivery behavior from a device may therefore be observed *in vivo* compared to *in vitro*, depending on the release kinetics of the device and the permeation or diffusion of the drug through the local tissue. Proof-of-principle studies of the release of a model radiolabeled molecule (^{14}C-mannitol) were therefore performed *in vivo* in order to confirm our *in vitro* results, and to demonstrate that the polymeric microreservoir devices could be used for multipulse *in vivo* drug delivery.

9.2 Materials and Methods

9.2.1 Materials

Poly(L-lactic acid) (**PLA**, M_w 194 Kilodaltons (Kd), Medisorb® 100 L) and poly(D,L-lactic-*co*-glycolic acid) polymer powders of molecular weights (M_w) 11 Kd (**PLGA11**, Medisorb® 5050 DL 2A) and 64 Kd (**PLGA64**, Medisorb® 5050 DL 4A) were obtained from Alkermes (Cincinnati, Ohio). 1,1,1,3,3,3-hexafluoroisopropanol (HFIP) was purchased from Sigma-Aldrich (St. Louis, MO). ^{14}C-mannitol was purchased from PerkinElmer Life Sciences (Boston, MA). ScintiSafe Plus 50% was purchased from Fisher Scientific (Suwanee, GA). Ideal 9144 Masking Tape was obtained from American Biltrite, Inc. (Lowell, MA).

9.2.2 Methods

9.2.2.1 Device Fabrication

Eight devices were fabricated and loaded with chemicals as described in Chapters 2 and 3. Device thicknesses ranged from 649 to 692 μm, with corresponding reservoir openings of 255–224 μm in diameter. Reservoir membranes were fabricated from approximately 12% by volume solutions of **PLGA11** and **PLGA64** in HFIP. Solutions were injected from a 1710RN 100 μL gas tight glass syringe with a 1" 31 gauge removable needle, blunt tip (part numbers 81030 and 0160831, both items from Hamilton Co., Reno, NV). Predicted membrane thicknesses were 150 μm for all devices. On each device, one reservoir having a **PLGA11** membrane and one reservoir having a **PLGA64** membrane were loaded with 0.1 μCi of ^{14}C-mannitol, for a total device loading of 0.2 μCi. Devices were sealed with 9144 Masking Tape and affixed to glass slides for stability for *in vitro* release studies. Devices were sealed with 9144 masking tape but not affixed to slides for *in vivo* release studies.

9.2.2.2 *In Vitro* ^{14}C-Mannitol Control Release Study

Devices were put in screw-cap jars containing 20 mL stirred 1X phosphate-buffered saline (PBS) at 37°C after drying and sealing. One mL samples of the medium were pipetted from the jars once per day, and fresh PBS was added to the release vessels to replace the volume of solution removed. Samples were pipetted into 7-mL glass scintillation vials, and five mL of Fisher Scientific ScintiSafe Plus 50% scintillation cocktail were added to each vial. The samples were analyzed on a Packard Tri-Carb liquid scintillation counter, Model U2200, using a ^{14}C counting protocol to monitor for release of ^{14}C-mannitol from the devices.

9.2.2.3 *In Vivo* ^{14}C-Mannitol Release Study

Female Fischer 344 rats weighing 150–175 g were obtained from Charles River (Wilmington, MA). Their water was supplemented with sucrose at a concentration of 15g/500ml Baltimore city water. Animals were housed individually in metabolic cages (Nalgene, Rochester, NY; Model #650-0100 for rats 150–300 g). Animals were allowed free access to rodent chow and were treated in accordance with the policies and principles of laboratory care of the Johns Hopkins University School of Medicine Animal Care and Use Committee.

Prior to flank implantation, microreservoir devices were sterilized using a Mark1-68 irradiator (JLS Shepherd, Glendale, CA) with a Cesium-137 source. Chips were sealed in autoclave bags and then exposed for 12 minutes to the source to equal a final gamma radiation dose of 48,000 Rad or 480 Gray. Upon flank implantation, devices were removed in a sterile fashion from the sealed bags and placed onto a sterile field.

Twenty-four hours prior to flank implantation, rats were weighed and placed individually into metabolic cages. The following day their urine and feces were removed from the collection vials to obtain a baseline radioactive count for each animal. Rats were then anesthetized with an intraperitoneal injection of 5mL/kg solution containing 25mg/mL ketamine/2.5 mg/mL xylazine and 14.25% ethanol (v/v). The left flank of the anesthetized rat was shaved and prepped with 70% ethanol and betadine. Under sterile conditions (sterile gloves, gowns, masks, sterile instruments and sterile fields), a 2-cm vertical incision was made in the flank. To accommodate the microreservoir device, a pocket was made by dissecting the subcutaneous tissue with sterile scissors. The sterilized device was then placed into the pocket and the incision was closed with staples. Animals then received a subcutaneous injection of the analgesic, buprenorphine, at 0.01 mg/kg, and were placed back into their metabolic cages. Cages were returned to the animal care facility once animals were fully alert and demonstrating no complications from the procedure. Urine and feces were collected from the cages and collection vials were rinsed clean daily to avoid any day to day contamination.

Control animals were weighed and caged individually in metabolic cages prior to flank injection to obtain baseline feces and urine radioactive counts. For flank injection, the animals were anesthetized and left flanks were shaved and prepped. The appropriate concentration of ^{14}C-mannitol was then injected subcutaneously in a 0.3 mL aliquot. Animals were returned in their cages to the central animal housing facility after they were fully alert. Urine and feces samples were removed periodically and counted for radioactivity.

Urine and feces samples were counted for radioactivity using Ready Safe scintillation fluid (Beckman Coulter, Inc, Fullerton, CA). A 250 μL urine sample was placed into a 7-mL scintillation vial, along with one mL of distilled water and five mL of scintillation fluid. Fecal samples were placed directly into five mL of scintillation fluid and counted. Each sample was counted using a Beckman LS3801 scintillation counter (Beckman Coulter, Fullerton, CA) for a

duration of two minutes. The conversion factor used was disintegrations per minute (dpm) = counts per minute (cpm)/.96 counting efficiency.

After experiments were concluded, all animals were euthanized by either CO_2 inhalation or a sodium pentabarbitol overdose (200 mg/kg, to effect). Microreservoir devices were removed for inspection.

9.3 Results and Discussion

The release results for the *in vitro* control devices having **PLGA11** and **PLGA64** membranes are shown in **Figure 9.1** below. The corresponding results for the *in vivo* release of ^{14}C-mannitol from devices are shown in **Figure 9.2** below.

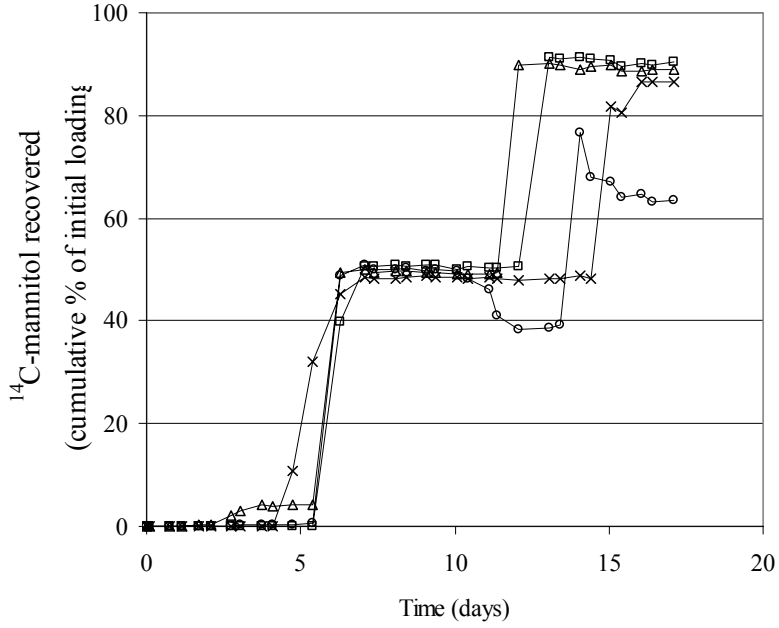

Figure 9.1 Cumulative percentage of initial ^{14}C-mannitol loading recovered over time from four devices having **PLGA11** and **PLGA64** reservoir membranes, each loaded with 0.2 μCi of ^{14}C-mannitol and maintained *in vitro* in PBS at 37°C.

Release of the ^{14}C-mannitol from devices *in vitro* was detected from the reservoirs having **PLGA11** membranes between five and six days, followed by release from the reservoirs having **PLGA64** membranes at 12 to 15 days. The total cumulative amount of ^{14}C-mannitol recovered ranged from 86 to 90%, excluding the device that showed a decrease in the cumulative amount of ^{14}C-mannitol over the course of the experiment (○ symbol in **Figure 9.1**). It is not clear why

this device showed different release behavior than the others, although it is possible that the mannitol could have been ingested by contaminant microorganisms (the devices were in saline solution at 37°C). The other three devices showed release of the ^{14}C-mannitol in two almost exactly equal pulses, and the range of release times for each type of membrane was relatively small, compared to release results previously presented in Chapter 4. Faster release was seen from these devices than for others at lower temperatures presented in Chapter 4.

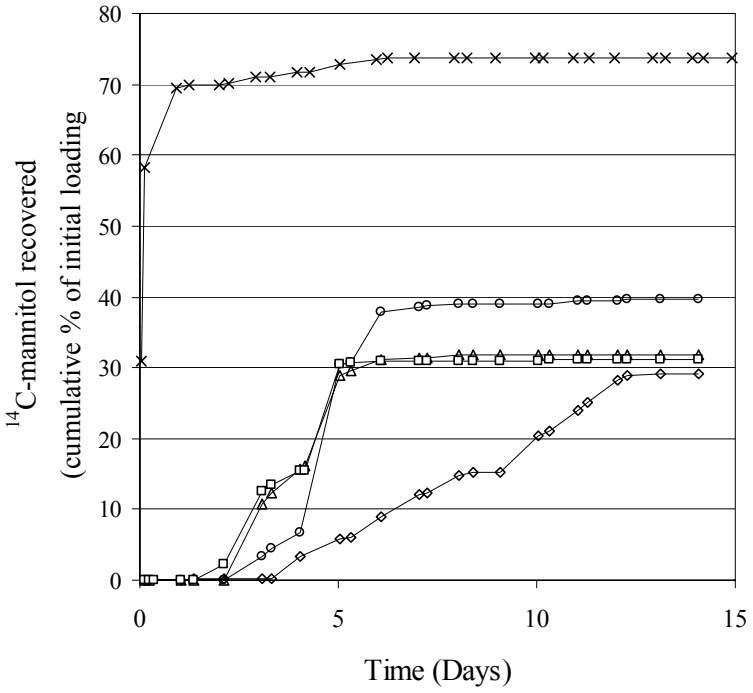

Figure 9.2 Cumulative percentage of initial ^{14}C-mannitol loading recovered over time from four devices (□△◇○) having **PLGA11** and **PLGA64** reservoir membranes, each loaded with 0.2 μCi of ^{14}C-mannitol and implanted subcutaneously in rats, and from one subcutaneous injection (×) of 0.1 μCi in a rat.

The observed release time *in vivo* of ^{14}C-mannitol from the reservoirs having **PLGA11** membranes ranged from two to four days, while the reservoirs having **PLGA64** membranes showed release between five and ten days. This was slightly greater variation than was seen for the devices *in vitro*. The release results for the devices implanted *in vivo* are similar to those for the *in vitro* devices, but the release times were faster. This is not surprising, as others have demonstrated more rapid release of chemicals from PLA[1,2] and PLGA[3] microspheres, as well as PLA and PLGA compression-molded implants[4] *in vivo* than *in vitro*. Additionally, the reader is referred to Chapter 10, in which a study to characterize the *in vivo* and *in vitro* degradation of

two of the membrane polymers showed in general faster degradation *in vivo* than *in vitro*. Although the *in vitro* release studies reported here were performed at 37°C in saline solution, this environment cannot reproduce the biological milieu to which the devices are exposed *in vivo* and which may contain other agents or molecules, such as enzymes, that aid polymer degradation. Another factor which may contribute to the observed faster release *in vivo* is the method by which the devices were sterilized (480 Gray γ-irradiation). Decreases in the molecular weight of PGA sutures as the γ-irradiation sterilization dosage is increased have been reported by others[5]. Although the dosage that was used to sterilize the microreservoir devices prior to implantation was much lower than the dosage at which the observed decreases in PGA suture molecular weight became significant, the very low initial molecular weight of the membrane polymers on the microreservoir devices may nevertheless be affected by the sterilization procedure. It is expected that increasing the molecular weight of the reservoir membrane materials would shift the release curves to later times. Replacing the **PLGA64** reservoir membrane with a higher molecular weight material might serve to more clearly separate the two pulses from a given device.

The recovered yield at 14 days post-implantation from the devices *in vivo* was 29–40% of the initial device loading. Approximately 74% of the injected control was recovered over the same time span. The higher recovery of the injected control is not surprising, as the ^{14}C-mannitol that is injected is in a volume of 0.3 mL, and forms a bolus with a large surface area from which it can diffuse away from the injection site. The microreservoir devices, in contrast, are loaded with ^{14}C-mannitol in solid form, which is located in a very small reservoir (120-130 nL in volume) and that has an opening of limited size (224–255 μm diameter reservoir openings) from which the mannitol can diffuse. These two factors could explain the low yield seen from the microreservoir devices *in vivo*.

The only report in the literature of *in vivo* drug delivery from a device similar to the one described here shows one pulse of Evans's blue dye from devices implanted subcutaneously in nude mice[4]. Comparative results obtained *in vitro* showed slower release than was observed *in vivo*, and neither quantitation of the amount of chemical released (% of initial loading released and/or detected) nor the duration of release *in vivo* were reported. In contrast, the results presented here from implanted polymeric microreservoir devices show release duration of two

days (with the exception of one device), and 29–40% of the loading detected over a span of two weeks.

9.4 Conclusions

The proof-of-principle studies reported here demonstrate the feasibility of delivering multiple pulses of drugs from the polymeric microreservoir devices *in vivo*. This has previously not been demonstrated by others. Further, even *in vitro* demonstration of multiple pulses from polymeric systems has typically required an applied stimulus (such as an electric field or ultrasound) or a change in the local environment (such as pH or temperature) in order to trigger drug release from the systems. Faster release was observed from devices implanted *in vivo* versus maintained *in vitro*, most likely due to enzymatic degradation and faster hydrolysis *in vivo*. Increasing the difference in molecular weights of the materials used for the reservoir membranes may therefore allow greater separation of the drug pulses from the device if so desired.

9.5 Acknowledgements

The *in vivo* release studies reported here were performed by Betty Tyler in the laboratory of Dr. Henry Brem, M.D., Department of Neurosurgery in the School of Medicine at Johns Hopkins University in Baltimore, MD.

9.6 References

1. C. Mallard, J. Coudane, I. Rault, and M. Vert, "The use of additives to modulate the release of a sparingly water soluble drug entrapped in PLA50 microparticles: *in vivo* investigation," *J. Microencapsulation* 17 (2000) 95–110.

2. C. Mallard, J. Coudane, I. Rault, and M. Vert, "*In vitro* delivery of a sparingly soluble compound from PLA50 microparticles," *J. Microencapsulation* 17 (2000) 13–28.

3. R. V. Diaz, I. Soriano, A. Delgado, M. Llabrés, and C. Evora, "Effect of surfactant agents on the release of ^{125}I-bovine calcitonin from PLGA microspheres: in vitro — in vivo study," J. Controlled Release 43 (1997) 59–64.

4. W. Vogelhuber, P. Rotunno, E. Magni, A. Gazzaniga, T. Spruß, G. Bernhardt, A. Buschauer, and A. Göpferich, "Programmable biodegradable implants," *J. Controlled Release* 73 (2001) 75–88.

5. D. K. Gilding and A. M. Reed, “Biodegradable polymers for use in surgery-polyglycolic/poly(lactic acid) homo- and copolymers:1,” *Polymer* 20 (1979) 1459–1464.

10 *In Vivo* Biodegradation of Reservoir Membrane Polymers

10.1 Introduction and Motivation

In previous chapters, we have demonstrated the feasibility of delivering multiple pulses of drugs from the polymeric microreservoir devices *in vitro* (Chapter 4) and *in vivo* (Chapter 9). It is of vital concern to understand the biocompatibility and/or biodegradation of the component materials of any implantable device when considering end-stage use in a patient. The implant must tolerate long-term exposure to the physiological environment, without inducing toxicity in the surrounding tissues. While the component materials of our drug delivery device (PLA and PLGA) have been extensively studied in regard to both biodegradation and biocompatibility[1], the literature is often specific, especially in the case of PLGA, to a particular molecular weight polymer, certain *in vitro* degradation conditions, a specific copolymer ratio[2,3], or even the size of the specimens studied[4–7]. Thus, it is important to study the biodegradation and biocompatibility of the specific materials used in our drug delivery device.

With the goal of understanding how the component materials of our device will degrade *in vivo*, we have investigated the biodegradation of two of the membrane materials (**PLGA4.4** and **PLGA64**) in a rat model. The biodegradation of the materials of interest was characterized by gel permeation chromatography (GPC) as well as differential scanning calorimetry (DSC). Both methods are commonly used to characterize the degradation of polymers. GPC provides molecular weight data, while DSC provides information about the glass transition and melting temperatures of a material, which can be correlated with both the molecular weight and degree of crystallinity of a polymer. Understanding the difference between material degradation behaviors *in vivo* versus *in vitro* is an important step in the development of a viable, long-term implantable drug delivery device.

10.2 Materials and Methods

10.2.1 Materials

Poly(L-lactic acid) (**PLA**, M_w 194 Kilodaltons (Kd), Medisorb® 100 L), poly(glycolic acid) (**PGA**, Medisorb® 100 PGA) and poly(D,L-lactic-*co*-glycolic acid) polymer powders

(50:50 mole ratio of lactic acid to glycolic acid units) of molecular weights (M_w) 4.4 Kd (**PLGA4.4**, Medisorb® 5050 DL 1A) and 64 Kd (**PLGA64**, Medisorb® 5050 DL 4A) were obtained from Alkermes (Cincinnati, Ohio). 1,1,1,3,3,3-hexafluoro-2-propanol (HFIP) was purchased from Sigma-Aldrich (St. Louis, MO). Mylar® sheets were donated from the laboratory of Dr. James Anderson (Case Western Reserve University, Cleveland, OH). Poly(methyl methacrylate) (PMMA) standards were obtained from Polysciences, Inc. (Warrington, PA).

10.2.2 Methods

10.2.2.1 Film Casting

Mylar® sheets were cleaned with Kimwipes® and acetone. Solutions of **PLA**, **PLGA4.4**, **PLGA64** (9 to 15 percent by volume) and **PGA** (1.4 to 5.5, or 15 percent by volume) were prepared in HFIP. A large area of Mylar® film was marked off with six layers of VWR brand time tape. The amount of polymer that was used in preparing each film was calculated using the density of the polymers, the cast area, and the desired thickness. The solutions were cast onto the Mylar® sheets in a hood, let dry until the films were partially opaque, and then transferred to a vacuum oven. The films were dried under vacuum at approximately 27 in Hg (8 kPa) and 80°C for 48 hours. After cooling, the films were cut into 2 cm × 1.25 cm rectangles, and the backs of the films were cleaned with acetone again before implantation.

10.2.2.2 Cage Fabrication

Test specimens of Mylar® backing, and Mylar® backing with **PLA**, **PGA**, **PLGA4.4**, and **PLGA64** polymer films were placed singly into cylindrical stainless steel wire mesh cages measuring approximately 3.5 cm long and 1.0 cm in diameter. The mesh from which the cages were made was type 310 stainless steel with a mesh size of 24, a wire diameter of 0.254 mm (0.01 in), and interstices measuring 0.8 × 0.8 mm (Cleveland Wire Cloth and Manufacturing Co, Cleveland, OH). Prior to cage fabrication, the mesh was sonicated in ethanol (Pharmaco Products Inc., Brookfield, CT) for 15 minutes, followed by a 10-minute rinse with distilled water. The material test specimens were ethylene oxide sterilized (Amsco model 2057 sterilizer, University

Hospitals of Cleveland, OH) using an exposure time of 1 hour and 45 minutes at 130°F and an outgassing time of 12 hours at 120°F prior to placement in the cages.

10.2.2.3 Film Implantation

10.2.2.3.1 Subcutaneous Cage Implant

Sterilized cages containing polymer films were implanted subcutaneously and bilaterally in the posterior back areas of 12 week old female Sprague-Dawley rats (Charles Rivers Laboratories, North Wilmington, MA), according to a previously published procedure[8] and observing IACUC and NIH animal care guidelines. Aerrane® (Baxter, Deerfield, IL) was used in a continuous analgesic stream to keep the animals unconscious during implantation. The rats were shaved and their skin scrubbed with surgical grade Betadine® (The Purdue Frederick Co., Stamford, CT). An incision 1.0 to 1.5 cm long was made in the skin about 2 cm above the tail and along the midline. Then, 0.5% Marcaine® solution (Abbott Laboratories, North Chicago, IL), a local anesthetic, was applied onto the incision to minimize post-operative discomfort. Blunt dissection was used to prepare an implant pocket in the facial plane beneath the panniculus carnosus muscle from the underlying tissue from the incision to just above the hip. The sterile cage containing the material was then introduced through the incision and positioned within the pocket and away from the incision site. The incision was closed with 9 mm stainless steel surgical wound clips (Becton Dickinson, Sparks, MD) and washed with Betadine®. Sterile surgical techniques were observed. In addition, empty cages were gas sterilized and implanted into a separate group of animals as controls. The rats were maintained on Purina Rat Chow and water *ad libitum* at the Animal Research Facilities of Case Western Reserve University on 12 hours light/dark cycles. All animals were sacrificed at day 21.

10.2.2.3.2 Direct Subcutaneous Implant

Polymer films and Mylar® controls were ethylene oxide sterilized and implanted without cages following the procedure described above, with one additional precaution. The size of the subcutaneous pocket was such that it would accommodate the film comfortably but not loosely. This precaution was taken in an attempt to minimize inflammatory response at the tissue-

material interface that could have resulted from the movement of the device within the pocket. Animals (n = 3) were sacrificed at 4, 7, 14, 21, 28, 35, 42, and 49 days.

10.2.2.3.3 In Vitro Controls

Samples of **PLA**, **PGA**, **PLGA4.4**, and **PLGA64** (n = 3) were placed in tissue culture polystyrene (TCPS) petri dishes (Becton Dickinson, Sparks, MD). Phosphate Buffer Saline (PBS) without Ca^{2+} and Mg^{2+} (Gibco Laboratories, Grand Island, NY) was added such that the films were completely submerged. The submerged films were maintained in a humidified atmosphere at 37°C (95% CO_2, 5% O_2) for 4, 7, 14, 21, 28, 35, 42, or 49 days.

10.2.2.4 Gel Permeation Chromatography (GPC)

After explantation and/or drying, one half of each polymer film (*in vivo* direct subcutaneous, *in vivo* cage, or *in vitro* control) was carefully removed from the Mylar® backing using a spatula and tweezers. The polymer residues were placed in 7-mL glass scintillation vials (VWR International, NJ) and one milliliter of HFIP was added to each vial using B-D 1 mL syringes. The vials were capped, wrapped with ParaFilm M® to prevent solvent evaporation, and left for approximately 24 to 48 hours to allow dissolution of the polymers. The vials were periodically agitated on a vortexer to aid polymer dissolution. Control samples of Mylar® and the **PGA**, **PLA**, **PLGA4.4**, and **PLGA64** powders (previously stored at –4°C in an airtight container with desiccant since receipt from the manufacturer) were prepared in a similar manner. In addition, samples of fibrous capsule retrieved from 42 day old implants of **PLA** and **PLGA4.4** were dissolved in HFIP using 7-mL glass vials. Tissue samples were left to dissolve for approximately five hours before GPC analysis was performed. The **PLA** and **PLGA4.4** polymer films from these tissue sections were prepared in the same manner as the Mylar® and other polymer samples. One sample of HFIP only, with no polymer in it, was prepared by letting it stand in a 1 mL B-D syringe for one minute.

After dissolution, all polymer solutions were transferred to 1-mL glass GPC vials (Waters Corporation, Milford, MA) using 1-mL B-D syringes and PTFE Minispike 0.2 μm syringe filters (Waters Corporation). The samples were analyzed in HFIP at 0.2 mL/min flow rate for either 40 or 45 minutes on a Waters GPC system consisting of a 515 HPLC Pump, 717_{plus} Autosampler, Styragel Guard Column, Styragel HR 4 and HR 3 columns, and 2410 refractive index detector.

Sample molecular weights were quantitated relative to PMMA standards of molecular weights 150,000, 125,000, 100,000, 75,000, 60,000, 30,000, 14,000, and 6,000 daltons. Data was analyzed using Millenium v.3.20 software.

10.2.2.5 Differential Scanning Calorimetry (DSC)

A 0.5 × 1.25 cm^2 strip was cut off of each film using tweezers and scissors. This strip was cut into three squares, which were placed in the bottom of a 50 μL aluminum DSC pan (PerkinElmer, Shelton, CT) with the polymer side facing the bottom of the pan (Mylar® side facing the lid), in order to provide optimal thermal contact of the polymer with the pan. A PerkinElmer universal crimper press was used to seal the pans with aluminum lids. Samples were analyzed on a PerkinElmer Diamond DSC with autosampler AS-6. Dry nitrogen was used as a purge gas. Pyris Manager version 5.0 was used to program and monitor the DSC and analyze data. **PLA** samples were heated to an upper temperature limit of 200°C in order to capture both the melting (T_m, results not reported here) and glass (T_g) transition temperatures, while the **PGA**, **PLGA4.4**, and **PLGA64** samples were heated to an upper temperature limit of 100°C. The experimental parameters (temperature limits and heating rates) are summarized in **Table 10-1.** Each sample was heated and cooled twice. The reported data are the T_g values obtained on the second heating cycle, after erasing the thermal history of and any irreversible effects present in each polymer film.

Table 10-1 Summary of experimental parameters for DSC analysis of polymer film samples degraded *in vitro* and *in vivo*.

Material	Sample Group	Lower Limit (°C)	Upper Limit (°C)	Number of Cycles	Isothermal Hold @ each endpoint	Rate
PLA	*in vitro*	-20	200	2	3 minutes	20°C/min
	in vivo	-65	200	2	3 minutes	20°C/min
PGA	*in vitro*	-20	100	2	3 minutes	20°C/min
	in vivo	-65	100	2	3 minutes	20°C/min
PLGA4.4	*in vitro*	-65	100	2	3 minutes	20°C/min
	in vivo	-65	100	2	3 minutes	20°C/min
PLGA64	*in vitro*	-65	100	2	3 minutes	20°C/min
	in vivo	-65	100	2	3 minutes	20°C/min

10.3 Results and Discussion

10.3.1 Film Casting

Several batches of films were made from each material. A Fowler micrometer was used to measure the thicknesses of the Mylar® substrates with cast polymer films, from which the thickness of the Mylar® substrate was subtracted in order to determine the thicknesses of the polymer films. The **PLA** films that were used were 67 μm thick, while the **PGA** films ranged in thickness from 76 to 133 μm, the **PLGA4.4** from 68 to 83 μm, and the **PLGA64** from 57 to 78 μm. The **PLA**, **PLGA4.4**, and **PLGA64** films were colorless and translucent in nature and adhered well to the Mylar® substrate. The **PGA** films, however, were white and opaque, and easily flaked off of the Mylar® substrate. The **PLGA4.4** film was slightly tacky at room temperature, due to the low T_g of this material (31.4°C reported by the manufacturer), while the other films were non-sticky.

10.3.2 Gel Permeation Chromatography (GPC)

Molecular weight results are shown in **Figure 10.1** to **Figure 10.4**. The dashed line on each graph indicates the average molecular weight measured for the powder standards of each polymer. Day zero cage and subcutaneous samples were unimplanted films taken from the same batches as those used for the cage and direct subcutaneous implants. The GPC software typically reports M_n (number average molecular weight), M_w (weight average molecular weight), and MP (the molecular weight corresponding to the maximum peak height) for a given peak. **Figure 10.1** to **Figure 10.4** show MP results.

The molecular weights reported by the software are not absolute values, but rather relative to the PMMA standards. Polyesters are typically analyzed in chloroform with polystyrene standards when performing GPC analysis. However, the insolubility of **PGA** in chloroform necessitated the use of 1,1,1,3,3,3-hexafluoro-2-propanol (HFIP) as a solvent for GPC analysis in this study. This solvent was used for GPC analysis of all the materials for experimental consistency. Although we used PMMA standards, which are used commercially in GPC analysis of polyesters in HFIP, we found that polyester samples analyzed in HFIP with PMMA standards yielded different molecular weight data than those run in chloroform using

polystyrene standards. Additionally, there was variation in the molecular weight values obtained for powder control samples that were run in different sample batches. Therefore, a correction factor was determined based on the molecular weight values obtained for powder controls in chloroform ($CHCl_3$) and HFIP. This correction factor was then applied to the molecular weight values obtained for the rest of the samples in a given batch. This allowed comparison of the experimentally obtained molecular weight values with the data reported by the manufacturer for the various polyester materials used in this study. The results and correction factors are summarized in the below. The molecular weight values reported in the text below for the **PLGA4.4**, **PLGA64**, and **PLA** samples have been corrected using the factors listed in **Table 10-2** below.

Table 10-2 Correction factors used in GPC calculations of molecular weight for **PLGA4.4**, **PLGA64**, **PLA**, and **PGA** samples.

Polymer	Manufacturer specified M_w (in $CHCl_3$)	Average M_w (in HFIP)	Average M_w (in $CHCl_3$)	Correction Factor $(M_{w,HFIP})/(M_{w,CHCl3})$
PLGA4.4	4,400	7,067/7,775	3,523	*2.006 or 2.207*
PLGA64	64,000	121,840/89,789/67,003	71,897	*1.69 or 1.249 or 0.93*
PLA (unpurified) (used for films)	194,000	120,881	NA	*0.623*
PLA (purified) (used for powder controls)	NA	143,757	303,760	*0.473*
PGA	Not characterized	143,950	NA	*NA*

10.3.2.1 Mylar® and HFIP

Mylar® control samples (results not shown) typically produced three peaks on the GPC chromatograms, at approximately 32,000 to 45,000, 2,000 to 2,500, and 800 daltons.

The sample of HFIP only (no polymer) showed peaks on the chromatogram at 760 and 520 daltons. The presence of a peak at 750 or 800 daltons on both the Mylar® and HFIP chromatograms indicates that it is intrinsic to the GPC system, most likely due to residual solvent from previous batches that used a different mobile phase.

Based on the results of these samples, the peaks at 2,000–2,500, ~800, and ~500 daltons were disregarded for most of the polymer samples and are not reported here. Additionally, peaks in the range of 35,000–45,000 were typically disregarded as due to the Mylar® if the samples had little visible polymer remaining on the surface of the Mylar® substrate. **Figure 10.1** to **Figure 10.4**, which show the GPC results for the **PLA**, **PGA**, **PLGA4.4**, and **PLGA64**, include the data for the molecular weight corresponding to the peak with the largest area on the

chromatogram (the main peak), although the discussion below includes any additional peaks that were present.

10.3.2.2 Fibrous Capsule Tissue With Implants

The explanted tissue surrounding the **PLA** film implant showed a visible fibrous capsule, with vascularization localized over less than one-half the area of the **PLA** film. Some of the capsule tissue looked yellowish, possibly indicating scar formation. The tissue samples showed a main peak on the GPC chromatograms around 185,000 daltons, while the **PLA** film that was removed from the unfixed tissue showed a main peak at 117,000 daltons (results not shown).

The tissue surrounding the **PLGA4.4** film implant showed a visible fibrous capsule with a much greater degree of tissue vascularization than was seen in the tissue surrounding the **PLA** film. Blood vessels were distributed throughout most of the tissue that was in contact with the surface of the implanted film. The tissue sample showed a main peak on the GPC chromatograms at around 190,000 daltons, which was also evident for the **PLGA4.4** film sample that was removed from the unfixed tissue.

Based on these results, peaks with a molecular weight of 190,000 or greater were typically disregarded from sample chromatograms as being due to biological material on the surface of the films. Exceptions will be noted below.

10.3.2.3 **PLA**

The GPC results for the **PLA** samples are shown in **Figure 10.1**. The **PLA** powder control samples had a main peak of ~290,000 (dashed line in **Figure 10.1**) and a secondary peak at ~10,000 daltons. The **PLA** cage control film samples (day zero cage samples) had a main peak of ~207,000, a 29% drop in molecular weight compared to the powder control, and secondary peaks at ~12,000 and 3,000–5,000 daltons. The **PLA** subcutaneous control film samples (day zero subcutaneous samples in **Figure 10.1**) showed a main peak at an average molecular weight of 166,000, a 43% drop in molecular weight compared to the powder control. A shoulder was also evident at 5,000–12,000 daltons.

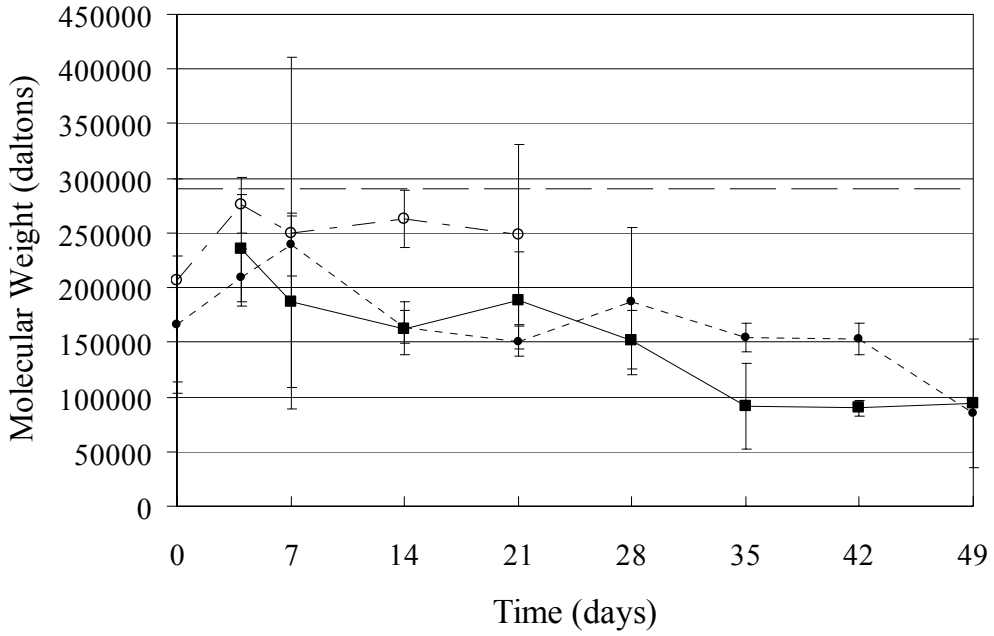

Figure 10.1 Measured peak molecular weight for **PLA** samples: - - - powder control samples, ■ *in vitro* samples, ● *in vivo* direct subcutaneous implants, ○ *in vivo* cage implants.

The **PLA** cage samples (○ in Figure 10.1) typically showed four peaks on the GPC chromatograms over the course of the study. The main peak was at approximately 147,000–435,000 daltons, with shoulder peaks at 25,000–30,000 and occasionally at 12,000–13,000 daltons. This high molecular weight main peak for the cage samples was disregarded as due to tissue or other biological material for one of the day seven samples, but the peak on the remaining samples chromatograms showed a trend of slightly decreasing molecular weight over time. Additionally, the day 42 **PLA** film sample that was removed from unfixed tissue (section 10.3.2.2) did not show a peak similar in molecular weight to that observed for the fibrous capsule tissue samples. This suggests that deposition of biological material in the surface of the **PLA** films was less pronounced than, for example, the **PLGA4.4** films, which will be discussed below. The shoulder peaks at approximately 25,000–30,000 and 12,000–13,000 daltons increased in size over time.

The **PLA** subcutaneous samples (● in **Figure 10.1**) showed a main peak that ranged in molecular weight over the course of the study from 270,000 down to 85,000 daltons, with a shoulder at 12,000–13,000 and a shoulder peak at 27,000 on one of the day seven explanted

samples. The high molecular weight peak at earlier time points seemed indicative of the decreasing molecular weight of the **PLA**. Two of the day 49 samples showed atypical results, having a main peak around the same molecular weight as that seen for Mylar®, as well as a secondary peak around 506,000–585,000 daltons. These very high molecular weight peaks at day 49 were disregarded as due to biological material on the surface of these two samples. These day 49 subcutaneous samples that showed atypical chromatograms were observed to have a much thinner layer of material on the Mylar® than the other subcutaneous **PLA** samples. It is possible that this material was actually deposited biological debris (material) which would be consistent with the observed ~500k dalton GPC peaks, rather than **PLA** remaining on the surface of the Mylar®.

The *in vitro* samples appeared to undergo degradation similar to that seen for the subcutaneous samples. The *in vitro* **PLA** samples (■ in **Figure 10.1**) showed one large main peak on the chromatograms, which ranged in molecular weight from 270,000 at day 4 down to 36,000 at day 49. This main peak showed a large variation in molecular weight for the day 49 samples.

10.3.2.4 **PGA**

The GPC results for the main peaks of the **PGA** samples are shown in **Figure 10.2** below. The **PGA** powder control samples had a main peak with an average molecular weight of ~155,000 (dashed line in **Figure 10.2**). A smaller peak was evident with a molecular weight ranging from 10,000 to 17,000 daltons (data not shown).

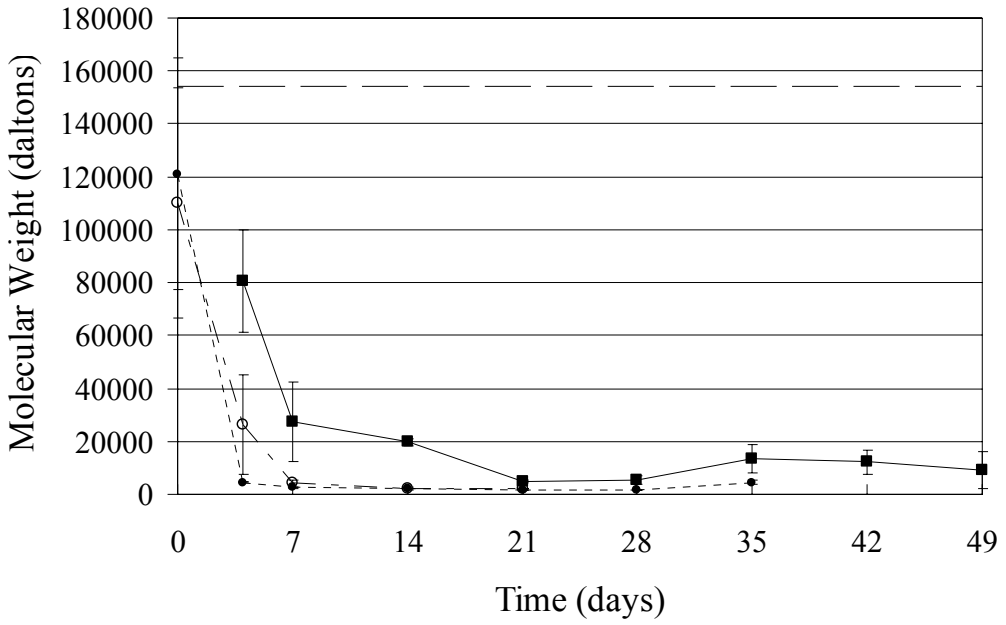

Figure 10.2 Measured peak molecular weight for **PGA** samples: - - - powder control samples, ■ *in vitro* samples, ● *in vivo* direct subcutaneous implants, ○ *in vivo* cage implants.

The **PGA** cage control film samples (day zero cage samples) had a main peak on the GPC chromatograms that had an average molecular weight of ~110,000, a 29% decrease in the molecular weight compared to the powder controls. Secondary peaks were also visible with molecular weights ranging from 5,000–12,000 and 14,000–19,000 daltons. The **PGA** subcutaneous control film samples (day zero subcutaneous samples in **Figure 10.2**) had a main peak with an average molecular weight of ~121,000 daltons (22% decrease in molecular weight from that of the powder control) and two smaller peaks with molecular weights ranging from 5,300–7,200 and 12,000–19,000 daltons (data not included in **Figure 10.2**).

The **PGA** cage samples (○ in **Figure 10.2**) typically showed three peaks on the GPC chromatograms. There was a large peak at approximately 350,000–400,000 daltons (which increased in molecular weight over time), two other peaks at around 38,000 and 2,000–6,000, and a shoulder at 10,000. The largest peak for two of the day 4 samples was at 38,000, while for the rest of the samples the main peak occurred at a molecular weight of 5,000 or less.

The **PGA** subcutaneous samples (● in **Figure 10.2**) for days 4, 7, 14, and 21 typically exhibited three peaks on the GPC chromatograms, similar to the cage samples. The main peak

was at approximately 5,000 daltons, with smaller peaks at ~40,000–55,000 and ~400,000 daltons, and a shoulder at 8,000–13,000 daltons. The ~40,000–55,000 peak and 8,000–13,000 shoulder decreased in size over time relative to the other peaks, while the ~5,000 peak increased in size relative to the other peaks. The chromatograms for the day 28 samples showed atypical shapes, with a main peak around 200,000 daltons and a secondary peak at ~1,400 daltons. The day 28, 35, 42, and 49 film samples were very different in appearance from the rest of the **PGA** subcutaneous samples. No white polymer was visible on the surface of the Mylar®, but a very thin, transparent film was present. These samples showed similar chromatogram peaks to the day 4, 7, 14, and 21 samples. The 400,000 dalton peak was larger in area than the 50,000 molecular weight peak for the day 35 samples, but decreased in size relative to the 50,000 peak for the day 42 and 49 samples.

A ~400,000 peak was seen on the chromatograms for nearly all of the *in vivo* **PGA** samples, but was absent from the **PGA** powder control and film control chromatograms. This peak is similar to that seen in the tissue samples, as well as the **PLGA4.4** *in vivo* and **PLGA64** direct subcutaneous samples that are discussed below.

The **PGA** *in vitro* samples (■ in **Figure 10.2**) typically showed three peaks on the GPC chromatograms, around 63,000–101,000, 17,000–25,000, and 6,000–9,000 daltons. The two highest molecular weight peaks showed a decrease in molecular weight and peak area over time. The 6,000–9,000 peak did not show a large decrease in molecular weight over the 49 days, but the peak area increased relative to the higher molecular weight peaks until this 6,000–9,000 molecular weight peak became the main peak (peak having the largest area) on the chromatograms. This is reflected by the large drop in molecular weight between days 4 and 49 shown in **Figure 10.2** for the *in vitro* **PGA** samples.

10.3.2.5 **PLGA4.4**

The GPC results for the **PLGA4.4** samples are shown in **Figure 10.3** below. The **PLGA4.4** powder controls (dashed line in **Figure 10.3**) showed a main peak on the GPC chromatograms at approximately 3,500 daltons. One batch of powder controls showed a shoulder at 18,000 to 19,000 daltons (data not shown).

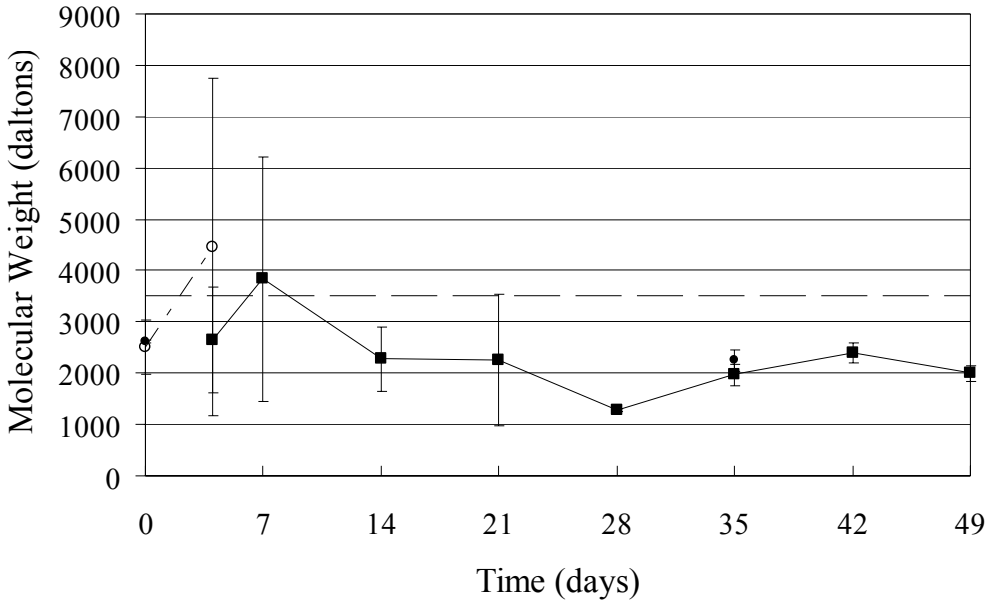

Figure 10.3 Measured peak molecular weight for **PLGA4.4** samples: - - - powder control samples, ■ *in vitro* samples, ● *in vivo* direct subcutaneous implants, ○ *in vivo* cage implants.

The **PLGA4.4** cage control film samples (day zero cage samples in **Figure 10.3**) had a main peak at approximately 2,500 daltons (a 29% decrease in molecular weight compared to the powder controls) with a shoulder at 18,000 daltons. The **PLGA4.4** subcutaneous control film samples (day zero subcutaneous samples in **Figure 10.3**) had a main peak on the chromatograms at an average molecular weight of ~2,600 daltons, and a shoulder peak at ~18,000 daltons. The **PLGA4.4** cage samples (○ in **Figure 10.3**) typically showed only one large peak on the GPC chromatograms at ~200,000 daltons. However, this peak was disregarded as due to biological material and therefore is not plotted in **Figure 10.3**. Occasionally a small peak was seen around 2,000 to 3,000 daltons. The **PLGA4.4** subcutaneous samples (● in **Figure 10.3**) typically showed a peak on the GPC chromatograms at ~200,000 daltons. This peak was shown on all of the day 7, 14, 42, and 49 day samples, as well as some of the day 21 and 35 samples. Similar to the **PLGA4.4** cage samples, this peak was disregarded as due to biological material on the surface of the Mylar® substrate and therefore is not shown in **Figure 10.3**.

The **PLGA4.4** *in vitro* samples (■ in **Figure 10.3**) exhibited many different peaks on the chromatograms. In general, not all of the samples had either the same chromatogram shape (number of peaks) or all of the same peak locations (molecular weights). Additionally, some

shoulder peaks were difficult to resolve due to their small area. The chromatograms for the day four samples showed a main peak at 1,500 or 2,800 daltons, or a main double peak at 1,800 and 3,500 daltons. One sample had a shoulder at 1,100 daltons, while another sample had a shoulder at 4,800 daltons. Two of the day seven samples exhibited double main peaks at 5,200 and 1,700–2,200 daltons, while the third sample had a peak at 6,000 daltons and a larger peak at 1,100 daltons. Similarly, two of the day 14 samples had peaks at 5,000 to 6,000 and 1,700 to 2,000 daltons, while the third sample had a double main peak at 3,000 and 1,700 daltons. The chromatograms for the day 21 and 28 samples were more consistent, showing two main peaks at 3,600–4,000 daltons, and 2,100–2,600 daltons. The day 35, 42 and 49 samples were also consistent, and all showed small peaks at 1,800–2,600 daltons.

10.3.2.6 **PLGA64**

The GPC results for the **PLGA64** are shown in **Figure 10.4** below. The chromatograms for the **PLGA64** powder control (dashed line in **Figure 10.4**) showed a main peak at ~72,000 daltons with shoulder peaks at 4,000 and 8,000 daltons.

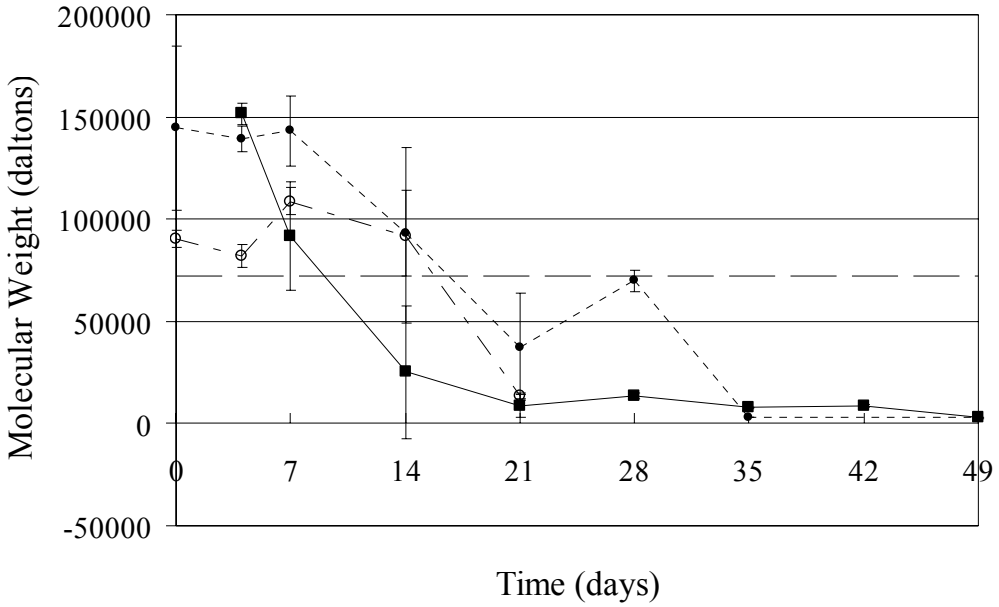

Figure 10.4 Measured peak molecular weight for **PLGA64** samples: - - - powder control samples, ■ *in vitro* samples, ● *in vivo* direct subcutaneous implants, ○ *in vivo* cage implants.

The chromatograms for the **PLGA64** cage control films (day zero cage samples in **Figure 10.4**) showed a main peak at around 90,000 daltons, with shoulders at around 14,000 and 4,500 daltons. This is a slight increase in the molecular weight of the main peak compared to the data obtained for the powder control.

The chromatograms for the **PLGA64** subcutaneous control films (day zero direct subcutaneous samples in **Figure 10.4**) showed a main peak at 135,000 daltons, with shoulders at 4,000–8,000 and 10,000–20,000 daltons. These control films also showed an increase in the molecular weight of the main peak compared to the powder controls.

The chromatograms for the **PLGA64** cage samples (○ in **Figure 10.4**) typically showed large peaks around 60,000–140,000 daltons with a shoulder at around 18,000 daltons. Two of the day 21 samples were tan or slightly reddish in color, and showed large peaks at 130,000–140,000 daltons. The **PLGA64** cage implants showed a trend of decreasing molecular weight over the course of the study.

The **PLGA64** subcutaneous samples (● in **Figure 10.4**) up to day 21 typically showed only one large peak at 45,000–155,000 daltons with only very occasional shoulder peaks around 12,000–16,000 daltons. One of the day 28 subcutaneous samples showed atypical results, exhibiting a high molecular weight peak at approximately 150,000 daltons. Two of the day 35 samples, as well as all of the day 42 and 49 samples, showed this same peak at a molecular weight that increased from around 260,000 to 320,000 daltons. This peak was interpreted as due to biological material on the surface of the films, and therefore was not included in **Figure 10.4**. The day 28, 35, and 42 samples also occasionally showed a small peak at 3,000–4,000 daltons. The **PLGA64** subcutaneous implants showed a trend of decreasing molecular weight over time.

The chromatograms for the *in vitro* **PLGA64** samples (■ in **Figure 10.4**) showed a main peak that started at 150,000 daltons on day four that rapidly decreased in molecular weight to approximately 63,000 daltons on one of the day 14 samples, and then disappeared. After day 14 the main peak most often appeared in the molecular weight range of 7,000–15,000 daltons until day 49, when it dropped to 2,500–3,000 daltons. A very small peak was also visible at approximately 3,500 daltons, which increased in relative size at days seven and 14, and that slowly decreased in molecular weight from day 21 to day 49.

10.3.3 Differential Scanning Calorimetry (DSC)

The results of the DSC analysis are summarized in **Figure 10.5** to **Figure 10.8**. Data points typically represent the average of T_g values obtained from three samples for a given material and time point. The absence of data points or error bars at a given time point is due to the absence of a T_g for two or more of the samples at that time point.

10.3.3.1 Mylar®

Mylar® control samples (results not shown) produced a small glass transition peak at approximately 99–102°C, and a baseline of approximately 0.037 milliWatts/°C. For comparison, a T_g of approximately 80°C has been reported in the literature for amorphous Mylar® heated at 10°C/minute[9]. Mylar® control samples were run with each batch of samples. This allowed for comparison of the Mylar® baseline and peaks with the sample results, in order to ensure that the thermal contribution from the Mylar® substrate did not interfere with the obtained sample results.

10.3.3.2 **PLA**

The measured T_g values of the **PLA** samples over the 49 days of the study are shown in **Figure 10.5** below. An average T_g of 52°C was measured for the **PLA** powder control samples (dashed line in **Figure 10.5**). The subcutaneous cage implants (○ symbols), direct subcutaneous implants (● symbols), and *in vitro* samples (■ symbols) did not show a clear trend of decreasing T_g in comparison to the powder control. The subcutaneous cage samples exhibited clearly visible T_g peaks for all time points. The direct subcutaneous implants also showed distinct T_g peaks for most samples up to 49 days. In contrast to these *in vivo* samples, only about half of the *in vitro* samples from days 14 or later had resolvable T_g peaks, and they were often much smaller in magnitude than those seen for the direct subcutaneous and the cage subcutaneous samples.

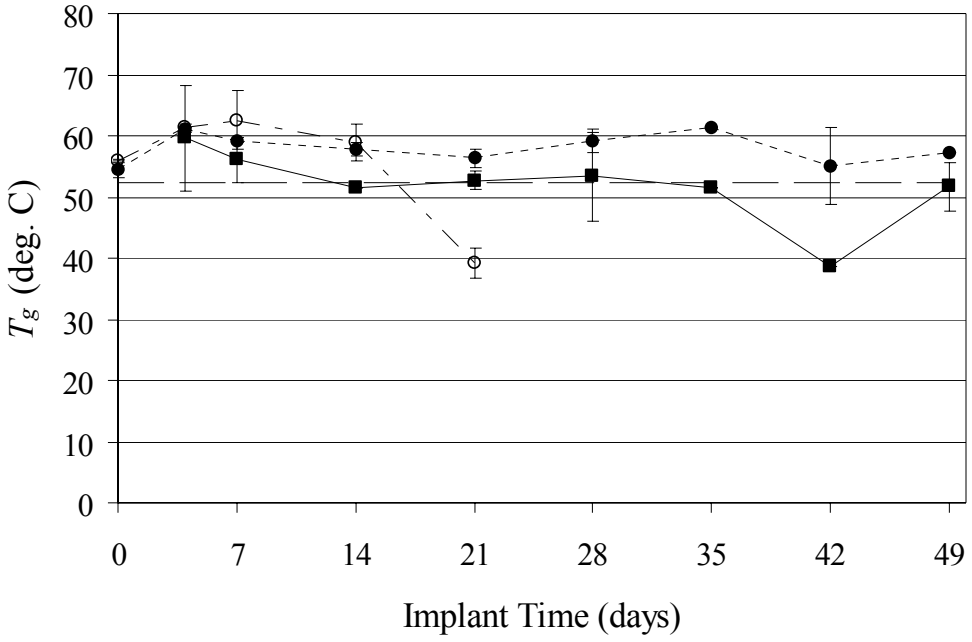

Figure 10.5 Measured T_g for **PLA** samples: - - - powder control samples, ■ *in vitro* samples, ● *in vivo* direct subcutaneous implants, ○ *in vivo* cage implants.

10.3.3.3 **PGA**

The measured T_g values for the **PGA** samples are summarized in **Figure 10.6** below. The average T_g measured for the **PGA** powder control samples (dashed line in **Figure 10.6**) was approximately 45°C. The subcutaneous cage samples (○ symbols) showed only a slight trend of decreasing T_g over the time period of the study, and the T_g peaks were very difficult to resolve on the day 14 and 21 samples. The **PGA** direct subcutaneous samples (● symbols) showed a decrease in the measured T_g between days four (40°C) and 21 (27°C). At day 28 the average T_g increased to approximately 50°C, and then decreased for the remaining three time points. The *in vitro* samples (■ symbols) showed a drop in the measured T_g from 25°C at day four to approximately 19°C at day seven. The average measured T_g for the *in vitro* samples plateaued at between 14 and 19°C for the rest of the time points.

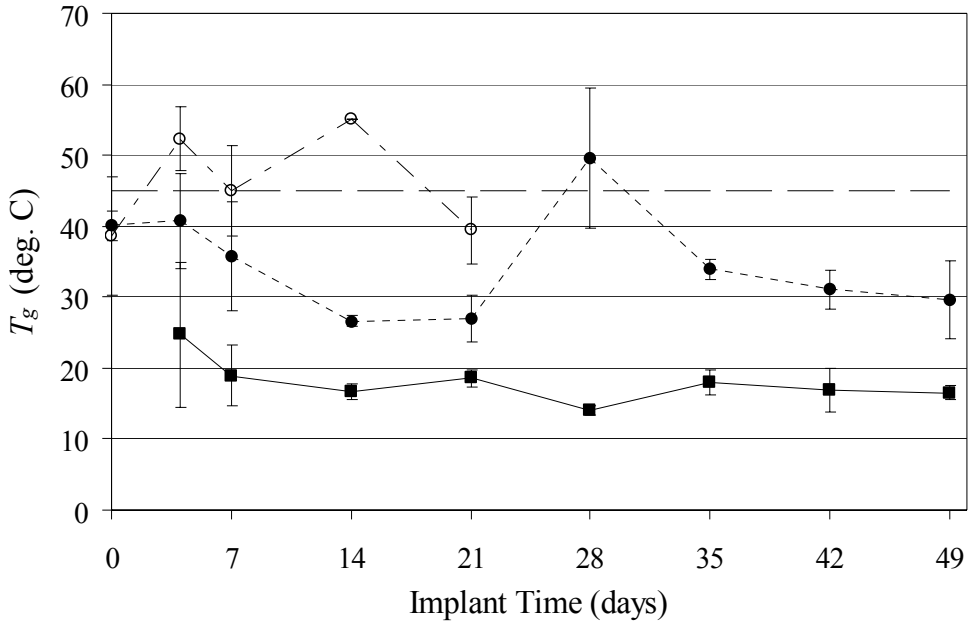

Figure 10.6 Measured T_g for **PGA** samples: - - - powder control samples, ■ *in vitro* samples, ● *in vivo* direct subcutaneous implants, ○ *in vivo* cage implants.

10.3.3.4 **PLGA4.4**

The measured T_g values for the **PLGA4.4** samples over the course of the study are summarized in **Figure 10.7** below. The powder control samples (dashed line in **Figure 10.7**) had an average T_g of 26°C. Neither the cage subcutaneous (○ symbols) nor the direct subcutaneous (● symbols) implant samples showed a decreasing T_g over time in comparison to the powder control. The direct subcutaneous samples had average measured T_g values greater than those of the powder controls for all time points of the study. The T_g peaks were very small and difficult to resolve for nearly all the samples at all time points for both the direct subcutaneous and the cage subcutaneous samples. The *in vitro* samples, in contrast, showed a decreasing trend in the T_g, from 9°C at four days to –7°C at 21 days. The T_g values obtained for the day 28 samples had a large amount of variation. After day 28 it became exceedingly difficult to reliably distinguish any T_g peaks for the *in vitro* samples, therefore no data for days 35, 42, and 49 are shown in **Figure 10.7**.

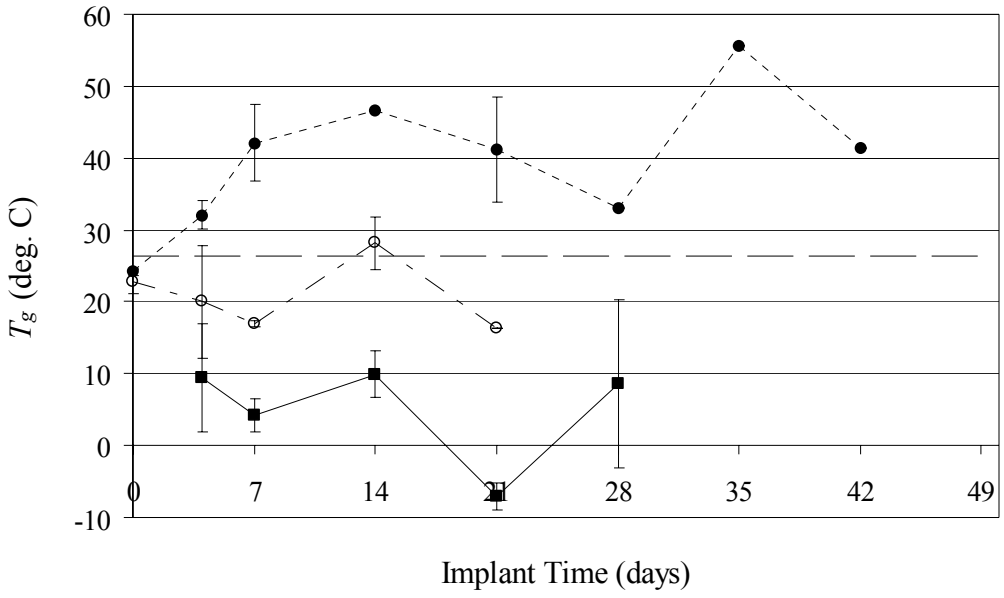

Figure 10.7 Measured T_g for **PLGA4.4** samples: - - - powder control samples, ■ *in vitro* samples, ● *in vivo* direct subcutaneous implants, ○ *in vivo* cage implants.

10.3.3.5 **PLGA64**

The measured T_g values of the **PLGA64** samples over the 49 days of the study are shown in **Figure 10.8** below. The powder control samples (dashed line in **Figure 10.8**) had an average measured T_g of 46°C. Both the direct subcutaneous (● symbols) and cage subcutaneous (○ symbols) implant samples showed only a very slight drop in measured T_g over 21 days compared to the powder controls, to 37°C for the direct subcutaneous samples, and to 43°C for the cage subcutaneous samples. The cage subcutaneous samples, with the exception of one sample at 21 days, all had clearly distinguishable T_g peaks. Similarly, the direct subcutaneous samples had distinct T_g peaks up to day 21, after which time no T_g peaks could be distinguished for any samples at the remaining time points (28, 35, 42, or 49 days). The *in vitro* samples had distinct T_g peaks out to day 35, but in contrast to the samples implanted *in vivo*, they showed a steady and large drop in the measured T_g, from 39°C at day four, to –23°C after 35 days.

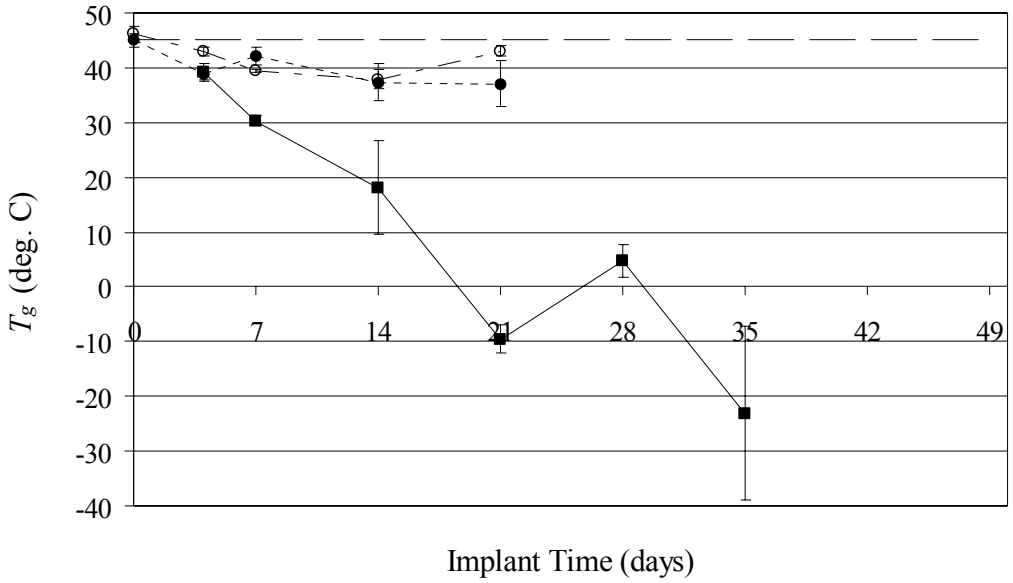

Figure 10.8 Measured T_g for **PLGA64** samples: - - - powder control samples, ■ *in vitro* samples, ● *in vivo* direct subcutaneous implants, ○ *in vivo* cage implants.

10.3.4 Discussion

10.3.4.1 Mylar®, HFIP, and Tissue Samples

The dissolution of the Mylar® and some tissue components in HFIP were unexpected results in this study. Mylar® is used in many applications whereby its chemical resistance is advantageous, and solubility of Mylar® in HFIP is not widely reported[10–12]. While the Mylar® control samples that were analyzed on the GPC were helpful in determining the Mylar® molecular weight, batch-to-batch variation in the reported molecular weights, as discussed in 10.3.2, made it difficult to interpret some chromatograms.

Filtration of the GPC samples prior to analysis was expected to remove any tissue or cell debris larger than 0.2 μm. However, extremely high molecular weight peaks were obtained for the tissue samples that were analyzed (see section 10.3.2.2), as well as for many of the polymer films that were implanted *in vivo*. This was particularly the case for the **PGA** and **PLGA4.4**, as well as some of the **PLGA64** and **PLA** *in vivo* samples at longer implantation times. Solubility of proteins in fluoroalcohols has been reported in the literature[13–16]. HFIP has been used to dissolve peptide aggregates[13], and has been shown to disrupt tertiary structure and strengthen

helical propensities of proteins[13,14]. If biological materials (proteins or collagen, for example) on the surface of the films are soluble in the HFIP, they may be the cause of this high molecular weight peak. Interestingly, the **PLA** film that was removed from the explanted tissue (at 42 days, see section 10.3.2.2) did not exhibit a high molecular weight peak from the biological material. This agrees with the results obtained for the **PLA** direct subcutaneous implant samples, which exhibited a biological material peak on the GPC chromatograms for only two of the day 49 samples, suggesting less deposition of biological material than was seen for the **PLGA4.4** samples. The chromatograms for the **PLGA4.4** film explanted at day 42 (see section 10.3.2.2), for example, showed only a peak from this biological material, and no peak due to the polymer itself. This also agrees with results obtained for the **PLGA4.4** direct subcutaneous implant samples, which indicated that the polymer rapidly degraded within the first seven days of the study, leaving no polymer on the Mylar® substrate at subsequent time points.

10.3.4.2 Biodegradable Polymers

A half-life ($t_{½}$) was determined for each sample group as the time period in which the experimentally measured average molecular weight dropped below one-half of the initial molecular weight for each sample group. The half-lives for each sample group are shown in **Table 10-3** below, and will be discussed in further detail in the sections below.

Table 10-3 Half-lives (time in days at which the average molecular weight of a sample group was one-half the initial molecular weight) for ~100 μm thick **PLA**, **PGA**, **PLGA4.4**, and **PLGA64** films degraded under various conditions.

Polymer	*In Vitro* Controls	*In Vivo* Direct Subcutaneous	*In Vivo* Cage Subcutaneous
PLA	28-35	49	>21
PGA	4-7	0-4	0-4
PLGA4.4	21-28	0-4	4-7
PLGA64	7-14	14-21	14-21

10.3.4.2.1 ***PLA***

The half-lives in **Table 10-3** of all of the **PLA** sample groups were larger than those for any of the other materials. This agrees with results in the literature which indicate that higher lactic acid content, as well as crystallinity of PLA samples, are correlated with slower degradation rates[2,3,5].

The GPC data for the **PLA** control films, as well as the control films for the other materials, typically showed a significantly lower molecular weight for the main peak than was measured for the powder controls. Other studies on solvent cast and vacuum-dried 50:50 PLGA films have shown similar behavior[5]. A 22% drop in molecular weight was reported for 85–100 μm thick films that were vacuum dried for 24 hours, with the hypothesis that the polymer degraded during fabrication. Between 17 and 40% loss in molecular weight has been reported for PLLA foams that were annealed above their T_m and then quenched and vacuum dried for 48 hours[5]. Processing conditions for the films analyzed in this study were similar (annealed above T_g while drying under vacuum for 48 hours) to the latter experiments.

While the GPC results indicate a steady slow loss of molecular weight for the **PLA** samples, the DSC results do not show a large change in the measured T_g over the course of the study. Two different types of phenomena have been reported in the literature with regard to DSC characterization of **PLA**, **PGA**, and **PLGA** degradation. The first type of behavior that has been observed is a decrease in the T_g of the polymer, reflecting a decrease in the molecular weight of the polymer chains and corresponding increase in the free volume of the polymer. The glass transition temperature (T_g) of a polymer and its molecular weight are related according to the following equation[17]:

$$T_g = T_g^{\infty} - \frac{2\rho N_A \theta}{\alpha_f M_n}$$

Equation 10-a

where T_g^{∞} = is the value of T_g for a polymer sample of infinite molar mass, ρ = polymer density, N_A = Avogadro's number, θ = contribution of one chain end to the free volume of the polymer, α_f = thermal expansion coefficient of the free volume, and M_n = number-average molar mass (molecular weight) of the polymer. The quantity ($2\rho N_A/M_n$) therefore represents the number of chain ends per unit volume. As the molecular weight of the polymer decreases, the number of chain ends per unit volume increases. The total contribution to the free volume due to the chain ends will therefore also increase, which is reflected in a lower measured T_g according to Equation 10-a (less thermal energy is needed to cause chain motion, since more free volume is already present). Physically this can be understood as the fact that for a higher concentration of

chain ends (lower chain molecular weight), greater free volume is present. Therefore, in order for short-range segmental motion to occur, correspondingly less thermal energy is required because the steric and energetic barriers to motion are smaller. This means that the onset of segmental motion, as reflected in the T_g, will occur at a lower temperature. Decreases in T_g due to a decrease in the molecular weight of the polymer have been observed in a number of studies that characterized PLA and PLGA degradation. Decreases in T_g over a period of up to 100 days have been observed for poly(D,L-lactic-co-glycolic acid) (50:50 ratio of lactide to glycolide) compression-molded samples[18] that were degraded at 37°C *in vitro*. Microspheres fabricated from poly(D,L-lactic acid) have also shown a decrease in the measured T_g over periods up to 250 days when degraded in saline at 37°C *in vitro*[19,20]. Similarly, microparticles made from both poly(D,L-lactic acid) and poly(D,L-lactic-co-glycolic acid) having a lactide:glycolide ratio of 75:25 showed decreases in their T_g's over the course of 120 days when degraded in saline at 37°C *in vitro*[21].

However, a second type of behavior has also been observed. An increase in the crystallinity of degrading polymer samples, as evidenced by higher T_g values and larger heats of fusion, has been observed for poly(glycolic acid)[22], poly(L-lactic acid)[23], and even poly(D,L-lactic-co-glycolic acid)[24] samples degraded in saline at 37°C *in vitro*. A hypothesis to explain this phenomena has been advanced, which proposes that as the polymer chains are degraded and cleaved into smaller chains, the oligomers that are formed can crystallize, resulting in the observed larger heats of fusion and higher T_g values[24]. Further, although one might expect that poly(D,L-lactic-co-glycolic acid) would not exhibit this behavior, due to the presumably random distribution of the lactic and glycolic acid units in the chain backbone, greater reactivity of glycolic units during ring-opening copolymerization of glycolide and lactide can lead to blocks of glycolide separated by as small as a single unit of lactide[25]. Faster hydrolysis of the glycolide regions of the PLGA copolymer might therefore leave behind crystallizable sequences of lactide.

In the case of the **PLA** samples investigated in this study, a number of different reasons might explain the observation that the T_g values for the various sample groups did not appear to decrease over the course of the study. The measured molecular weight even after 49 days is still considerably larger (85,000 for the direct subcutaneous samples and 94,000, on average, for the *in vitro* samples) than the molecular weights measured for the other materials in this study. It may be that, according to Equation 10-a, the change in molecular weight was not significant

enough to be reflected in a change in the T_g of the samples. Additionally, crystallization of oligomers of the L-lactic acid may have counteracted any drop in the T_g due to the decrease in molecular weight of the chains.

10.3.4.2.2 ***PGA***

The more rapid degradation of the **PGA** relative to the **PLA**, as evidenced by the shorter half-lives in **Table 10-3,** can be explained by the greater hydrophilicity of the **PGA**. Other studies of PLGA copolymers have demonstrated more rapid *in vitro* and *in vivo* degradation of 50:50 (L:G) copolymers than other copolymers having higher fractions of lactic acid (75:25 or 85:15), which was attributed to the more hydrophilic nature of the glycolic acid units[2,3,5]. A very rapid and large decrease in molecular weight was seen for all of the **PGA** sample groups in this study.

The *in vitro* **PGA** samples had visible white polymer film present on the Mylar® out to day 49, which was easily removed from the surface of the Mylar®, while the *in vivo* samples had visible **PGA** up to day 21. Therefore, although a peak was typically seen on the **PGA** GPC chromatograms at approximately 38,000 daltons, similar to the molecular weight value obtained for the Mylar® controls, it seems unlikely that this peak is due to the Mylar® for many of the samples because of the ease with which the PGA could be separated from the Mylar® substrates. The **PGA** chromatograms were often bimodal, suggesting heterogeneous degradation. As was explored in Chapter 5, size-dependent degradation has been reported in the literature[5,6]. One study found more rapid molecular weight loss in thick (100 μm) PLGA films compared to thin (10 μm) films, but both types of films exhibited bimodal chromatograms[5]. The size of the samples used in this study (133 μm or less) is plausibly within the range where heterogeneous degradation may occur, and the results presented in Chapter 5 support this hypothesis.

The DSC results for the **PGA** material do not initially appear to correlate well with the GPC results. The **PGA** direct subcutaneous samples show the expected behavior (a decrease in the measured molecular weight reflected by a drop in the T_g values) over the first 21 days of the study, but the day 28 samples showed a sudden increase in the measured T_g. This may be explained by our observations that the surface of two of the three explanted samples at this time point had tan and reddish patches on their surfaces. The presence of this biological material most likely caused the increase in the measured T_g. Although the day 35, 42, and 49 samples

subsequently showed a decrease in the measured T_g values, these values were still higher than those obtained for the day four to 21 samples. However, the higher measured T_g values for the explanted samples from these last three time points of the study may be explained by the fact that the Mylar® substrates had no visible **PGA** (thick white film) remaining on their surfaces, but instead a thin, translucent white film with some tan patches. Thus the T_g that was measured is most likely that of the biological residue on the surface of the explanted Mylar® film, and not that of the **PGA** material. The **PGA** cage samples also exhibited high T_g values and a high molecular weight peak on the GPC chromatograms, which it seems likely are both due to biological residue on the surface of the films, even though no biological material was visible when the explanted films were inspected with the naked eye. Although the *in vitro* **PGA** samples did not show a large drop in the measured T_g, the initial drop followed by a plateau is similar to the molecular weight results obtained by the GPC analysis.

10.3.4.2.3 ***PLGA4.4***

Both the GPC and DSC results indicated that the **PLGA4.4** degraded extremely rapidly *in vivo* and that it left only reminiscent traces of the polymer film on the Mylar® substrate after seven days. This hypothesis was confirmed by the visual inspection of the **PLGA4.4** *in vivo* samples that was performed. Even after just seven days of implantation (both in the cage as well as directly under the skin of the animals), the films appeared to have only a very thin translucent coating on their surface, which could not reliably be identified as either polymer or biological material. The GPC results showed a large molecular weight peak similar to that observed in the tissue samples (see section 10.3.2.2) for all of the cage samples and most of the direct subcutaneous samples. Further, peaks at or less than the molecular weight specified by the manufacturer (4,400 daltons) were visible on very few of the *in vivo* sample chromatograms. These results support the hypothesis that the **PLGA4.4** degraded rapidly *in vivo*. The molecular weight of the **PLGA4.4** samples could be characterized out to 49 days *in vitro*, however, most likely due to the slower degradation *in vitro* compared to *in vivo*, as evidenced by the larger half-life for the *in vitro* sample group in **Table 10-3**. Faster degradation rates of PLGA copolymers *in vivo* compared to *in vitro* have been reported in the literature, with the hypothesis that local accumulation of acidic degradation products may autocatalyze further degradation[4].

The high T_g values measured for the **PLGA4.4** samples that were implanted *in vivo* may be explained by the biological material that appeared to cause the high molecular weight peak (~200,000 daltons) on the GPC chromatograms. Evidence that these two phenomena are related may be found in the fact that the **PLGA4.4** direct subcutaneous samples from days four and 28, which did not exhibit a high molecular weight peak (~200,000 daltons) on the GPC chromatograms had lower T_g values than the samples at other time points (see **Figure 10.7**). The difficulty in resolving T_g peaks for the **PLGA4.4** *in vitro* samples after day 28 correlates well with the GPC results, which indicated a very low molecular weight (~2,000 daltons) at or after 28 days. Further, visual inspection of the *in vitro* film samples prior to GPC or DSC preparation revealed that the samples for days 35, 42, and 49 had only a very sparse opaque white powder present. All of these indications suggest that the **PLGA4.4** degraded very rapidly and that most of the polymer had been removed from the Mylar® substrate by the time the GPC and DSC analyses were performed.

10.3.4.2.4 ***PLGA64***

The GPC results showed that the molecular weight of the **PLGA64** samples took 35 days to plateau when implanted *in vivo*, indicating that this material degraded more slowly than both the **PGA** and the **PLGA4.4**. The half-lives in **Table 10-3** suggest that this material degraded slightly more rapidly *in vitro* than *in vivo*, but this is not a conclusive result due to the large variation in sample molecular weights (as evidenced by the large error bars for the day seven, 14, and 21 samples in **Figure 10.4**).

The day 21 **PLGA64** direct subcutaneous samples showed noticeably broader peaks on the GPC chromatograms than samples explanted at earlier time points. The appearance of a high molecular peak (due to biological material) on one of the day 28 samples, similar to that seen for the **PGA** and **PLGA4.4** *in vivo* samples, suggests that the period around 21 to 28 days may be critical for the onset of rapid degradation of the polymer. Further, the **PLGA64** cage samples at day 21 showed a slight increase in the measured T_g, and two of the explanted films at this time point were tan and red in color. The presence of this biological debris on the surface of the polymer film again seems correlated with a higher measured T_g, and the appearance of the biological material after day 21 for both sets of *in vivo* samples (cage as well as direct subcutaneous) suggests a change in the immune response at that time frame. An increase in the

degradation rate of the polymer during this period or alternatively solubilization of the low molecular weight oligomers during this period may have caused a greater immune response in the animal, with correspondingly increased localization of cells that may have deposited biological material on the surface of the **PLGA64** films. The GPC results for the *in vitro* **PLGA64** samples also indicate that this polymer rapidly degrades over the first 21 days after implantation, but the molecular weight did not plateau even after 49 days of implantation.

The **PLGA64** samples implanted *in vivo* showed a higher measured T_g than the *in vitro* samples up to day 21, which correlates well with the higher molecular weight measured for these *in vivo* samples over the same time period.

10.4 Summary and Conclusions

Polymer films of **PLA**, **PGA**, and **PLGA** of two different molecular weights were fabricated on Mylar® substrates for an *in vivo* study of their biodegradation. The gel permeation chromatography and differential scanning calorimetry analyses indicate that the **PGA** degrades the most rapidly *in vivo*, followed by the **PLGA4.4, PLGA64**, and **PLA**. In general, more rapid degradation of the materials occurred *in vivo* than *in vitro*, most likely due to the autocatalytic effect of acidic degradation products that accumulate locally near the implant. This trend supports the results presented in Chapter 9, which indicated that release from the microreservoir devices was more rapid *in vivo* than *in vitro*, presumably due to the faster degradation rates of the membrane polymers *in vivo*. The GPC and DSC results suggest the presence of biological material on the surface of the explanted films (particularly the **PLGA4.4**, **PGA,** and **PLGA64** at longer implantation times).

10.5 Acknowledgements

The *in vivo* and *in vitro* degradation studies reported here were performed by Gabriela Voskerician in the laboratory of Dr. James M. Anderson, M.D., Ph.D., Departments of Biomedical Engineering and Macromolecular Science, and Institute of Pathology in the School of Medicine at Case Western Reserve University in Cleveland, OH. Joyce Chan and Grace Kim performed sample preparation for the GPC and DSC analyses at MIT.

10.6 References

1. J. M. Anderson and M. S. Shive, "Biodegradation and biocompatibility of PLA and PLGA microspheres," *Adv. Drug Deliv. Rev.* 28 (1997) 5–24.

2. R. A. Miller, J. M. Brady, and D. E. Cutright, "Degradation rates of oral resorbable implants (polylactates and polyglycolates): rate modification with changes in PLA/PGA copolymer ratios," *J. Biomed. Mater. Res.* 11 (1977) 711–719.

3. L. Lu, S. J. Peter, M. D. Lyman, H.-L. Lai, S. M. Leite, J. A. Tamada, S. Uyama, J. P. Vacanti, R. Langer, and A. G. Mikos, "*In vitro* and *in vivo* degradation of porous poly(DL-lactic-*co*-glycolic acid) foams," *Biomaterials* 21 (2000) 1837–1845.

4. S. M. Li, H. Garreau, and M. Vert, "Structure-property relationships in the case of the degradation of massive aliphatic poly-(α-hydroxy acids) in aqueous media, Part 1: Poly(DL-lactic acid)," *Journal of Materials Science: Materials in Medicine* 1 (1990) 123–130.

5. L. Lu, C. A. Garcia, and A. G. Mikos, "*In vitro* degradation of thin poly(DL-lactic-*co*-glycolic acid films)," *J. Biomed. Mater. Res.* 46 (1999) 236–244.

6. I. Grizzi, H. Garreau, S. Li, and M. Vert, "Hydrolytic degradation of devices based on poly(DL-lactic acid) size-dependence," *Biomaterials* 16 (1995) 305–311.

7. M. Vert, J. Mauduit, and S. Li, "Biodegradation of PLA/GA polymers: increasing complexity," *Biomaterials* 15 (1994) 1209–1213.

8. M. S. Shive, "*In vivo* studies of biomedical polymers," M.S. thesis, Department of Biomedical Engineering, Case Western Reserve Univ., Cleveland, OH, 1998.

9. N. A. Bailey, J. N. Hay, and D. M. Price, "A study of the enthalpic relaxation of poly(ethylene terephthalate) by conventional and modulated temperature differential scanning calorimetry," Proceedings of the Twenty-Seventh Conference of the North American Thermal Analysis Society, September 20–22, 1999, Savannah, Georgia, pp. 731–736.

10. "Polyethylene Terephthalates" in The Merck Index, 13th edition, Eds: M.J. O'Neill, A. Smith, P.E. Heckelman, J.R. Obenchain, Jr., J.A.R. Gallipeau, M.A. D'Arecca, S. Budavari, Merck & Co., Inc., Whitehouse Station, NJ (2001) 1359.

11. "Mylar® Chemical Properties," DuPont Teijin Technical Data Sheet H-37250-1, http://www.dupontteijinfilms.com/datasheets/mylar/productinfo/properties/h37250-1.pdf, DuPont Teijin, Wilmington, DE (1995).

12. "Polyethylene terephthalate," in CRC Handbook of Polymer-Liquid Interaction Parameters and Solubility Parameters, A.F.M. Barton, CRC Press, Boca Raton, FL (1990) 202–206.

13. K. Gast, A. Siemer, D. Zirwer, and G. Damaschun, "Fluoroalcohol-induced structural changes of proteins: some aspects of cosolvent-protein interactions," *Eur. Biophys. J.* 30 (2001) 273–283.

14. J. Cort, and N. Andersen, "Formation of a molten-globule-like state of myoglobin in aqueous hexafluoroisopropanol," *Biochem. Biophys. Res. Commun.* 233 (1997) 687-691.

15. N. Andersen, R. Dyer, R. Fesinmeyer, F. Gai, A. Liu, J. Neidigh, and H. Tong, "Effect of hexafluoroisopropanol on the thermodynamics of peptide secondary structure formation," *J. Am. Chem. Soc.* 121 (1999) 9879–9880.

16. N. Hirota, K. Mizuno, and Y. Goto, "Cooperative α-helix formation of B-lactoglobulin and melittin induced by hexafluoroisopropanol," *Protein Sci.* 6 (1997) 416–421.

17. R. J. Young, P. A. Lovell, Introduction to Polymers, 2nd edition, Chapman and Hall, London (1996) 299.

18. W. Vogelhuber, P. Rotunno, E. Magni, A. Gazzaniga, T. Spruß, G. Bernhardt, A. Buschauer, and A. Göpferich, "Programmable biodegradable implants," *J. Controlled Release* 73 (2001) 75–88.

19. T. G. Park, "Degradation of poly(D,L-lactic acid) microspheres: effect of molecular weight," *J. Controlled Release* 30 (1994) 161–173.

20. M. F. Gonzalez, R. A. Ruseckaite, and T. R. Cuadrado, "Structural changes of polylactic-acid (PLA) microspheres under hydrolytic degradation," *J. Appl. Polym. Sci.* 71 (1999) 1223–1230.

21. G. Reich, "Use of DSC to study the degradation behavior of PLA and PLGA microparticles," *Drug Development and Industrial Pharmacy* 23 (1997) 1177–1189.

22. R. M. Ginde and R. K. Gupta, "In vitro chemical degradation of poly(glycolic acid) pellets and fibers," *J. Appl. Polym. Sci.* 33 (1987) 2411–2429.

23. C. Migliaresi, L. Fambri, and D. Cohn, "A study on the in vitro degradation of poly(lactic acid)," *J. Biomater. Sci. Polymer Edn.* 5 (1994) 591–606.

24. T. G. Park, "Degradation of poly(lactic-co-glycolic acid) microspheres: effect of copolymer composition," *Biomaterials* 16 (1995) 1123–1130.

25. D. K. Gilding and A. M. Reed, "Biodegradable polymers for use in surgery—polyglycolic/poly(lactic acid) homo- and copolymers:1," *Polymer* 20 (1979) 1459–1464.

11 Conclusions and Future Work

11.1 Summary of Results

The results presented in this thesis clearly show the viability of using the polymeric microreservoir device to achieve multipulse delivery of drugs both *in vitro* and *in vivo*. While many other systems, such as three-dimensionally printed structures and compression molded devices, could also be used to deliver multiple pulses of drugs, thus far no proof-of-principle results have been reported. Therefore, the design we have developed and reported here represents a new class of device for controlled release drug delivery.

11.2 Future Work

While the results presented here demonstrate proof-of-principle of the device operation and give us some understanding of the factors that can affect system performance, further study will only serve to improve both our understanding as well as the functioning of the system.

11.2.1 Membrane Degradation and Opening

As was discussed extensively in Chapter 5, the degradation mechanisms of the PLGA copolymers that comprise the reservoir membranes are quite complicated. The local environmental temperature and pH can affect the degradation rate of the membranes and therefore change the time at which the drugs are released from the reservoirs. Additionally, the dimension dependence of the PLGA degradation rate and nonlinearity of the degradation rate as a function of polymer molecular weight make prediction of membrane degradation time difficult without prior *in vitro* and *in vivo* characterization.

While the GPC characterization of polymer degradation in Chapter 5 suggested that perhaps membrane opening is correlated with the polymer molecular weight dropping below 5,000–7,000 daltons, the results reported in Chapter 7, which showed a large amount of water uptake and membrane swelling during the course of a typical release experiment, suggest that there may also be a mechanical component which helps dictate membrane opening. Further elucidation of the mechanisms by which the membranes open will aid in gaining further control over device performance. Alternatively, other biodegradable materials, such as polyanhydrides,

polydioxanone, or polyethylene carbonate, may ultimately prove more amenable to achieving greater control over the release time of drugs from the devices.

11.2.2 Drug Chemistry

A number of the studies reported here aimed to gain an understanding of whether the drug itself that is released from the microreservoir device plays a role in changing the observed release time from the reservoirs. While some results appeared to indicate that this was indeed the case, other studies seemed to support the theory that the molecular weight of the drug did not affect release time. In the case of BCNU and IAP, the large partitioning coefficients calculated for the **PLGA4.4** membrane material in Chapter 6 seemed to support the observed diffusion-type release behavior of these molecules from the microreservoir device that was observed in Chapter 4. On the other hand, studies that investigated the effect of drug molecular weight and reservoir loading on the release time and membrane swelling (Chapter 7) showed no significant differences between ^{14}C-glucose and higher molecular weight polymers of ^{14}C-dextran (10,000, 40,000, and 70,000 molecular weights). While the lipophilicity of the drug, rather than the molecular weight, may ultimately prove to be the determining factor for the release kinetics, at present the only way to understand the interaction between the drug and membrane material is to investigate each drug on an individual basis. More systematic study of this issue may help to delineate a set of general guidelines or expectations for release kinetics, based on certain characteristics of the drugs of interest (such as molecular weight, functional groups, pKa, partition coefficient, or hydrodynamic radius, for example) that would allow device performance to be predicted with confidence. Further, ameliorative measures may be developed that could eliminate the effects of drug chemistry on device performance. For example, coating the inside of the reservoirs with a barrier layer of a hydrophilic material (such as a starch or sugar) might prevention diffusional release of small lipophilic molecules such as BCNU through the reservoir membranes prior to membrane opening.

11.2.3 *In Vivo* Drug Release

While the results presented in Chapter 9 show that *in vivo* drug delivery from the microreservoir device is possible, much more thorough study and testing will be necessary before this device will become a clinical reality. The need for a better correlation between *in*

vitro and *in vivo* results seen in general for PLGA-based drug delivery systems necessitates more extensive testing and redesign of these systems even when reproducible *in vitro* performance has been achieved. The rapid release times as well as closely spaced pulses that were observed for ^{14}C-mannitol released from these devices *in vivo* suggest that the first step towards robust *in vivo* device performance may be to increase the difference in molecular weights of the materials used for the reservoir membranes in order to achieve more distinctly separated pulses from the device.

Once reproducible *in vivo* device performance has been achieved, demonstration of device efficacy for treatment of a disease condition would provide the ultimate confirmation of device utility.

11.3 Conclusions

The work reported here represents the first demonstration in the literature of multipulse chemical delivery from a polymeric reservoir-based system without reliance on external stimuli. This device could potentially be used in applications where pulsatile delivery of potent molecules is desired for maximum therapeutic efficacy, such as hormone treatments or multi-dose vaccines. The separation of the drug formulations (reservoir contents) from the release formulations (reservoir membranes) may permit greater flexibility in device design and performance than is currently available for other implantable polymeric drug delivery systems, allowing greater applicability to a wider range of clinical indications.

Appendices

A Factors Affecting Measured Fluorescence

A.1 Introduction

It is well known that several factors may affect the measured fluorescence of a molecule. Most notable of these are the pH[1] and ionic strength[2,3] of the solution that contains the fluorescent molecule, and photobleaching[4–6]. Several of the studies reported in Chapter 3 and Appendix B that investigated the accuracy of the microinjector apparatus used sodium fluorescein or fluorescein-labeled dextran as the marker molecule. Fluorescein has many desirable properties, including high fluorescence yield and high water solubility. However, its fluorescence is significantly pH-dependent, and it can undergo rapid photobleaching under exposure to high or even moderate intensity light. Several studies were therefore conducted to determine if the changes in fluorescence caused by pH, the related factors of conductivity and ionic strength, and photobleaching were significant enough to explain some of the variation in fluorescence measured in the different studies.

A.2 Materials and Methods

A.2.1 Materials

Fluorescein sodium salt was purchased from Sigma-Aldrich (St. Louis, MO). Solutions of sodium fluorescein were made using either phosphate buffered saline (PBS) or milliQ deioinized water.

A.2.2 Methods

A.2.2.1 Photobleaching: Microinjected Cuvettes

For the first set of experiments, a sodium fluorescein solution of 1.32×10^{-2} mol/L was microinjected into cuvettes. The procedure that was used was similar to that described in Chapter 3. Series of one, two, three, four, or five injections of 19.57, 49.72, 99.98, and 149.7 nL were performed. Two series of microinjections were performed. The first set was performed with both ambient lighting (overhead fluorescent lights as well as natural light from nearby windows) and

stage lighting on the microscope. The second set was performed with only stage lighting on the microscope. The overhead lights were turned off and the blinds were drawn on the windows to block as much natural light as possible. To each cuvette were added three milliliters of deionized water. The cuvettes were covered with Parafilm M® and shaken.

The fluorescence (fluorescence counts/sec) of each cuvette was measured using λ_{exc} = 494 nm and λ_{emi} = 520 nm on a spectrofluorometer (Photon Technology International, Lawrenceville, NJ) having an L-201M Illumination System, LPS-220 Lamp Power Supply, A1010 Arc Lamp Housing, two Model 101 Computer-Controlled Monochromators, MP-1 Sample Compartment, Model 814 Analog/Photon-Counting Photomultiplier Detector, SC-500 Shutter Controller, Computer Interface, and PTI Felix v.1.42a software on a Dell Optiplex 466/Le computer. The concentration of fluorescent label in each cuvette (C_c) was calculated by subtracting the background fluorescence of a cuvette of deionized water (blank), and dividing by the slope in (fluorescence counts/sec)/(mol/L) of a standard curve. The measured microinjected volume V_{meas} was then calculated by using the volume of solution in the cuvette (V_c), the appropriate dilution factors (D_i), and the concentration of the fluorescently labeled solution in the syringe (C_{init}) as follows:

$$V_{meas} = \frac{(V_C \times C_C)}{(C_{init} \times D_i)}$$

Equation 0-a

A.2.2.2 Photobleaching: Pipetted Cuvettes

Twenty microliters of a sodium fluorescein solution of 1.41×10^{-2} mol/L were pipetted into a cuvette containing three milliliters of phosphate buffered saline (PBS), n = 3. The solutions in these cuvettes were then diluted twice sequentially by pipetting 20 μL of the solution from each cuvette into a fresh cuvette with three milliliters of PBS. This procedure was used to produce two sets of cuvettes, designated A and B. Set A was kept wrapped in foil and not exposed to any light, while set B cuvettes were placed on the stage of the PZMT Trinocular stereo microscope with 13338 Adapter Ring Light, R-8-8-WPI01 fiber optic ring light, and NOVA Novaflex fiber optic light source (World Precision Instruments, Sarasota FL) for five minutes, with the microscope stage light on the lowest setting, the overhead lights off, and the

window blinds closed. The fluorescence of both sets of cuvettes was measured on the spectrofluorometer. Both sets of cuvettes were then placed on the microscope stage for eight minutes, with the same conditions as for the initial light exposure of set B. The fluorescence of the cuvettes was then measured again on the spectrofluorometer.

A.2.2.3 Ionic Strength and pH

Various dilutions of PBS were made in order to more thoroughly investigate the effect of ionic strength and pH on the measured fluorescence of fluorescein sodium salt solutions. As received 10X PBS was diluted to 9X, 7X, 5X, 3X, and 1X solutions using milliQ deionized water. Fluorescein sodium salt solution (1.3 μmolar) was pipetted in 25, 50, or 100 μL increments into polystyrene cuvettes, and three milliliters of the PBS dilution of interest was added to the cuvette. This was repeated in triplicate for each volume size and PBS dilution, for a total of 54 samples ($3 \times 3 \times 6 = 54$). The fluorescence of each cuvette was then measured on the spectrofluorometer as described previously. The pH values of the samples were measured using a Corning model 430 pH meter.

A.2.2.4 pH and Conductivity: Release Studies

Data from a number of release studies were compiled in order to determine if pH and conductivity effects on the observed fluorescence are significant over the course of a typical release study. Eleven devices were loaded with sodium fluorescein for *in vitro* release experiments. The cumulative percentage of the initial fluorescein loading was measured over time. The experiments were stopped at various points, ranging from 7 to 180 elapsed days. The pH of the release medium was measured using a Corning model 430 pH meter and the conductivity was measured using a Fisher Scientific Digital Conductivity Meter on the 20,000 microohm (μohm) setting.

A.3 Results and Discussion

A.3.1 Photobleaching: Microinjected Cuvettes

The results for the microinjected cuvettes are shown in **Figure A.1** and **Figure A.2** below.

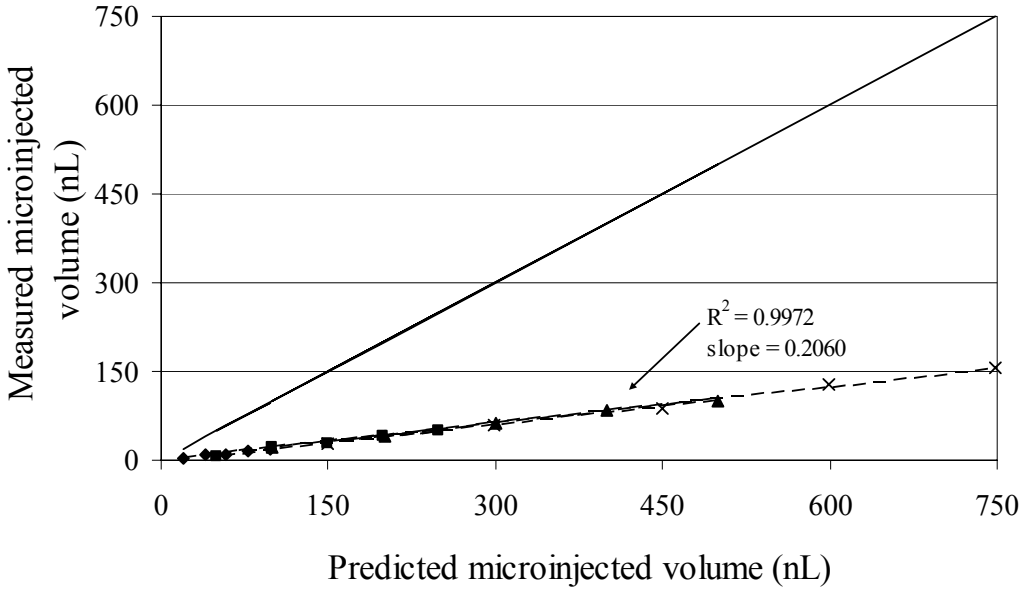

Figure A.1 Measured microinjected volume versus predicted microinjected volume (solid line) for bleached sodium fluorescein microinjected from a 10 μL syringe: ○ 19.57 nL injections, × 49.72 nL injections, ● 99.98 nL injections, ■ 149.7 nL injections. Solid line indicates theoretical predicted microinjected volume, dashed line is linear least squares fit to experimental data points.

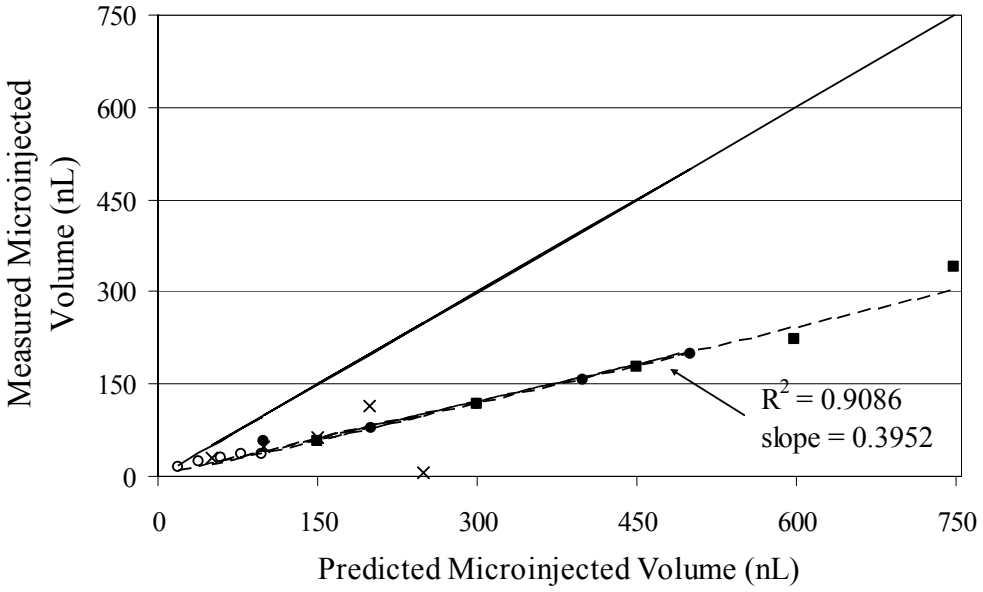

Figure A.2 Measured microinjected volume vs. predicted microinjected volume (solid line) for unbleached sodium fluorescein microinjected from a 10 μL syringe: ○ 19.57 nL injections, × 49.72 nL injections, ● 99.98 nL injections, ■ 149.7 nL injections. Solid line indicates theoretical predicted microinjected volume, dashed line is linear least squares fit to experimental data points.

Solid lines indicate the predicted (theoretical) microinjected volume, while the experimentally obtained data are shown by the different symbols. A linear least-squares fit to the experimental data was used to determine R^2 and the slope of the line. This fit is shown by the dashed lines in **Figure A.1** and **Figure A.2**.

The "bleached" fluorescein results shown in **Figure A.1** indicate that the measured microinjected volume was only approximately 20% of the predicted volume. For the unbleached samples, shown in **Figure A.2**, the measured microinjected volume was approximately 40% of the predicted value. The 20% lower fluorescence seen for the "bleached" samples in **Figure A.1** suggests that the ambient and natural lighting to which the samples were exposed (overhead fluorescent lighting and natural light from the windows in the laboratory) caused measurable loss in fluorescence in this experimental setup. However, more importantly, the large difference between the measured and predicted volumes for both sets of samples indicates that the stage lighting on the microscope, which was present for both sets of microinjections, may account for the majority of the loss in the measured fluorescence. This most likely explains the low percentages of microinjected sodium fluorescein that were measured in some of the studies detailed in Appendix B for the studies that investigated the effect of the syringe volume on the accuracy of microinjection.

A.3.2 Photobleaching: Pipetted Cuvettes

Table A-1 shows the initial and final average measured fluorescence and standard deviation for sets A and B cuvettes, as well as the calculated loss in fluorescence, in percent, due to the light exposure between the two sets of fluorescence measurements.

Table A-1 Measured fluorescence of sodium fluorescein solution pipetted into cuvettes. Set A cuvettes received only eight minutes of exposure to microscope stage lighting, while Set B had an initial five-minute exposure to the microscope stage lighting, followed by a second exposure of eight minutes.

	Fluorescence (counts/sec)	**Standard Deviation (counts/sec)**	**Standard Deviation (% of Average)**
Set A initial average:	1804667	91817	5.09
Set A final average:	1663333	91566	5.50
Percent decrease:	**7.83**		
Set B initial average:	1913667	17926	0.94
Set B final average:	1763667	12741	0.72
Percent decrease:	**7.84**		

Contrary to what was expected, the set B cuvettes, which had an initial light exposure of five minutes before the first set of fluorescence measurements were taken, showed a higher average fluorescence than set A, which did not have any initial light exposure. However, this result is not statistically significant, as the average values plus or minus one standard deviation overlap for the two sets of cuvettes. Additionally, the difference between the averages for the two sets of measurements is only approximately five to six percent ((1913667-1804667)/1913667 × 100 = 5.7%), which may simply be due to a slight variation in pipetting the concentrated solution of sodium fluorescein.

Although standard deviations of each individual reading were not recorded for these samples, typically the standard deviation for a given reading is between 1 and 3 %. The decrease in fluorescence measured after the second light exposure is larger than this typical standard deviation for a single reading, as well as the standard deviations for the averaged initial readings (0.94% and 5.09%), and the differences between the average values of counts/sec for set A and set B. This indicates that the photobleaching caused by the eight-minute exposure to the microscope stage lighting was significant enough to be measurable, and confirms the results reported in section 0, which showed a significant loss in fluorescence for samples that were microinjected without precautions to minimize the exposure to ambient light. However, some of this loss in fluorescence may be due to the light exposure that the samples received while they were being read in the spectrofluorometer. The samples were exposed to the excitation light (75 watt xenon lamp) of the spectrofluorometer for three seconds, and this may contribute to the measured photobleaching.

Further confirmation of these results can be found in the literature. The photobleaching of free (0.01 μM PBS solution) and bound (surface-labeled microspheres) fluorescein has been experimentally studied and theoretically modeled by others[4]. Air saturated free fluorescein solutions were found to bleach approximately 50 % after 80 minutes of exposure to a 100 W mercury arc lamp with a 450–490 nm excitation filter block, but were bleached only approximately 8 % after ten minutes of photobleaching under the same conditions. This 8% loss in fluorescence is similar to the magnitude of photobleaching seen in the study reported here.

A.3.3 Ionic Strength and pH

The measured fluorescence values of various amounts of microinjected sodium fluorescein are shown in **Figure A.3** for six different ionic strengths of PBS.

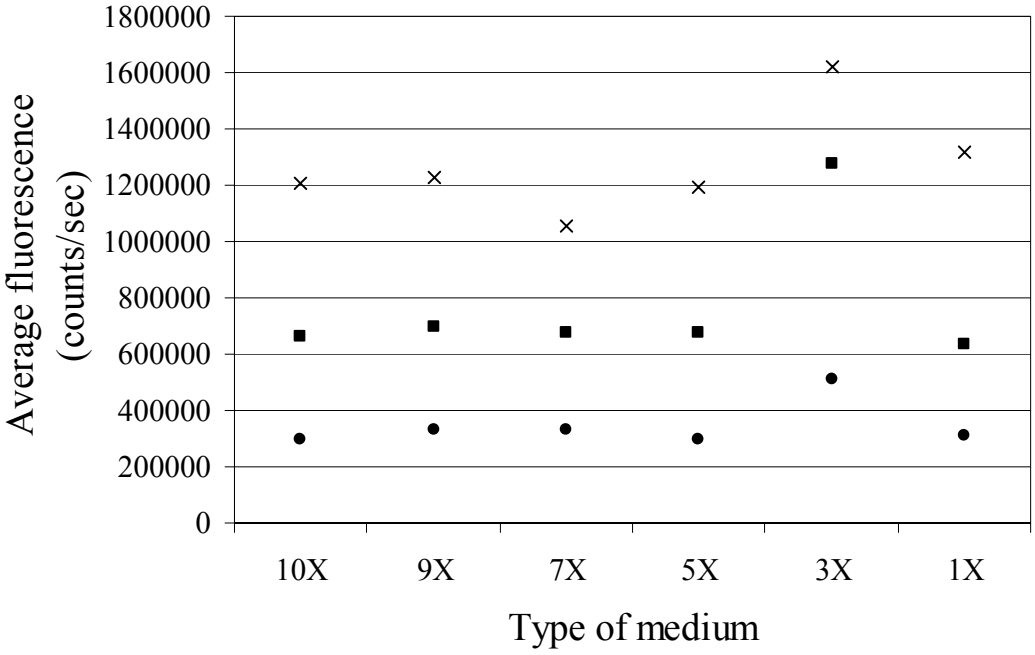

Figure A.3 Measured fluorescence of various microinjected amounts of sodium fluorescein (● 1.1 nmol, ■ 2.2 nmol, × 4.4 nmol) in PBS of different ionic strengths. Ionic strength is greatest for 10X PBS.

Overall, the samples show a slight decreasing trend of measured fluorescence as the ionic strength is increased from 1X up to 10X. This can be explained by the fact that as the ionic strength of the release medium increases, greater screening of the fluorescent species and thus faster quenching occurs, leading to a lower measured fluorescence[2]. Another way in which to understand these results is to plot the fluorescence of the samples as a function of the medium pH. The pH is inversely related to the ionic strength (as ionic strength and hence [H+] concentration increase, the pH decreases), and thus we would expect the measured fluorescence to decrease as the pH decreases. This is exactly what is experimentally observed, as shown in **Figure A.4** below.

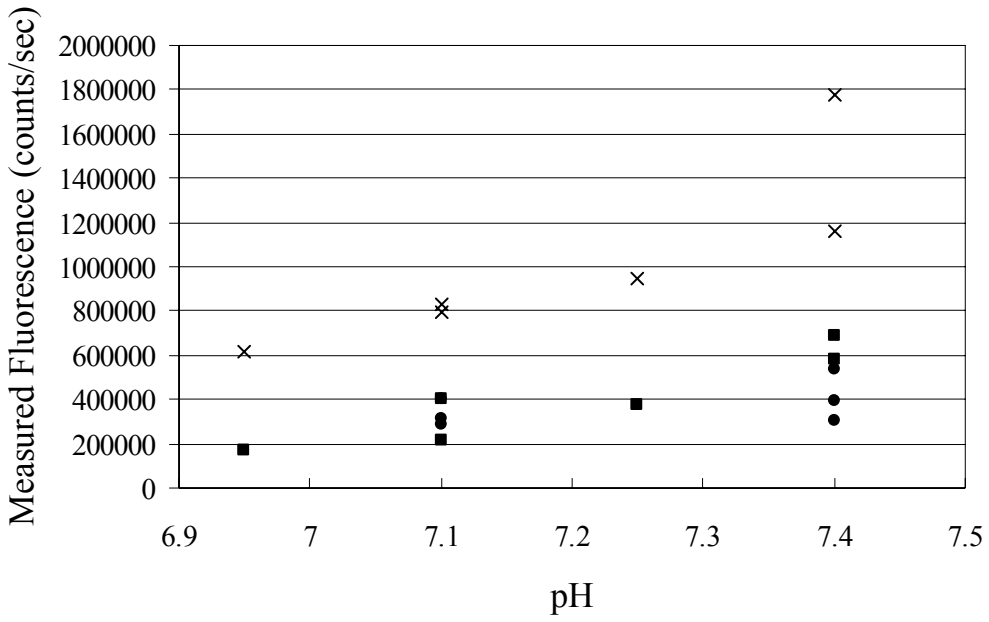

Figure A.4 Measured fluorescence of cuvettes having different amounts of sodium fluorescein (● 1.1 nmol, ■ 2.2 nmol, × 4.4. nmol) in different ionic strengths of PBS, as a function of pH.

These results quite clearly show that the sodium fluorescein becomes more fluorescent as the release medium pH is increased ([H+] concentration decreases, ionic strength decreases, and thus the screening effect becomes less significant), and that this effect is quite large. Approximately a threefold increase in measured fluorescence was seen for 4.2 nmol of sodium fluorescein (× symbol in **Figure A.4**) as the pH was increased from 6.95 to 7.4.

A.3.4 pH and Conductivity

Results from a variety of release studies were collated with pH and conductivity measurements in order to determine whether the phenomena discussed thus far are significant over the course of a typical release study. **Figure A.5** below shows the compiled measurements of release media pH versus the time (in days) at which the eleven release studies were concluded.

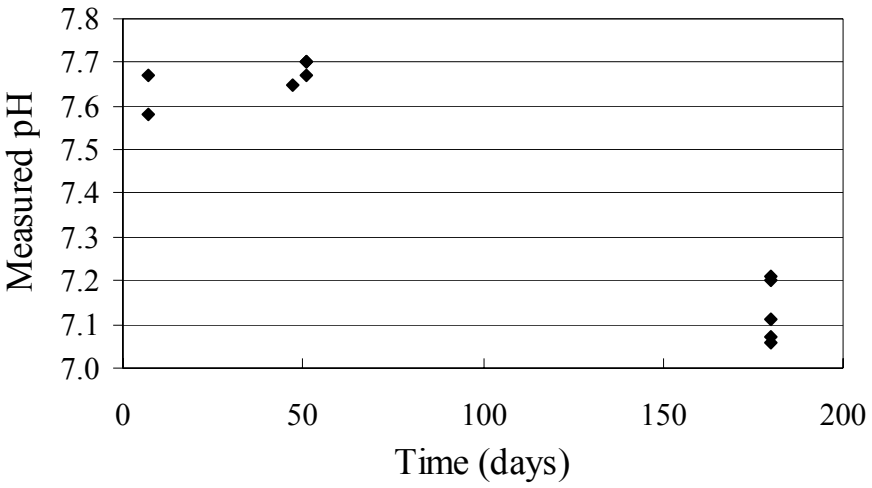

Figure A.5 Measured media pH over time for various release experiments.

Although the experiments were performed in phosphate buffered saline, a drop in pH was seen as the length of the studies increased. This decrease in pH over time is most likely due to the release of lactic acid and glycolic acid monomers from the device substrate and membranes as the device degrades over the course of the experiment. Based on the results discussed in section A.3.3 above, we would therefore expect the cumulative amount of fluorescence measured at the conclusion of the release studies to show a decrease over time. This is indeed the case, as shown in **Figure A.6** below. The measured cumulative percentage of loading released showed a marked decrease over the time period that was investigated.

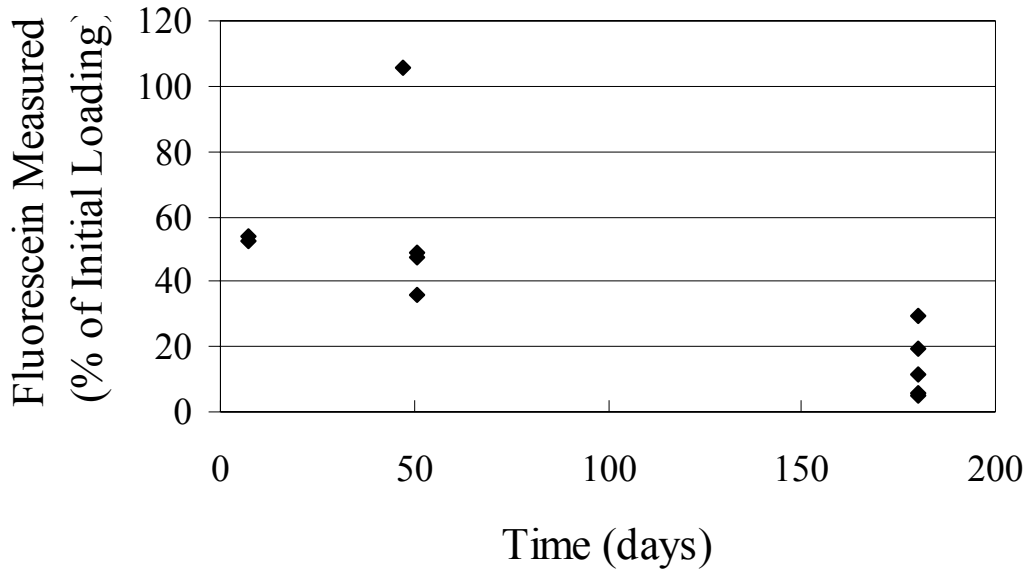

Figure A.6 Cumulative percentage of initial fluorescein loading measured at the conclusion of various release experiments.

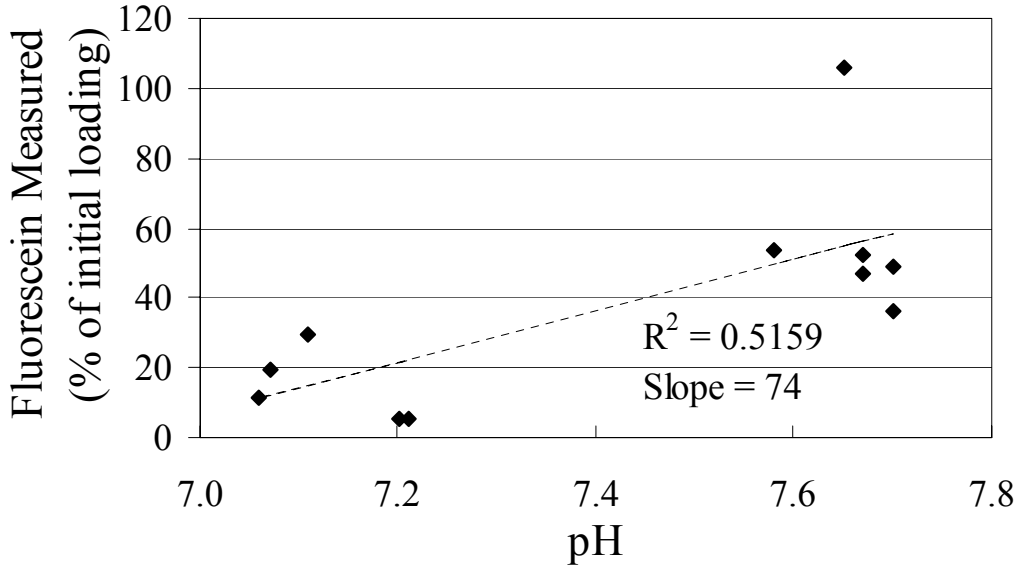

Figure A.7 Percentage of initial fluorescein loading measured at the conclusion of various release experiments, as a function of pH.

Combining the results from **Figure A.5** and **Figure A.6**, **Figure A.7** shows that the measured cumulative percentage of loading released shows a decreasing trend as the pH

decreases. This is consistent with our results shown in Figure A.4 that show lower fluorescence for a given amount of fluorescein as the pH is decreased (and therefore charge screening and fluorescence quenching are increased). However, this plot does not take into account that the devices that were left in the release media for the longest amount of time most likely had the largest amount of photobleaching from ambient light. Some of the decrease in measured fluorescence is thus due to photobleaching and not to the drop in pH. In fact, the fluorescence of fluorescein as a function of pH has been studied and showed less pH sensitivity than we have found[1]. A decrease in the measured fluorescence of fluorescein (normalized to the fluorescence measured above pH 8.2) has been reported as the pH was decreased. The normalized fluorescence decreased from 99.2% at pH 7.73, to 95.8% at pH 7.48, and to 82.7% at pH 6.99. Thus over the pH range measured for our *in vitro* release devices (7.06–7.7 in **Figure A.5** and **Figure A.7**), we would expect to see a difference in measured fluorescence of only approximately 17%. The significantly greater observed drop in measured fluorescence may therefore be attributed to photobleaching, as was discussed in sections A.3.1 and A.3.2 above.

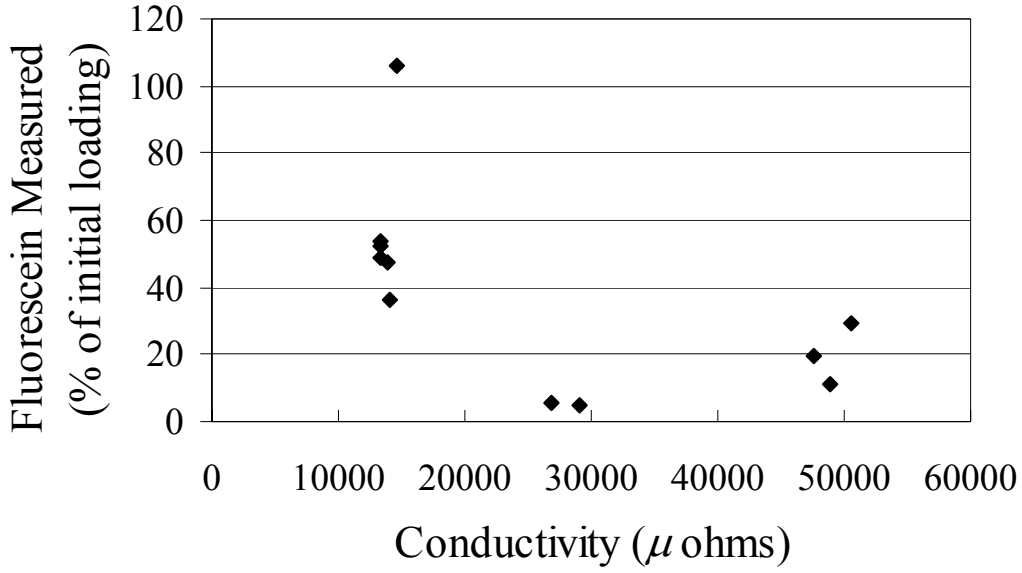

Figure A.8 Percentage of initial fluorescein loading measured at the conclusion of various release studies, as a function of release media conductivity.

Finally, **Figure A.8** above shows the percentage of the initial fluorescein loading recovered for these eleven microreservoir devices as a function of the release media conductivity, which is inversely proportional to the pH ($pH = -\log_{10}[H+]$). As the conductivity of the release

medium increases, the measured amount of fluorescein drops. This phenomenon is due to the faster quenching rate and shorter lifetime of the fluorescent species as the charge screening increases at higher ionic strengths[2].

A.4 Summary and Conclusions

The studies presented here clearly show that sodium fluorescein is very sensitive to 1) photobleaching and 2) the related variables of pH, ionic strength, and conductivity. Furthermore, the effects of these variables on the fluorescence of the molecule appear to be significant over the time scale of a typical release study, as they are most likely exacerbated by 1) production of acidic degradation products from the PLGA membranes on the microreservoir device, and 2) concentration of the saline solution due to continuous evaporation of the release media over time. Therefore, radiolabeled molecules were used for all of the release studies reported in this thesis in order to eliminate as many factors as possible that might affect accurate quantitation of the microreservoir device performance.

A.5 References

1. H. Diehl and R. Markuszewski, "Studies on fluorescein-VII. The fluorescence of fluorescein as a function of pH." *Talanta* 36 (1989) 416–418.

2. B. Verity and S. W. Bigger, "The dependence of quinine fluorescence quenching on ionic strength," *International Journal of Chemical Kinetics* 28 (1996) 919–923.

3. M. E. Morrison, R. C. Dorfman, and S. E. Webber, "Fluorescence quenching kinetics of phenanthrene covalently bound to sodium poly (acrylate-*co*-acrylamide): effects of ionic strength and counterion," *J. Phys. Chem.-U.S.* 100 (1996) 15187–15197.

4. L. Song, E. J. Hennink, I. T. Young, and H. J. Tanke, "Photobleaching kinetics of fluorescein in quantitative fluorescence microscopy," *Biophys. J.* 68 (1995) 2588–2600.

5. L. Song, "Photobleaching Kinetics of Fluorescein in Quantitative Fluorescence Microscopy," Delft University Press, Delft, The Netherlands, 1996.

6. L. Lindqvist, "A flash photolysis study of fluorescein," *Arkiv för Kemi* 16 (1960) 79–138.

B Microinjector Accuracy

B.1 Introduction

As was discussed in Chapter 3, a number of factors may affect the performance of the microinjector and therefore the amount of drug that is loaded into the reservoirs. The effects of drug solvent and surface geometry were investigated in Chapter 3, and it was found that both of these variables affected the measured microinjected volume to a quantifiable degree. However, two other factors may also affect the volume of solution that is delivered from the microinjector, namely the volume of the syringe that is used, and the amount of time that elapses between injections. Therefore, the goal of the microinjector studies reported here was to quantify the effect of these two variables on the microinjector performance in order to determine whether or not their effect on the amount of drug loaded into the microreservoir devices was significant.

B.2 Materials and Methods

B.2.1 Materials

Fluorescein-dextran, M_w~70,000 daltons, was obtained from Molecular Probes (Eugene, OR). Fluorescein sodium salt was obtained from Sigma-Aldrich (St. Louis, MO). Ideal 9144 Masking Tape was obtained from American Biltrite, Inc. (Lowell, MA).

B.2.2 Methods

B.2.2.1 Effect of Syringe Volume

The first variable that may affect the amount of solution that is delivered from the microinjector is the volume of the syringe that is used in the microinjector. The dispensing of liquid from the syringe is controlled by the rotation of an internal seated screw. The screw has a defined pitch such that rotation of the screw causes the plunger seat to move the syringe plunger a certain distance. A single rotation of the screw corresponds to one step, which is equal to the plunger seat moving a distance of 0.000125". For a syringe having a specified volume $V_{syringe}$, the volume that will be injected as the plunger seat moves one step (V_{step}) can be calculated as follows:

$$V_{step} = \left(\frac{V_{syringe}}{L_{syringe}} \right) \times \frac{0.000125"}{step}$$

Equation B-a

where $L_{syringe}$ is the distance that the plunger moves in order to inject $V_{syringe}$. For example, the plunger in a ten μL syringe moves approximately 2.36" in order to inject the entire volume of the syringe. Therefore, it has a volume per step of:

$$V_{step} = \left(\frac{10\mu L}{2.36"} \right) \times \left(\frac{1000nL}{1\mu L} \right) \times \left(\frac{0.000125"}{step} \right) = 0.529nL / step$$

Similarly, a 100 μL syringe has a volume of 5.29 nL/step, since the value of $L_{syringe}$ is the same for both the ten and 100 μL syringes and only $V_{syringe}$ differs by a factor of ten. The microinjector can therefore only dispense volumes that are integer multiples of the step size for a given syringe, and smaller volume syringes will have a greater resolution (smaller volume per step) than larger volume syringes.

Polystyrene cuvettes (4.5 mL, Labnet International, Woodbridge, NJ) having four optical windows were microinjected with different volumes of sodium fluorescein solution. One, two, three, four, or five injections were performed with the programmed volume per injection set to 20, 50, 100, or 150 nL. Solutions were injected from either a ten or 50 μL syringe with a 31 gauge, 2", blunt tip stainless steel metal hub needle (part 91031). To each cuvette were added three milliliters of deionized water. The cuvettes were covered with ParaFilm M® and shaken. The microinjected solutions were then further diluted by pipetting 50 μL from each cuvette into a second cuvette that contained three milliliters of deionized water.

The fluorescence (fluorescence counts/sec) of each cuvette was measured using λ_{exc} = 494 nm and λ_{emi} = 520 nm on a spectrofluorometer (Photon Technology International, Lawrenceville, NJ) having an L-201M Illumination System, LPS-220 Lamp Power Supply, A1010 Arc Lamp Housing, two Model 101 Computer-Controlled Monochromators, MP-1 Sample Compartment, Model 814 Analog/Photon-Counting Photomultiplier Detector, SC-500 Shutter Controller, Computer Interface, and PTI Felix v.1.42a software on a Dell Optiplex

466/Le computer. The concentration of fluorescent label in each cuvette (C_c) was calculated by subtracting the background fluorescence of a cuvette of deionized water (blank), and dividing by the slope in (fluorescence counts/sec)/(mol/L) of a standard curve. The measured microinjected volume V_{meas} was then calculated by using the volume of solution in the cuvette (V_c), the appropriate dilution factors (D_i), and the concentration of the fluorescently labeled solution in the syringe (C_{init}) as follows:

$$V_{meas} = \frac{(V_C \times C_C)}{(C_{init} \times D_i)}$$

Equation B-b

B.2.2.2 Effect of Elapsed Time Between Microinjections

As was discussed in Chapter 3, evaporation of the drug solution in the needle can cause consequent concentration of the solution and variation in the measured volume of solution that is microinjected. While the studies reported in Chapter 3 showed that the vapor pressure of the solvent clearly affected the measured microinjected volume due to evaporation, the effect of elapsed time between microinjections was not quantified. Therefore, a series of experiments was performed in order to determine if increasing the elapsed time between microinjections would affect the measured concentration. A 50 μL syringe with a 31 gauge needle was used to inject 18.48 nL of a fluorescein sodium solution onto a clean glass slide, followed by an injection onto the surface of a polystyrene cuvette. The elapsed time between the test injection on the glass slide and the injection into a cuvette was varied from one to four minutes. Four mL of deionized water were added to each cuvette before the fluorescence was measured on the spectrofluorometer using the procedures described in section B.2.2.1 above.

B.3 Results and Discussion

B.3.1 Effect of Syringe Volume

Syringes having volumes of ten and 50 μL were used to determine the effect of syringe volume on the accuracy of the microinjector. A 1.3×10^{-4} mol/L solution of fluorescein sodium in water was loaded into the syringes. The MICRO4 microinjector controller was programmed to

deliver 20, 50, 100, or 150 nL per injection. The actual volumes injected were multiples of 19.57, 49.72, 99.98, and 149.7 nL for the ten μL syringe, and multiples of 18.48, 47.52, 97.68, or 147.8 nL for the 50 μL syringe.

Figure B.1 shows the measured microinjected volume vs. predicted microinjected volume for the sodium fluorescein solution microinjected from the ten μL syringe, while the results for the 50 mL syringe are shown in **Figure B.2**.

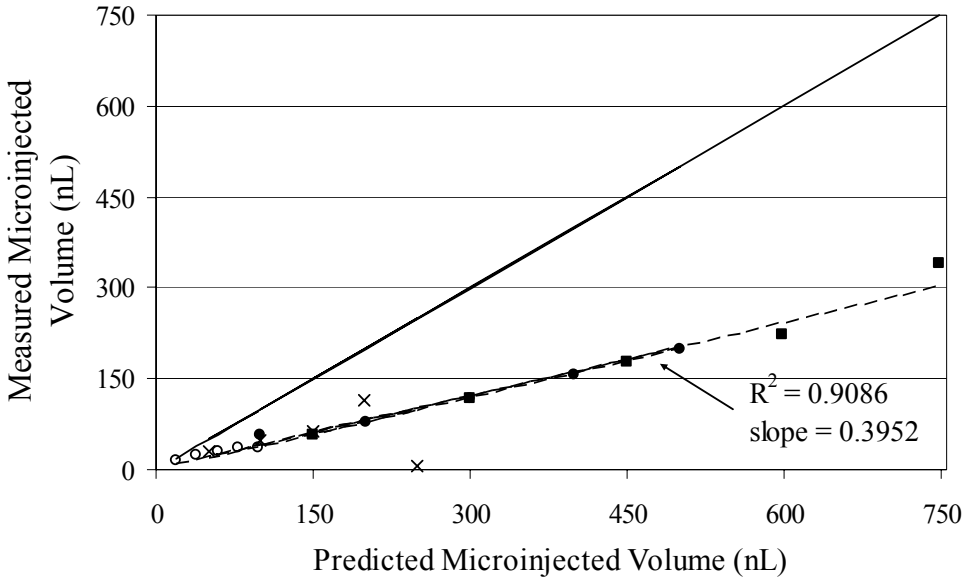

Figure B.1 Measured vs. predicted microinjected volume for multiple injections of sodium fluorescein solution from a ten μL syringe: ○ 20 nL injections, × 50 nL injections, ● 100 nL injections, ■ 150 nL injections, solid line indicates theoretical predicted microinjected volume, dashed line indicates least-squares best fit to data points.

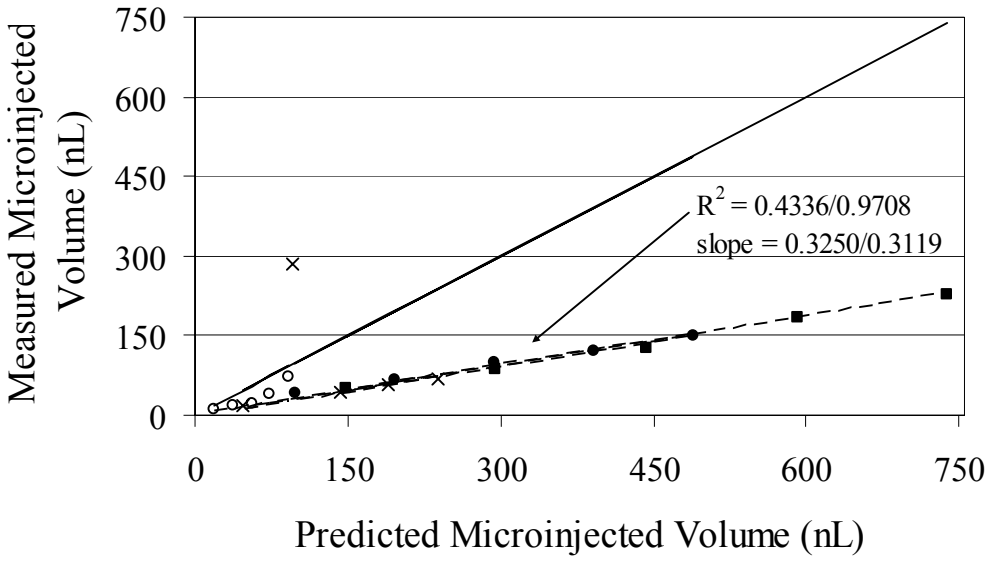

Figure B.2 Measured (calculated) vs. predicted microinjected volume for multiple injections of sodium fluorescein solution from a 50 μL syringe: ○ 20 nL injections, × 50 nL injections, ● 100 nL injections, ■ 150 nL injections, solid line indicates theoretical predicted microinjected volume, dashed line indicates least-squares best fit to data points. R^2 and slope values calculated with/without 95.04 nL outlier.

The ten μL syringe results indicate a measured microinjected volume of approximately 40% (slope = 0.3952) of the predicted microinjected volume, on average, while the 50 μL results show approximately 30% (slope = 0.3250) of the predicted microinjected volume. The slopes and R^2 values indicated in **Figure B.2** were calculated for the 50 μL syringe samples both with and without the 95.04 nL outlier (2 x 47.52 nL injections). The small overall measured volumes may be due to the rapid photobleaching of fluorescein, which was discussed in Appendix A. The difference in the average measured microinjected volumes, however, indicates that the volume of the syringe affects the accuracy of the microinjector. This is not surprising, as the smaller syringe has a smaller volume per step and therefore a better resolution. Improper rotation of the internal microinjector screw by one step, for example, would create an error of 0.529 nL for a ten μL syringe, but an error of 2.65 nL for a 50 μL syringe. For a programmed microinjected volume of 20 nL, these errors would turn out to be 2.65% and 13.25% of the programmed volume. This difference in syringe resolution could therefore explain the greater accuracy of the ten μL syringe as evidenced by the larger slope of the curve in **Figure B.1**. From this set of experiments,

we concluded that the syringe volume did have a measurable, although small, effect on the accuracy of microinjection.

B.3.2 Effect of Elapsed Time Between Microinjections

Although the results that were presented in Chapter 3 suggested an evaporation effect due to solvent vapor pressure, reconciliation of experimentally obtained values with predicted values was difficult. However, varying the time between microinjections of a solution and then measuring the microinjected amount of solute can provide a qualitative measure of whether evaporation significantly affects the microinjected volumes of interest for our studies.

A solution of fluorescein sodium in water was injected into polystyrene cuvettes. The elapsed time between a test injection on a glass slide and the injection into the cuvette was varied from one to four minutes. The results of the experiment are shown in Figure B.3 below.

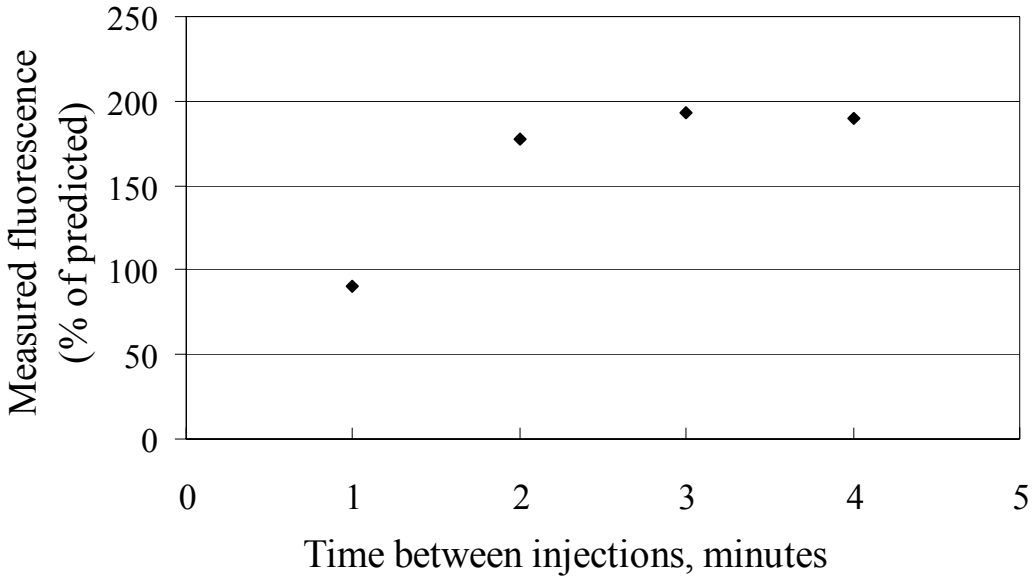

Figure B.3 Measured fluorescence as a function of elapsed time between microinjections.

At one minute, the measured fluorescence is approximately equal to the predicted fluorescence. This may represent a balance between the three phenomena of concentration of the solution due to evaporation, photobleaching, and decreased wetting due to an increase in the solution viscosity as the solvent evaporates. As is expected, when the time between microinjections is increased, the measured fluorescence also increases. This is most likely due to the evaporation of the solvent and corresponding increase in concentration of the droplet, similar

to the results seen for ^{14}C-iodoantipyrine in section 3.3.1.1. Predicted values of the adjusted concentration in the solution droplets can be obtained using the following equations from Chapter 3:

$$RT \ln\left(\frac{P}{P_0}\right) = \gamma \frac{V_m}{R_m}$$

Equation B-c

$$Z = P\left(\frac{1}{2\pi MRT}\right)^{\frac{1}{2}}$$

Equation B-d

$$N_L = Z \times S_A \times t$$

Equation B-e

We assumed a pendant droplet volume of 18.48 nL, T = 290°K (20°C), and an initial solution concentration of 0.0132 mol/L. The calculated concentrations for the droplets after one, two, three, or four minutes of elapsed time are shown in **Table B-1** below.

Table B-1 Calculated concentrations of fluorescein sodium droplets after one, two, three, or four minutes elapsed time between microinjections.

Solution	V_{inj} (nL)	P (kPa)	Elapsed Time (sec)	Adjusted Concentration (mol/L)
Water	18.48	3.2000115	60	0.013200508
	18.48	3.2000115	120	0.013201016
	18.48	3.2000115	180	0.013201524
	18.48	3.2000115	240	0.013202033

While our theoretical calculations show an increase in the droplet concentration, it is not a large enough increase to account for the experimentally observed doubling of the measured fluorescence. As was discussed in Chapter 3, the most obvious reason for this is that the vapor pressure calculations do not account for the continuing decrease in the size of a given droplet due to evaporation. As the droplet shrinks, the vapor pressure will increase, thereby further increasing the vapor pressure and hence the evaporation rate.

This increase in concentration as the elapsed time increases seems to plateau at times longer than three minutes. One explanation for this might be that after approximately three

minutes, equilibrium is reached between the driving force to evaporate the solution from inside the needle, and the geometry of the liquid surface. From Equation B-c it can be seen that the vapor pressure P is proportional to $\exp(R_m^{-1})$, where R_m is the mean radius of curvature of the liquid surface. As the solution evaporates from the end of the needle, the liquid surface becomes flatter and the radius of curvature increases. In the case of a completely flat, planar surface, the radius of curvature becomes infinite. From Equation B-c it is evident that as the radius of curvature increases, the vapor pressure decreases. The vapor pressure and thus the driving force for evaporation will be zero when the quantity $(\gamma V_m)/(RTR_m)$ is equal to one. Alternatively, the plateau region seen in **Figure B.3** may arise when the photobleaching rate of the fluorescein exactly counteracts the evaporation and hence concentration rate.

B.4 Conclusions

The studies presented here clearly show that the microinjection method that is used to load the devices with chemicals has a number of variables that can affect the accuracy of loading. First, the syringe volume appears to have a large effect on the microinjected volume. Larger volume syringes will have a correspondingly larger volume per step when used with the microinjector. This leads to less accuracy than can be achieved with smaller volume syringes. Additionally, greater elapsed time between microinjections appeared to increase the amount of solute that was measured for a given microinjected volume, most probably due to concentration of the solution within the syringe needle as the solvent evaporated.

Precautions were typically taken during loading of devices for a release study to minimize the effects of these two variables. At least one test microinjection was always performed on a glass slide just prior to microinjection of a drug solution into a reservoir on a given device in order to minimize the effect of evaporation. When loading reservoirs with drug solutions, ten μL syringes were typically used for ^{14}C labeled chemicals, although 50 or 100 μL syringes were used for ^{125}I chemicals, and a 100 μL syringe was used to load ^{3}H-heparin. While the syringe volume may partially explain the variability seen for the amounts of ^{125}I labeled chemicals recovered over the course of the release studies presented in Chapter 4, the devices loaded with ^{3}H-heparin from a 100 μL syringe showed generally very reproducible and high amounts of loading released over the course of the release studies. Therefore, it is more likely that other factors such as the counting efficiency and sensitivity of the scintillation counters for

the various isotopes, as well as the partition coefficients of the chemicals, play a larger role in the determination of the measured amount of chemical released from the devices.

A more critical issue for *in vitro* prototypes with regard to microinjector accuracy may be the fabrication of the reservoir membranes. Typically microinjection of the membrane solutions is performed with a 100 μL syringe due to the large volume of solution required when fabricating membranes in a batch of devices. The greater inaccuracy of the larger volume syringes, combined with the high vapor pressure of the solvent in which the membrane polymers are dissolved, may generate greater than expected variability in the volume of reservoir membrane polymers injected into the reservoirs. This could affect the final membrane thicknesses, which in turn may affect their degradation and the subsequent time at which release of chemicals from the reservoirs is observed, as discussed in Chapter 5. A more thorough study to correlate the predicted microinjected volume with the actual membrane thickness may prove valuable.